



**HAL**  
open science

# Interactions entre les Spirosilane de Martin et Base de Lewis coordination, frustration et nouveau ligand anionique

Fabrizio Medici

► **To cite this version:**

Fabrizio Medici. Interactions entre les Spirosilane de Martin et Base de Lewis coordination, frustration et nouveau ligand anionique. Chimie organique. Université Paris sciences et lettres, 2017. Français. NNT : 2017PSLET029 . tel-04343678

**HAL Id: tel-04343678**

**<https://theses.hal.science/tel-04343678>**

Submitted on 14 Dec 2023

**HAL** is a multi-disciplinary open access archive for the deposit and dissemination of scientific research documents, whether they are published or not. The documents may come from teaching and research institutions in France or abroad, or from public or private research centers.

L'archive ouverte pluridisciplinaire **HAL**, est destinée au dépôt et à la diffusion de documents scientifiques de niveau recherche, publiés ou non, émanant des établissements d'enseignement et de recherche français ou étrangers, des laboratoires publics ou privés.

# THÈSE DE DOCTORAT

of the university of Paris Science and Lettre  
PSL Research University

Interactions Between the Martin's Spirosilane and Lewis Bases:  
Coordination, Frustration and New Anionic Ligands

**Ecole doctorale n°406**

Chimie Moléculaire de Paris Centre

**Spécialité** Chimie Moléculaire

**Soutenue par Fabrizio MEDICI**  
**le 13 décembre 2017**

Dirigée par **Louis FENSTERBANK**  
**Gilles LEMIÈRE**

## COMPOSITION OF THE JURY :

Mme. DÍEZ-GONZÁLEZ Silvia  
Imperial College London, Rapporteur

M. TSUYOSHI Kato  
Laboratoire Hétérochimie Fondamentale  
et Appliquée, Rapporteur

Mme. VIDAL Virginie  
L'École Nationale Supérieure de Chimie  
de Paris, Examineur

M. DAGORNE Samuel  
Institut de Chimie de Strasbourg,  
Examineur

M. AMOURI Hani  
Université Pierre et Marie Curie,  
President

M. FENSTERBANK Louis  
Université Pierre et Marie Curie,  
Directeur de thèse

M. LEMIÈRE Gilles  
Université Pierre et Marie Curie,  
invité



*To Sara and my Family*



*I have a friend who's an artist and has sometimes taken a view which I don't agree with very well. He'll hold up a flower and say "look how beautiful it is," and I'll agree. Then he says "I as an artist can see how beautiful this is but you as a scientist take this all apart and it becomes a dull thing," and I think that he's kind of nutty. First of all, the beauty that he sees is available to other people and to me too, I believe. Although I may not be quite as refined aesthetically as he is ... I can appreciate the beauty of a flower. At the same time, I see much more about the flower than he sees. I could imagine the cells in there, the complicated actions inside, which also have a beauty. I mean it's not just beauty at this dimension, at one centimeter; there's also beauty at smaller dimensions, the inner structure, also the processes. The fact that the colors in the flower evolved in order to attract insects to pollinate it is interesting; it means that insects can see the color. It adds a question: does this aesthetic sense also exist in the lower forms? Why is it aesthetic? All kinds of interesting questions which the science knowledge only adds to the excitement, the mystery and the awe of a flower. It only adds. I don't understand how it subtracts."*

Richard Feynman



## Acknowledgements

This thesis work was done at the Université Pierre et Marie Curie in the laboratory of the IPCM under the supervision of Professor Louis Fensterbank, financed by the PSL.

First, I want to thank you the jury for having accepted to judge this work: Dr. DÍEZ-GONZÁLEZ Silvia from the Imperial College of London; Dr. TSUYOSHI Kato from the Laboratoire Heterochimie Fondamentale et Applique; Dr. VIDAL Virginie from L'École Nationale Supérieure de Chimie de Paris; Dr. DAGORNE Samuel from L'Institut de Chimie de Strasbourg; Dr. AMOURI Hani from l'Université Pierre et Marie Curie.

I want to thank Louis because he has accepted and supported my application allowing me to do this thesis in the MACO team. I learned a lot thanks to him, but really a lot, he has allowed me to grow as a chemist and personally, and in the end I really enjoyed his humor, probably because it is similar to mine. So thank you really much for believing in me and for having helped me.

Thanks also to my younger boss Gilles, together we have made a great chemistry, also if not always appreciate from the other, but hey I really like my subject, even though sometimes I complained. He was always available to answer my question or to discuss new ideas, or to make some office Foot-basket, it is great to have such a relationship between a student and a supervisor. Indeed, both Louis and Gilles they always listened and respect my ideas, they never clip my wing and I think that this is one of the best qualities of a boss. And also thank you to have allowed me to be a handyman.

Of course I thank all the permanents of the MACO team, for their great advice, the humor and the help they gave to me and to all the team.

And what can we say about the other members of the team and the friends from the other teams? Well I love you guys, other than chemistry knowing I'd spend the day with you made me even more enthusiastic to come to the lab. Thank you for the patience and for having borne me, especially my French that I admit still needs a small review, my untameable Italian style and for my music which may have caused some bearable disturbance, but hey it is not my fault if you listen bad music. I will miss you... I will miss you...

Thank you also to my friend outside the lab, The Italian's Group, present and not.. I absolutely love being your friend you helped me to feel less of home nostalgia. We laughed so much and made so many stupid things, (e quanto non è stato bello lamentarsi dei francesi insieme), we are epic. Honestly, among all the people I knew during this experience I found

true friends, really the best. To remember also the friends left in Italy, few but good, thank you very much.

Returning in university I have to thank all the person that help me, Geoffrey and Lise-Marie for have solved all the structure which I brought to them, it was a pleasure to work with you. As also if I do not so much Mass analysis, they were some nasty sample but thanks to Omar we do it. I cannot forgot to thanks the NMR's girls, Aurelie&Claire, I so much enjoyed spend time with you, I learn so much on NMR and thanks to you I fallen in love with this technique, also if I need more entrainment on the interpretation. How many times have you pulled me out of trouble, even if I did not do anything and a bug on the system appeared and how much time I ask to add an experience or something on the NMR, I loss the count. Of course thanks to our gestionaire and secretaries to had facilitate my work.

Time for the family now so... I switch to Italian. Che dire, come si può non ringraziare la famiglia. Grazie davvero per aver creduto in me e per avermi sostenuto in questa avventura, in tutti questi anni, dalla nascita, ammetto che ve ne ho fatte passare di tutti i colori non so come avete fatto a sopportarmi. L'aiuto che mi avete dato in questi ultimi anni, come nei miei periodi peggiori, è insostituibile e non potrò mai dirvi grazie abbastanza. A mia Madre perché, va beh la mamma è la mamma, quel tuo lato da chiocchia mi ha salvato in molti casi e ci ho fatto parecchio affidamento, grazie per avermi preso a calci nel sedere, metaforicamente e non, per darmi una svegliata, spero di averti un poco ripagata dei tuoi sforzi, grazie per avermi trasmesso la passione della lettura dei giochi e anche l'empatia verso il prossimo, di quella troppa forse eheh ma va bene così, oltre alla passione della cucina del nuoto proprio una gran mamma. A mio Padre, che è un riferimento come mia madre, grazie per avermi insegnato a sciare a guidare, anche se il temperamento e il sangue caldo quelli gli ho ereditati dalla mamma eheheh, per avermi trasmesso la tua abilità da bricoleur e la passione per smontare e sistemare le cose oltre a saper fare un barbecue, ma soprattutto a essere un uomo, non te lo ho mai detto perché son timido e non riesco a parlare con te di queste cose, ma spero di diventare un uomo anche solo la metà di quello che sei te sarebbe un onore. A mio fratello, uno migliore non puoi trovarlo, con le nostre passioni in comune ci siamo divertiti un sacco e continuiamo ancora, mi spiace non essere stato lì con te in questi anni come fratello maggiore quando avevi bisogno, ma vedo che te la sei cavata egregiamente. Ai nonni, grazie perché siete fantastici e premurosi come sempre, e fuori di testa quel tanto che basta per rendervi ancora più unici. È sempre fantastico venire da voi e passare una bella giornata di relax, nonostante i lavoretti richiesti che si fanno sempre con piacere. Grazie anche agli altri nonni,

anche se non ci siete più non potrò mai dimenticarvi. Ovviamente ringrazio anche la famiglia della mia fidanzata con cui è sempre un piacere passare del tempo.

Ultima ma non sicuramente per importanza, anzi, Sara la mia ragazza... ci sarebbero un sacco di cose da dire ma lei sa già tutto, ma grazie davvero sei fantastica.



# Summary

<b>Acknowledgements .....</b>	<b>.....</b>
<b>Summary.....</b>	<b>.....</b>
<b>Abbreviations .....</b>	<b>1</b>
<b>General Introduction.....</b>	<b>7</b>
<b>I. Introduction.....</b>	<b>13</b>
<b>I.1 Hypercoordination in Silicon Chemistry.....</b>	<b>13</b>
I.1.1 Introduction .....	13
<b>I.2 Hypercoordinate Silicon.....</b>	<b>14</b>
I.2.1 Invoking the <i>d</i> orbitals.....	15
I.2.2 Three-Centre Four-Electron .....	17
I.2.3 Hypercoordination or hypervalence? .....	19
I.2.4 Hypercoordinate silicon in organic chemistry .....	20
<b>I.3 Martin's Spirosilane .....</b>	<b>24</b>
<b>I.4 Results and Discussion .....</b>	<b>34</b>
<b>II. Interaction Between Martin's Spirosilane and N-Heterocyclic Carbenes .....</b>	<b>41</b>
<b>II.1 N-Heterocyclic Carbenes .....</b>	<b>42</b>
II.1.1 Introduction .....	42
II.1.2 Electronic properties of NHC.....	43
<b>II.2 NHC-Silicon Interactions.....</b>	<b>49</b>
<b>II.3 Results and Discussion .....</b>	<b>55</b>
II.3.1 Synthesis of the NHC used in this study .....	55
II.3.2 Adducts formation.....	57
<b>III. Martin's Spirosilane as a New Partner in FLP Chemistry</b>	<b>75</b>
<b>III.1 Bibliography.....</b>	<b>75</b>
III.1.1 Frustrated Lewis Pair: from the concept to applications.....	76
III.1.2 NHCs and silicon in Frustrated Lewis Pair chemistry .....	85
<b>III.2 Results and Discussion .....</b>	<b>94</b>

III.2.1	Assessing the Lewis acidity of the Martin's spirosilane .....	94
III.2.2	Attempts to split hydrogen .....	95
III.2.3	Attempts to activate carbon dioxide.....	99
III.2.4	Reaction with formaldehyde .....	101
III.2.5	Reaction with benzyl alcohol .....	103
III.2.6	Reaction with 1,3-cyclopentadione .....	105
<b>IV.</b>	<b>Anionic NHC Carbenes Bearing a Siliconate Moiety.....</b>	<b>111</b>
IV.1	Anionic NHC Carbene : from Synthesis to Metals Coordination and Catalysis 112	
IV.2	Results and Discussion .....	117
IV.2.1	Deprotonation of the abnormal adduct 29.....	117
IV.2.2	Metal complex with 29.....	118
IV.2.3	Metal complexes with the 28 .....	119
IV.2.4	Computational investigations .....	125
<b>V.</b>	<b>Configurational Stability at the Pentacoordinate Silicon Adducts .....</b>	<b>129</b>
V.1	Introduction on Silicon Chirality .....	129
V.2	Configurational Stereomutation at Pentacoordinate Species.....	130
V.3	Configurational Stereomutation in Martin's Spirosilane Adduct .....	132
V.4	Configurational Stability of NHC-Si and $\alpha$ NHC-Si Adducts .....	135
	<b>General Conclusion .....</b>	<b>141</b>
	<b>Experimental Section .....</b>	<b>145</b>
Chapter I	.....	148
Chapter II	.....	149
	Synthesis of Carbenes .....	149
	Synthesis of NHC-Martin's Adducts .....	152
Chapter III	.....	155
	Hydrogen Activation Reactions .....	155
	Activation of the Carbon Dioxide .....	158
	Interactions between 7 and phosphine .....	160
	Synthesis of the Formaldehyde adducts .....	160
	Synthesis of the benzyl alcohol adducts.....	162

Synthesis of the 1,3-cyclopentanedione adduct .....	163
<b>Chapter IV .....</b>	<b>164</b>
Selenium Derivatives .....	169
<b>Chapter V.....</b>	<b>171</b>
Separation of 29 .....	171
Separation of 26 .....	172
Separation of 57 .....	172
Separation of 58 .....	173
<b>Crystallographic Data.....</b>	<b>175</b>
<b>Figure's Index .....</b>	<b>181</b>
<b>Scheme's Index.....</b>	<b>184</b>
<b>Table's Index.....</b>	<b>188</b>



# **Abbreviations**



**2c-1e:** 2 centre-1 electron

**3c-4e:** 3 centre-4 electrons

**9-BBN:** 9-Boracyclo[3.3.1c]nonane

**18-c-6:** 1,4,7,10,13,16-hexaoxacyclooctadecane

**aIPr:** Abnormal 1,3-bis(2,6-diisopropylphenyl)-imidazolyliden

**aItBu:** abnormal 1,3-di-*tert*-butyl-imidazolyliden

**Ar:** Aryl

**bipy:** 2,2'-bipyridine

**CAAC:** Cyclic Alkyl Amino Carbene

**CD:** Circular Dichroism

**COD:** 1,5-cyclooctadiene

**DCC:** N,N'-dicyclohexylcarbodiimide

**DCM:** Dichloromethane

**DDQ:** 2,3-dichloro-5,6-dicyano-1,4-benzoquinone

**DFT:** Density Functional Theory

**Dipp:** 2,6-diisopropylphenyl

**DMAP:** 4-Dimethylaminopyridine

**DMF:** N,N-Dimethylformamide

**DMSO:** Dimethyl sulfoxide

**eV:** Electronvolt

**FLP:** Frustrated Lewis Pair

**HOMO:** Highest Occupied Molecular Orbital

**HRMS:** High Resolution Mass Spectroscopy

**IDM:** 1,3-dimethyl-imidazolylidene

**IMes:** 1,3-dimesityl-imidazolylidene

**IPr:** 1,3-bis(2,6-diisopropylphenyl)-imidazolylidene

**ItBu:** 1,3-di-*tert*-butyl-imidazolylidene

**LUMO:** Lowest Unoccupied Molecular Orbital

**Mes:** 2,4,6-trimethylphenyl, mesityl

**NHC:** N-Heterocyclic Carbene

**NMR:** Nuclear Magnetic Resonance

**ORTEP:** Oak Ridge Thermal Ellipsoid Plot

**SIMes:** 1,3-dimesityl-4,5-dihydro-imidazolylidene

**SPP:** Square Planar Pyramid

**TASF:** Tris(dimethylAmino)Sulfonium diFluorotrimethylsilicate

**TBAF:** TetraButylAmmonium Fluoride

**TBP:** Trigonal Bi-Pyramid

**TfOH:** Triflic acid

**THF:** Tetrahydrofurane

**THT:** Tetrahydrothiophene

**TMEDA:** N,N,N',N'-tetramethylethan-1,2-diamine

**TMP:** 2,2,6,6-tetramethylpiperidine

**TMSCF<sub>3</sub>:** Trifluoromethyltrimethylsilane, Ruppert's reagent

**WCA:** Weakly Coordinate Anion



# **General Introduction**



Silicon and its derivatives play a prominent position in everyday life, just think that our computers and cell phones are based on silicon electronics as well as a considerable amount of polymers used in the most different applications. However, this element has not only found a use in the world of materials and electronic, but its derivatives have distinguished themselves as key reagent in chemistry, just think of the Hiyama reaction, one of the most famous cross-coupling reactions. This extraordinary success is mainly due to the Lewis acidity of silicon and its ability to become hyper-coordinated, unlike carbon, belonging to the same group, which can form a maximum of four bonds. In fact, structures in which silicon has five or six different bonds, thus apparently breaking the octet rule, are not so rare. This work will start with the examination of this characteristic, which will allow us to better understand the reactivity of Martin's spiro-silane, our protagonist. The purpose of this thesis is in fact, the study of interactions that may present this particular Lewis acid with Lewis bases, particularly N-Heterocyclic Carbenes.

NHCs are characterized by a high stability and great versatility, due to the possibility to modify the structure by customizing the substituents. In summary, it is possible to modulate their electronic and steric properties, which explains the immense potential of this particular class of carbenes and why they have found a wide use in the most different fields of chemistry. However, in the literature few examples of the synthesis and investigation of silicon(IV) derivatives, not derived from halogenate precursors, with NHCs has been reported.

Our study has allowed the discovering of new fascinating unique compounds and due to their nature, different applications were envisioned. Indeed, in our systems herein a Lewis acid and base are present and characterised by a high steric hindrance. We look at their potential applications as Frustrated Lewis Pairs chemistry. Moreover, a part of the compounds synthesised during this work, can be the platform for the chemistry of anionic ligands. Finally, the chirality of the pentacoordinate siliconate structure was explored, especially the configurational stability of some silicon adducts we obtained.



# **Chapter I**

## **Introduction**



# I. Introduction

This chapter will be focused on the silicon element, with a particular emphasis on its extracoordinate derived structures. Some synthetic utilities of pentacoordinate silicon intermediates in organic chemistry will be also presented. In addition, a second part of this first chapter will try to provide an overview of the literature about the Martin's spiroasilane from its first synthesis to applications.

## I.1 Hypercoordination in Silicon Chemistry

### I.1.1 Introduction

Etymologically, the word silicon comes from the Latin word *silex* meaning flint. In terms of abundance in the earth crust, it represents the second element with 28% (after oxygen 47%), and is found in its silica form,  $\text{SiO}_2$ , the base constituent of the amorphous glass and also, of the crystalline quartz (Figure I.1).

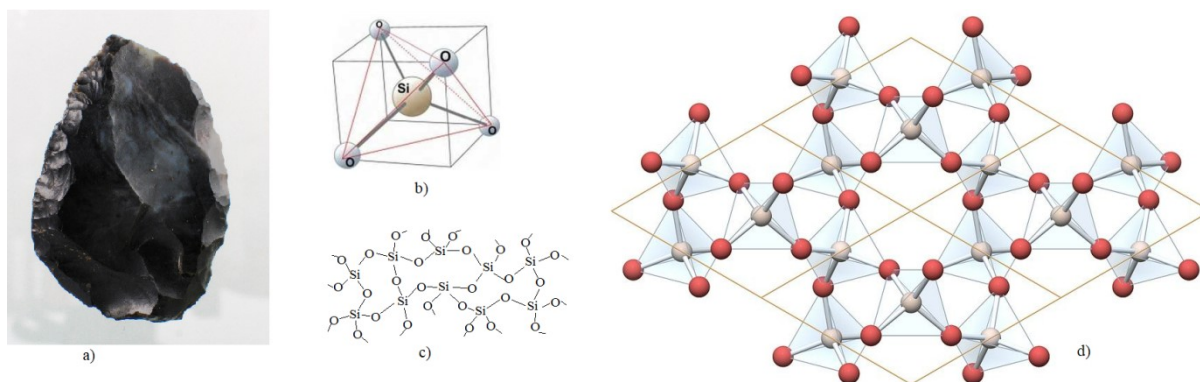


**Figure I.1** a) Fragment of flint; b) Base unit cell of silica; c) Disordered 3D network typical of glass; d) Ordered 3D network typical of the crystalline form of silica quartz.

The synthesis of the pure element was a troubled story.<sup>1</sup> Lavoisier in 1787 hypothesized that silica must be the oxide of a new element.<sup>2</sup> Although Sir Humphry Davy was unable to isolate it with his electrochemical apparatus, he coined the term “silicium”.<sup>3</sup> Guy-Lussac and Thenard obtained a reddish-brown solid, by heating metallic potassium in

<sup>1</sup> M. E. Weeks, *J. Chem. Educ.* **1932**, 9, 1386

<sup>2</sup> A. Lavoisier, *Traité Élémentaire de Chimie*, Paris, Cuchet, **1789**, vol. 1, 174

<sup>3</sup> D. Humphry, "Electro chemical researches, on the decomposition of the earths; with observations on the metals obtained from the alkaline earths, and on the amalgam procured from ammonia", *Philosophical Transactions of the Royal Society of London*, **1808**, 98, 333–370

presence of  $\text{SiCl}_4$ . This was probably a really impure form of amorphous silicon.<sup>4</sup> Finally J. J. Berzelius in 1824 isolated the pure element by heating potassium in a silica container.<sup>5</sup> The properties of this element were deeply studied during the two last centuries, allowing for the discovery of a wide range of applications from computer manufacturing, that is probably the most known application, solar cell for its semiconductive properties to chemistry. One of the most peculiar properties of silicon is the possibility to exceed the tetracoordination, which is not possible for the carbon element, and therefore exhibiting hypercoordination.<sup>6</sup> This feature has strongly attracted the interest of chemists for the potential application in organic and inorganic chemistry, such as the discovery of new reactivities or new intriguing structures.

## I.2 Hypercoordinate Silicon

As we all know, silicon belongs to the same group of carbon. Its electronic configuration is  $1s^2 2s^2 2p^6 3s^2 3p^2$  and therefore to complete its configuration to reach the complete octet,<sup>7</sup> it only requires four covalent bonds. Despite this basic rule, it is possible to find different compounds based on this element with apparently five or six “covalent” bonds. However, silicon is not the only main group element with this “ability” to reach hypercoordination, and sulfur and phosphorus belong as well to this exclusive club. The Langmuir-Lewis theory and the quantum mechanical theory, that worked really well on molecules like  $\text{Cl}_2$ ,  $\text{PH}_3$ ,  $\text{H}_2\text{S}$  and also with metal complexes,<sup>8</sup> began to face some difficulties with molecules like  $\text{PCl}_5$ ,  $\text{DMSO}$  or  $\text{HClO}_4$ , where the participation of the  $d$  orbitals in the formation of this extra bonds was invoked. Finally, an alternative theory to the involvement of  $d$  orbitals was also proposed.

---

<sup>4</sup> Gay-Lussac, L. J. Thenard, "Recherches Physico-Chimiques," *Imprimerie de Crapelet, Paris*, **1811**, Vol. 1, 313-314; Vol 2, 54-65

<sup>5</sup> J. J. Berzelius, "On the Results of Some Chemical Analyses, and the Decomposition of Silica", *Annals of Phil.*, **1824**, *111*, 24, 1214

<sup>6</sup> C. Chuit, R. J. P. Corriu, C. Reye, J. C. Young, *Chem. Rev.* **1993**, *93*, 1371–1448.

<sup>7</sup> a) G. N. Lewis, *J. Am. Chem. Soc.* **1916**, *38*, 762–785. b) I. Langmuir, *J. Am. Chem. Soc.* **1919**, *41*, 868–934

<sup>8</sup> a) C. A. Coulson: *Valence*. 2nd Edit., *Oxford University Press*, Oxford **1961**. b) C. J. Ballhausen and H. B. Gray: *Molecular Orbital Theory*. Benjamin, New York **1964**. c) L. Pauling: *Nature of the Chemical Bond*. 3rd Edit., *Cornell University Press*, New York **1960**. d) R. J. Gillespie, R. S. Nyholm, *Progr. in Stereochem.*, **1958**, *2*, 261.

## I.2.1 Invoking the $d$ orbitals

Since the very first years of studies in chemistry at school, the complex phenomenon of hypervalence has been preferentially rationalised invoking the  $d$  orbitals. It is a simple and easy-to-understand approach to get out of an intricate problem.

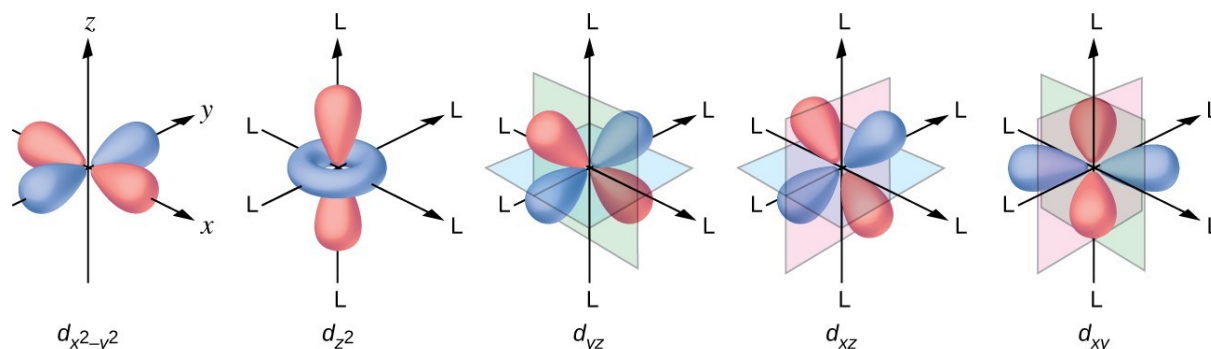


**Figure I.2** Schematic representation of the  $d$  atomic orbitals

Kwart and King analysed in-depth the nature of the  $d$  orbitals and their interactions with the ligand, classifying them in:  $\sigma$ ,  $\pi$ , and  $\delta$  (non-bonding) bonding interaction.<sup>9</sup>

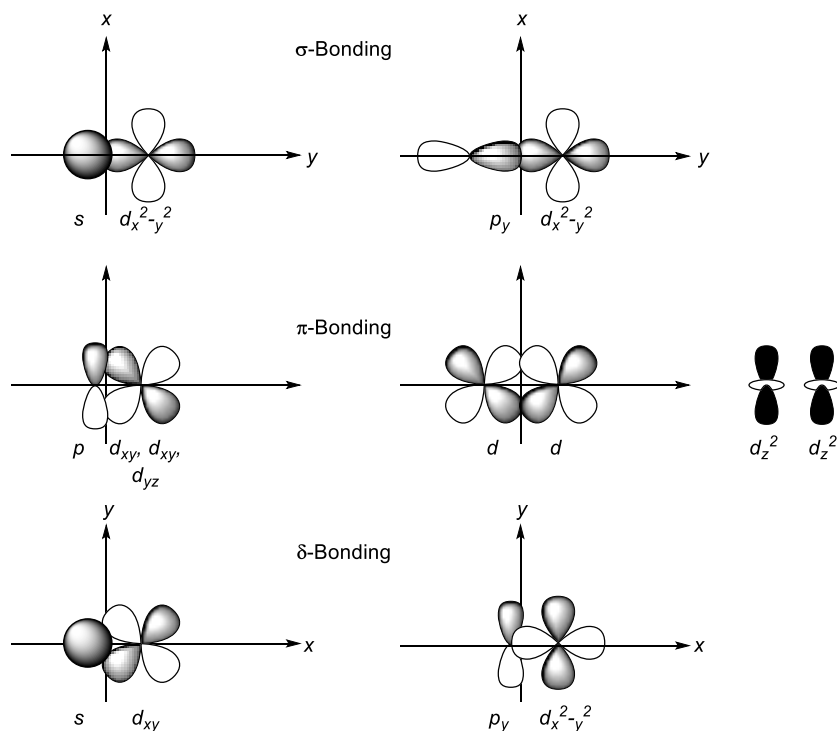


**Figure I.3** Example of  $\sigma$ ,  $\pi$  and  $\delta$  bonding

<sup>9</sup> H. Kwart, K. King, *D-Orbitals in the Chemistry of Silicon, Phosphorus and Sulfur*, Springer Science & Business Media, 2012.

In 1963, Gillespie focused his studies on the two different geometries that can adopt the pentacoordinate molecules: a trigonal bipyramid and a square planar pyramid. He described them using the d orbitals hybridisation, five  $sp^3d$ , and the lone pairs present in the valence shell.<sup>10</sup> With the investigations of the repulsion energies between lone pair and between the bond electrons, Gillespie could predict the preferential structure that can adopt a five-coordinated molecule (Figure I.4).

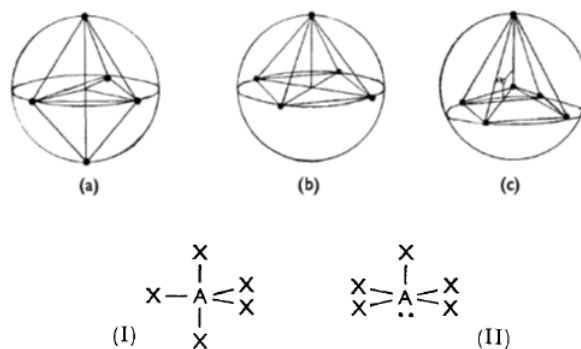


**Figure I.4** Equilibrium arrangements for electron pairs on the surface of a sphere repelling each other according to a force law of the form  $1/r^n$ . (a) and (b) are the most stable arrangements for  $n = \infty$ . (c) is the form of the square-pyramidal configuration for  $n < \infty$ ; preferential conformation of  $AX_5$  molecules (I) and  $AX_5E$  (II).

The hybridisation concept was highlighted in a recent paper of Oestreich and co-workers,<sup>11</sup> to describe the hypervalence of silicon.

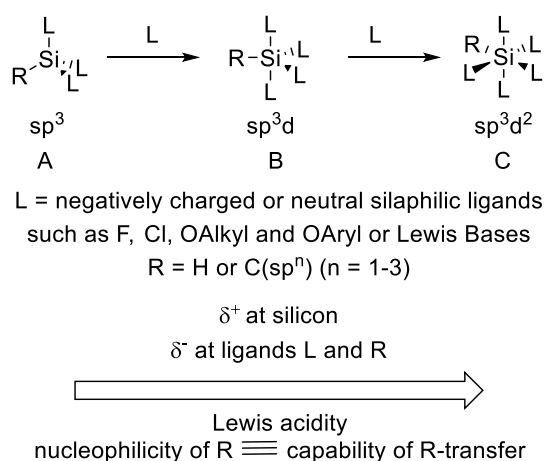


**Figure I.5** Hybridisation and electron density in hypervalent silicon

<sup>10</sup> a) R. J. Gillespie, *J. Chem. Soc. Resumed* **1963**, 0, 4679–4685. b) R. J. Gillespie, *J. Chem. Soc. Resumed* **1963**, 0, 4672–4678. c) R. J. Gillespie, *J. Chem. Soc. Resumed* **1952**, 0, 1002–1013

<sup>11</sup> S. Rendler, M. Oestreich, *Synthesis* **2005**, 2005, 1727–1747.

Using the valence bond theory, one can imagine the passage from the  $sp^3$  hybridisation in the tetravalent silicon (A), to the  $sp^3d$  and  $sp^3d^2$  for the pentacoordinate (B) and hexacoordinate (C) respectively. Logically speaking, it is expected from the silicon atom to get richer in electron upon coordination of an extra ligand and expansion of the coordination sphere, but experimentally the opposite has been observed. Hybridisation of the orbitals, has as consequence a loss of  $s$  character, meaning a depletion of electron density and so, an enhanced Lewis acidity on the central atom (see figure above).

### I.2.2 Three-Centre Four-Electron

The other theory to rationalize the hypercoordination is based on the three-centre four-electron concept developed by Rundle and Pimentel.<sup>12</sup> Rundle in 1963 introduced the concept of hypervalent bond and applied it to explain the bond's nature in polyhalide ions.<sup>13</sup> Thanks to Musher's work it was possible to extend the theory to other systems.<sup>14</sup> He defined a molecule as hypervalent when, there is a so-called donor atom that exceeds the valence allowed by the traditional theory.

**Errore. Il segnalibro non è definito.** These hypervalent bonds are formed from the interaction of a bonding and a nonbonding atomic orbital. As shown in figure I.6, silicon is in a  $sp^3$  hybridization state when tetravalent, the passage to the pentavalent form implied the engagement of a  $p$  orbital in a hypervalent bond, silicon is in a  $sp^2$  hybridisation state. The hexacoordinate species request to involve another  $p$  orbital, the silicon is in a  $sp$  hybridisation state.

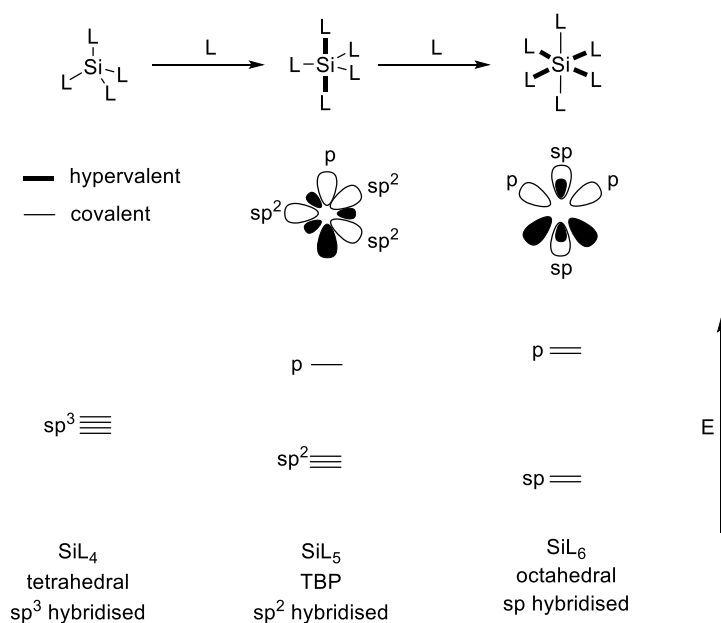


**Figure I.6** Orbital picture and hybridisation of silicon complex

In the three MO obtained in hypervalent species, (Figure I.7) it can be noticed how, in the case of the non-bonding orbital, a node is localized on the central atom.

<sup>12</sup> a) R. E. Rundle, *J. Chem. Phys.* **1949**, *17*, 671–675. b) G. C. Pimentel, *J. Chem. Phys.* **1951**, *19*, 446–448.

<sup>13</sup> R. E. Rundle, *Surv. Prog. Chem.* **1963**, *1*, 81–131.

<sup>14</sup> J. I. Musher, *Angew. Chem. Int. Ed. Engl.* **1969**, *8*, 54–68.

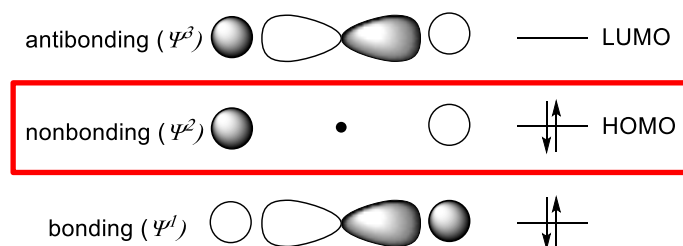


**Figure I.7** Molecular orbital diagram of three-centre four-electron molecule

The presence of this node results in the migration of the electronic density from the silicon to the ligands. For this reason, the central atom in extracoordinate compounds possesses an enhanced Lewis acidity compared to the tetracoordinate one.

The 3c-4e theory has been further corroborated by the work of Alekseev and co-workers, in which they demonstrated that the  $d$  orbitals of silicon are too much diffuse to participate in the bonds formation.<sup>15</sup>

<sup>15</sup> S. N. Tandura, M. G. Voronkov, N. V. Alekseev, in *Struct. Chem. Boron Silicon*, Springer, Berlin, Heidelberg, **1986**, pp. 99–189.

### I.2.3 Hypercoordination or hypervalence?

Once the nature of this “extra-bond” was discussed, a new problem appeared: is it better to use the term hypercoordination or hypervalence?<sup>16</sup> The term Hypervalent was firstly introduced by Musher in 1969,<sup>14</sup> and during the following years was more and more used to refer to molecules in which the coordination number exceed the valence number.<sup>7</sup> In 1930 Sugden suggested the existence of a 2c-1e covalent bond to explain the hypervalency without breaking the octet rule.<sup>17</sup> Rundle and Pimentel<sup>18</sup> with their 3c-4e theory, derived from that of Sugden, stated that there are only two electrons bonding which are localized on the ligands. In the years also the definition proposed by Musher was criticised, although in this definition the octet expansion theory was rejected in favour of the Rundle-Pimentel theory. All of these theories showed that in these “extra-bonded” compounds the valence of the central atom is not affected at all, so the term hypervalence does not have any logical meaning. Indeed, in 1984, Schleyer suggested the term “Hypercoordination”<sup>19</sup> to name that species, as this provides an empirical description of their structure without calling into question the nature of the bond (Figure I.8).

Despite these last suggestions and evidence that confirm the validity of the octet rule for the main group elements including the case of the hypercoordinate molecules, in the

<sup>16</sup> W. B. Jensen, *J. Chem. Educ.* **2006**, *83*, 1751.

<sup>17</sup> S. Sugden, *The Parachor and Valency.*, G. Routledge, London, **1930**.

<sup>18</sup> a) R. E. Rundle, *J. Chem. Phys.* **1949**, *17*, 671–675. b) G. C. Pimentel, *J. Chem. Phys.* **1951**, *19*, 446–448.

<sup>19</sup> P. von R. van Schleyer, *Chem. Eng. News Arch.* **1984**, *62*, 4.

### Hypervalent compounds . . .

SIR: Anthony Arduengo’s letter (Nov. 28, 1983, page 3) may be misleading. No genuinely “hypervalent” compounds of carbon are known. One must distinguish between “hypercoordination” and “hypervalence.” Coordination is the number of nearest neighbors; valence is the number of electron pairs involved in bonding. Hypercoordinated carbon is common.

There are hundreds of neutral compounds with structures secured by x-ray crystallography where the carbon coordination is five, six, seven, or even eight (see my comments, page 13 in H. C. Brown’s “The Non-Classical Ion Problem,” Plenum Press, 1977, and Olah and Prakash, *Chemistry in Britain*, **1983**, page 916). These include metal alkyls, carboranes, metal carbide carbonyl clusters, etc.

The bonds in such hypercoordinate molecules are partial and carbon has no more than eight valence electrons. While molecules like  $\text{CLi}_6$  [*J. Am. Chem. Soc.*, **105**, 5932 (1983)] and the interesting (but not really “hypervalent”) cases discussed by J. C. Martin [*Science*, **22**, 509 (1983)] apparently have 10 electrons formally associated with carbon, analyses of the bonding (also carried out by Prof. Karl Jug, Hannover) show that “hypervalent carbon” is not involved.

The “extra” electrons beyond the usual octet occupy orbitals which are nonbonding or antibonding with regard to carbon. The maximum valence which can be exhibited by carbon appears to be four.

**Paul von Ragué Schleyer**  
*Universität Erlangen-Nürnberg*  
*West Germany*

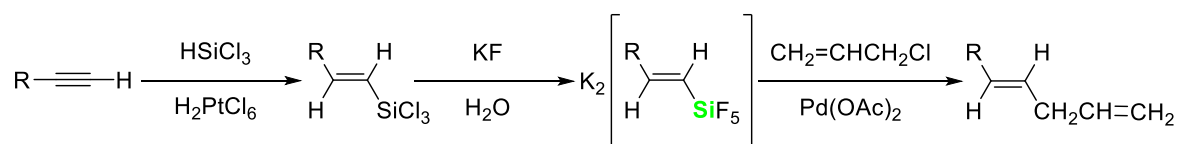
**Figure I.8** Original letter of Pr. Schleyer

textbooks the “expansion of the octet” and the term hypervalence are still commonly used.<sup>20</sup> From now on, the term hypercoordination will be preferentially used.

#### I.2.4 Hypercoordinate silicon in organic chemistry

Hypercoordination of silicon cannot be seen as a simple laboratory curiosity, since it has proved to be really useful in chemistry. An example of application is the C-C bond formation, one of the most interesting challenges in organic synthesis, and in the years different approaches have been developed from metal-catalysed one<sup>21</sup> to organocatalysed one.<sup>22</sup>

Kumada was probably the first to have developed a reaction mediated by a hypercoordinate silicon species (Scheme I-1).<sup>23</sup>



**Scheme I-1** First C-C bond formation with organosilane by Kumada *et al.*

As we can see, this reaction involves hexacoordinate species, organopentafluorosiliconates, that were made by reaction between a terminal alkyne and trichlorosilane, in presence of a catalytic amount of hexachloroplatinic acid followed by the addition of an excess of potassium fluoride. The subsequent reaction using an excess of allyl chloride with palladium(II) acetate as catalyst gave the corresponding 1,4-diene.

In this article, Kumada<sup>23</sup> showed that this reaction works principally with allyl bromide and chloride in moderate yield, but extension to substituted allyl derivatives gave also the corresponding dienes in poor yield though. These first examples demonstrate the great potentiality of organosilane.

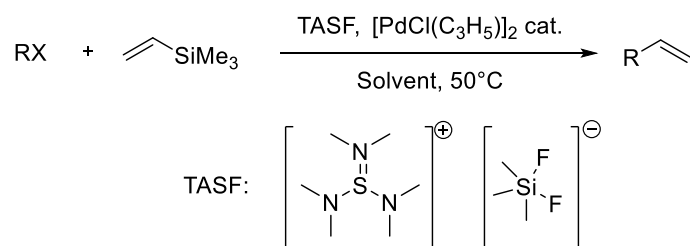
It is probably the work of Hiyama that shed light on the role of silicon derivatives in cross-coupling chemistry,<sup>24</sup> making them a powerful tool in the hand of the chemist.

<sup>20</sup> a) R. J. Gillespie, E. A. Robinson, *Inorg. Chem.* **1995**, *34*, 978–979. b) J. C. Martin, *Science* **1983**, *221*, 509–514.

<sup>21</sup> J. F. Hartwig, *Nature* **2008**, *455*, 314–322.

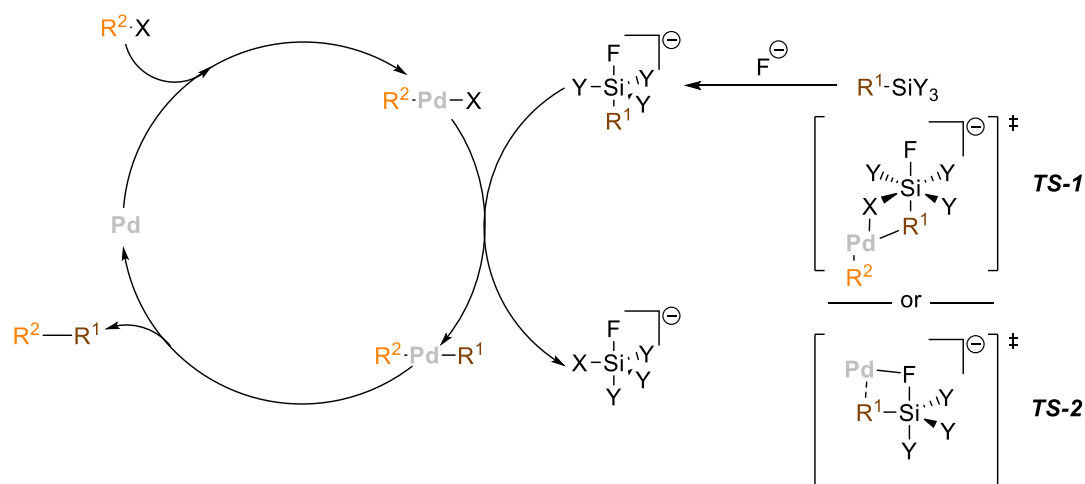
<sup>22</sup> C. Grondal, M. Jeanty, D. Enders, *Nat. Chem.* **2010**, *2*, 167–178.

<sup>23</sup> J. Yoshida, K. Tamao, M. Takahashi, M. Kumada, *Tetrahedron Lett.* **1978**, *19*, 2161–2164.



**Scheme I-2** General example of the first reported Hiyama cross-coupling

The reaction proceeds between an aryl/alkyl halide and a tetracoordinate organosilane, in the presence of a fluoride source, TASF, and a palladium complex as catalyst. This system resulted to be simpler as compared to the one of Kumada, since it is not necessary to isolate the organopentafluorosiliconate intermediate. As reported by Hiyama, and previously noticed by Kumada<sup>23</sup> and Hallberg,<sup>25</sup> a hypercoordinate intermediate is involved in the transmetallation step rationalizing the importance, of TASF. As depicted in scheme I-3, the following mechanism was proposed.



**Scheme I-3** Proposed catalytic cycle for of Pd-catalysed cross-coupling of organosilicon reagent

The reaction starts with the oxidative addition of the organohalide to the palladium and in the same time the addition of a fluoride onto the organosilane derivative, thus generating the pentacoordinate siliconates as key reagent. The change of coordination, as it is known, entails a modification of the electronic density and as a consequence, the weakening of the Si-C bond that results in the transfer of the R group from silicon to palladium. At this

<sup>24</sup> Y. Hatanaka, T. Hiyama, *J. Org. Chem.* **1988**, 53, 918–920.

<sup>25</sup> A. Hallberg, C. Westerlund, *Chem. Lett.* **1982**, 11, 1993–1994.

point, reductive elimination occurs to lead to the final coupled product and the regeneration of the palladium catalyst.

Since 1988, the Hiyama reaction has been widely studied<sup>26</sup> and some variation has been proposed. In particular, Denmark showed that the reaction works really well when using silanol-based complex instead of silanes. He also postulated the following intermediate for the transmetalation step (Figure I.9).<sup>27</sup>

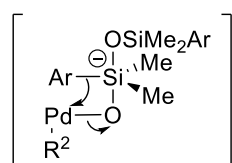
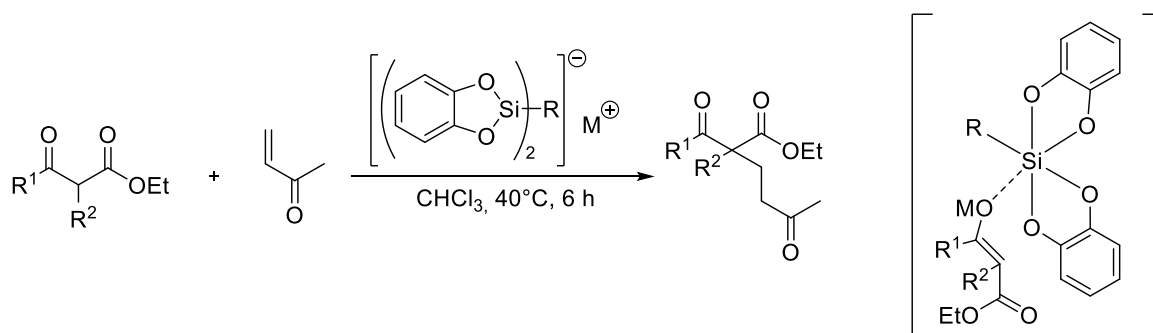


**Figure I.9** Denmark's intermediate for silanol-based cross-coupling

Over the years, hypercoordinate silicon intermediates have become increasingly important, in organic chemistry and now have been found in a large variety of reactions. In 2001, Hosomi<sup>28</sup> demonstrated how a hypercoordinate bis-catecholato silconate is capable to catalyse the Michael addition of  $\beta$ -keto ester to enones, through the formation of a hexacoordinate intermediate.



**Scheme I-4** In bracket the active hypercoordinate compound in the Hosomi's example

In 2005, Leighton and co-workers,<sup>29</sup> proposed a cyclosilane able to allylate aldehyde in enantioselective manners, through the formation of a hypercoordinate intermediate. This concept was reprised by them in 2012,<sup>30</sup> for the asymmetric allylation of  $\beta$ -diketone. They

<sup>26</sup> S. E. Denmark, A. Ambrosi, *Org. Process Res. Dev.* **2015**, *19*, 982–994.

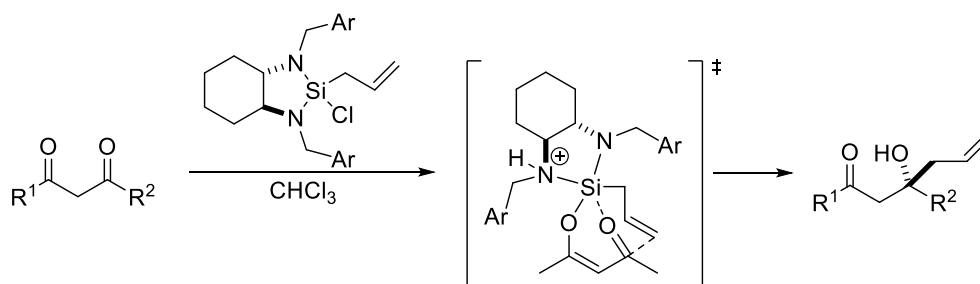
<sup>27</sup> S. A. Tymonko, R. C. Smith, A. Ambrosi, M. H. Ober, H. Wang, S. E. Denmark, *J. Am. Chem. Soc.* **2015**, *137*, 6200–6218.

<sup>28</sup> J. Tateiwa, A. Hosomi, *Eur. J. Org. Chem.* **2001**, *2001*, 1445–1448.

<sup>29</sup> X. Zhang, K. N. Houk, J. L. Leighton, *Angew. Chem.* **2005**, *117*, 960–963.

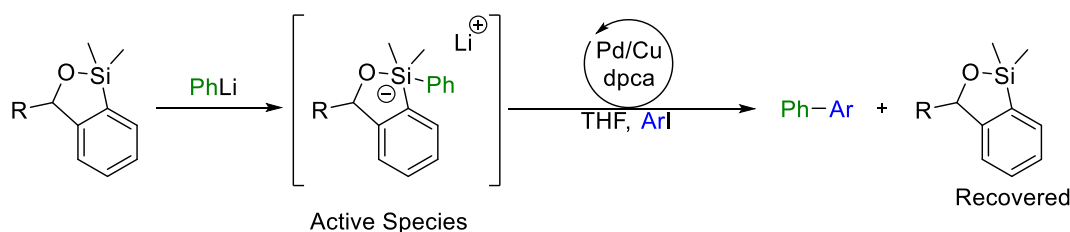
<sup>30</sup> W. A. Chalifoux, S. K. Reznik, J. L. Leighton, *Nature* **2012**, *487*, 86–89.

explained the difference in regioselectivity and enantioselectivity by invoking the variation of the intermediate conformation.



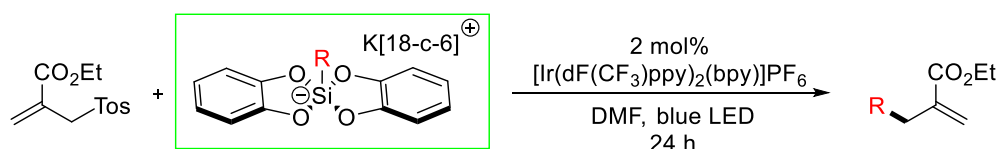
**Scheme I-5** General intermediate proposed by Leighton

Meanwhile Amos B. Smith *et al.*,<sup>31</sup> described the 1-oxa-2-silacyclopentene as an excellent “transfer reagent” for cross-coupling reaction between organohalides and organolithium derivatives. The latter are known for their sensitivity and the difficult handling conditions they impose. Indeed, organolithium compounds can easily transfer the nucleophilic group to the silicon centre, which becomes extracoordinate and in the right conditions, can release the carbanion nucleophile to allow the cross-coupling reaction.



**Scheme I-6** Cyclosilane as transfer reagent

Recently, our group has been interested in the behaviour and reactivity of silicon extracoordinate species, in particular the derivatives of the bis-catecholato-siliconate to generate alkyl radicals.<sup>32</sup> Basically by photooxidation, these derivatives are prone to easily release a carbon centred radical, due to the specific electronic properties of the hypercoordinate silicon compounds.



**Scheme I-7** Pentacoordinate siliconate as radical precursor

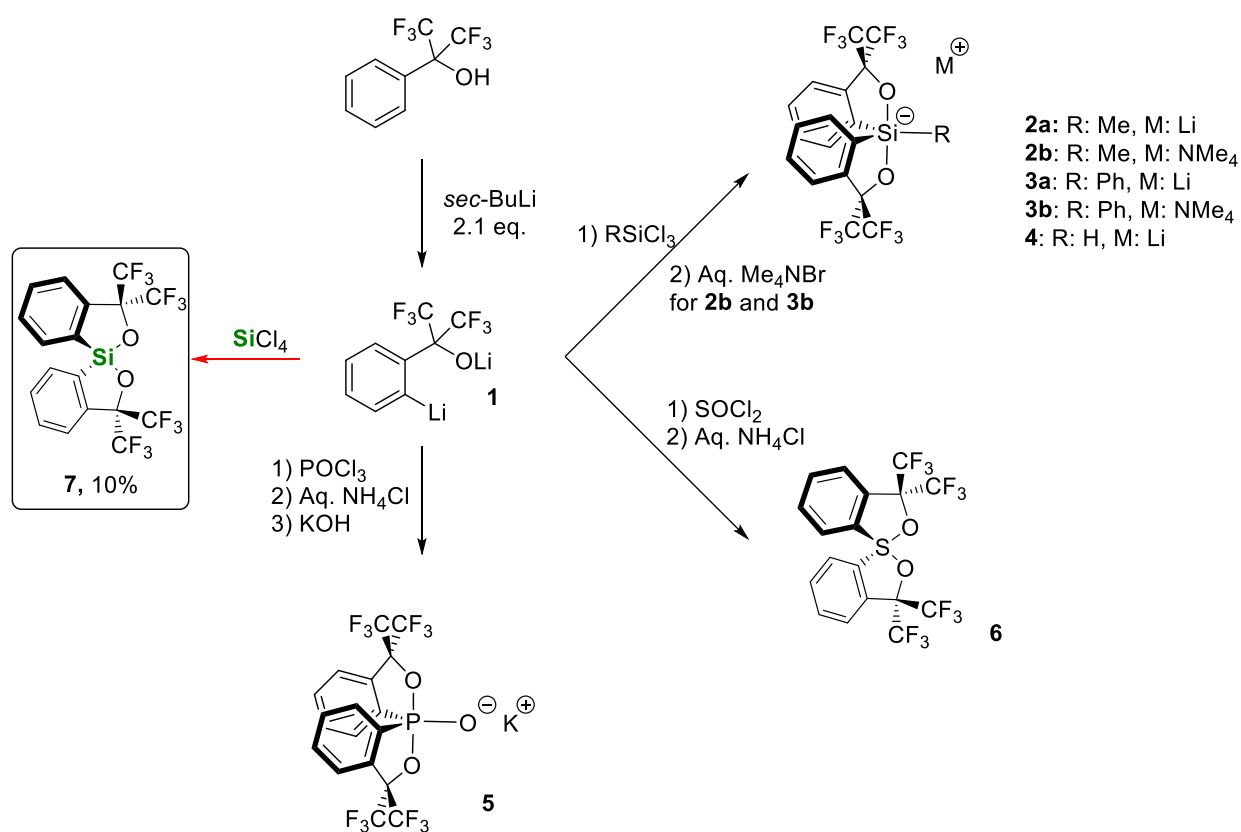
<sup>31</sup> a) A. B. Smith, A. T. Hoye, D. Martinez-Solorio, W.-S. Kim, R. Tong, *J. Am. Chem. Soc.* **2012**, *134*, 4533–4536. b) D. Martinez-Solorio, B. Melillo, L. Sanchez, Y. Liang, E. Lam, K. N. Houk, A. B. Smith, *J. Am. Chem. Soc.* **2016**, *138*, 1836–1839.

<sup>32</sup> V. Corcé, L.-M. Chamoreau, E. Derat, J.-P. Goddard, C. Ollivier, L. Fensterbank, *Angew. Chem. Int. Ed.* **2015**, *54*, 11414–11418.

These few examples highlight the potentiality of hypercoordinate silicon species and their increasing role in chemistry for the development of new reactivities.<sup>33</sup>

### I.3 Martin's Spirosilane

The first part of this chapter was dedicated to the properties of silicon especially in hypercoordinate species. The second part will focus on the Martin's spiro-silane, a tetravalent silicon(IV) Lewis acid, from its first synthesis to recent developments. The first synthesis was reported by J. C. Martin and co-workers in 1979.<sup>34</sup> In this seminal work, the authors were motivated in finding new methodologies for the synthesis of hypercoordinate species based on silicon, sulfur and phosphorus. Interestingly they could obtain different derivatives starting from the dilithiated form of the 1,1,1,3,3,3-hexafluoro-2-phenyl-2-propanol used, as a bidentate ligand (Scheme I-5).



**Scheme I-8** Reactions scheme for the synthesis of the hypercoordinate compounds from hexafluorocumyl alcohol

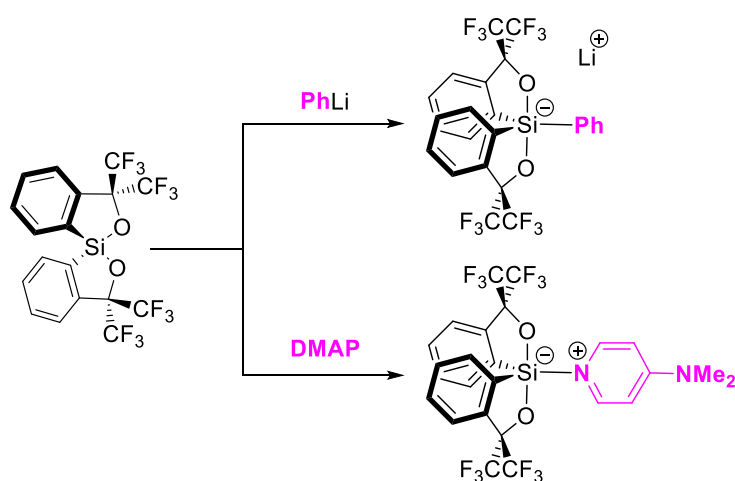
<sup>33</sup> a) Y. Deng, Q. Liu, A. B. Smith, *J. Am. Chem. Soc.* **2017**, *139*, 9487–9490. b) T. Komiyama, Y. Minami, T. Hiyama, *ACS Catal.* **2017**, *7*, 631–651. c) M. Benaglia, S. Guizzetti, L. Pignataro, *Coord. Chem. Rev.* **2008**, *252*, 492–512. d) S. Rendler, M. Oestreich, *Synthesis* **2005**, *2005*, 1727–1747.

<sup>34</sup> E. F. Perozzi, J. C. Martin, *J. Am. Chem. Soc.* **1979**, *101*, 1591–1593.

The dianionic species **1** was obtained treating the starting alcohol with two equivalent of *sec*-BuLi, that was then reacted with CH<sub>3</sub>SiCl<sub>3</sub>, PhSiCl<sub>3</sub>, SOCl<sub>2</sub>, POCl<sub>3</sub> or SiCl<sub>4</sub>. In the case of the alkyl or aryl silane the pentacoordinate derivatives, **2a-3a**, was obtained in good yields, 79%-70%, it was also possible to perform the cation metathesis from lithium to tetramethylammonium. The hydrosiliconate **4** was supposed by Martin and co-workers due to the impossibility to purify it or to found the Si-H signal in the proton NMR. Compounds **5** and **6** were obtained in moderate yield 50% and 45% respectively.

The compounds represented herein, turned out to be highly stable, due to the formation of five-membered rings<sup>35</sup> favoured by the presence of the gem-dialkyl effect (Thorpe-Ingold effect).<sup>36</sup> Furthermore, for the pentacoordinate species, the presence of two electronegative oxygen atoms, connected to a carbon atom bearing two electro-withdrawing groups, in the apical position is known to have a strong contribution to the stability of these compounds.<sup>37</sup>

In this thesis, we have been mainly interested in the reactivity of spiroasilane **7**. This intriguing spiranic structure with a silicon(IV) in junction is obtained by treating **1**, the dilithiated form of hexafluorocumulacohol, with tetrachlorosilane. Martin's spiroasilane **7**, possesses a relatively high Lewis acidity owing to the presence of electron-withdrawing ligands. In terms of reactivity, it reacts with anionic and neutral nucleophile, such as phenyllithium or DMAP, to afford the corresponding anionic or neutral pentacoordinate silicon products (Scheme I-9).



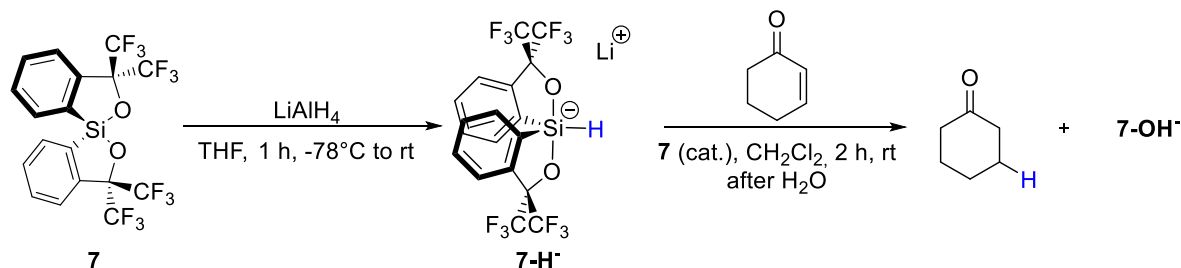
**Scheme I-9** Reaction with different nucleophiles

<sup>35</sup> J. C. Martin, E. F. Perozzi, *J. Am. Chem. Soc.* **1974**, *96*, 3155–3168

<sup>36</sup> a) R. M. Beesley, C. K. Ingold, J. F. Thorpe, *J. Chem. Soc. Trans.* **1915**, *107*, 1080–1106. b) C. K. Ingold, *J. Chem. Soc. Trans.* **1921**, *119*, 305–329.

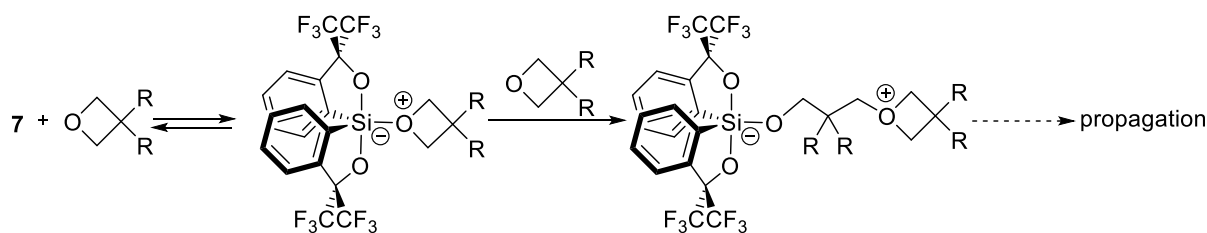
<sup>37</sup> a) R. Hoffmann, J. M. Howell, E. L. Muetterties, *J. Am. Chem. Soc.* **1972**, *94*, 3047–3058. b) E. L. Muetterties, R. A. Schunn, *Q. Rev. Chem. Soc.* **1966**, *20*, 245–299.

Martin,<sup>38</sup> also noticed that **7** can react with a source of hydride such as LiAlH<sub>4</sub> in order to generate the hydrosiliconate derivative. This latter compound proved to be able to achieve the reduction of different carbonyl-containing molecules (Scheme I-10). A catalytic amount of spiroasilane **7** is required to activate the substrate by coordination of the oxygen.



**Scheme I-10** Synthesis of hydrosiliconate **7-H<sup>-</sup>** and its application in the enone's reduction

Martin's spiroasilane Lewis acidity and oxophilicity were the two crucial factors in the reactivity described by Chien and co-workers.<sup>39</sup> Indeed, they have employed it as an initiator for the polymerisation of oxetanes (Scheme I-11).



**Scheme I-11** polymerisation of oxetanes

It is well-known that silicon has a high affinity with fluoride.<sup>40</sup> Moreover, fluoride can have a considerable impact on human health<sup>41</sup> and for these reasons, it is necessary to monitor its quantity in drinking water and in food, and if necessary, to be able to uptake it. Different systems for detection have been proposed, from ion-selective sensor to ion chromatography,<sup>42</sup>

<sup>38</sup> S. K. Chopra, J. C. Martin, *J. Am. Chem. Soc.* **1990**, *112*, 5342–5343.

<sup>39</sup> B. Xu, C. P. Lillya, J. C. W. Chien, *J. Polym. Sci. Part Polym. Chem.* **1992**, *30*, 1899–1909.

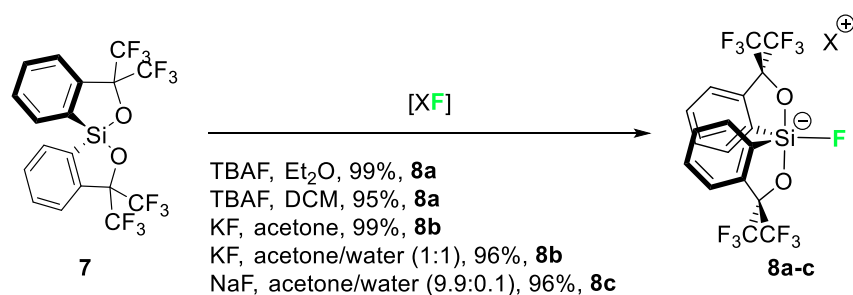
<sup>40</sup> a) R. Damrauer, A. J. Crowell, C. F. Craig, *J. Am. Chem. Soc.* **2003**, *125*, 10759–10766. b) J. W. Larson, T. B. McMahon, *J. Am. Chem. Soc.* **1985**, *107*, 766–773.

<sup>41</sup> a) J. K. Fawell, K. Bailey, W. H. Organization, *Fluoride in Drinking-Water*, World Health Organization, **2006**. b) S. Ayoob, A. K. Gupta, *Crit. Rev. Environ. Sci. Technol.* **2006**, *36*, 433–487. c) M. Kleerekoper, *Endocrinol. Metab. Clin.* **1998**, *27*, 441–452. d) P. Singh, M. Barjatiya, S. Dhing, R. Bhatnagar, S. Kothari, V. Dhar, *Urol. Res.* **2001**, *29*, 238–244. e) E. B. Bassin, D. Wypij, R. B. Davis, M. A. Mittleman, *Cancer Causes Control* **2006**, *17*, 421–428.

<sup>42</sup> a) R. De Marco, G. Clarke, B. Pejic, *Electroanalysis* **2007**, *19*, 1987–2001. b) M. A. G. T. van den Hoop, R. F. M. J. Cleven, J. J. van Staden, J. Neele, *J. Chromatogr. A* **1996**, *739*, 241–248.

but of more interest to us are the molecular sensors. They are compounds that can be affected by a structural change, when they undergo coordination with a specific target, that can be analysed by UV-Vis, fluorescence or NMR spectroscopy.<sup>43</sup> For these reasons, Martin's spiro-silane was investigated by our group as a potential molecular sensor.<sup>44</sup>

As shown before, hypercoordination of **7** results in a deep structural change that should affect the UV-Vis and fluorescence spectra. Different sources of fluoride were investigated, in different conditions affording the compounds **8a-c** in excellent yield (Scheme I-12).



**Scheme I-12** Reactivity of **7** toward different fluoride source

The UV-vis spectra did not give an appreciable result, because no sufficient difference between the two compounds was noticed, as opposed to the fluorescence spectra (Figure I-10).

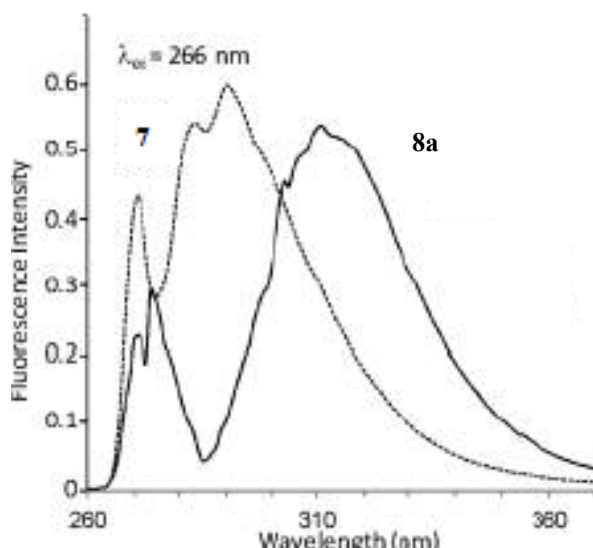


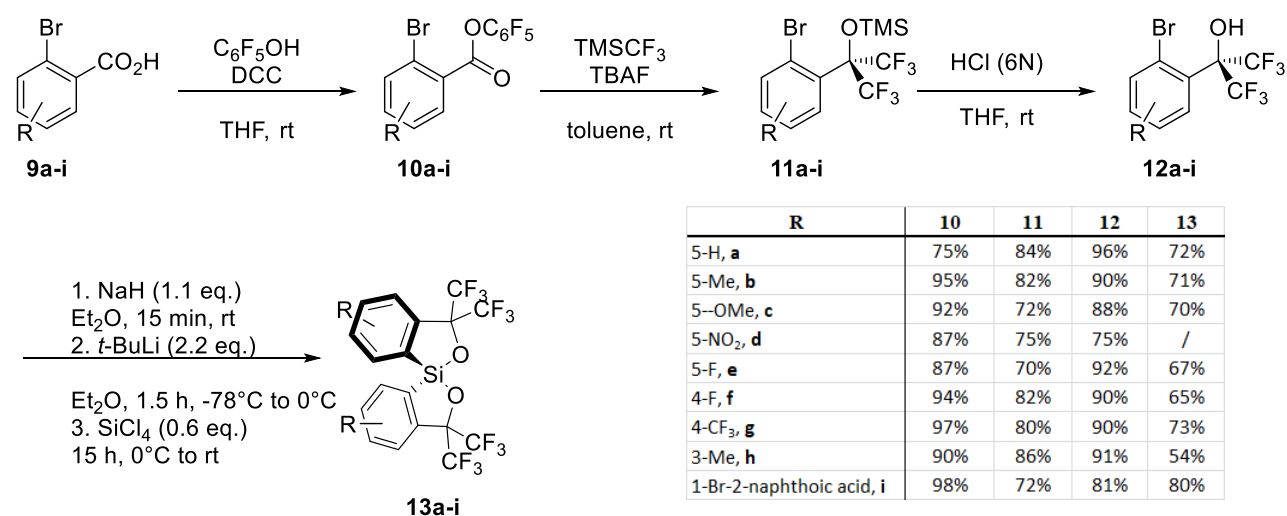
**Figure I.10** Fluorescence spectra ( $\lambda_{\text{ex}} = 266 \text{ nm}$ ) of **7** and **8a** in DCM

<sup>43</sup> a) Z. Xu, S. K. Kim, J. Yoon, *Chem. Soc. Rev.* **2010**, *39*, 1457–1466. b) A.-F. Li, J.-H. Wang, F. Wang, Y.-B. Jiang, *Chem. Soc. Rev.* **2010**, *39*, 3729–3745. c) E. J. Cho, J. W. Moon, S. W. Ko, J. Y. Lee, S. K. Kim, J. Yoon, K. C. Nam, *J. Am. Chem. Soc.* **2003**, *125*, 12376–12377.

<sup>44</sup> H. Lenormand, J.-P. Goddard, L. Fensterbank, *Org. Lett.* **2013**, *15*, 748–751

In this case, it is possible to discern the two different compounds. Indeed, fluoride coordination generates a redshift of the maximum of emission, from 290 nm to 311 nm, as well as a change in the shape of the curve, thus making it possible to monitor the uptake. It has been demonstrated that **7** can detect fluoride anion down to a threshold of 10  $\mu\text{M}$ , concentration close to that found in drinking water.

Our group has been also interested in the development of new synthetic strategies to obtain analogues of **7** with a modified aromatic system (Scheme I-13).<sup>45</sup>



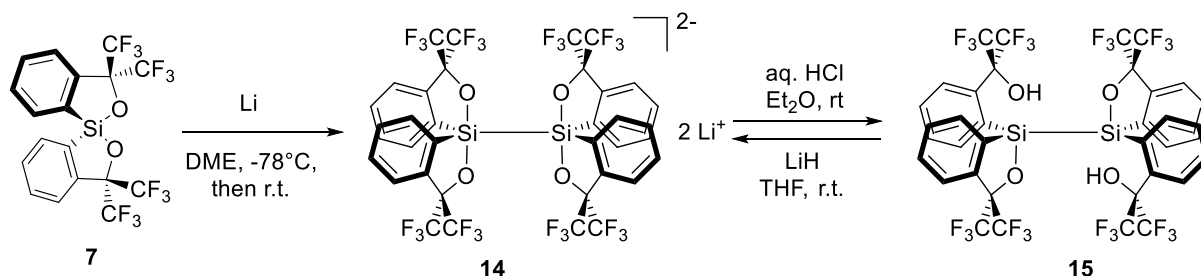
**Scheme I-13** Synthesis of the modified spirosilane **13a-i**

By means of this route, it has been possible to synthesise a variety of precursors with both electron-withdrawing and electron-donating substituents. The synthetic approach starts from derivatives of 1-bromo-2-benzoic acid, that are commercially available. The first step consists in the synthesis of an activated ester (**10a-i**) using pentafluorophenol in presence of DCC. The formation of this type of ester is necessary for the subsequent use of the Prakash reagent (TMSCF<sub>3</sub>) instead of hexafluoroacetone, as trifluoromethylating agent, in presence of TBAF. Two consecutive nucleophilic additions occurred on the benzylic carbon generating the corresponding silyl ether (**11a-i**). Subsequent treatment with hydrochloric acid leads to the corresponding alcohol (**12a-i**). The precursors have been synthesized from good to excellent yields. Finally, Martin's derivatives were obtained in good yield, except for the nitro-substituted, due to the incompatibility between the functional group and the organolithium. In

<sup>45</sup> H. Lenormand, V. Corcé, G. Sorin, C. Chhun, L.-M. Chamoreau, L. Krim, E.-L. Zins, J.-P. Goddard, L. Fensterbank, *J. Org. Chem.* **2015**, *80*, 3280–3288.

all these cases, dianionic intermediates are generated by deprotonation and halogen-metal exchange.

Some years before this work, Pr. Kano reported an interesting paper in which Martin's spirosilane was used as starting material for the synthesis of disilane.<sup>46</sup>



**Scheme I-14** Synthesis and reactivity of disilicate **14**

A reducing-coupling occurs when **7** is treated with a slight excess of Li(0) leading to the disilicate **14** as a dilithium salt. Treating **14** with tetrabutylammonium bromide allows the exchange of the countercation. From the tetrabutylammonium salt, an X-ray structure was obtained (Figure I.11).

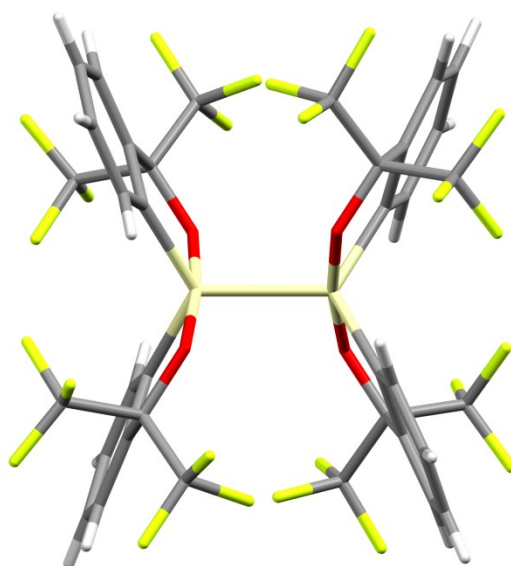
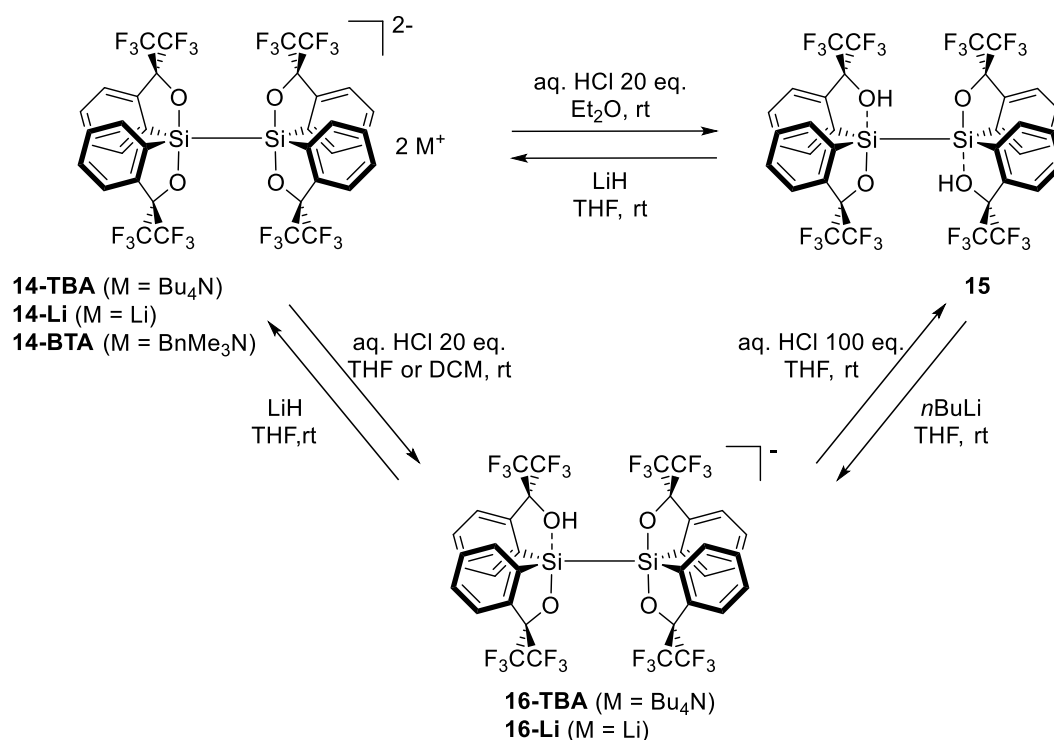


**Figure I.11** X-ray structure of **14**·TBA (CCDC: 692252), the countercation is omitted for clarity.

The structure shows how the silicon atoms are connected by a  $\sigma$  bond. Bond orbital analysis stated that the hybrid orbitals of both silicon atoms are almost in a  $sp^2$  ( $s^{0.93}p^{1.61}$ ) hybridisation state. therefore the Si-Si  $\sigma$  bond derived from the overlap of two  $sp^2$  hybrid

<sup>46</sup> N. Kano, H. Miyake, K. Sasaki, T. Kawashima, N. Mizorogi, S. Nagase, *Nat. Chem.* **2010**, *2*, 112–116.

orbitals, a phenomenon known in literature where there are disilenes displaying a Si-Si bond between two  $sp^2$  hybrid orbitals<sup>47</sup>, but characterised also for the presence of a double bond instead of only a single bond. He illustrated that in acid conditions the rupture of the two Si-O bond takes place to afford the corresponding alcohols. Kano also demonstrated that an interconversion between the disiliconate **14**, the silylsiliconate **16**, and the disilane **15** could operate (Scheme I-15), with the variation of the pH.<sup>48</sup>



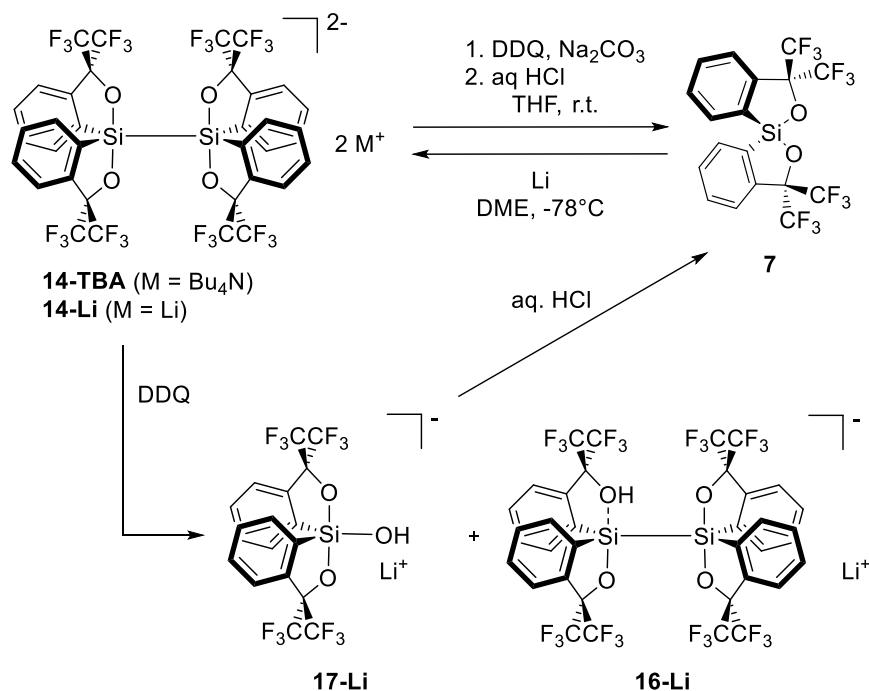
**Scheme I-15** Interconversion among the Disiliconates, silylsiliconates and Disilane

It is worthy to note that in these interconversion reactions, the Si-Si bond is not affected at all, highlighting the high strength of it.

<sup>47</sup> a) G. Raabe, J. Michael, *The Chemistry of Organic Compounds*, Patai, S & Rappoport Z., Wiley **1989**, Part. 2, Ch. 17, 1015-1142. b) R. Okazaki, R. West, *Chemistry of Stable Disilenes*, *Adv. Organomet. Chem.*, **1996**, 39, 231-273. c) M. Kira, T. Iwamoto, *Progress in the Chemistry of Stable Disilenes*, *Adv. Organomet. Chem.*, **2006**, 54, 73-148.

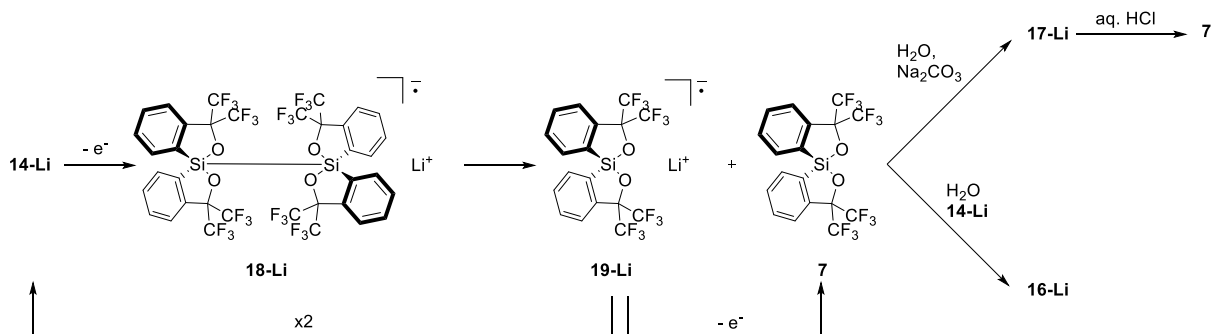
<sup>48</sup> N. Kano, K. Sasaki, H. Miyake, T. Kawashima, *Organometallics* **2014**, 33, 2358–2362.

A year later Kano found some oxidative conditions to break the solid Si-Si bond (Scheme I-16).<sup>49</sup>



**Scheme I-16** Oxidative bond cleavage of **14-M**

Treatment of **14-Li** with two equivalents of DDQ in presence of a base followed by the quenching with HCl give **7** quantitatively. It is interesting to note that without any base the hydroxysiliconate is obtained along with the silylsiliconate. For this reaction, Kano proposed the following mechanism (Scheme I-17).



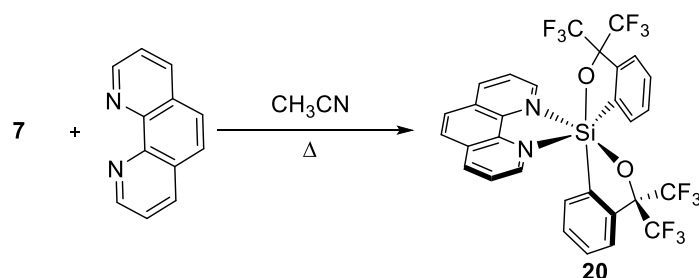
**Scheme I-17** Proposed mechanism for Si-Si cleavage

Oxidation of **14-Li** through electronic transfer leads to the corresponding anion radical **18-Li**. Indeed, abstraction of one electron from the  $\sigma$  Si-Si bond causes the rupture of the weakened bond. As a result, spirosilane **7** is obtained along with the corresponding anion

<sup>49</sup> N. Kano, H. Miyake, K. Sasaki, T. Kawashima, *Heteroat. Chem.* **2015**, *26*, 183–186.

radical. This latter can follow two different pathways: dimerization allowing for the regeneration of the disiliconate **18-Li** while oxidation generates **7**. Hydrolysis of **7** in presence of a base gave the hydroxysiliconate **17-Li**, that after treatment with HCl affords the final product. On the other hand, hydrolysis in presence of **14-Li** afforded **16-Li** as the only product.

Up to now, it has been demonstrated how Martin's spirosilane is prone to provide pentacoordinate complexes with a wide variety of nucleophiles. A single example of hexacoordinate species from Martin's spirosilane **7** has also been reported by Farnham *et al.*<sup>50</sup> in 1984 by complexation with 1,10-phenanthroline (Scheme I-18).



**Scheme I-18** Synthesis of the phenanthroline's adduct **20**

The complex formation was confirmed by X-Ray diffraction (Figure I.12).

Surprisingly, in the X-ray structure, it was noticed that the two oxygen atoms are not in *trans* position as expected. It can be a consequence of the chelating nature of the phenanthroline, forcing the other ligands in a more constrained conformation. Indeed, if the two oxygen were in *trans* positions, the two phenyl ring were obliged to be in a too constraint conformation.

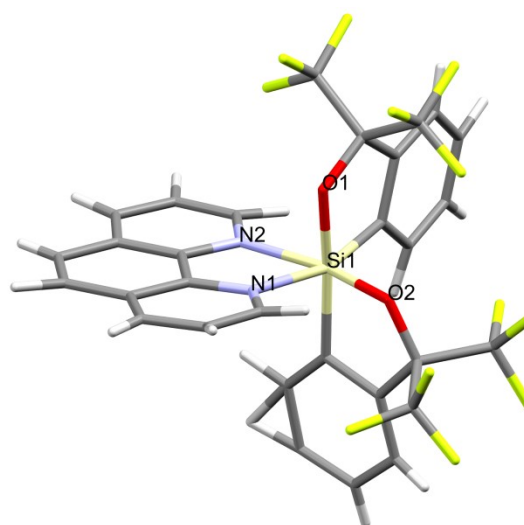


**Figure I.12** X-Ray structure of **20**

NMR studies were performed, in particular, the <sup>19</sup>F NMR gave some interesting clue (Figure I.13).

<sup>50</sup> W. B. Farnham, J. F. Whitney, *J. Am. Chem. Soc.* **1984**, *106*, 3992–3994.

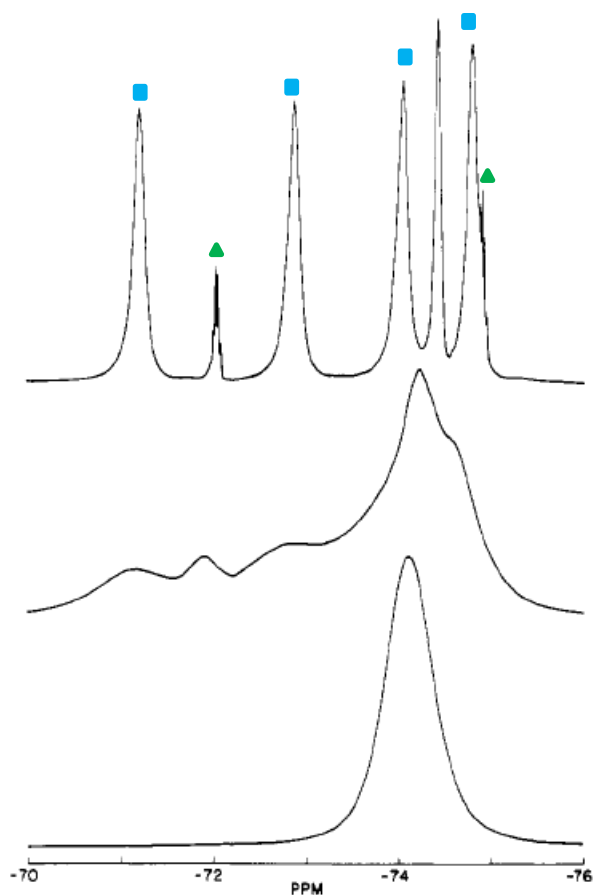
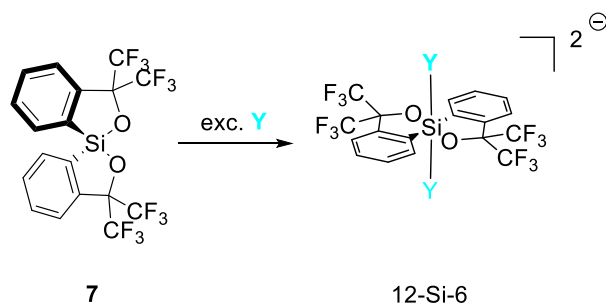


**Figure I.13**  $^{19}\text{F}$ NMR of **20** at different T (*dioxane- $d_8$* )

At room temperature, according to the  $^{19}\text{F}$  NMR, different isomers are present in solution. The major isomer (blue square), apparently the one corresponding to the X-Ray structure with a  $\text{C}_1$  symmetry, displays four diastereotopic  $\text{CF}_3$  group. A minor pair of quadruplet (green triangle), where  $\text{CF}_3$  groups are equivalents two by two, and a single peak of another minor isomer (orange star), in which all the  $\text{CF}_3$  groups are equivalent. The variable temperature NMR experiments showed a coalescence of the signals into one broad singlet, indicating ligands permutations. Farnham indicates a dissociation/recombination process of the phenanthroline that allows the passage from one to another isomer. Other experiments regarding hexacoordination were performed by Stevenson *et al.*<sup>51</sup> with monodentate nucleophiles. They treated **7** with a large excess of nucleophile: TBAF, pyridine,  $(\text{C}_6\text{F}_5)\text{Li}$ , in order to obtain the 12-Si-6 structures (Scheme I-19).

<sup>51</sup> W. H. Stevenson, J. C. Martin, *J. Am. Chem. Soc.* **1985**, *107*, 6352–6358.

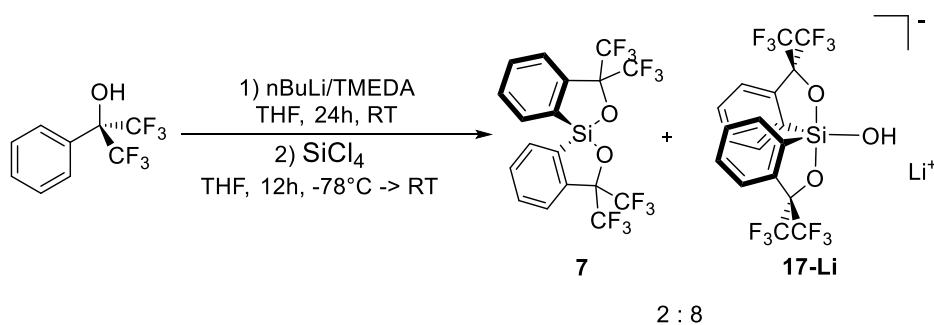


**Scheme I-19** General reaction between **7** with a large excess of nucleophile

Although a variety of nucleophile and conditions were tested, they were not able to isolate any hexacoordinate structure. Indeed, Stevenson and co-workers explained this behaviour due to structural features that favoured the 10-Si-5 structure instead the 8-Si-4 or the 12-Si-6.<sup>52</sup>

## I.4 Results and Discussion

In this thesis, the first attempted synthetic approach to spirosilane **7** was a slightly modified version of the original one developed by Martin (Scheme I-20). Starting from the hexafluorocumylalcohol, *n*-BuLi/TMEDA mixture was used to deprotonate the alcohol and also the hydrogen in *ortho*-position, to lead to the dilithiated compound as previously mentioned.

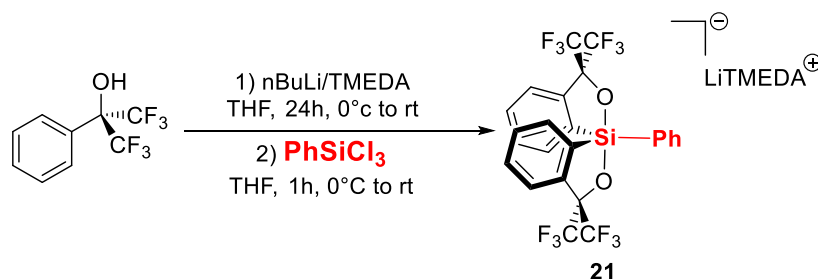


**Scheme I-20** First synthetic attempt

Following the reported procedure we were not able to obtain Martin's spirosilane **7** in good and reproducible yields.

<sup>52</sup> W. H. Stevenson, S. Wilson, J. C. Martin, W. B. Farnham, *J. Am. Chem. Soc.* **1985**, *107*, 6340–6352.

Due to problems of reproducibility and difficulties to obtain **7** with a good purity on a large scale, we decided to modify the synthetic approach. Inspired by the work of Stevenson and Martin,<sup>51</sup> PhSiCl<sub>3</sub> was used instead of SiCl<sub>4</sub> (Scheme I-21).



**Scheme I-21** Synthesis of Ph-Martin Spirosilane

Phenylsiliconate **21** was isolated in good and reproducible yields, even when the reaction was carried out on 25 g of starting hexafluorocumyl alcohol (102 mmol). The first step was quite similar to the previous one, with the formation of the dilithiated intermediate followed by the addition of PhSiCl<sub>3</sub>. Incidentally, TMEDA was still present as deduced from the <sup>1</sup>H NMR spectrum (Figure I.14), probably coordinated to the lithium cation.

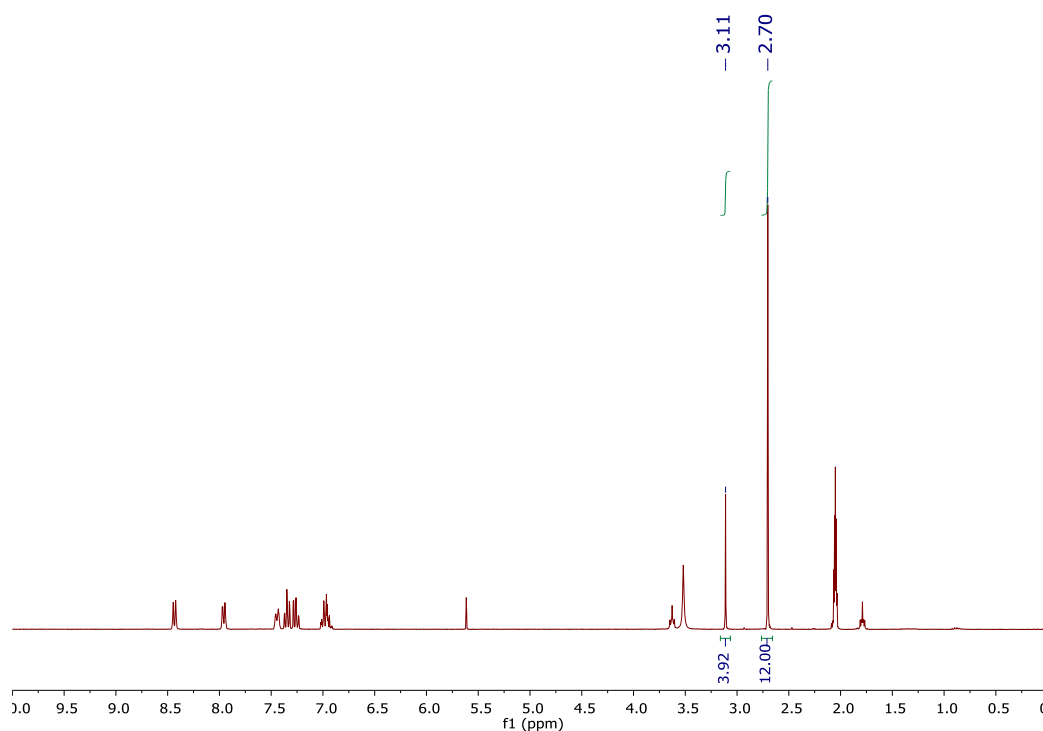
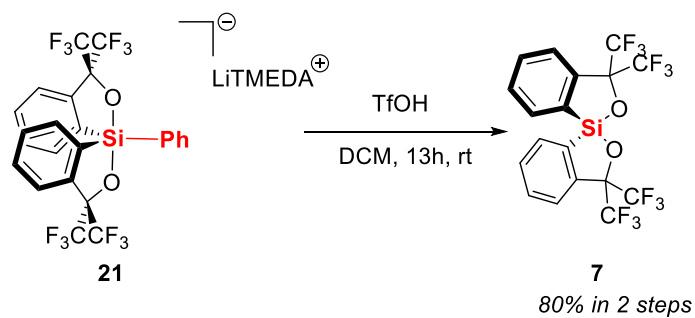


**Figure I.14** <sup>1</sup>H NMR spectra ((CD<sub>3</sub>)<sub>2</sub>CO) of **21**. \* THF.

The product previously obtained was then treated with triflic acid in DCM in order to accomplish a selective protodesilylation on the phenyl group.



**Scheme I-22** Final step of Martin's spirosilane synthesis

The desired tetracoordinate spirosilane was efficiently obtained in two steps with a very good efficiency and reproducibility. The  $^1\text{H}$  NMR spectrum of pure Martin's spirosilane is depicted in the figure below.

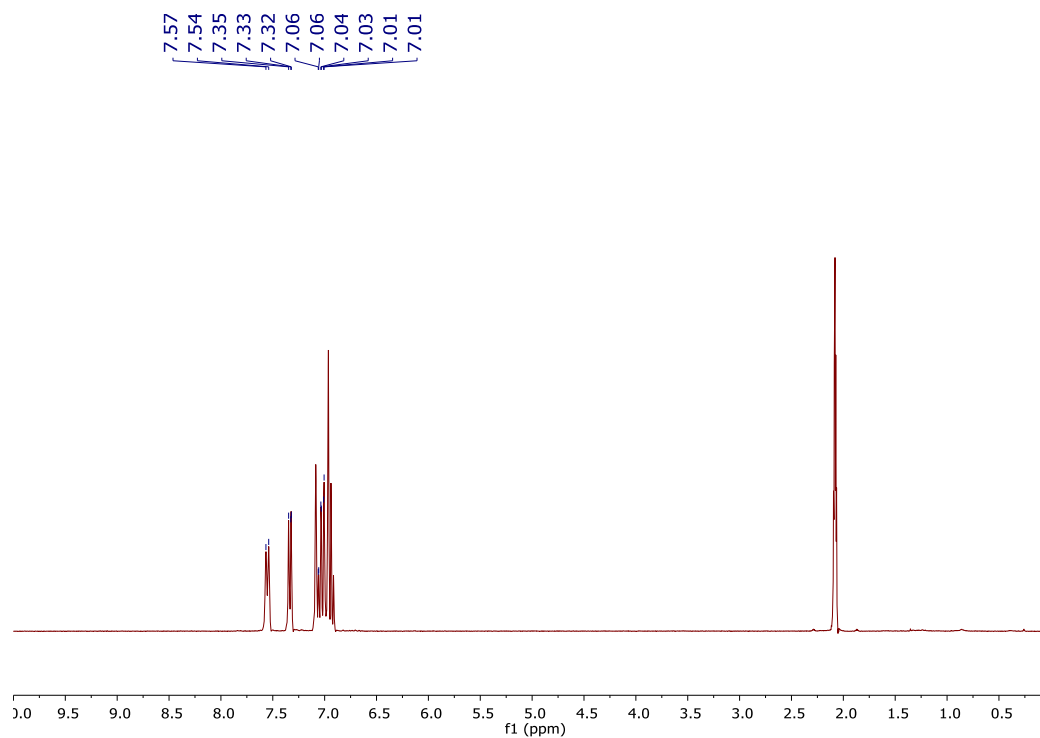


**Figure I.15**  $^1\text{H}$ NMR (toluene- $d_8$ ) of Martin's spirosilane

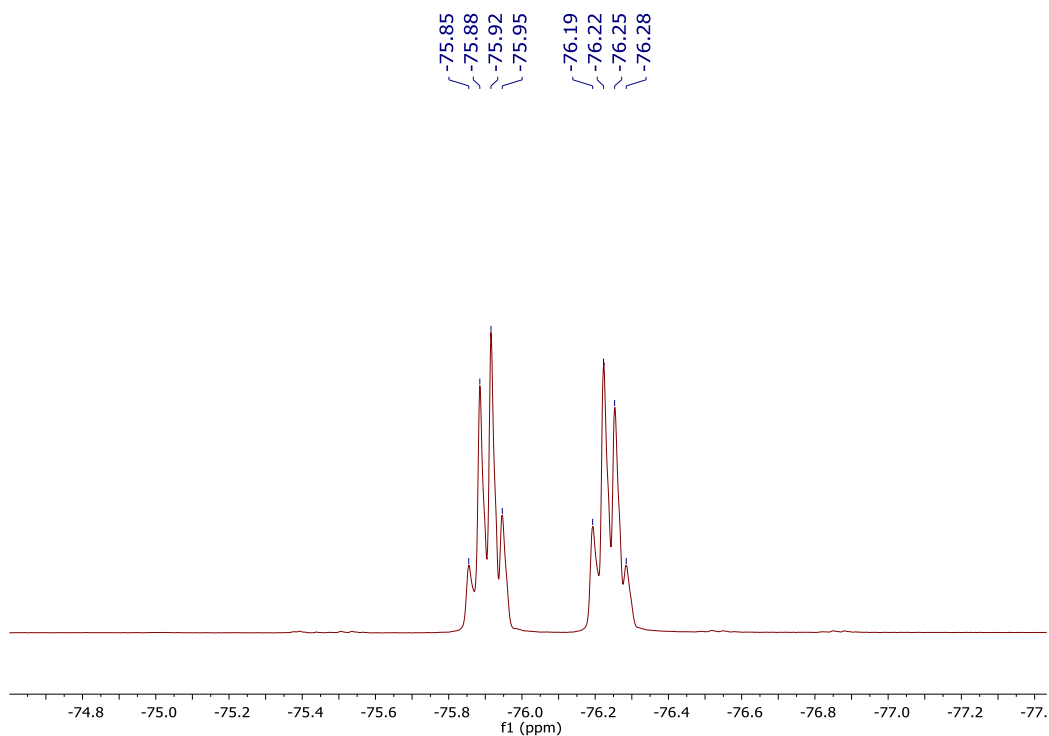


**Figure I.16**  $^{19}\text{F}$ NMR (toluene- $d_8$ ) of Martin's spiroilane

The  $^{19}\text{F}$  NMR spectrum (Figure I.16) clearly shows the equivalence of the  $\text{CF}_3$  groups two by two. Interestingly, performing the NMR experiment in a more coordinating solvent such as acetone results in the appearance a broad singlet due to a rapid ligand permutation at the NMR timescale through a pseudorotation mechanism (*vide infra*).

In conclusion, an excellent synthetic pathway for the reproducible synthesis of Martin's spiroilane on large scale was developed. In the following chapters, it will be discussed about the level of interaction of spiroilane **7** with different Lewis base, in particular with some NHC carbenes and the applications of these systems.



**Chapter II**  
**Interaction Between The Martin's**  
**Spirosilane and N-Heterocyclic Carbenes**



## II. Interaction Between Martin's Spirosilane and N-Heterocyclic Carbenes

Carbenes are defined as neutral compounds of divalent carbon. In these molecules, the carbon atom possesses six valence electrons and can adopt a linear or bent structure.



**Figure II.1** Linear and bent structure of carbene

They were firstly hypothesised in 1903 by Büchner during his studies on cyclopropanation of ethyl diazoacetate with toluene.<sup>53</sup> Some years later, in 1912, Staudinger was able to convert alkenes to cyclopropanes using diazomethane and methylene.<sup>54</sup> However it was only in 1954 that Doering demonstrated the synthetic utility of these molecules in organic chemistry,<sup>55</sup> while we had to wait until 1964 with Fischer demonstrating their utility in organometallic chemistry.<sup>56</sup> In the successive decades the chemistry of carbene had extraordinarily increased finding applications in a huge number of chemistry fields.<sup>57</sup> By now, there are several classes of carbene, each one with its peculiar properties and application.<sup>58</sup> In this thesis and especially in this chapter we will focus our attention on the N-Heterocyclic Carbenes.

<sup>53</sup> E. Buchner, L. Feldmann, *Berichte Dtsch. Chem. Ges.* **1903**, *36*, 3509–3517.

<sup>54</sup> H. Staudinger, O. Kupfer, *Berichte Dtsch. Chem. Ges.* **1912**, *45*, 501–509.

<sup>55</sup> W. von E. Doering, A. K. Hoffmann, *J. Am. Chem. Soc.* **1954**, *76*, 6162–6165.

<sup>56</sup> E. O. Fischer, A. Maasböl, *Angew. Chem. Int. Ed. Engl.* **1964**, *3*, 580–581.

<sup>57</sup> a) S. Würtemberger-Pietsch, U. Radius, T. B. Marder, *Dalton Trans.* **2016**, *45*, 5880–5895. b) W. Kirmse, *Carbene Chemistry*, Elsevier, **2013**. c) D. Martin, M. Melaimi, M. Soleilhavoup, G. Bertrand, *Organometallics* **2011**, *30*, 5304–5313. d) P. de Frémont, N. Marion, S. P. Nolan, *Coord. Chem. Rev.* **2009**, *253*, 862–892. e) S. Marrot, F. Bonnette, T. Kato, L. Saint-Jalmes, E. Fleury, A. Baceiredo, *J. Organomet. Chem.* **2008**, *693*, 1729–1732. f) A. J. Arduengo, R. Krafczyk, *Chem. Unserer Zeit* **1998**, *32*, 6–14.

<sup>58</sup> J.-M. Collinson, J. D. E. T. Wilton-Ely, S. Díez-González, *Catal. Commun.* **2016**, *87*, 78–81.

## II.1 N-Heterocyclic Carbenes

### II.1.1 Introduction

N-Heterocyclic Carbenes (NHCs) represent a special class of carbenes, characterised by the presence of a ring containing a divalent carbon and at least one nitrogen atom within the ring structure, some examples are: pyrrolylidene (Cyclic Alkyl Amino Carbenes, CAAC), imidazolylidene, benzimidazolylidene, triazolylidene etc... (Figure II.2)

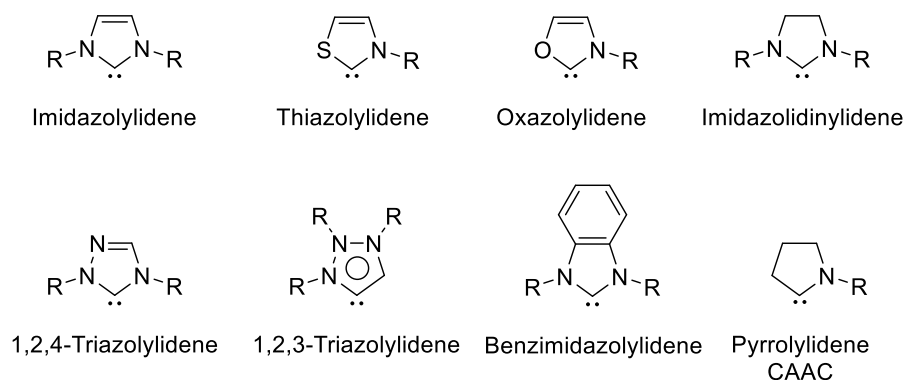
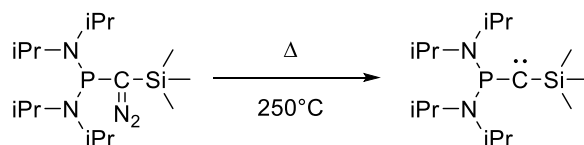


**Figure II.2** Some class of NHC carbene

Over the years, the library of heteroaromatic rings applied to the carbene chemistry has been well implemented whose properties can be modulated by changing the substituents on the ring and/or on the heteroatom. A peculiarity of NHC lies in their high stability whereas the majority of first synthesized carbenes were very short-living species.<sup>59</sup> In early sixties, Wanzlick demonstrated how the presence of an amino group near the carbenic carbons can dramatically increase its stability.<sup>60</sup> However, despite this finding, we had to wait until 1988 to observe the first isolable carbene thanks to the work of Bertrand and co-workers.<sup>61</sup> They reported the synthesis of an isolable carbene that was stable for weeks in benzene solution (Scheme II-1).



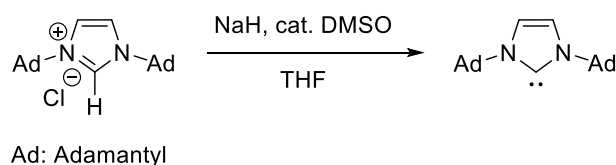
**Scheme II-1** Synthesis of the phosphinocarbene used by Bertrand and co-workers in their studies

<sup>59</sup> H. D. Roth, *Nature* **2001**, *412*, 598–601.

<sup>60</sup> a) H.-W. Wanzlick, H.-J. Kleiner, *Chem. Ber.* **1963**, *96*, 3024–3027. b) H.-W. Wanzlick, F. Esser, H.-J. Kleiner, *Chem. Ber.* **1963**, *96*, 1208–1212. c) H.-W. Wanzlick, *Angew. Chem.* **1962**, *74*, 129–134. d) H.-W. Wanzlick, H.-J. Kleiner, *Angew. Chem.* **1961**, *73*, 493–493.

<sup>61</sup> A. Igau, H. Grutzmacher, A. Baceiredo, G. Bertrand, *J. Am. Chem. Soc.* **1988**, *110*, 6463–6466.

A few years later, in 1991, Arduengo and co-workers published an article<sup>62</sup> dealing with the synthesis (Scheme II-2), isolation and X-Ray characterisation (Figure II.3) of a very stable and bottleable imidazolylidene.



**Scheme II-2** Synthesis of 1, 3-di(1-adamantyl)imidazole-2-ylidene

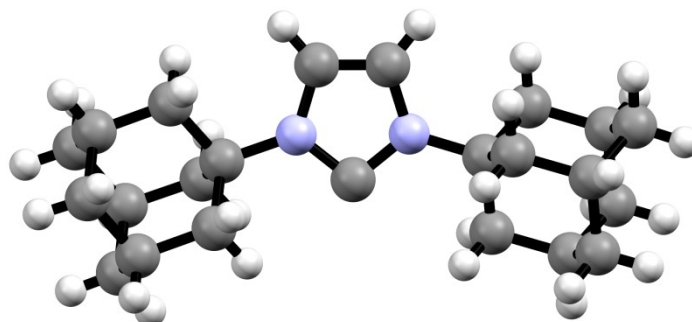


**Figure II.3** X-Ray structure of 1, 3-di(1-adamantyl)imidazole-2-ylidene (CCDC number: 1283930)

This first NHC was synthesised from the imidazolium salt by a deprotonation reaction using one equivalent of sodium hydride and a catalytic amount of DMSO. With this tremendous breakthrough, Arduengo gave the input for the development of the carbene chemistry, that allowed the discovery an incredible amount of new applications.<sup>63</sup>

### II.1.2 Electronic properties of NHC

As implied by the definition of carbene, due to the presence of a six valence electrons carbon, they can adopt a linear or bent geometry. The linear one is characterised by a *sp*-hybridized carbenic carbon atom in which two energetically degenerated *p* orbitals are present (Figure II-4).

<sup>62</sup> A. J. Arduengo, R. L. Harlow, M. Kline, *J. Am. Chem. Soc.* **1991**, *113*, 361–363.

<sup>63</sup> N-Heterocyclic Carbenes: From Laboratory Curiosities to Efficient Synthetic Tools, *RSC Catalysis Series No. 6*, Edited by Silvia Díez-González, Royal Society of Chemistry **2011**

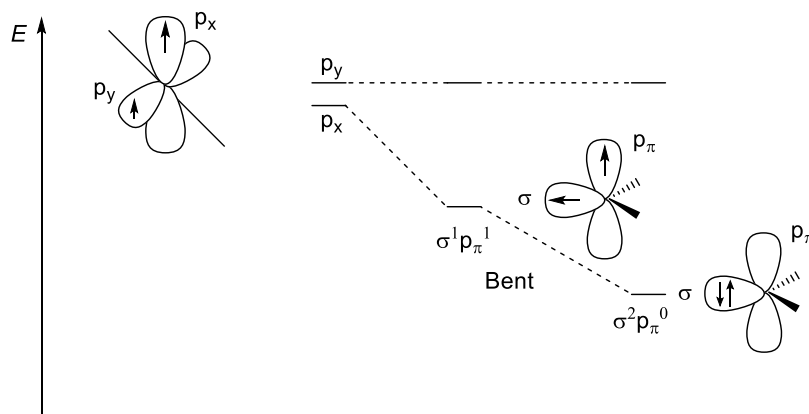


**Figure II.4** Frontier orbitals and electron configurations for carbene carbon atoms

However, it is easier to find the  $sp^2$ -hybridised state, where the two non-bonding electrons occupy the two empty orbitals with a parallel spin orientation, leading to a triplet ground state,  $\sigma^1 p_\pi^1$ . However, both electrons can occupy the  $\sigma$  orbital, with antiparallel spin orientation, which represents the singlet ground state  $\sigma^2 p_\pi^0$ . One of the factors that favours one state to the other is the energy gap between the  $\sigma$  and  $p_\pi$  orbitals: the higher is this gap, the more favoured is the singlet state. Quantum calculations have stated that an energy gap of 2 eV is required to stabilize this latter state.<sup>64</sup> In this chapter, we will focus only on the carbenes in their singlet state.<sup>65</sup>

With the presence of an empty  $p$  orbital on the carbenic carbon, the lone pair present on the nitrogen atom can be involved in a  $\pi$ -donation, generating an ylidic limit form that stabilises the singlet state (Figure II.5).

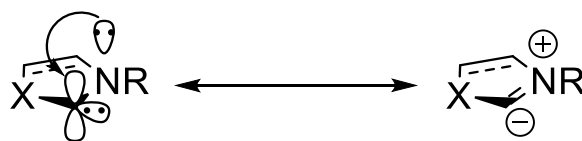


**Figure II.5** Representation of the limit forms of the carbene in NHCs

DFT calculation,<sup>66</sup>  $^{13}\text{C}$  NMR,<sup>67</sup> XPS (X-Ray photoelectron spectroscopy)<sup>68</sup> and neutron diffraction,<sup>69</sup> carried out by Arduengo and co-workers, tend to indicate that the first

<sup>64</sup> R. Hoffmann, G. D. Zeiss, G. W. Van Dine, *J. Am. Chem. Soc.* **1968**, *90*, 1485–1499.

<sup>65</sup> D. Bourissou, O. Guerret, F. P. Gabbaï, G. Bertrand, *Chem. Rev.* **2000**, *100*, 39–92.

<sup>66</sup> D. A. Dixon, A. J. Arduengo, *J. Phys. Chem.* **1991**, *95*, 4180–4182.

<sup>67</sup> A. J. Arduengo, D. A. Dixon, K. K. Kumashiro, C. Lee, W. P. Power, K. W. Zilm, *J. Am. Chem. Soc.* **1994**, *116*, 6361–6367.

<sup>68</sup> A. J. Arduengo, H. Bock, H. Chen, M. Denk, D. A. Dixon, J. C. Green, W. A. Herrmann, N. L. Jones, M. Wagner, R. West, *J. Am. Chem. Soc.* **1994**, *116*, 6641–6649.

mesomeric form is favoured rather the ylidic one, especially in the case of the imidazolylidene, where the HOMO correspond to the lone pair centred on the carbene carbon.

However a couple of years later, Frenking claimed that the methodology used by Arduengo for mapping the electronic density was not enough relevant.<sup>70</sup> He then proposed, at the same time of Apeloig and Schwarz,<sup>71</sup> a different method based on isodesmic calculation,<sup>72</sup> reaching the conclusion that imidazolylidene is partially aromatic. This result was also used to explicate the higher stability of imidazolylidene compare to that of imidazolidinylidenes with a saturated backbone.

The concept applied to the nitrogen-based system can be extended making them more general: if the inductive effect is considered,  $\sigma$ -electron-withdrawing groups increase the gap present between the  $\sigma$  and  $p_\pi$  orbitals, favouring the singlet state. If instead, we consider the mesomeric effect,  $\pi$ -electron-donating substituent are able to stabilise the carbene *via* interaction with the lone pair present on the heteroatom, favouring the bent structure.

Nevertheless, it is necessary to consider also the steric effect of the substituents. Independently from the type of carbene, bulky substituents are prone to kinetically stabilise the system. In addition, if the resulting electronic effect becomes negligible, it is up to the steric effect to determine the multiplicity of the ground state. For instance, if we compare the dimethylcarbene<sup>73</sup> with the di(*t*-butyl)carbene<sup>74</sup> and the diadamantylcarbene,<sup>75</sup> only the first one is able to reach the singlet state, while the other can only access the triplet state. This behaviour is a consequence of the broadening of the C-C-C angle, caused by the presence of bulky substituents that destabilises the singlet state (Figure II.6).

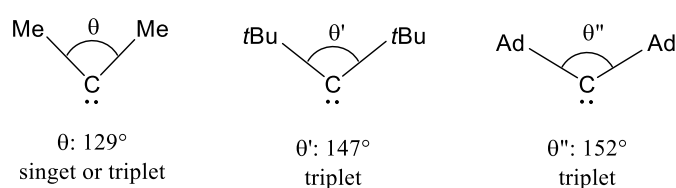


**Figure II.6** Consequence of steric effect on multiplicity state

<sup>69</sup> A. J. Arduengo, H. V. R. Dias, D. A. Dixon, R. L. Harlow, W. T. Klooster, T. F. Koetzle, *J. Am. Chem. Soc.* **1994**, *116*, 6812–6822.

<sup>70</sup> C. Boehme, G. Frenking, *J. Am. Chem. Soc.* **1996**, *118*, 2039–2046.

<sup>71</sup> C. Heinemann, T. Müller, Y. Apeloig, H. Schwarz, *J. Am. Chem. Soc.* **1996**, *118*, 2023–2038.

<sup>72</sup> W. J. Hehre, R. Ditchfield, L. Radom, J. A. Pople, *J. Am. Chem. Soc.* **1970**, *92*, 4796–4801.

<sup>73</sup> a) C. A. Richards, S.-J. Kim, Y. Yamaguchi, H. F. Schaefer, *J. Am. Chem. Soc.* **1995**, *117*, 10104–10107. b) D. A. Modarelli, S. Morgan, M. S. Platz, *J. Am. Chem. Soc.* **1992**, *114*, 7034–7041.

<sup>74</sup> J. E. Gano, R. H. Wettach, M. S. Platz, V. P. Senthilnathan, *J. Am. Chem. Soc.* **1982**, *104*, 2326–2327.

<sup>75</sup> D. R. Myers, V. P. Senthilnathan, M. S. Platz, M. Jones, *J. Am. Chem. Soc.* **1986**, *108*, 4232–4233.

Electronic properties of NHC can also be quantified experimentally and, over the years, different methods have been used and proposed.

One of the methods is based on the  $pK_a$  evaluation. Alder,<sup>76</sup> Streitwieser,<sup>77</sup> Cheng,<sup>78</sup> Toth<sup>79</sup> and O'Donoghue<sup>80</sup> in the last twenty years have fully investigated it, analysing a large number of NHC carbene precursors, by monitoring the deprotonation reaction in DMSO or H<sub>2</sub>O with different spectroscopic methods. From the data, it was observed that imidazolium possesses  $pK_a$  values around 25 while protonated NHCs with sulfur or oxygen instead of a nitrogen result to be more acidic. Imidazolium salts prove to be slightly more acidic than their unsaturated counterpart. An expanded ring with more than five atoms has its acidity dropped down with a  $pK_a$  value rising around 29. Triazoliums on the other side display an increased acidity with a  $pK_a$  around 17.0 (Figure II.7).

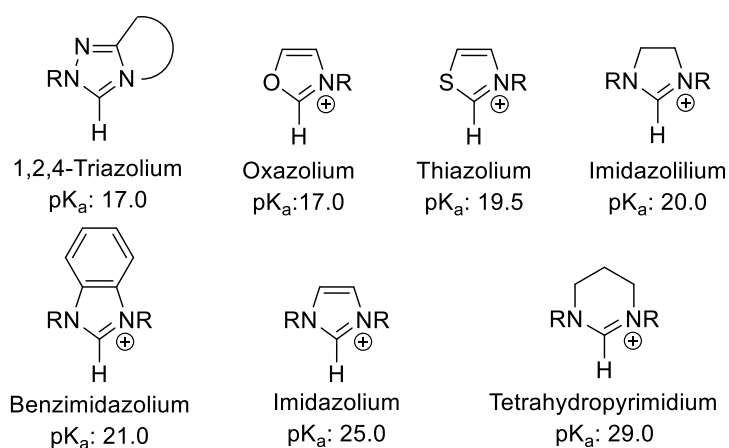


**Figure II.7** NHC classes used in  $pK_a(\text{H}_2\text{O})$  evaluation put in a decreasing acidity scale

These examples clearly point out the impact of the substituents on the Lewis basicity of the carbene, indeed modulation of it can emphasize the basicity and the application related to it. The nucleophilicity ( $N$ ) as a function of the  $N$ -substituent of the carbene is another interesting parameter to evaluate. In 2016, Lupton and Mayr were the first to assess the nucleophilicity in this term<sup>81</sup> and performed nucleophilic addition of various NHCs on a

<sup>76</sup> R. W. Alder, P. R. Allen, S. J. Williams, *J. Chem. Soc. Chem. Commun.* **1995**, 0, 1267–1268.

<sup>77</sup> Y.-J. Kim, A. Streitwieser, *J. Am. Chem. Soc.* **2002**, *124*, 5757–5761.

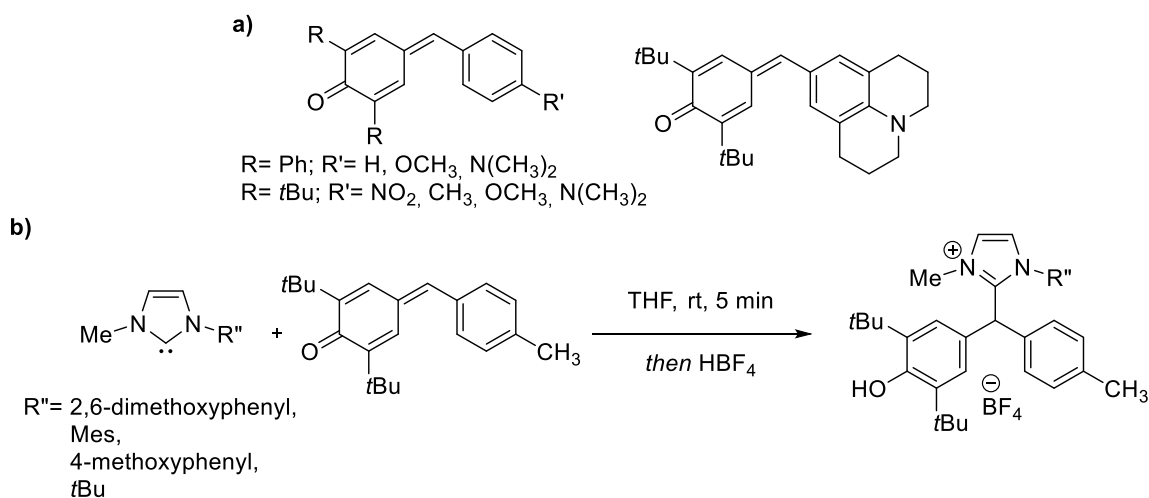
<sup>78</sup> Y. Chu, H. Deng, J.-P. Cheng, *J. Org. Chem.* **2007**, *72*, 7790–7793.

<sup>79</sup> T. L. Amyes, S. T. Diver, J. P. Richard, F. M. Rivas, K. Toth, *J. Am. Chem. Soc.* **2004**, *126*, 4366–4374.

<sup>80</sup> a) R. S. Massey, C. J. Collett, A. G. Lindsay, A. D. Smith, A. C. O'Donoghue, *J. Am. Chem. Soc.* **2012**, *134*, 20421–20432. b) E. M. Higgins, J. A. Sherwood, A. G. Lindsay, J. Armstrong, R. S. Massey, R. W. Alder, A. C. O'Donoghue, *Chem. Commun.* **2011**, *47*, 1559–1561.

<sup>81</sup> A. Levens, F. An, M. Breugst, H. Mayr, D. W. Lupton, *Org. Lett.* **2016**, *18*, 3566–3569.

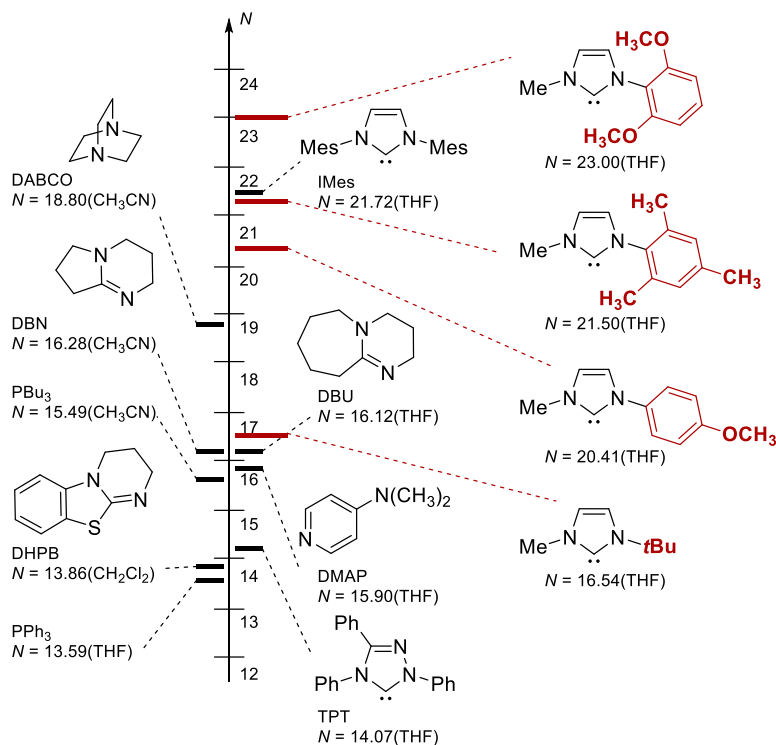
Michael acceptor such as *p*-quinone methides, for the evaluation of the *N* value (Scheme II-3).<sup>82</sup>



**Scheme II-3** a) Electrophiles used by Lupton in his studies; b) Reaction used to calculate the nucleophilicity

To date, this method has been widely used to examine more than a thousand of nucleophilic and electrophilic compounds.<sup>83</sup> Using this reaction, Lupton could determine the nucleophilicity and *N* values shown in the following figure (red compounds).

**Figure II.8** Nucleophilicity parameters measured by Lupton

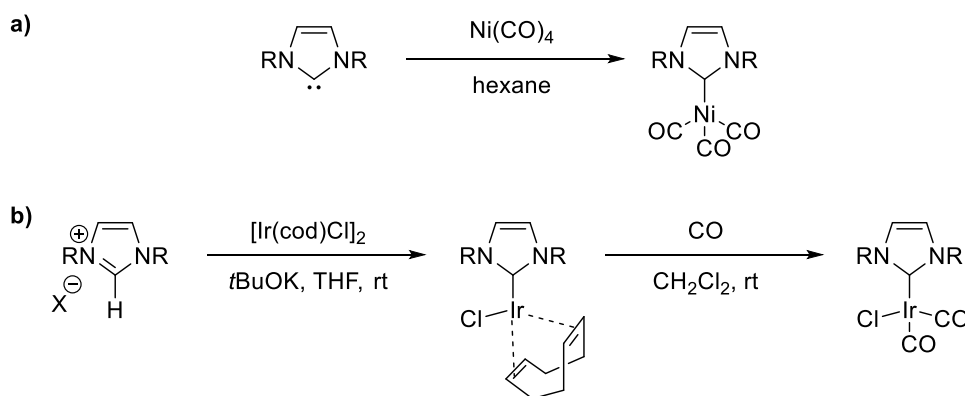


As expected the phosphine resulted to be less nucleophilic than the carbenes. It is also interesting to denote that in this scale, the *t*Bu derivative proved to be less nucleophilic than the dimethoxyphenyl derivative or even the mesityl derivative.

<sup>82</sup> H. Mayr, A. R. Ofial, *J. Phys. Org. Chem.* **2008**, *21*, 584–595. b) H. Mayr, T. Bug, M. F. Gotta, N. Hering, B. Irrgang, B. Janker, B. Kempf, R. Loos, A. R. Ofial, G. Remennikov, et al., *J. Am. Chem. Soc.* **2001**, *123*, 9500–9512.

<sup>83</sup> Access to all constants is provided at: Mayr, H. Database of Nucleophilicities and Electrophilicities. <http://www.cup.uni-muenchen.de/oc/mayr/DBintro.html>

Another method for the evaluation of the electronic properties of NHC is based on the Tolman Electronic Parameter (TEP),<sup>84</sup> using InfraRed spectroscopy. The variation of the CO stretching of a Ni(CO)<sub>4</sub> derivatives is measured and by comparison with the value of the pure nickel tetracarbonyl it gives an indication of the  $\sigma$  donor properties of the ligand. Initially Ni(CO)<sub>4</sub> was used to form the metal complexes<sup>85</sup> but due to its high toxicity, other transition metal complexes have been preferred, in particular iridium derivatives<sup>86</sup> (Scheme II-5).



**Scheme II-4** Synthetic pathway used by Dorta (a) and Plenio (b)

The more electron donating the ligand, the more electron-rich the metal and therefore due to the  $\pi$ -backbonding donation in the  $\pi^*_{\text{CO}}$  anti-bonding orbital, a weakening of the C=O bond is observed. The TEP values (cm<sup>-1</sup>) for imidazolylidene are: ItBu: 2048.9, IMes: 2049.3, IPr: 2050.2 and IDM: 2051.2. This value shows how starting from ItBu to IDM we have a decreasing of the  $\pi$ -backbonding donation meaning that ItBu is the most donor.<sup>87</sup>

In conclusion, the possibility to use different heteroatoms and also the tuning of the different substituents give access to a wide range of NHCs, each one with its particular properties that opens the path to a wide amount of applications.

<sup>84</sup> C. A. Tolman, *Chem. Rev.* **1977**, 77, 313–348.

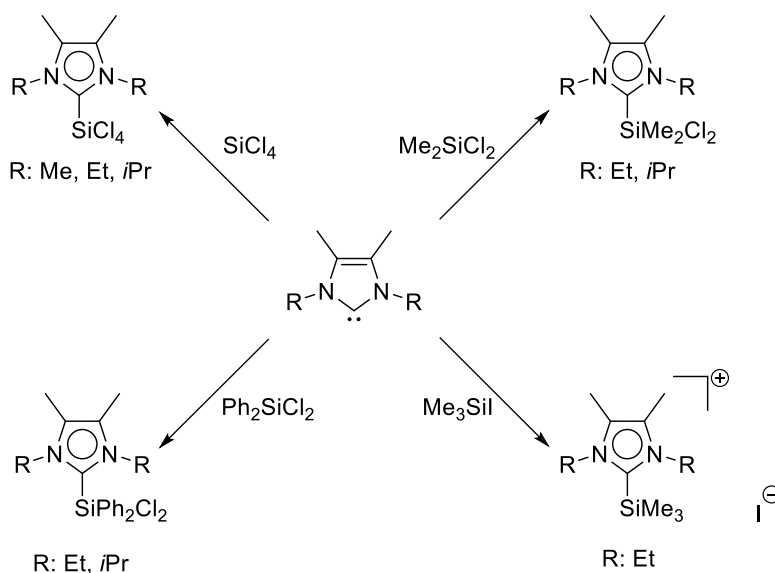
<sup>85</sup> R. Dorta, E. D. Stevens, N. M. Scott, C. Costabile, L. Cavallo, C. D. Hoff, S. P. Nolan, *J. Am. Chem. Soc.* **2005**, 127, 2485–2495.

<sup>86</sup> S. Leuthäuser, D. Schwarz, H. Plenio, *Chem. – Eur. J.* **2007**, 13, 7195–7203.

<sup>87</sup> D. J. Nelson, S. P. Nolan, *Chem. Soc. Rev.* **2013**, 42, 6723–6753.

## II.2 NHC-Silicon Interactions

The first study on the interaction between a NHC and silane derivatives was reported by Kuhn in 1995, few years later after the work of Arduengo. In this study, Kuhn<sup>88</sup> was able to isolate the first neutral NHC-SiCl<sub>x</sub>R<sub>y</sub> adducts using different source of starting halosilane (Scheme II-5).



**Scheme II-5** First examples of NHC-Silanes realised by Kuhn

Addition of the dimethylcarbene to chlorosilanes mostly led to neutral pentacoordinate silicon(IV) adducts displaying a TBP geometry with an average Si-C(imidazole) distance of 1.91 Å. In contrast, when trimethyliodosilane was used, a tetracoordinate cationic adduct was obtained. This was due to the lower energy of the Si-I bond as compared to that of Si-Cl, and also the larger size of the iodine atom which resulted in the elimination of the iodide to form the cationic species. Fourteen years later, some penta- and hexacoordinate NHC complexes derived from SiF<sub>4</sub> and SiBr<sub>4</sub> were also obtained by the group of Roesky.<sup>89</sup>

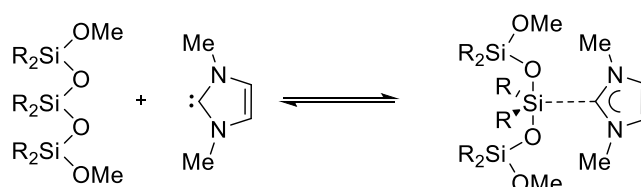
Surprisingly, after this first example of Silicon-NHC interaction, no other studies have been reported for more than a decade. In 2007, the group of Bacciredo<sup>90</sup> used polysiloxanes, for the protection of some NHC carbenes. The idea was to use a weak Lewis acid in order to

<sup>88</sup> N. Kuhn, T. Kratz, D. Bläser, R. Boese, *Chem. Ber.* **1995**, *128*, 245–250

<sup>89</sup> R. S. Ghadwal, S. S. Sen, H.W. Roesky, G. Tavcar, S. Merkel, D. Stalke, *Organometallics* **2009**, *28*, 6374–6377.

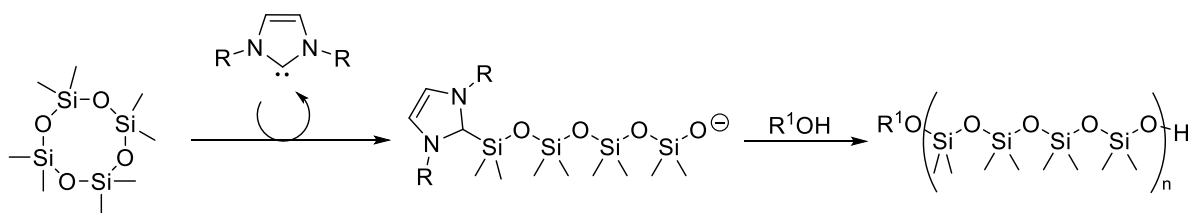
<sup>90</sup> F. Bonnette, T. Kato, M. Destarac, G. Mignani, F. P. Cossío, A. Bacciredo, *Angew. Chem. Int. Ed.* **2007**, *46*, 8632–8635.

mask the reactivity of the carbenic function towards air and moisture. For this purpose, they took advantage of the hydrophobicity and chemical resistance of polysiloxanes to protect the carbene through its complexation to the silicon atoms. They suggested pentacoordinate silicon species as intermediates which was supported by DFT calculations (Scheme II-6). Interestingly, when the polysiloxane-carbene mixture was placed in an organic solution, the reactivity of the carbenes was perfectly recovered.



**Scheme II-6** Polysiloxane for the protection of carbene

The same year, the Baceiredo group<sup>91</sup> described also the ring opening polymerisation of cyclotetrasiloxane catalysed by a NHC carbene.

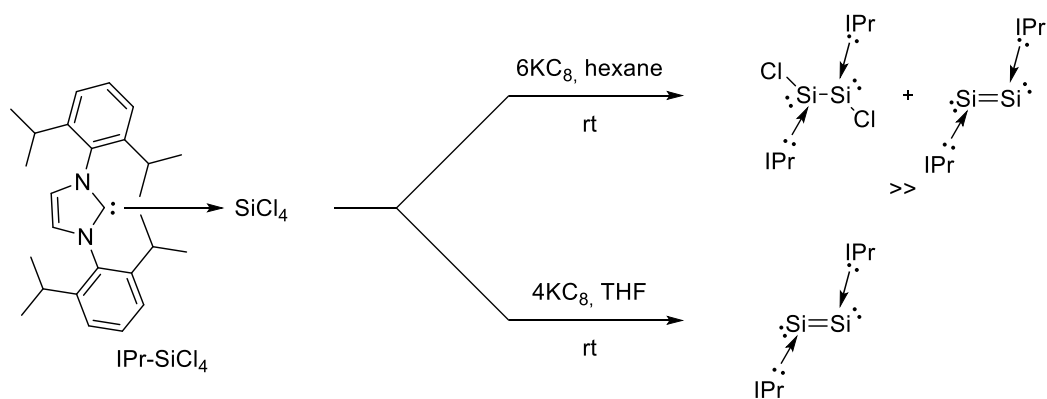


**Scheme II-7** Polymerisation of polysiloxane

In 2008, Robinson used NHCs to stabilize low-valent silicon compounds in which the silicon atom is present in formal oxidation states +I and 0 by treatment of  $\text{IPr-SiCl}_4$  with  $\text{KC}_8$  reducing agent (Scheme II-8).<sup>92</sup>

<sup>91</sup> M. Rodriguez, S. Marrot, T. Kato, S. Stérin, E. Fleury, A. Baceiredo, *J. Organomet. Chem.* **2007**, 692, 705–708.

<sup>92</sup> Y. Wang, Y. Xie, P. Wei, R. B. King, H. F. Schaefer, P. von R. Schleyer, G. H. Robinson, *Science* **2008**, 321, 1069–1071.



**Scheme II-8** Synthetic strategy adopted by Robinson to stabilize low-valent oxidation states of silicon

In the first case, using a large excess of  $\text{KC}_8$  led to the formation of a major product with the silicon atom at the +I oxidation state, while a minor product was a Si(0) derivative. By varying the conditions, specifically the amount of the reducing agent, this minor Si(0) compound could be obtained selectively. They were able to isolate and characterise the two different species, thanks to the enhanced stability reached through the carbene complexation. In fact, NHC acted as a lone pair donor able to stabilise thermodynamically and kinetically the compounds. Similar stabilizations were reported by the same group involving Cy-CAAC<sup>93</sup> and the group of Driess reported as well the synthesis of stabilised Si(0) species with dicarbene ligands.<sup>94</sup>

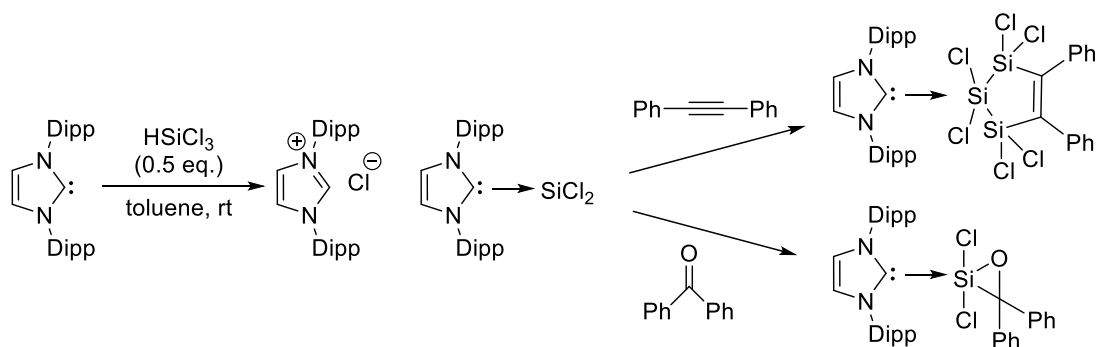
In 2009 Roesky and co-workers reported that in presence of trichlorosilane, IPr afforded the corresponding NHC-dichlorosilylene adducts.<sup>95</sup> This Si(II)-stabilized compound could react in mild conditions with diphenylacetylene and benzophenone, giving the corresponding pentacoordinate complexes (Scheme II-9).<sup>96</sup>

<sup>93</sup> K. C. Mondal, P. P. Samuel, H. W. Roesky, R. R. Aysin, L. A. Leites, S. Neudeck, J. Lübben, B. Dittrich, N. Holzmann, M. Hermann, et al., *J. Am. Chem. Soc.* **2014**, *136*, 8919–8922.

<sup>94</sup> Y. Xiong, S. Yao, S. Inoue, J. D. Epping, M. Driess, *Angew. Chem. Int. Ed.* **2013**, *52*, 7147–7150.

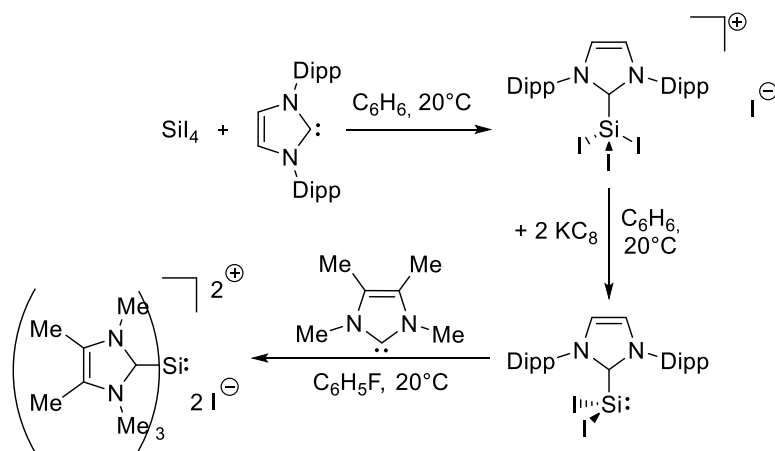
<sup>95</sup> R. S. Ghadwal, H. W. Roesky, S. Merkel, J. Henn, D. Stalke, *Angew. Chem. Int. Ed.* **2009**, *48*, 5683–5686.

<sup>96</sup> R. S. Ghadwal, S. S. Sen, H. W. Roesky, M. Granitzka, D. Kratzert, S. Merkel, D. Stalke, *Angew. Chem., Int. Ed.* **2010**, *49*, 3952–3955.



**Scheme II-9** Dichlorosilene stabilised by IPr and its reactivity

Other examples of syntheses with NHC-stabilized dibromo<sup>97</sup> and diiodosilylene<sup>98</sup> were reported by Filippou and co-workers. In both cases they started from the corresponding tetrahalosilane that formed the expected cationic adduct in presence of IPr. Subsequent reduction using potassium graphite allows them to obtain the desired Si(II) complex. Intriguingly, addition of 1,3,4,5-tetramethyl-imidazol-2-ylidene (IMe<sub>4</sub>) to the NHC-stabilised diiodosilylene led to the dicationic Si(II) complex [Si(IMe<sub>4</sub>)<sub>3</sub>]<sup>2+</sup> after replacement of both iodides and the IPr ligand (Scheme II-10)



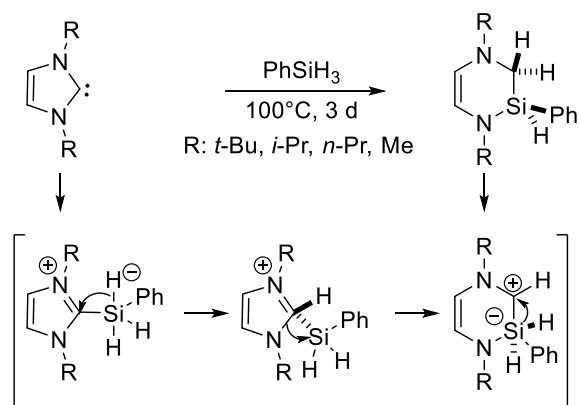
**Scheme II-10** Synthesis of the Filippou's complex

In 2012, Radius described examples of ring expansion of NHCs by insertion reaction of hydrosilanes into the C-N bond (Scheme II-11).<sup>99</sup> It is worth to note that several pentacoordinate silicon intermediate are involved in the proposed mechanism.

<sup>97</sup> A. C. Filippou, O. Chernov, G. Schnakenburg, *Angew. Chem. Int. Ed.* **2009**, *48*, 5687–5690

<sup>98</sup> A. C. Filippou, Y. N. Lebedev, O. Chernov, M. Straßmann, G. Schnakenburg, *Angew. Chem. Int. Ed.* **2013**, *52*, 6974–6978.

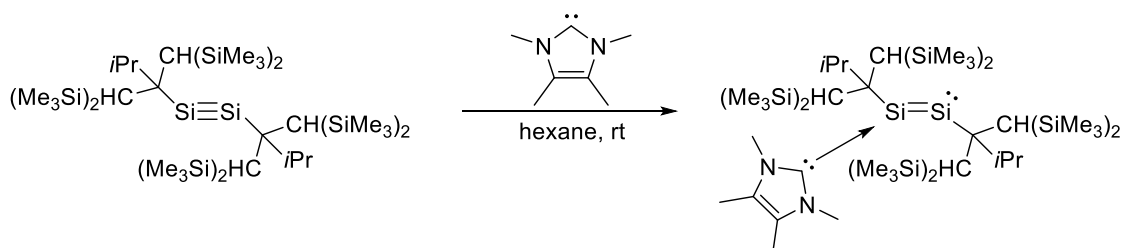
<sup>99</sup> D. Schmidt, J. H. J. Berthel, S. Pietsch, U. Radius, *Angew. Chem. Int. Ed.* **2012**, *51*, 8881–8885.



**Scheme II-11** Example of ring opening reaction described by Radius

From a mechanistic point of view, it was suggested that a first formal insertion of the carbene into the Si-H proceeds followed by the nitrogen shift to the silicon atom yielding a pentacoordinate intermediate (Scheme II-11). Finally, a hydride transfer takes place to give the final product. This mechanism was validated by Hemberger some years later by means of DFT calculations.<sup>100</sup>

Reaction of a Si≡Si moiety, firstly synthesized in 2004 by Sekiguchi,<sup>101</sup> was a pioneering result obtained by Sekiguchi and Driess (Scheme II-12).<sup>102</sup>



**Scheme II-12** Disilyne stabilised by NHC

This reaction give some interesting output: first, the coordination of the carbene induced the passage from a triple to a double bond since from the X-Ray structure an elongation of the Si-Si bond from 2.06 Å to 2.19 Å is noticeable and comparable to the 2.20 Å of disilenide  $\text{RHSi}=\text{SiR}^*\text{Li}(\text{dme})_3^+$ .<sup>103</sup> Second, aside the equivalent of carbene used in the reaction, no product of bi-coordination was formed.

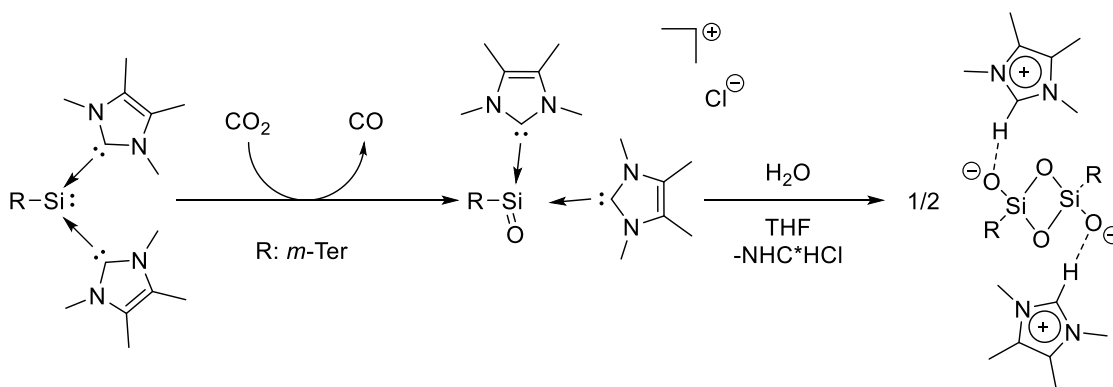
<sup>100</sup> P. Hemberger, A. Bodi, J. H. J. Berthel, U. Radius, *Chem. – Eur. J.* **2015**, *21*, 1434–1438.

<sup>101</sup> A. Sekiguchi, R. Kinjo, M. Ichinohe, *Science* **2004**, *305*, 1755–1757.

<sup>102</sup> T. Yamaguchi, A. Sekiguchi, M. Driess, *J. Am. Chem. Soc.* **2010**, *132*, 14061–14063.

<sup>103</sup> R. Kinjo, M. Ichinohe, A. Sekiguchi, *J. Am. Chem. Soc.* **2007**, *129*, 26–27.

Inoue and co-workers applied NHC to stabilise the silicon analogue of acylium ion, disclosing also some interesting reactivity (Scheme II-13).<sup>104</sup>



**Scheme II-13** Silicon-based acylium ion

Starting from a stabilised silylene, the reduction of carbon dioxide was possible, obtaining the silicon acylium analog, silacylium. Subsequently, treatment with water gave rise to the cyclotetrasiloxanediol dianion with imidazolium salt as counteranion. DFT studies proposed a mechanism involving as intermediate the formation of a silyl carboxylate that converts into a silanoic derivative. The latter is able to react with another silanoic moiety, thanks to the Si=O---Si=O interactions. Rearrangement of this species gives the product.

The studies mentioned previously represent an overview of the field born from the interaction between N-Heterocyclic Carbenes and silicon derivatives. Despite the difficulty to itemise all of them in an exhaustive manner, all the emphasized cases display a common thread, the stabilization brought by NHCs.<sup>105</sup> A remarkable element shared by all these examples is the use of silylene or halosilanes as source of silicon. Moreover, excepted for the examples showed by Khun *et al.*,<sup>88</sup> in most cases no hypercoordinate complexes seem to be stable enough to be isolated, probably because the silicon species involved were too reactive or not hindered enough. Consequently, as soon as a pentacoordinate compound was obtained, a rearrangement occurred to restore the four-coordinate species, probably more favoured in this kind of derivatives.

Inspired by this foreword, we decided to investigate the interaction of a presumably hindered silicon-based Lewis acid, like the Martin's spiro-silane, with some NHCs. In

<sup>104</sup> S. U. Ahmad, T. Szilvási, E. Irran, S. Inoue, *J. Am. Chem. Soc.* **2015**, *137*, 5828–5836.

<sup>105</sup> a) D. Lutters, C. Severin, M. Schmidtman, T. Müller, *J. Am. Chem. Soc.* **2016**, *138*, 6061–6067. b) T. Fukuda, H. Hashimoto, H. Tobita, *J. Am. Chem. Soc.* **2015**, *137*, 10906–10909. c) T. Böttcher, S. Steinhauer, L. C. Lewis-Alleyne, B. Neumann, H.-G. Stammer, B. S. Bassil, G.-V. Rösenthaler, B. Hoge, *Chem. – Eur. J.* **2015**, *21*, 893–899. d) T. Böttcher, S. Steinhauer, B. Neumann, H.-G. Stammer, G.-V. Rösenthaler, B. Hoge, *Chem. Commun.* **2014**, *50*, 6204–6206.

particular, due to its peculiar hindrance and high Lewis acidity, formation of pentacoordinate adducts is expected to be favoured.

## II.3 Results and Discussion

Firstly, to start the investigation it was necessary to choose and synthesize the appropriate NHC carbenes. We selected four imidazolylidenes which follow an increasing scale of hindrance according to their percent buried volumes:<sup>106</sup> IDM, IMes, ItBu and IPr which are represented in figure II.9. The possibility to synthesise them in a quite simple manner on grams-scale and their good literature background were also important criteria for their selection.

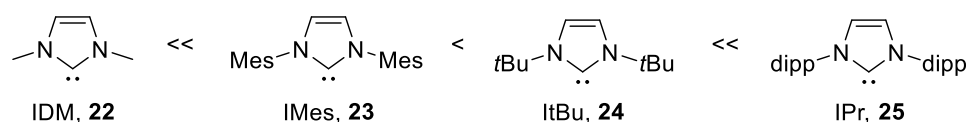
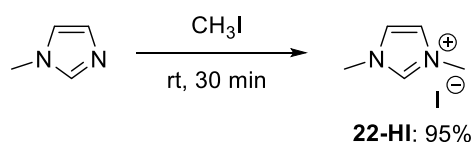


**Figure II.9** NHCs used for this study in steric hindrance scale

### II.3.1 Synthesis of the NHC used in this study

For the synthesis of IDM (**22**), the imidazolium iodide precursor (**22-HI**) was prepared, following a literature procedure<sup>107</sup> consisting in the treatment of N-methylimidazole with iodomethane (Scheme II-14).



**Scheme II-14** synthesis of the precursor IDM

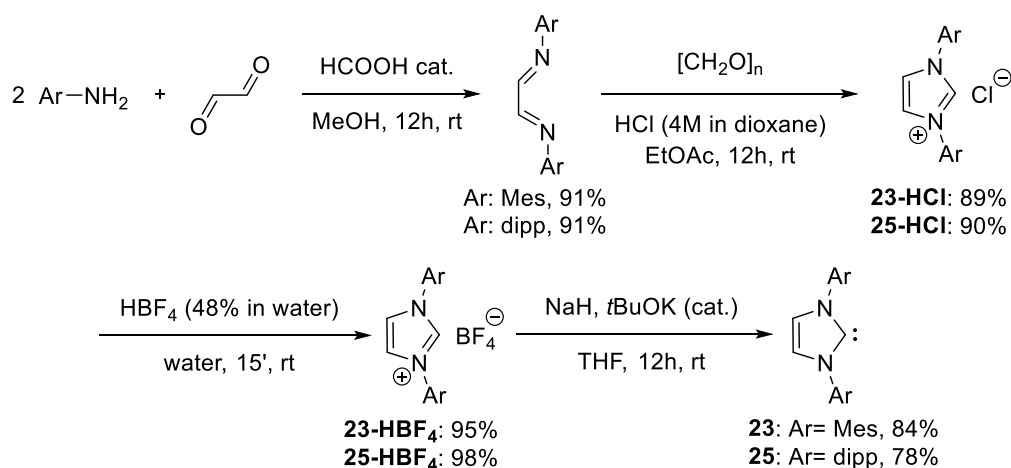
The product was prepared in excellent yield as a pale yellow solid. The following step was the deprotonation, required to obtain the carbene. Different approaches were tested: from treatment with NaHMDS to the more sophisticated NaH in presence of a catalytic amount of tBuOK, unfortunately, in the first case the starting material was recovered, while in the latter case, a sticky dark oil was obtained. <sup>1</sup>H NMR analysis of the crude of this latter reaction, showed the presence of the desired product **22**. Distillation of the oil, allowed for the isolation

<sup>106</sup> H. Clavier, S. P. Nolan, *Chem. Commun.* **2010**, 46, 841–861.

<sup>107</sup> S. Gardner, T. Kawamoto, D. P. Curran, *J. Org. Chem.* **2015**, 80, 9794–9797.

of different not identified degradation products. In 1992 Arduengo already described that IDM is stable in solution of THF stored at  $-30^{\circ}\text{C}$  for several days, while the conservation in its pure form leads to degradation over time.<sup>108</sup> For this reason, it was decided to not isolate the free carbene but to generate it *in situ*.

For the synthesis of IMes (**23**) and IPr (**25**), a modified version of the protocol described by Nolan and co-workers (Scheme II-15) was used.<sup>109</sup>



**Scheme II-15** Synthesis of carbenes **23** and **25**

The first synthetic step is the formation of the diimine by condensation of the corresponding aniline on glyoxal catalysed by formic acid. The next step is the formation of the five-membered ring by addition of paraformaldehyde in presence of hydrochloric acid leading to the formation of the corresponding imidazolium chloride. It is worth to note that the chloride salt can be directly used to perform the deprotonation step in order to get the free carbene.<sup>110</sup> In our case, following the example of Nolan, we opted for an anion metathesis with the tetrafluoroborate anion that results to be more adequate for the deprotonation step. The last step is the deprotonation performed with sodium hydride and a catalytic amount of potassium tert-butoxide, this afforded the two compound **23** and **25** in good yields. The last NHC carbene synthesised was the ItBu. Following the literature procedure for the generation of the tetrafluoroborate precursor,<sup>111</sup> it is possible to obtain it in a one-pot reaction.

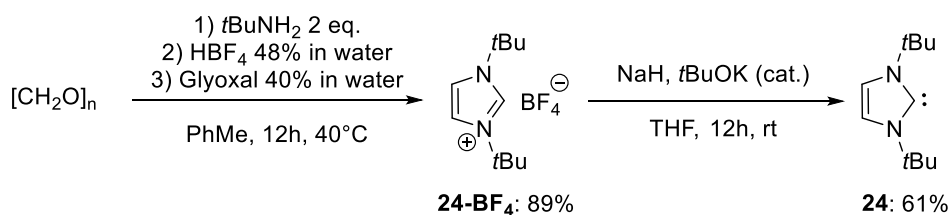
<sup>108</sup> A. J. Arduengo, H. V. R. Dias, R. L. Harlow, M. Kline, *J. Am. Chem. Soc.* **1992**, *114*, 5530–5534.

<sup>109</sup> X. Bantreil, S. P. Nolan, *Nat. Protoc.* **2011**, *6*, 69–77.

<sup>110</sup> G. Schnee, A. Bolley, F. Hild, D. Specklin, S. Dagherne, *Catal. Today* **2017**, *289*, 204–210.

<sup>111</sup> W. A. Herrmann, V. P. W. Böhm, C. W. K. Gstöttmayr, M. Grosche, C.-P. Reisinger, T. Weskamp, *J. Organomet. Chem.* **2001**, *617–618*, 616–628.

Deprotonation was achieved with the above-mentioned method (Scheme II-16). This carbene was obtained in a lower yield due to the higher solubility of the product in THF.

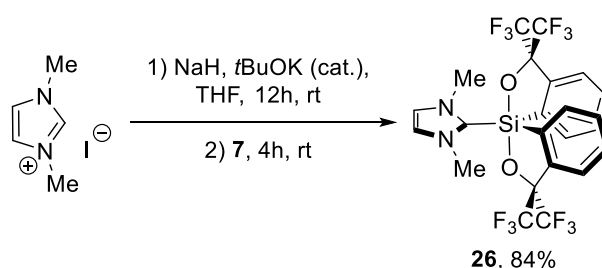


**Scheme II-16** Synthetic strategy for **24**

## II.3.2 Adducts formation

### II.3.2.1 Interaction of Martin's spiroasilane with IDM

Now that we have been able to synthesise the protagonists namely the Martin's spiroasilane **7** and the NHC carbenes, we turned our attention to their interactions. We first started our study by examining the reactivity of IDM, the smallest dimethyl NHC towards the silicon Lewis acid. Since the isolation of the free carbene was quite difficult, we accomplished an *in situ* deprotonation (Scheme II-17).



**Scheme II-17** Interaction between Martin's spiroasilane **7** and IDM

The proton abstraction was carried out using sodium hydride and a catalytic amount of potassium tert-butoxide, allowing the *in situ* generation of the free carbene. The subsequent addition of Martin's spiroasilane **7** to the reaction mixture afford the adduct **26** in 84% yield as a white solid after purification. This Lewis adduct turned out to be very stable and inert to moisture as it could resist to an aqueous workup, which attests the strength of the interaction. From  $^1\text{H}$  NMR analysis is clearly visible the structural change that affected the Martin's spiroasilane due to the coordination of the carbene with a splitting of the aromatic protons (Figure II.10). For the adduct, four distinct signals are observed, with an important chemical

shift as compared to the  $^1\text{H}$  NMR of silane **7** due to electronic density perturbation. The pentacoordinate nature of the silicon atom was confirmed by  $^{29}\text{Si}$  NMR spectroscopy displaying a chemical shift of - 83 ppm ( $\delta = 7.5$  ppm for **1**) that is in accordance with other known pentacoordinate derivatives and thus excluding the formation of adducts with other valences.<sup>112</sup>

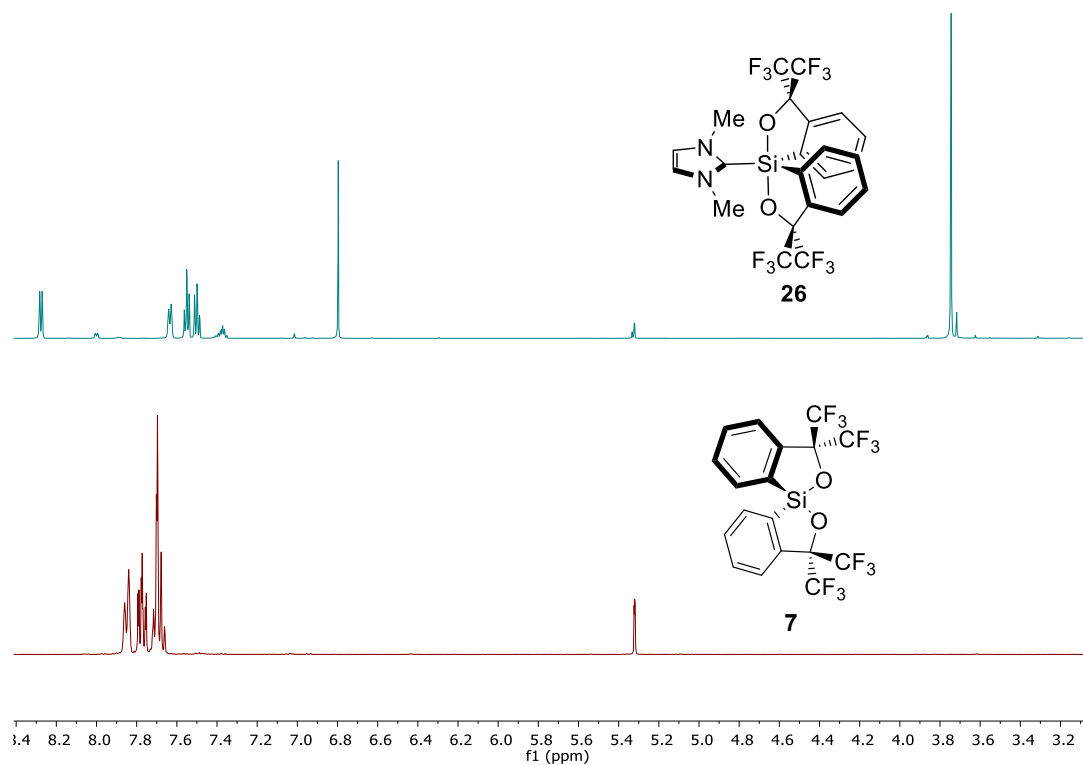


**Figure II.10** comparison of the  $^1\text{H}$  NMR of **7** (red) and **26** (blue).  $\text{CD}_2\text{Cl}_2$

Slow evaporation of a solution of **26** in dichloromethane provided crystals suitable for X-Ray diffraction that confirmed the pentacoordinate silicon structure.

<sup>112</sup> a) A. H. J. F. de Keijzer, F. J. J. de Kanter, M. Schakel, V. P. Osinga, G. W. Klumpp, *J. Organomet. Chem.* **1997**, 29; b) J. A. Cella, J. D. Cargioli, E. A. Williams, *J. Organomet. Chem.* **1980**, 13.

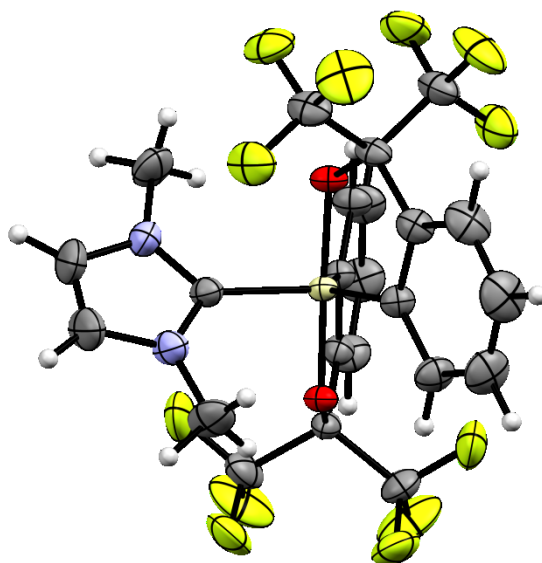


**Figure II.11** ORTEP representation of **26**, ellipsoid 50% probability.

The adduct crystallises in the centrosymmetric orthorhombic *Pbca* group and, as expected, with a trigonal-bipyramidal geometry, characterised by a O-Si-O angle of 178.05°. To the best of our knowledge, no stable complex between IDM and silicon are known. One of the few examples of this type of interaction was reported, as aforementioned, by Radius and co-workers.<sup>99</sup> For this reason, our result with the IDM will be compared with the 1,3-dimethylimidazolidin-2-ylidene silicon derivatives (**NHC-Rosch.**) obtained by Rosenthaler and co-workers (Figure II.12).<sup>113</sup>

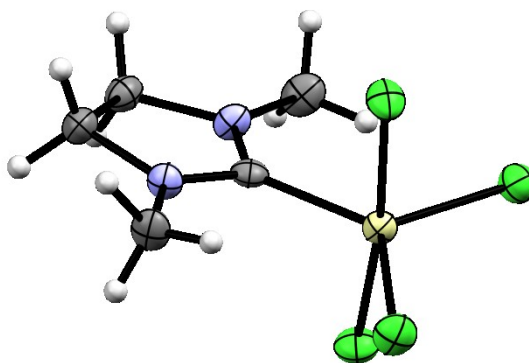


**Figure II.12** ORTEP representation of the NHC-Si derivatives of Rosenthaler

The Si-C is about 1.94 Å in **26**, longer than the average Si-C bond distance of 1.85 Å, this bond length is also slightly longer than the one in the **NHC-Rosch.**, with a distance of 1.92 Å. This difference is ascribable to the steric hindrance that, as we can clearly see, is higher in Martin's spirosilane than SiCl<sub>4</sub>. The NHC occupies the equatorial position but does

<sup>113</sup> T. Böttcher, B. S. Bassil, L. Zhechkov, T. Heine, G.-V. Rösenthaler, *Chem. Sci.* **2012**, *4*, 77–83.

not lie in the equatorial plane having a dihedral angle of  $-45.75^\circ$  clearly visible in the next figure.

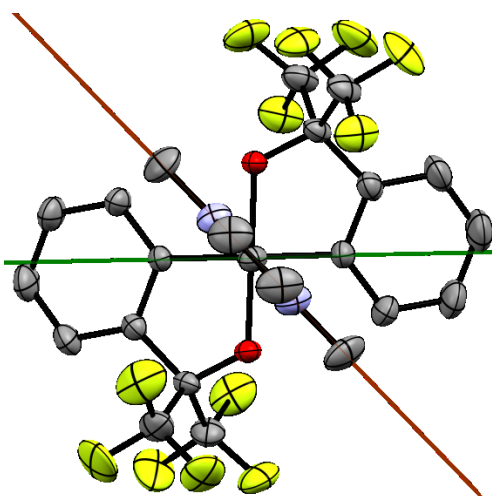
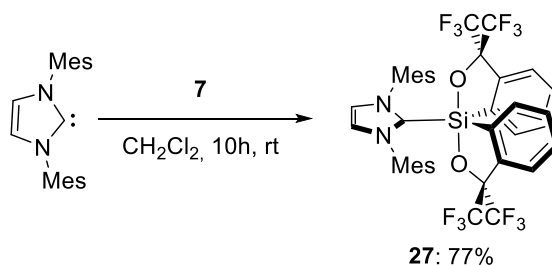


**Figure II.13 26** X-Ray structure divided in quadrant

If we divided the adducts in quadrants, using the O-Si-O axis and the equatorial axis, it is possible to observe how the methyl groups occupy the two free quadrants where the trifluoromethyl groups are not present in order to minimise the interaction. Once again, it is an undeniable effect of the steric hindrance, and this phenomenon will be a common trend in the structures that we will present throughout this chapter.

### II.3.2.2 Interaction of Martin's spirosilane with IMes

The next imidazolylidene studied was the IMes **23**, characterised by an enhanced steric hindrance around the reactive divalent carbon. In this case, we could start directly from the free carbene as mentioned previously. When mixing IMes with spirosilane **7**, the complete formation of the normal Lewis adduct **27** was still observed (Scheme II-18).



**Scheme II-18** Formation of the normal adduct **27** by interaction between Martin's spirosilane **7** and IMes **23**

The complex obtained is air-stable and only after ten hours in water, it was observed the full decomposition, leading to the formation of the corresponding imidazolium and hydroxysiliconate form of the Martin's spirosilane (Figure II.14).

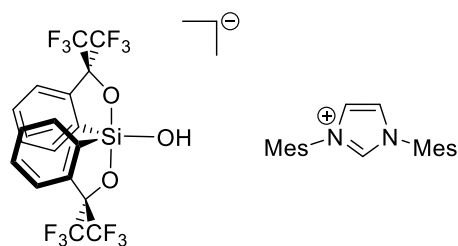


**Figure II.14** Decomposition product of **27** after water treatment.

Slow evaporation of a solution of adduct **27** in dichloromethane afforded crystals suitable for X-Ray diffraction.

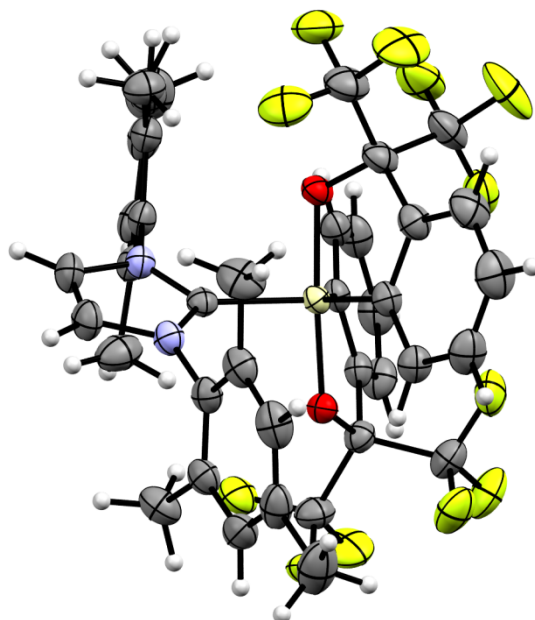


**Figure II.15** ORTEP representation of **27**, 50% probability ellipsoid. For the sake of clarity the second molecule of adduct present in the asymmetric unit is omitted

As anticipated, the structure presents some common features with the previous ones, such as the trigonal bipyramidal geometry. The inclination of the plane containing the imidazole ring displays a dihedral angle of  $-32.4^\circ$ . The asymmetric unit is composed of two molecules (one omitted for clarity in the previous figure), belonging to the  $P2_1/n$  space group, of the monoclinic family.

The steric hindrance of the IMes being higher than IDM, a slight increase of the Si-C bond length was observed, finding a value of  $1.96 \text{ \AA}$  ( $1.94 \text{ \AA}$  for **26**). The elongation of the Si-O bond to  $0.02 \text{ \AA}$  was also observed. Finally, a distortion of O-Si-O angle due to the

hindrance was found, measuring  $176.7^\circ$ , two degrees of difference by comparison with IDM adduct **26**. This distortion from the ideal geometry could be a reason to explain why the Si-C bond was not so much affected. The  $^{13}\text{C}$  NMR characterisation of adduct **27** allowed us to bring out an intriguing fact: the presence of two quadruplets in the aliphatic region (Figure II.15).

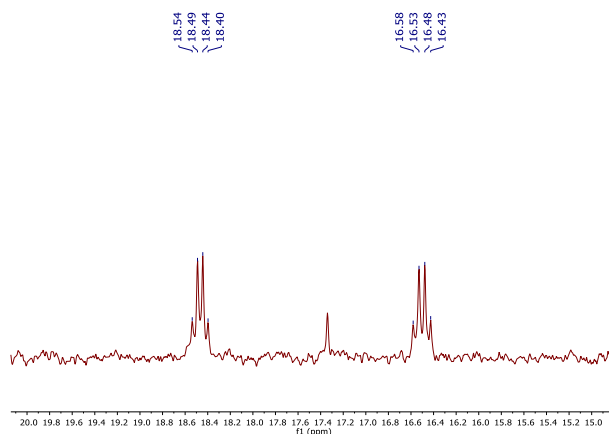


**Figure II.16**  $^{13}\text{C}$  NMR spectrum detail of **27**

Due to the proton decoupled nature of the experience, the only nucleus prone to

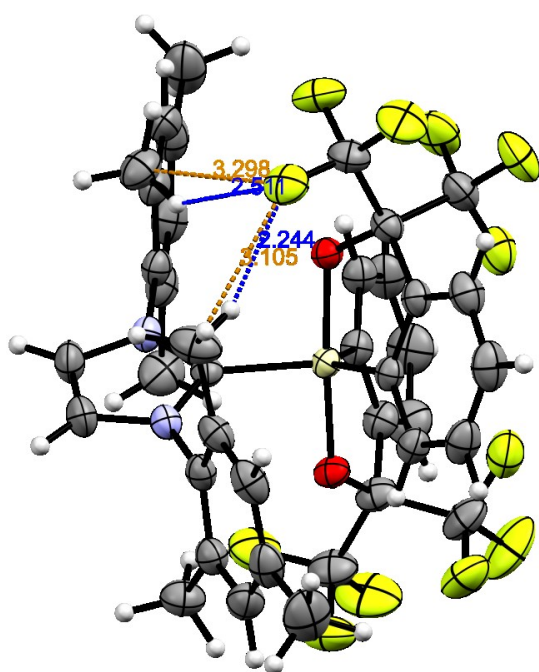


**Figure II.17** C-F (orange), H-F (blue) distance.

couple with carbon is the fluorine. As stated before, these two signals fall in the range of aliphatic carbons and actually correspond to two methyls of the mesityl groups. Nevertheless, at least ten bonds of distance separate them to the closest fluorine atom. It is incongruous to envisage a through-bond coupling with  $^{10}J$  constants about 4 Hz. We found out through a literature survey that a “through-space” coupling between the  $\text{CF}_3$  and the  $\text{CH}_3$  groups was likely.<sup>114</sup> Different theories have justified this particular coupling, the most affirmed one is by

Contreras and co-workers.<sup>115</sup> They rationalised this

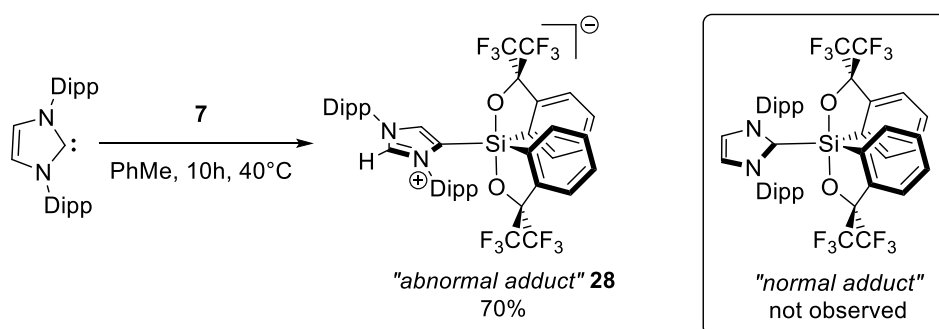
<sup>114</sup> a) F. B. Mallory, C. W. Mallory, in *eMagRes*, John Wiley & Sons, Ltd, **2007**. b) J. W. Lyga, R. N. Henrie, G. A. Meier, R. W. Creekmore, R. M. Patera, *Magn. Reson. Chem.* **1993**, *31*, 323–328.

<sup>115</sup> a) I. D. Rae, A. Staffa, A. C. Diz, C. G. Giribet, M. C. R. Deazua, et al., *Aust. J. Chem.* **1987**, *40*, 1923–1940. b) R. H. Contreras, C. G. Giribet, M. A. Natiello, J. Perez, I. D. Rae, J. A. Weigold, *Aust. J. Chem.* **1985**, *38*, 1779–1784. c) M. A. Natiello, R. H. Contreras, *Chem. Phys. Lett.* **1984**, *104*, 568–571.

phenomenon as an interaction between a lone pair present on fluorine and the  $\sigma^*$  orbital of the sterical opposed C-H bond. In other words, it can be described as the propagation of the Fermi contact term<sup>116</sup> through space, mediated by a third atom, in the majority of the case, one hydrogen (Figure II.17).

### II.3.2.3 Interaction of Martin's spirosilane with IPr

The third NHC investigated was the IPr **25** which possesses a higher steric hindrance than the previously used NHCs. When the Martin's spirosilane was treated with one equivalent of IPr at room temperature in toluene, <sup>1</sup>H NMR and <sup>19</sup>F NMR monitoring of the reaction showed no particular interaction. Indeed, the spectra of the mixture were more or less a superimposition of both starting materials. This result tends to indicate that the two Lewis partners behaved as a Frustrated Lewis Pair. However, over time the system evolved smoothly towards the formation of a well-defined product presenting a loss of symmetry of the carbene moiety as deduced from the <sup>1</sup>H NMR spectrum. This new product was ascribed to the abnormal adduct **28** (Scheme II-19) where the silicon reacted with one of the carbon atoms in the backbone position of the carbene. Conducting the reaction at higher temperature, namely 40 °C, allowed for the complete conversion and the new adduct **28** was isolated in 70% yield. Interestingly, it is known from the literature that IPr forms in the presence of borane B(C<sub>6</sub>F<sub>5</sub>)<sub>3</sub>, the most encountered acid partner in FLP chemistry, only the normal adduct whereas in our case the abnormal adduct is obtained.<sup>117</sup> This result could attest for the high Lewis acidity and steric hindrance of spirosilane **7**. It also suggests that **7** could offer interesting features for its use as new acid partner in FLP chemistry (see chapter 3).



**Scheme II-19** Synthesis of abnormal adduct **28**

<sup>116</sup> W. Kutzelnigg, *Theor. Chim. Acta* **1988**, 73, 173–200.

<sup>117</sup> P. A. Chase, D. W. Stephan, *Angew. Chem. Int. Ed.* **2008**, 47, 7433–7437.

The following figure displays the  $^1\text{H}$  NMR spectrum of abnormal adduct **28**. Surprisingly, the eight methyl groups and the four methines are non-equivalents. This is due to the loss of symmetry of the carbene moiety and also the stereogenicity of the silicon moiety.

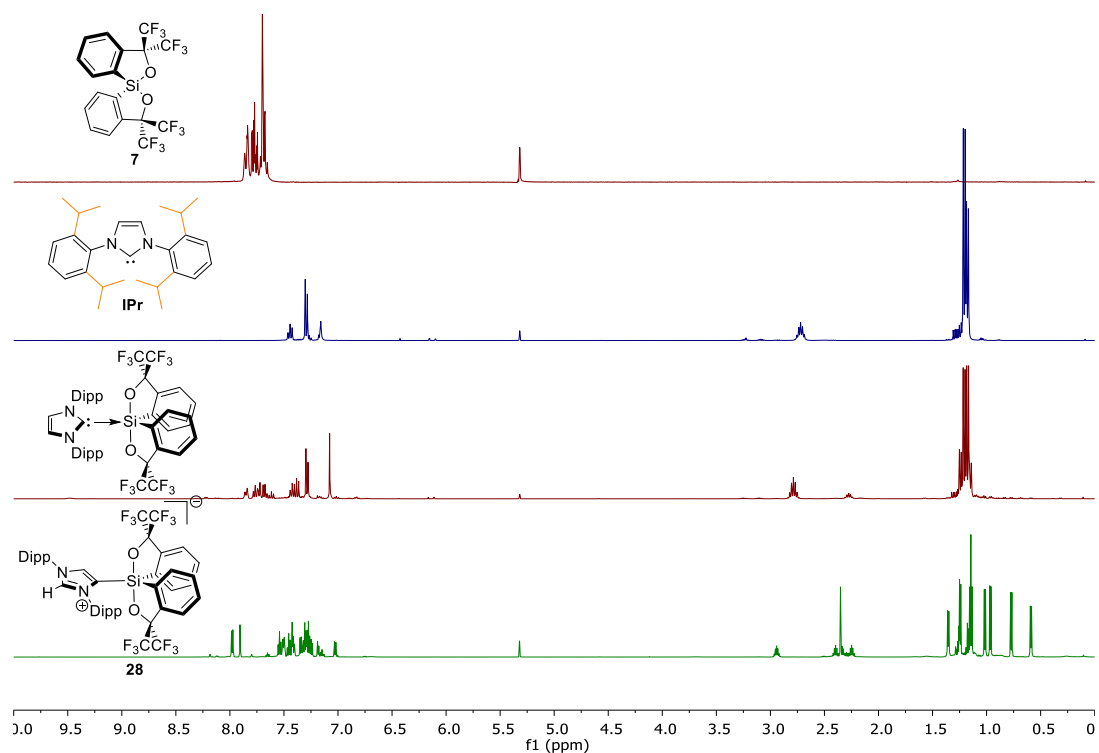


**Figure II.18** Comparison between the  $^1\text{H}$  NMR in the aliphatic area of **IPr** and **28** in  $\text{CD}_2\text{Cl}_2$

Delightfully, suitable crystals for X-Ray diffraction by slow evaporation of a dichloromethane solution of **28** was obtained. The crystallographic structure is depicted in the following figure.

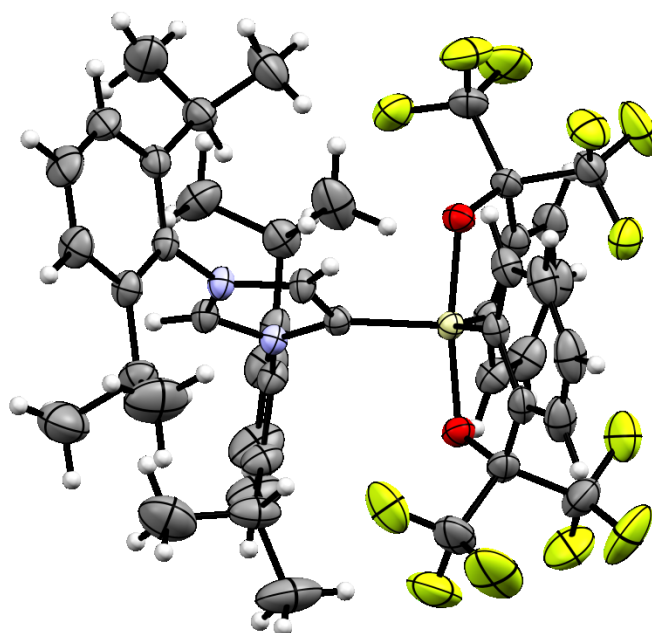


**Figure II.19** ORTEP representation of **28** ellipsoid 50% probability.

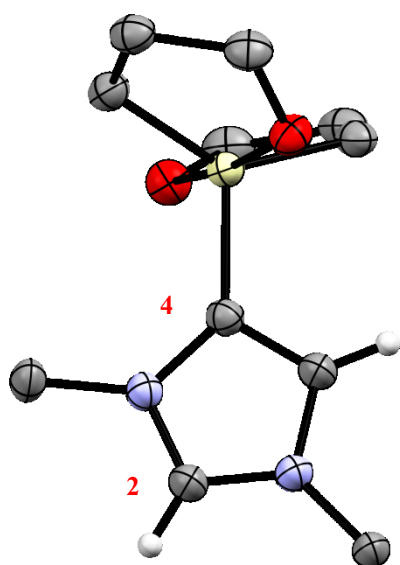


**Figure II.20** ORTEP Cross section of **28**. Highlighted the imidazole ring.

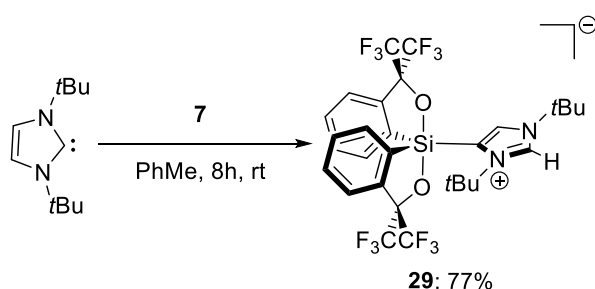
corresponding imidazolylidene.<sup>118</sup>

The crystal belongs to the *P-1* space group, having a triclinic asymmetric unit. We can see how the steric release has a great influence on the length of the Si-C bond, measuring 1.909(1) Å, quite inferior compared to the one in adduct **27** and also compared to the “unhindered” IDM adduct **26**. In addition, the dihedral angle between the equatorial plane and the plane containing the heterocyclic ring is about 27.5°. On the other hand, the O-Si-O angle is quite far from the ideal 180°, measuring 170.77° making **28** a highly distorted trigonal bipyramid. The strength of the interaction between the carbene moiety and the spiroasilane in the abnormal adduct **28** seems to be higher than in the previous normal adducts. This could be attributed the better sigma-donor ability of mesoionic carbenes over the

<sup>118</sup> D. J. Nelson, S. P. Nolan, *Chem. Soc. Rev.* **2013**, 42, 6723–6753.

### II.3.2.4 Interaction of Martin's spirosilane with ItBu

The last carbene considered for this study was the ItBu that possesses a hindrance level between the IMes and the IPr according the calculated percent buried volume. As in the previous cases, we could start directly from the free carbene form. The reaction between the spirosilane **7** and ItBu led as well exclusively to the abnormal adduct **29** at room temperature. This behaviour has already been observed by Tamm between ItBu and the borane  $B(C_6F_5)_3$ .<sup>119</sup> It is worth mentioning that the abnormal adduct is neutral and could be easily purified by chromatography on silica gel.



**Scheme II-20** Synthesis of abnormal adduct **29**

Similarly to the previous adduct, the proton NMR spectrum clearly showed the desymmetrization of the carbene moiety characterised by the presence of two signals ascribable to the two *tert*-butyl groups. Slow evaporation of a dichloromethane solution of **29** allows for the formation of suitable crystals for X-Ray diffraction (Figure II-21).

<sup>119</sup> D. Holschumacher, T. Bannenberg, C. G. Hrib, P. G. Jones, M. Tamm, *Angew. Chem. Int. Ed.* **2008**, *47*, 7428–7432.

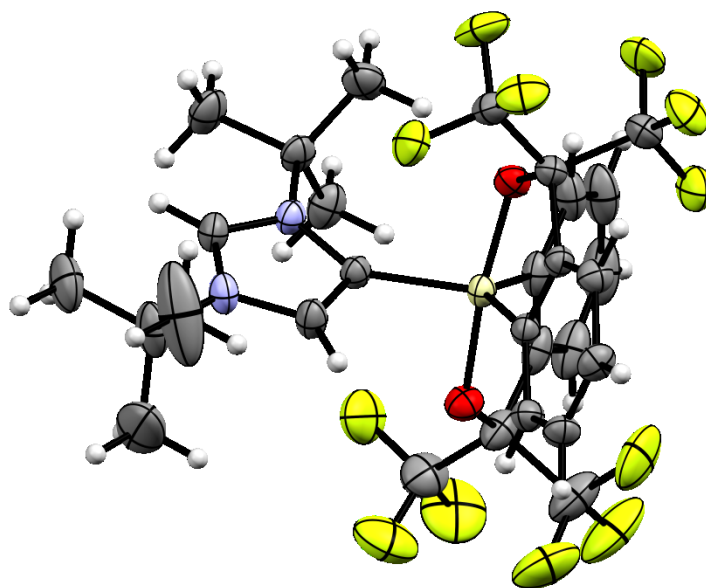


**Figure II.21** ORTEP representation of **29**, ellipsoid 50% probability.

The crystal belongs to the  $P2_1/n$  space group with a monoclinic asymmetric unit. The Si-C distance is about 1.928(1) Å, a value between **28** and **26**. A counterbalance of this elongation by comparison with the similar abnormal adduct **28** is the weaker distortion of the silane scaffold and a O-Si-O angle of 173.38°. Once again a dihedral angle between the equatorial plane and the plane containing the heterocyclic ring was found, measuring -32.4°.

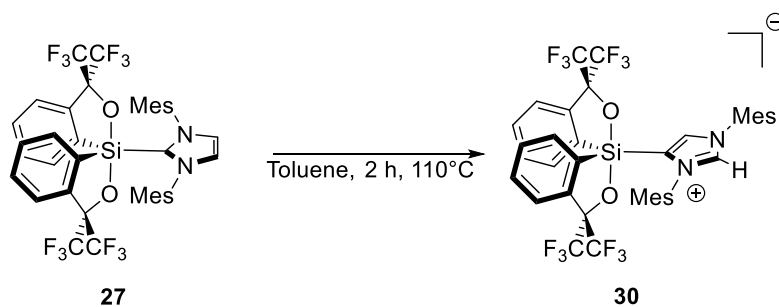
### II.3.2.5 Normal-to-abnormal rearrangement of IMes

Normal-to-abnormal rearrangements of Lewis adducts obtained from NHC carbenes are known to proceed with metal complexes<sup>120</sup> such as trialkylgallium<sup>121</sup> or aluminium.<sup>122</sup> We were interested to see whether the corresponding abnormal adduct of the mesityl derivative **27** could be obtained through this type of rearrangement. When the reaction reaction was conducted in refluxing toluene (Scheme II-21), the adduct **27** underwent rearrangement to form the corresponding abnormal adduct **30** as the major product. However, it was difficult to purify this product to properly characterize it.

<sup>120</sup> a) B. M. Day, K. Pal, T. Pugh, J. Tuck, R. A. Layfield, *Inorg. Chem.* **2014**, 53, 10578; b) B. M. Day, T. Pugh, D. Hendriks, C. Fonseca Guerra, J. Evans, F. M. Bickelhaupt, R. A. Layfield, *J. Am. Chem. Soc.* **2013**, 135, 13338; c) R. H. Crabtree, *Coordination Chemistry Reviews* **2013**, 257, 755.

<sup>121</sup> M. Uzelac, A. Hernan-Gomez, D. R. Armstrong, A. R. Kennedy, E., *Chem. Sci.* **2015**, 6, 5719.

<sup>122</sup> G. Schnee, O. N. Faza, D. Specklin, B. Jacques, L. Karmazin, R. Welter, C. Silva Lopez, S. Dagorne, *Chem. Eur. J.* **2015**, 21, 17959.



**Scheme II-21** NMR comparison between the *n*NHC adduct with I-Mes (red) and the mixture *n*NHC/*a*NHC (green). Tol-*d*<sub>8</sub>.

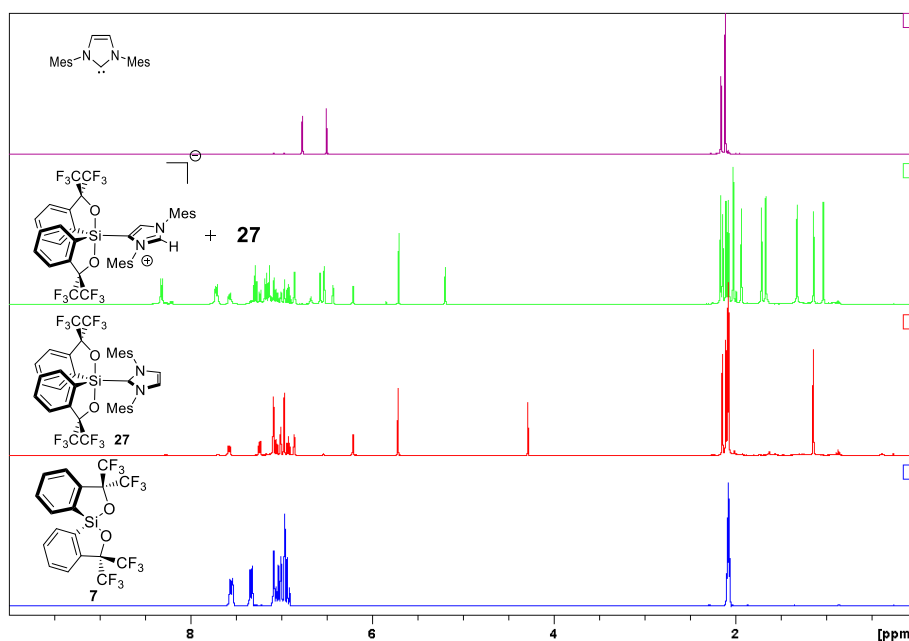
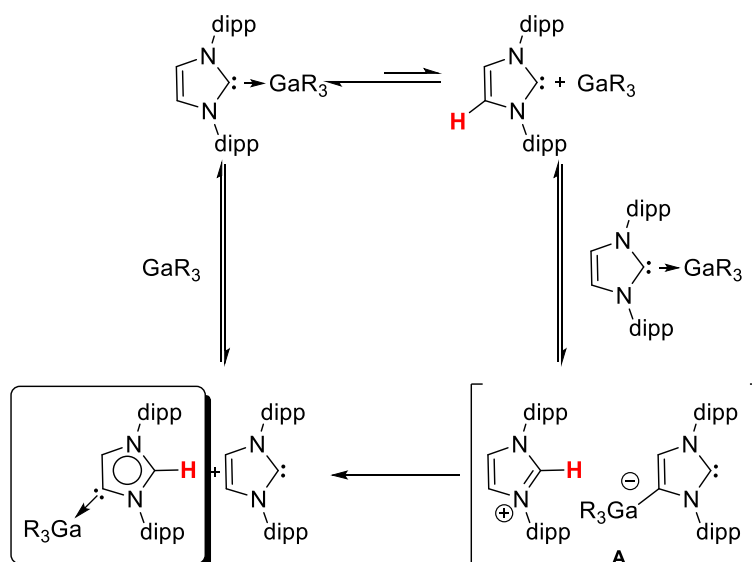


**Figure II.22** Comparison of the NMR spectra of **27** at room temperature (red) and at 80 °C (green)

### II.3.2.6 Mechanism for the normal-to-abnormal rearrangement

Different theories have been proposed to rationalize the formation of the abnormal NHC adducts from the normal ones and could differ according to the metal and the carbene involved. Hevia and co-workers suggested the following mechanism for the isomerisation of IPr-GaR<sub>3</sub> adduct (R = CH<sub>2</sub>SiMe<sub>3</sub>), supported by kinetic, NMR and DFT studies (Scheme II-22).<sup>123</sup>

<sup>123</sup> M. Uzelac, A. Hernán-Gómez, D. R. Armstrong, A. R. Kennedy, E. Hevia, *Chem. Sci.* **2015**, *6*, 5719–5728.

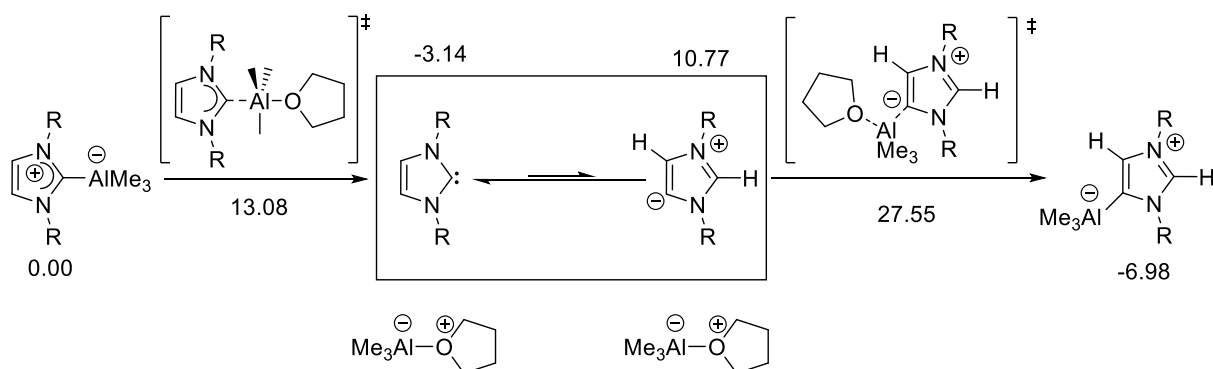


**Scheme II-22** Mechanism formation of abnormal adduct proposed by Hevia

An equilibrium between the coordinated and the non-coordinated forms of the IPr-GaR<sub>3</sub> complex would operate. Then the free carbene present in this latter form would be capable to deprotonate at the C4 position, triggering the migration of the Ga(III) and leading to the ionic pair **A** consisting in the imidazolium and the deprotonated form of abnormal adduct. This system evolves and leads to abnormal adduct through proton exchange. Experimentally, it is observed that the presence of an excess of GaR<sub>3</sub> slows down the rearrangement, whereas an excess of IPr tends significantly accelerates it which is in agreement with the proposed mechanism.

At the same time, the group of Dagorne suggested another pathway for the normal-to-abnormal isomerisation in THF of ItBu-AlMe<sub>3</sub> adduct based on kinetic and DFT studies.<sup>124</sup> The mechanism starts with the solvent coordination to the aluminium centre, leading to the formation of THF-AlMe<sub>3</sub> complex and the free ItBu. This latter is in equilibrium with the much less stable isomeric aItBu by about 14 kcal.mol (Scheme II-23) which readily reacts with the previously formed THF-AlMe<sub>3</sub> to provide the aItBu-AlMe<sub>3</sub> adduct.

<sup>124</sup> G. Schnee, O. Nieto Faza, D. Specklin, B. Jacques, L. Karmazin, R. Welter, C. Silva López, S. Dagorne, *Chem. – Eur. J.* **2015**, *21*, 17959–17972.



**Scheme II-23** DFT-computed (M06/def2-SVP) mechanism for the normal-to-abnormal NHC rearrangement in the presence of THF proposed by Dagorne and coworker. Gibbs free energies in THF solution.

### II.3.2.7 DFT calculations

To gain further insights into the thermodynamics of the NHCs-silane **7** interactions, DFT calculation at the B3LYP-D3 and M05-2X levels were performed. First, the geometrical parameters obtained with both methods fit well with the X-Ray crystallographic structures with notably a good estimation of the Si-C bond lengths.

NHC	d(exp) Si-C	B3LYP-D3		M05-2X	
		d <sub>Si-C</sub>	$\Delta H/\Delta G$	d <sub>Si-C</sub>	$\Delta H/\Delta G$
<b>22</b>	1.943	1.958	-42.5/-27.7	1.950	-40.7/-25.2
<b>23</b>	1.956	1.965	-48.1/-25.8	1.963	-36.6/-19.1
<b>24</b>	-	2.025	-24.8/-6.9	2.018	-17.9/+0.5
<b>25</b>	-	1.967	-38.5/-18.3	1.955	-31.9/-8.7

**Table II.1** Thermodynamic parameters obtained by DFT calculations for the formation of normal adduct.

Distance are given in Å and energies in Kcal.mol<sup>-1</sup>

Some trends can be stressed from both methods. The formation of the normal adducts resulted to be highly dependent on the steric bulk on the NHC. Indeed, the exothermicity of the Lewis adducts formation decreased by 10 kcal.mol<sup>-1</sup> between **26** and **28** about 25 Kcal.mol<sup>-1</sup> between **26** and **29**. In addition, a high charge transfer of about 0.45 from all the NHCs to **7** has been deduced from NBO analysis. The gain of electron density is mainly redistributed to the bistrifluoro alkoxy ligands while the charge at the silicon remains approximately unchanged, from +1.21 to +1.15. Regarding abnormal adducts, the calculated Si-C distance is slightly longer with both methods than the one deduced from the X-Ray

structure, which probably indicates an overall underestimation of the bond strength and consequently, of the *a*NHC-Si interaction.

NHC-Si	d(exp) Si-C	B3LYP-D3		M05-2X	
		d <sub>Si-C</sub>	ΔH/ΔG	d <sub>Si-C</sub>	ΔH /ΔG
<b>26</b>	-	1.934	11.2/10.6	1.926	10.8/9.41
<b>27</b>	-	1.932	11.5/6.21	1.936	6.2/5.6
<b>28</b>	1.910	1.938	3.7/0.2	1.926	6.4/1.1
<b>29</b>	1.928	1.962	-6.8/-9.0	1.936	-8.0/-10.4

**Table II.2** Thermodynamic parameters obtained by DFT calculations for normal-to-abnormal adducts interconversion. Distance are given in Å and energies in Kcal.mol<sup>-1</sup>

Interestingly and also fully consistent with our experimental findings, calculations showed that the larger the steric demand of the NHC, the higher the stability of the abnormal adduct over the normal adduct.



**Chapter III**  
**Martin's Spirosilane a New Partner in**  
**FLP Chemistry**



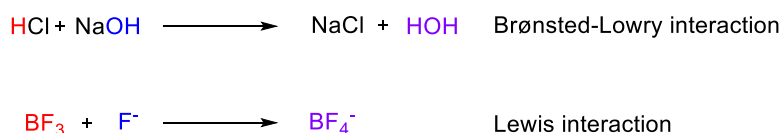
# III. Martin's Spirosilane as a New Partner in FLP Chemistry

## III.1 Bibliography

1923 is one of the most important years in the history of chemistry, due to the enunciation of one of its cornerstone: the theory of Lewis acid and base.<sup>125</sup>

Simple and elegant, this concept splits the compounds into two categories, one at which belong all the molecules capable of accepting a pair of electron, the acids, and one capable of donating one electron pair, the bases. This theory can be seen as a generalisation of the one stated by Brønsted<sup>126</sup> and Lowry<sup>127</sup> that referred only to the protons transfer.

This assumption, now elementary, is in part responsible of the astonishing development of chemistry of the XX century and it is also the base concept of the Frustrated Lewis Pairs (FLPs) chemistry discussed in this chapter. It is known that reaction between a Brønsted acid and base gave as a result the corresponding salt through a proton transfer, whereas in the case of a reaction between a Lewis acid and a Lewis base, an adduct is usually obtained (Scheme III-1). In both cases, the resulting compound do not exhibit the properties of the reactants: a quenching reaction has happened.



**Scheme III-1** Examples of Brønsted adduct formation (up) and Lewis adduct formation (bottom)

The chemistry of Frustrated Lewis Pairs emanates from the absence of this quenching phenomena due to the steric hindrance of the two partners.

<sup>125</sup> G. N. Lewis, *Valence and the Structure of Atoms and Molecules*, Chemical Catalog Com.; New York, **1923**.

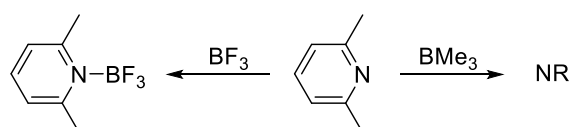
<sup>126</sup> J. N. Brønsted, *Recl. Trav. Chim. Pays-Bas* **1923**, *42*, 718–728.

<sup>127</sup> T. M. Lowry, *J. Soc. Chem. Ind.* **1923**, *42*, 43–47.

### III.1.1 Frustrated Lewis Pair: from the concept to applications

While the concept of FLP is quite recent, the presence of some Lewis acids and bases that do not form the classical adduct has been known for a long time.

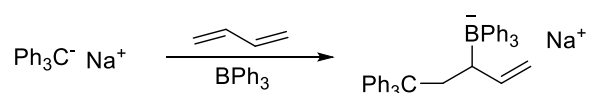
The first example of this peculiar behaviour was shown by Brown in 1942,<sup>128</sup> during his studies on the interaction of pyridine with different borane. In the majority of the case, he isolated the expected classical adducts, but with lutidine, although he was able to coordinate  $\text{BF}_3$ , no adduct was obtained with  $\text{BMe}_3$  (Scheme III-2).



**Scheme III-2** Brown's experiments.

Investigation through molecular models suggests that the steric hindrance of both Lewis partners is the main supporter of this phenomenon. Indeed, it prevents the interaction of the two moieties avoiding the formation of an adduct.

Some years later, Wittig and Benz illustrated that benzyne is generated in situ, in presence of triphenylphosphine and triphenylborane, a *o*-phosphorus borate adduct was obtained instead of the classical adduct.<sup>129</sup> Tochtermann, also, observed the formation of a “trapping product” always instead of the expected adduct (Scheme III-3).<sup>130</sup>



**Scheme III-3** Tochtermann trapping product.

It has been 60 years after the seminal work of Brown, that the last piece of the puzzle comes to light. In 1998, Erker published a paper describing the reaction between the tris(pentafluorophenyl)borane and a phosphorus ylide. Stone, Massey and Park were the firsts to synthesise this particular borane and they isolate some adducts with it.<sup>131</sup> It possesses a very high Lewis acidity and also an important steric hindrance, that granted it some

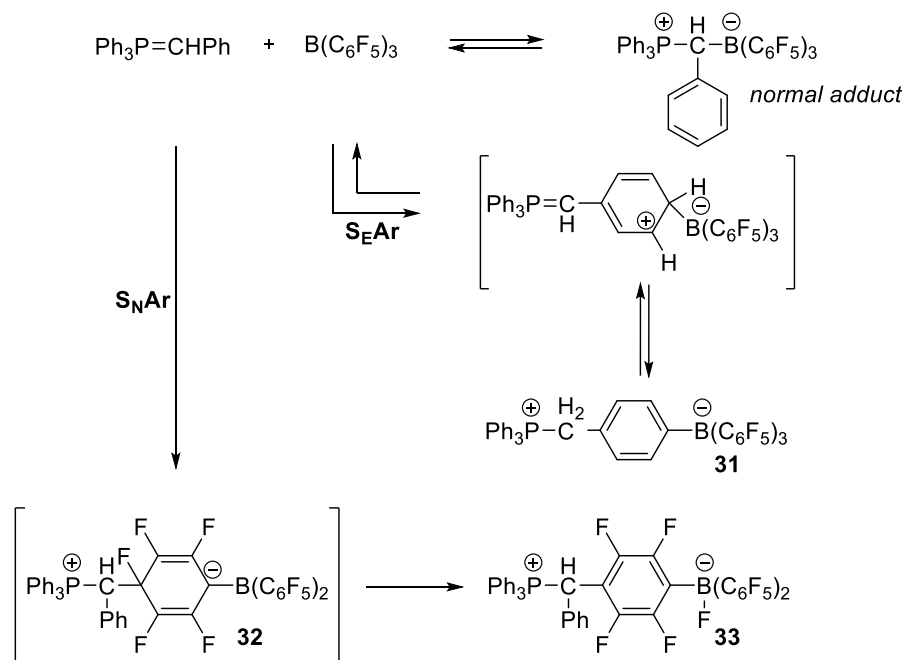
<sup>128</sup> H. C. Brown, H. I. Schlesinger, S. Z. Cardon, *J. Am. Chem. Soc.* **1942**, *64*, 325–329.

<sup>129</sup> G. Wittig, E. Benz, *Chem. Ber.* **1959**, *92*, 1999–2013.

<sup>130</sup> W. Tochtermann, *Angew. Chem. Int. Ed. Engl.* **1966**, *5*, 351–371.

<sup>131</sup> A. G. Massey, A. J. Park, F. G. A. Stone, *Proc. Chem. Soc.* **1963**, 212.

interesting properties. It has been discovered a competition between the formation of the normal adduct and an electrophilic aromatic substitution pathway or a third pathway characterised by a nucleophilic substitution.<sup>132</sup>



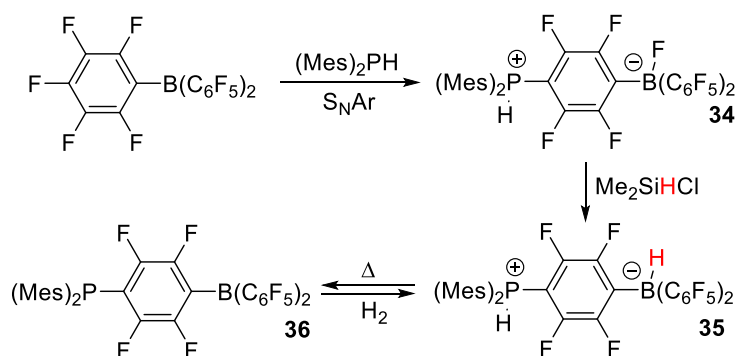
**Scheme III-4** Reactivity of tris(pentafluorophenyl) borane and a phosphorus ylide

The two reactants were found to be in equilibrium with the classical acid-base Lewis adduct. But, when the mixture was heated at  $55^\circ\text{C}$ , another equilibrium was observed. In that case, the product **31** coming from an electrophilic aromatic substitution at the para position of the phenyl ring of the ylide was obtained. The product proved to be thermolabile, indeed, if the reaction was heated at  $55^\circ\text{C}$  for more than 24 h, a third irreversible reaction pathway was noticed. A nucleophilic aromatic substitution product, **32**, is formed through the attack of the ylide to the para position of one of the pentafluorophenyl ring. A subsequent fluoride rearrangement gave access to the final product **33**.

In 2006 Stephan and co-workers used the tris(pentafluorophenyl)borane and a hindered secondary phosphine, as previously shown by Erker. In this case, the product **34** formed by aromatic nucleophilic substitution was obtained.<sup>133</sup>

<sup>132</sup> S. Döring, G. Erker, R. Fröhlich, O. Meyer, K. Bergander, *Organometallics* **1998**, *17*, 2183–2187.

<sup>133</sup> G. C. Welch, R. R. S. Juan, J. D. Masuda, D. W. Stephan, *Science* **2006**, *314*, 1124–1126.



**Scheme III-5** First example of FLP

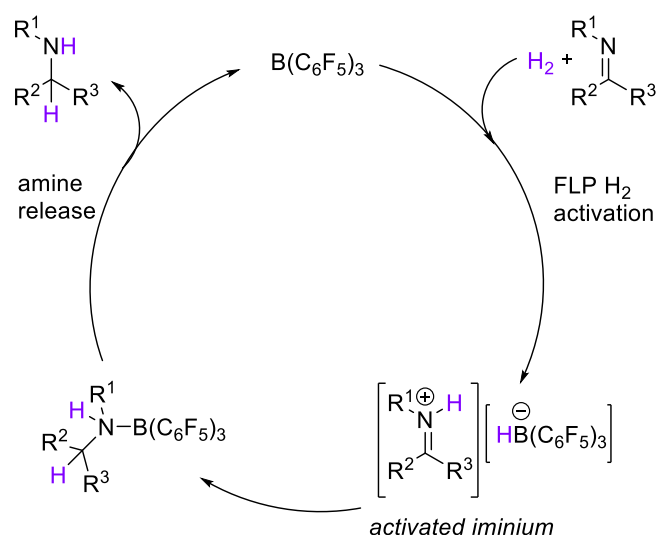
NMR investigations confirmed the presence of a hydrogen on the phosphorus while fluorine was present on the boron atom. Consequently, reaction with chlorodimethylsilane triggered the metathesis between the fluoride on boron and the hydride present on the silane (in red in the previous scheme) to afford **35** as a moisture and air-stable compound. Stephan and co-workers observed that the stoichiometric loss of H<sub>2</sub> occurred when a solution of zwitterionic compound **35** in toluene was heated at 100°C, leading to **36**. The revolutionary behaviour of this molecule is that at 25°C in presence of hydrogen the restoration of **35** can be achieved. To gain further insight, NMR kinetic studies were performed.

This experiment marked the birth of the concept of Frustrated Lewis Pairs. Starting from the “simple” hydrogen splitting, it was envisioned to use FLP in catalysis. One of the first example, was the imine reduction reported by Stephan and co-workers using **35** as catalyst.<sup>134</sup> The desired product could be obtained in good yield and no by-products were noticed. In-depth investigations demonstrated that the rate of reduction is widely affected by the basicity of the nitrogen than by the steric hindrance present on it. This consideration implicated that the first step is the protonation by the phosphonium rather than the hydride attack on the electrophilic carbon. In order to verify this hypothesis, the same experiment was performed using Cy<sub>3</sub>P(C<sub>6</sub>F<sub>4</sub>)BH(C<sub>6</sub>F<sub>5</sub>)<sub>2</sub>, in which a proton is absent. As expected the reaction did not occur, corroborating the importance of the basicity of the nitrogen.

A year after, the group of Stephan also demonstrated that hindered imines could themselves be used as the Lewis base partners to split hydrogen (Scheme III-6).<sup>135</sup>

<sup>134</sup> P. A. Chase, G. C. Welch, T. Jurca, D. W. Stephan, *Angew. Chem. Int. Ed.* **2007**, *46*, 8050–8053.

<sup>135</sup> P. A. Chase, T. Jurca, D. W. Stephan, *Chem. Commun.* **2008**, *0*, 1701–1703.



**Scheme III-6** Catalytic cycle proposed for the imine reduction

As stated before, the imine acts as the substrate and also as the FLP Lewis base partner by splitting the hydrogen and generating the activated iminium salt. Hydride migration from boron to the electrophilic carbon afforded the weak coordinated amino-borane complex that easily releases the final product, regenerating the catalyst.

Few years later, the asymmetric version has been introduced thanks to the work of Klankermayer and co-workers. They have evaluated the hydrogenation reaction of different imines, using as catalyst a chiral borane, derived from (+)- $\alpha$ -pinene (Figure III.1).<sup>136</sup>

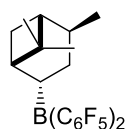
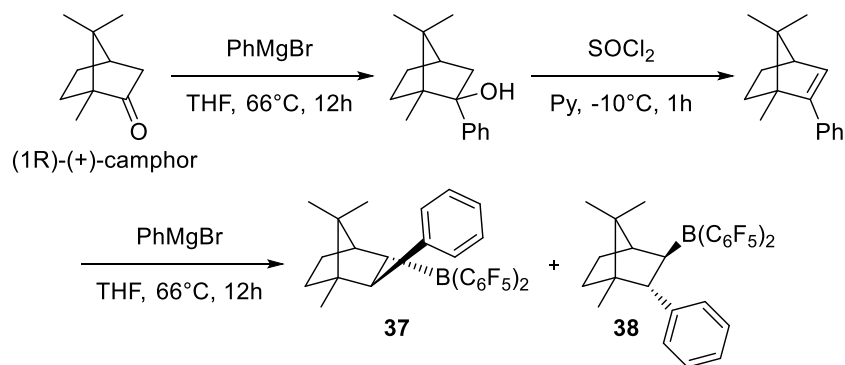


**Figure III.1** chiral borane derived from the (+)- $\alpha$ -pinene

Despite only 10% ee was reached, this experiment represents an important proof of concept and another important step in the evolution of FLP. In 2010, Klankermayer again reported the first example of efficient enantioselective hydrogenation mediated by a chiral FLP. He assumed that the chirality had to be incorporated in the Lewis acid structure, for this reason (1R)-(+)-camphor was elected as the ideal structural motif.<sup>137</sup>

<sup>136</sup> D. Chen, J. Klankermayer, *Chem. Commun.* **2008**, 0, 2130–2131.

<sup>137</sup> D. Chen, Y. Wang, J. Klankermayer, *Angew. Chem. Int. Ed.* **2010**, 49, 9475–9478.



**Scheme III-7** Synthesis of chiral borane **37** and **38**

The overall synthesis gave an easy access to two diastereoisomeric boranes in 1:4 ratio, **37**, **38** (Scheme III.7), however, it was not possible to separate the two compounds. It was then performed the hydrogen splitting, with the diastereoisomeric mixture, in presence of tri-tertbutylphosphine (Figure III.2).

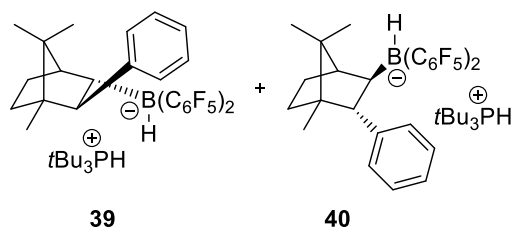


**Figure III.2** Activated form of catalyst

A deeper study showed that the FLP system **37**/*t*Bu<sub>3</sub>P performs the hydrogen splitting in a faster way than the other FLP couple, so under kinetic control it was possible to obtain the two diastereoisomers in pure form. The chiral activity was evaluated in the hydrogenation of substituted imine using the diastereoisomerically pure compounds **39** and **40**; they were able to reach moderate to good enantiomeric excess, from 48% to 83%, in mild conditions.

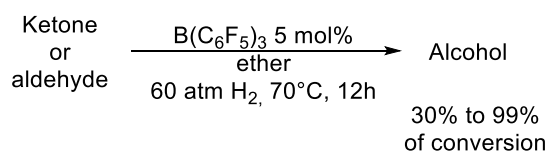
In the next years, different substrates from silyl enol ether, enamines and enones, were successfully reduced in a selective manner.<sup>138</sup>

Up to now, only nitrogen-based substrates were analysed since more problems came out when carbonyl function are involved. Erker *et al.* described how the intramolecular FLP Mes<sub>2</sub>PCH<sub>2</sub>CH<sub>2</sub>B(C<sub>6</sub>F<sub>5</sub>)<sub>2</sub> reacted with benzaldehyde in irreversible manners.<sup>139</sup> Repo's group

<sup>138</sup> J. Paradies, *Synlett* **2013**, 24, 777–780.

<sup>139</sup> P. Spies, G. Erker, G. Kehr, K. Bergander, R. Fröhlich, S. Grimme, D. W. Stephan, *Chem. Commun.* **2007**, 0, 5072–5074.

reported that  $B(C_6F_5)_3$  deoxygenates but did not reduce aromatic carbonyl compounds.<sup>140</sup> Ashley and O'Hare were able to reduce  $CO_2$  in presence of  $(C_6F_5)_2BOMe$  and hydrogen, but with a conspicuous degradation of the borane.<sup>141</sup> Nevertheless, computational studies performed by Privalov's group<sup>142</sup> and Wang's group<sup>143</sup> have demonstrated the viability of the ketone hydrogenation. Finally, in 2014, once again due to the work of Stephan and co-workers, this challenge was achieved.<sup>144</sup> The degradation's problem, encountered by Ashley, was overcome by an judicious choice of the FLP system, in particular, it was required a system able to split hydrogen but not too much acidic in order to avoid the reaction with the B-C bond. Suitable candidates are the borane-oxyborate, like  $(C_6F_5)BCH(C_6F_5)OB(C_6F_5)_3$ .<sup>145</sup> Another alternative can be the use of ether derivatives as Lewis base FLP partners as it is shown that FLP systems containing this functional group, can activate hydrogen.<sup>146</sup> The first attempt involved diethyl ether as base which enabled the ketone hydrogenation, albeit in poor yield, 30%. Optimisation of the reaction allows them to reach good conversion from 32% with cyclohexanaldehyde, to 99% with dipropylketone (Scheme III-8). Isopropyl ether gave also a good result.



**Scheme III-8** General condition for hydrogenation reaction

In the proposed mechanism, borane and ether are in equilibrium between the classical adduct and the FLP form. This latter is the active species, able to split the hydrogen, with the hydride located on the boron atom, while the proton is stabilised by interactions between the ether and the carbonyl. This associated form made the electrophilic carbon more susceptible to undergo the hydride attack allowing the formation of the alcohol. From this point, hydrogenation mediated by FLPs continued to gain importance. Other than the organic system, also organometallic compounds were used, in particular, the Erker's group result

<sup>140</sup> M. Lindqvist, N. Sarnela, V. Sumerin, K. Chernichenko, M. Leskelä, T. Repo, *Dalton Trans.* **2012**, *41*, 4310–4312.

<sup>141</sup> A. E. Ashley, A. L. Thompson, D. O'Hare, *Angew. Chem. Int. Ed.* **2009**, *48*, 9839–9843.

<sup>142</sup> J. Nyhlén, T. Privalov, *Dalton Trans.* **2009**, *0*, 5780–5786.

<sup>143</sup> H. Li, L. Zhao, G. Lu, F. Huang, Z.-X. Wang, *Dalton Trans.* **2010**, *39*, 5519–5526.

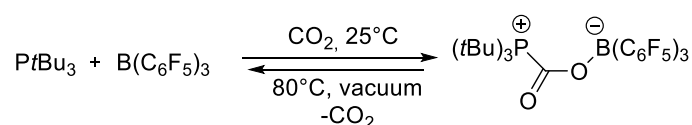
<sup>144</sup> T. Mahdi, D. W. Stephan, *J. Am. Chem. Soc.* **2014**, *136*, 15809–15812.

<sup>145</sup> L. E. Longobardi, C. Tang, D. W. Stephan, *Dalton Trans.* **2014**, *43*, 15723–15726.

<sup>146</sup> L. J. Hounjet, C. Bannwarth, C. N. Garon, C. B. Caputo, S. Grimme, D. W. Stephan, *Angew. Chem. Int. Ed.* **2013**, *52*, 7492–7495.

really active in this field, using ferrocene derivatives.<sup>147</sup> From the pioneering work of Klankermayer,<sup>137</sup> other have successfully joined the asymmetric field obtaining good result, Repo and co-workers used an N-Heterocyclic N/B FLP to reduce ketimines, obtaining a 37% of ee.<sup>148</sup> Liu and Du used a chiral bis-borane obtaining an ee of 74-88%.<sup>149</sup> More recently Erker's group used a chiral ferrocene-based phospho-borane for the asymmetric imine reduction.<sup>150</sup> In 2016 Kremper and co-workers described what they call an "inverse" FLP in which there is an organosuperbase coupled with a weak Lewis acid, that are able to split hydrogen.<sup>151</sup>

Beyond these examples of H<sub>2</sub> activation, Frustrated Lewis Pairs can also react with other small molecules like CO<sub>2</sub>, SO<sub>2</sub>, N<sub>2</sub>O, CO and also alkyne, alkene and more. In the last decades, the attention around the chemistry connected to carbon dioxide arose due to the environmental issues. The aim of this research field is to use CO<sub>2</sub> as a carbon feedstock. The first example of an FLP interacting with carbon dioxide is by Mömming *et al.* in 2009,<sup>152</sup> they were able to obtain the carboxylic derivatives mixing tri-*tert*butyl phosphine and B(C<sub>6</sub>F<sub>5</sub>)<sub>3</sub> in bromobenzene in an atmosphere of CO<sub>2</sub> (Scheme III-9).



**Scheme III-9** Reversible CO<sub>2</sub> binding

As shown previously, one oxygen atom coordinates to the boron atom, the acidic site, while the phosphine undergoes a nucleophilic attack on the electrophilic carbon generating the zwitterionic species. Moreover, the process is reversible. It was possible also to pass from an intermolecular system to an intramolecular one, like (Mes)<sub>2</sub>PCH<sub>2</sub>CH<sub>2</sub>B(C<sub>6</sub>F<sub>5</sub>)<sub>2</sub>. From this first example, different systems for the trapping of carbon dioxide were designed, using nitrogen-based Lewis base,<sup>153</sup> bisborane,<sup>154</sup> organometallic species<sup>155</sup> and other.<sup>156</sup> Beyond the

<sup>147</sup> G. Erker, *Dalton Trans.* **2011**, 40, 7475–7483.

<sup>148</sup> V. Sumerin, K. Chernichenko, M. Nieger, M. Leskelä, B. Rieger, T. Repo, *Adv. Synth. Catal.* **2011**, 353, 2093–2110.

<sup>149</sup> Y. Liu, H. Du, *J. Am. Chem. Soc.* **2013**, 135, 6810–6813.

<sup>150</sup> K.-Y. Ye, X. Wang, C. G. Daniliuc, G. Kehr, G. Erker, *Eur. J. Inorg. Chem.* **2017**, 2017, 368–371.

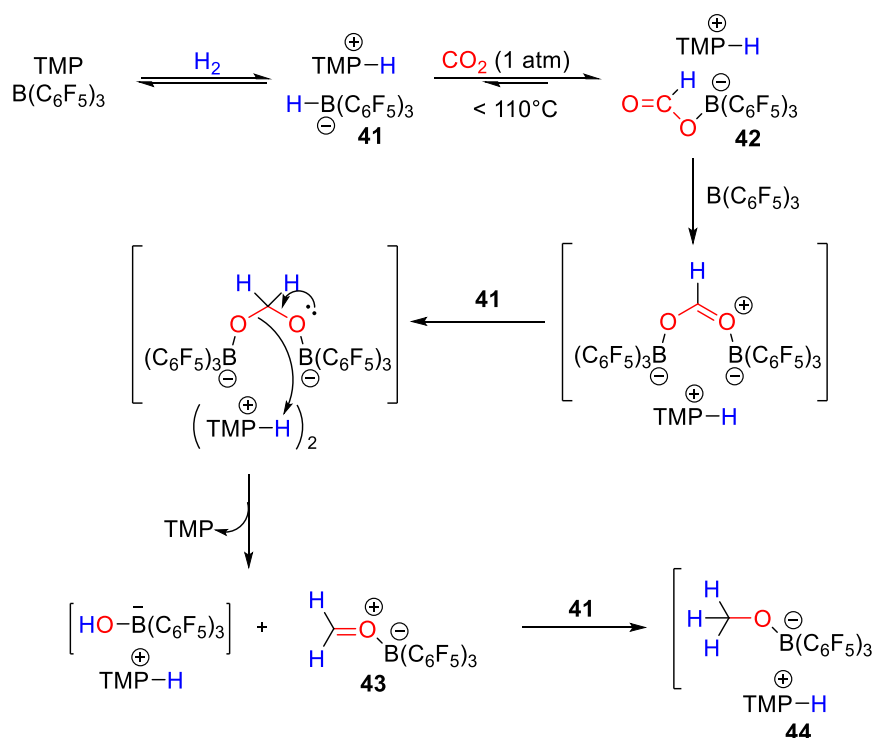
<sup>151</sup> S. Mummadi, D. K. Unruh, J. Zhao, S. Li, C. Kremper, *J. Am. Chem. Soc.* **2016**, 138, 3286–3289.

<sup>152</sup> C. M. Mömming, E. Otten, G. Kehr, R. Fröhlich, S. Grimme, D. W. Stephan, G. Erker, *Angew. Chem. Int. Ed.* **2009**, 48, 6643–6646.

<sup>153</sup> A. E. Ashley, A. L. Thompson, D. O'Hare, *Angew. Chem. Int. Ed.* **2009**, 48, 9839–9843.

<sup>154</sup> X. Zhao, D. W. Stephan, *Chem. Commun.* **2011**, 47, 1833–1835.

uptake of carbon dioxide, it results of higher interest the transformation of it in useful building block for the chemical industry. The first attempt of CO<sub>2</sub> reduction, using FLPs, was realized by Ashley and O'Hare, using the pair formed by B(C<sub>6</sub>F<sub>5</sub>)<sub>3</sub> and TMP.<sup>153</sup> In order to reduce it, the FLP system was “activated” with hydrogen, followed by insertion of carbon dioxide in the B-H bond, generating the formatoborate species, **42**, with tetramethylpiperidinium as counter-cation (Scheme III-10).



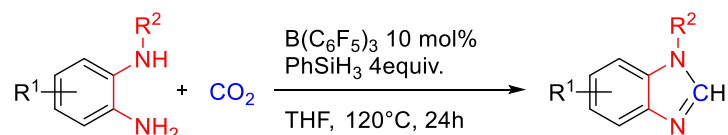
**Scheme III-10** Proposed mechanism for the CO<sub>2</sub> reduction

The subsequent complexation of the tris(pentafluorophenyl)borane on the acyl oxygen generates the diborane intermediate, that it is susceptible to hydride reduction giving the acetal derivatives, that in protic media, decomposes to the corresponding formalborate **s**, and hydroxyborate. Compound **43** possess a high nucleophilicity, it can undergo easily a reduction affording the methanol-borane derivatives **44**. Consequent thermolysis, allowed them to liberate methanol as final product. Only a year later, Piers and co-workers, were able to perform the tandem catalytic deoxygenation of CO<sub>2</sub>, employing the same system aforementioned, with a slight excess of borane, and an excess of triethylsilane, methane was

<sup>155</sup> O. J. Metters, S. J. K. Forrest, H. A. Sparkes, I. Manners, D. F. Wass, *J. Am. Chem. Soc.* **2016**, *138*, 1994–2003.

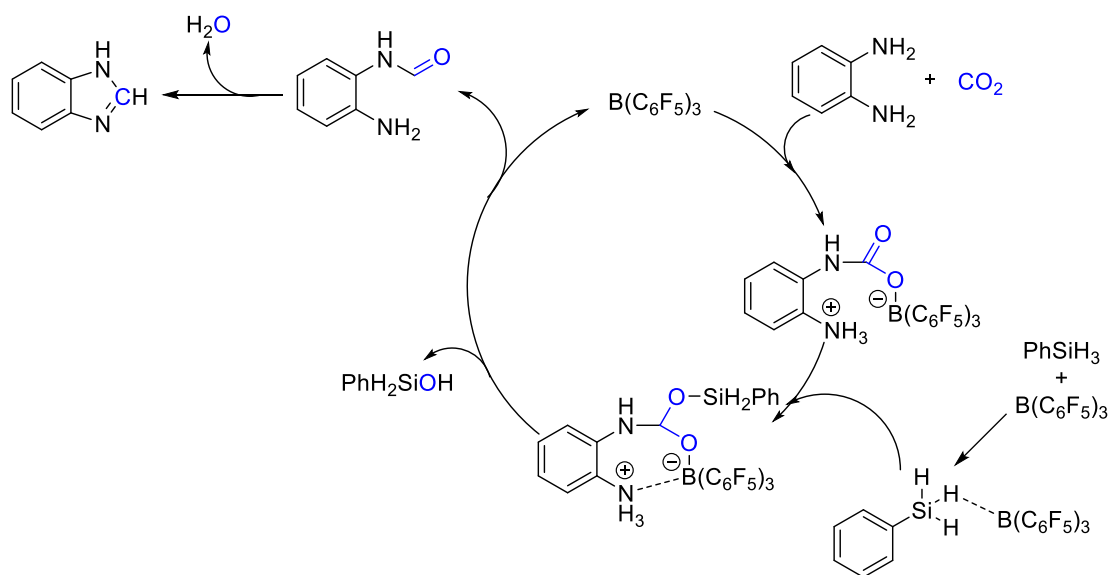
<sup>156</sup> L. J. Hounjet, C. B. Caputo, D. W. Stephan, *Angew. Chem. Int. Ed.* **2012**, *51*, 4714–4717.

obtained.<sup>157</sup> Wang *et al.* were able to obtain a methanol-borane derivative, like **44**, using as catalytic couple  $PtBu_3$  and 9-BBN.<sup>158</sup> It has to be mentioned also, the great work of Sun and co-workers in the diamine cyclization.<sup>159</sup> They started from *ortho*-phenylenediamines and by reduction of  $CO_2$ , they were able to synthesise the corresponding benzimidazoles (Scheme III-11).



**Scheme III-11** General reaction conditions for the synthesis of benzimidazoles

They were able to extend this reaction to different substrates with yields fluctuating between 53% to 95%, containing electron-donor or withdrawing group, with heteroaromatic ring in the backbone and also from unhindered to hindered substituents on the amine group. NMR studies allowed them to postulate of a simple but elegant mechanism (Scheme III-12).



**Scheme III-12** Proposed mechanism for benzimidazoles formation

Starting with the FLP activation of carbon dioxide, the N- $CO_2$ -borane adduct is obtained. Consequent reaction with phenylsilane, previously activated by another molecule of  $B(C_6F_5)_3$ , generate the silyloxy group. Decoordination of the borane and formation of the

<sup>157</sup> A. Berkefeld, W. E. Piers, M. Parvez, *J. Am. Chem. Soc.* **2010**, *132*, 10660–10661.

<sup>158</sup> T. Wang, D. W. Stephan, *Chem. Commun.* **2014**, *50*, 7007–7010.

<sup>159</sup> Z. Zhang, Q. Sun, C. Xia, W. Sun, *Org. Lett.* **2016**, *18*, 6316–6319.

silanol was followed by the generation of the formamide derivatives, that after dehydration and cyclisation, the desired product was achieved.

Other than experimental work, also theoretical calculations were performed in order to understand the activation of carbon dioxide, it has to be mentioned the works of Fontaine and Co-worker,<sup>160</sup> Roy *et al.*<sup>161</sup> and Stephan and co-workers.<sup>162</sup>

FLPs are not only limited to the activation of hydrogen and carbon dioxide, but they can also react with: CO,<sup>163</sup> SO<sub>2</sub>,<sup>164</sup> N<sub>2</sub>O,<sup>165</sup> also applications in radical chemistry with NO, were accomplished.<sup>166</sup>

FLPs were also recently involved in the study of Phospha-Stork<sup>167</sup> and Phospha-Claisen<sup>168</sup> reaction, otherwise quite unknown in the literature.

### III.1.2 NHCs and silicon in Frustrated Lewis Pair chemistry

#### III.1.2.1 Silicon-based FLP

After this introduction to the chemistry of the Frustrated Lewis Pairs, we will emphasize the studies involving silicon and NHCs. The first report of silicon as Lewis acid partner in FLP was proposed by Manners and co-workers,<sup>169</sup> using Me<sub>3</sub>SiOTf and TMP as a base. Although this couple did not split hydrogen, it was able to quantitatively dehydrogenate Me<sub>2</sub>NH\*BH<sub>3</sub> forming trimethylsilane and the piperidinium salt. Silylium ion remains the

---

<sup>160</sup> a) R. Declercq, G. Bouhadir, D. Bourissou, M.-A. Légaré, M.-A. Courtemanche, K. S. Nahi, N. Bouchard, F.-G. Fontaine, L. Maron, *ACS Catal.* **2015**, *5*, 2513–2520. b) M.-A. Courtemanche, M.-A. Légaré, L. Maron, F.-G. Fontaine, *J. Am. Chem. Soc.* **2014**, *136*, 10708–10717.

<sup>161</sup> L. Roy, B. Ghosh, A. Paul, *J. Phys. Chem. A* **2017**, *121*, 5204–5216.

<sup>162</sup> J. J. Chi, T. C. Johnstone, D. Voicu, P. Mehlmann, F. Dielmann, E. Kumacheva, D. W. Stephan, *Chem. Sci.* **2017**, *8*, 3270–3275.

<sup>163</sup> M. Sajid, L.-M. Elmer, C. Rosorius, C. G. Daniliuc, S. Grimme, G. Kehr, G. Erker, *Angew. Chem. Int. Ed.* **2013**, *52*, 2243–2246.

<sup>164</sup> M. Sajid, A. Klose, B. Birkmann, L. Liang, B. Schirmer, T. Wiegand, H. Eckert, A. J. Lough, R. Fröhlich, C. G. Daniliuc, et al., *Chem. Sci.* **2012**, *4*, 213–219.

<sup>165</sup> E. Otten, R. C. Neu, D. W. Stephan, *J. Am. Chem. Soc.* **2009**, *131*, 9918–9919.

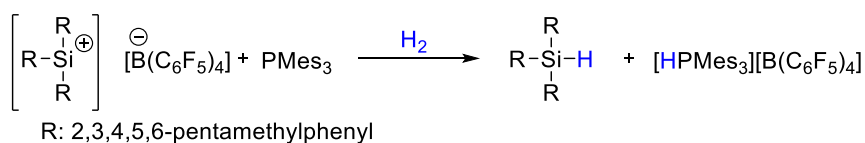
<sup>166</sup> A. J. P. Cardenas, B. J. Culotta, T. H. Warren, S. Grimme, A. Stute, R. Fröhlich, G. Kehr, G. Erker, *Angew. Chem. Int. Ed.* **2011**, *50*, 7567–7571.

<sup>167</sup> Y. Hasegawa, C. G. Daniliuc, G. Kehr, G. Erker, *Angew. Chem. Int. Ed.* **2014**, *53*, 12168–12171.

<sup>168</sup> G.-Q. Chen, G. Kehr, C. Mück-Lichtenfeld, C. G. Daniliuc, G. Erker, *J. Am. Chem. Soc.* **2016**, *138*, 8554–8559.

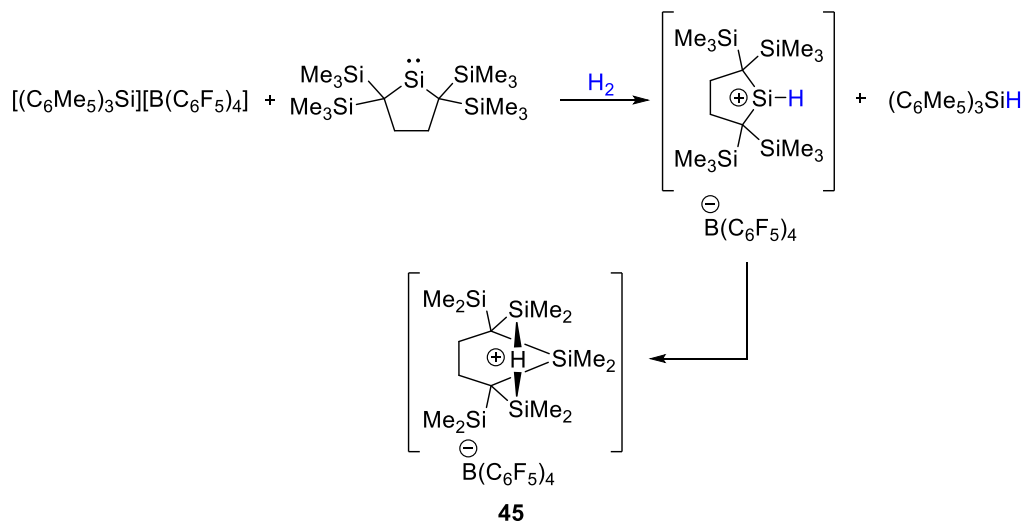
<sup>169</sup> G. R. Whittell, E. I. Balmond, A. P. M. Robertson, S. K. Patra, M. F. Haddow, I. Manners, *Eur. J. Inorg. Chem.* **2010**, *2010*, 3967–3975.

centre of the attention in silicon-based Frustrated Lewis Pairs, and in 2011 Müller and co-workers finally achieved the splitting of hydrogen with this kind of system (Scheme III-13).<sup>170</sup>



**Scheme III-13** Silyl ion split hydrogen

A triarylsilylium stabilized with a borate was prone in the presence of a bulky phosphine to activate hydrogen in an irreversible manner. Later, the Muller's group reported again on the activation of hydrogen and carbon dioxide using different system based on different phosphines. FLP behaviours was observed only when tertbutyl, mesityl and pentafluorophenyl derivatives were used. Moreover, tritertbutyl and tricyclohexyl phosphines also turned out to activate carbon dioxide.<sup>171</sup> The same group of Muller used for the first time a silylene as Lewis base in partnership with a silylium ion (Scheme III-14).<sup>172</sup>



**Scheme III-14** Hydrogen activation and rearrangement of silylium cation

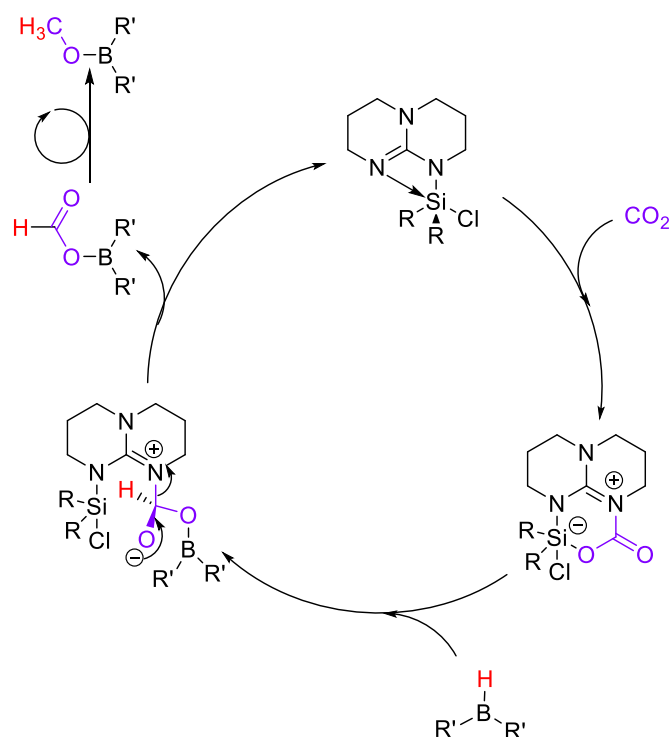
In the scheme III-14, it is shown that the silylene efficiently activates the hydrogen molecule, but the resulting silylium cation due to its instability rearrange in the compound **45**. DFT calculations suggested a mechanism based on a 1,3-methyl group shift which was

<sup>170</sup> A. Schäfer, M. Reißmann, A. Schäfer, W. Saak, D. Haase, T. Müller, *Angew. Chem. Int. Ed.* **2011**, *50*, 12636–12638.

<sup>171</sup> M. Reißmann, A. Schäfer, S. Jung, T. Müller, *Organometallics* **2013**, *32*, 6736–6744.

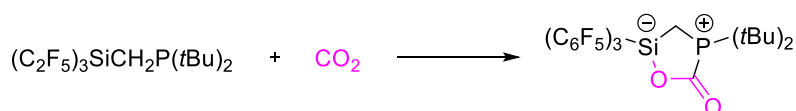
<sup>172</sup> A. Schäfer, M. Reißmann, A. Schäfer, M. Schmidtman, T. Müller, *Chem. – Eur. J.* **2014**, *20*, 9381–9386.





**Scheme III-16** First proposed catalytic cycle

In 2015, Mitzel and co-workers synthesised an intramolecular and neutral silicon-phosphorus FLP able to activate  $\text{CO}_2$  (Scheme III-17). To the best of our knowledge, this system represents the only example of a silicon-based FLP in which the Lewis acid partner is not a silylium but a tetracoordinate silicon species.<sup>176</sup>

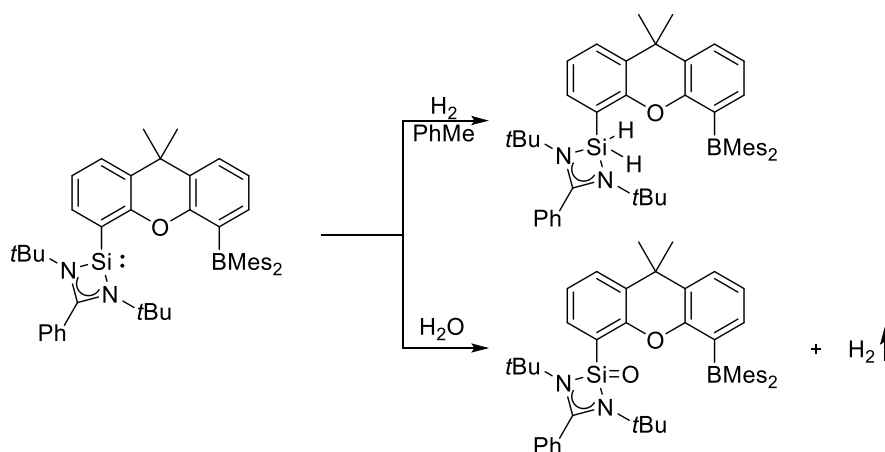


**Scheme III-17** Mitzel's adduct

Recently, Driess and co-workers have reported the activation of small molecules and also the dehydrogenation of water afforded by an intramolecular silylene-borane FLP (Scheme III-18).<sup>177</sup>

<sup>176</sup> B. Waerder, M. Pieper, L. A. Körte, T. A. Kinder, A. Mix, B. Neumann, H.-G. Stammer, N. W. Mitzel, *Angew. Chem. Int. Ed.* **2015**, *54*, 13416–13419.

<sup>177</sup> Z. Mo, T. Szilvási, Y.-P. Zhou, S. Yao, M. Driess, *Angew. Chem. Int. Ed.* **2017**, *56*, 3699–3702.



**Scheme III-18** Hydrogen activation and dehydrogenation of water

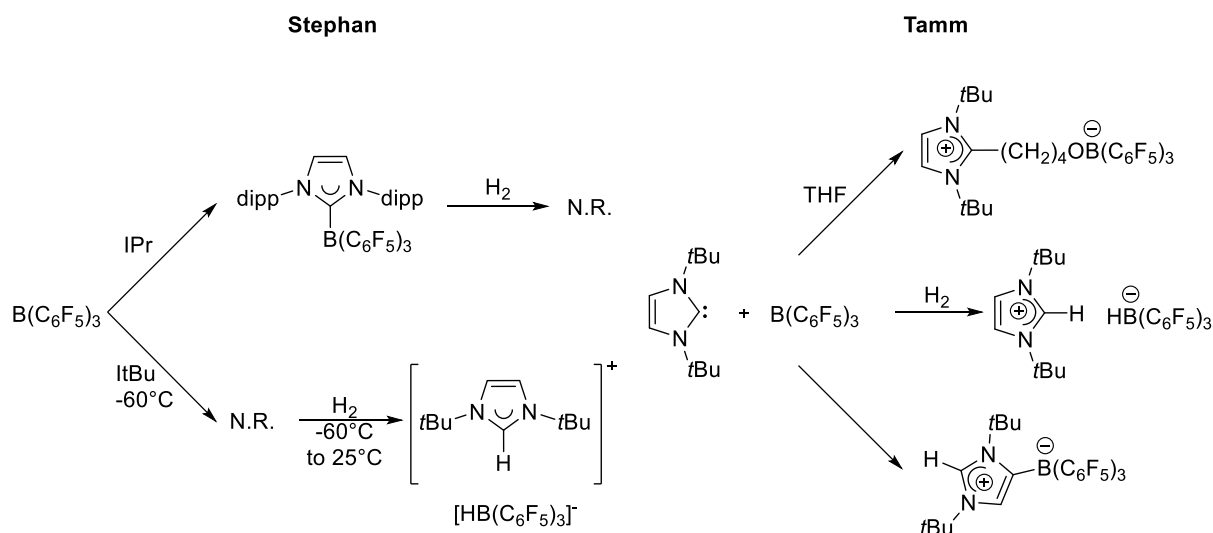
Despite they could not obtain crystal suitable for X-Ray diffraction, High-Resolution NMR studies, allow them the identification of the two compounds. Indeed, proton NMR confirmed the presence of two hydrogens on the silicon atom, however, the presence of a signal at -15 ppm in the boron spectrum, indicates a tetracoordinate species, so a B---H interaction is suggested.

### III.1.2.2 Use of NHC in FLP chemistry

Regarding NHC carbenes, it is well-known that in general, they are more  $\sigma$ -donor and basic than phosphines and it is easy to modify their steric and electronic properties. The possible use of NHCs as partner in FLP chemistry has quickly appeared. In particular Stephan<sup>178</sup> and Tamm<sup>179</sup> independently reported the efficient heterolysis of hydrogen by a carbene-borane FLP system (Scheme III-19).

<sup>178</sup> P. A. Chase, D. W. Stephan, *Angew. Chem. Int. Ed.* **2008**, *47*, 7433–7437.

<sup>179</sup> D. Holschumacher, T. Bannenberg, C. G. Hrib, P. G. Jones, M. Tamm, *Angew. Chem. Int. Ed.* **2008**, *47*, 7428–7432.



**Scheme III-19** First time NHC were employed in FLP chemistry

The first notable difference is the use of two different carbenes in the investigation of Stephan while Tamm concentrated his attention on the ItBu. In the case of Stephan, reaction between borane and IPr generated the simple acid-base adduct that results to be inert towards hydrogen. It is also inactive towards olefins and it decomposed rapidly in solution after sometimes. By contrast, mixing ItBu with  $B(C_6F_5)_3$  at room temperature gave a mixture of products, included some aromatic substitution derivatives. But, if the reaction was performed at  $-60^\circ C$ , no interaction between the two moieties were observed, however, addition of  $H_2$  to the cooled solution resulted in the heterolytic splitting of the gas. On the other side, Tamm reported that this FLP system was able to open THF with the oxygen bonded to the boron and the carbon bonded to the carbene. Purging hydrogen in a toluene solution of the two compounds ended in the heterolytic split of hydrogen, confirming the frustrated behaviour. Unexpected was the result of the last test performed by Tamm, in which NHC and tris(pentafluorophenyl)borane were mixed without a third reactant. In this case, only a product was recovered, resulting to be inactive to hydrogen activation. Additional analysis reveals the formation of an abnormal adduct, where the electrophile is located at the backbone carbon. This particular result encouraged us to consider our compounds as potential FLP partner.

Some years later Hoshimoto *et al.*, were able to synthesise an NHC-borane system that is able to pass from the state of classical Lewis adduct to the state of FLP (Figure III.3).<sup>180</sup>

<sup>180</sup> Y. Hoshimoto, T. Kinoshita, M. Ohashi, S. Ogoshi, *Angew. Chem.* **2015**, *127*, 11832–11837.

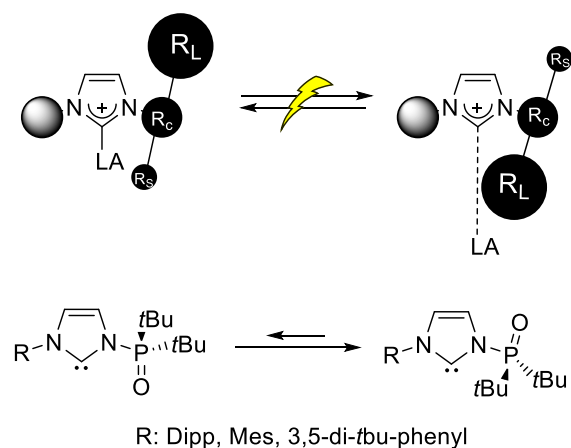
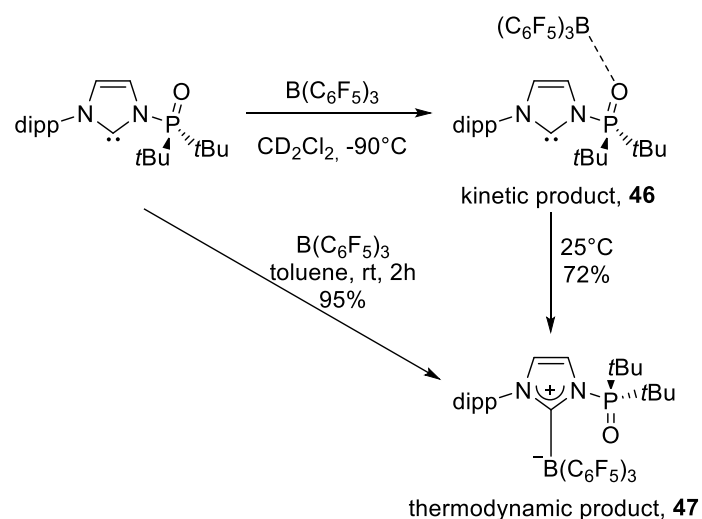


**Figure III.3** Top: classical adduct transformed in FLP; bottom: Hoshimoto's system

Their ideal system has to fulfil these conditions: one nitrogen atom should have a substituent bearing a large group and a small one linked to it. Rotation of the N-central atom bond has to drastically change the spatial environment around the carbene centre. Interconversion from the classic adduct to the FLP had to be stimulated by external source. For this, they synthesised the N-phosphanyl-substituted imidazole (bottom part of scheme III-22). The steric hindrance was evaluated using the percent buried volume, confirming the great spatial difference, from 40 to 50%, plus, theoretical calculation found a rotation barrier of approximately  $12 \text{ kcal mol}^{-1}$ , quite low and accessible. Treatment of the Dipp-derivatives with tris(pentafluorophenyl)borane at  $-90^\circ\text{C}$  in dichloromethane, under kinetic control, resulted in the quantitative conversion in the borane-oxygen coordination product, **46**, that heated at  $25^\circ\text{C}$ , converts in the classical Lewis adduct, **47**. This latter compound can also be obtained directly, thermodynamic control, from a toluene solution of the starting material at room temperature.



**Scheme III-20** Synthesis and conversion of **46** and **47**

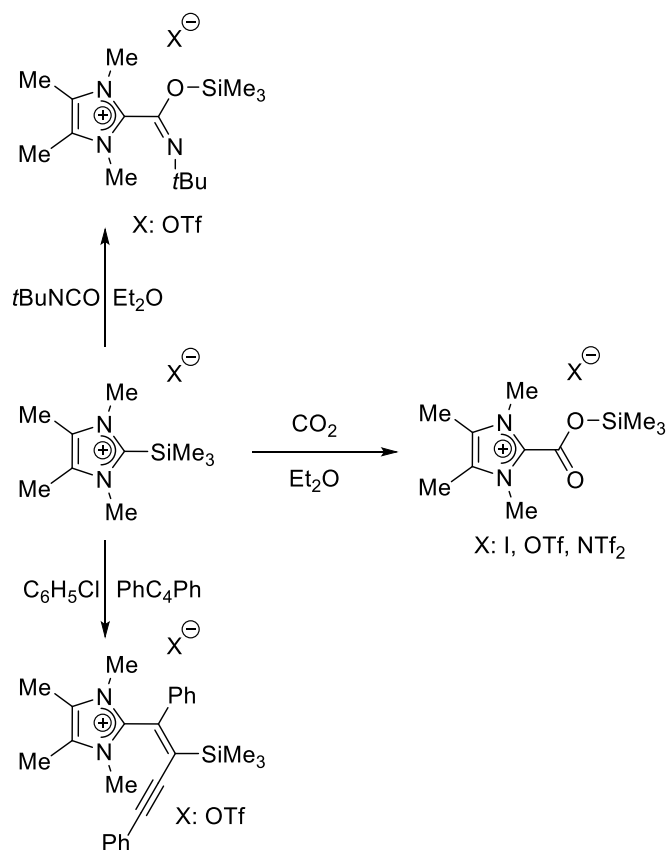
Heterolytic cleavage experiments gave the results expected, indeed at the diminution of the R's group size, Dipp>Mes>3,5-di-*t*butylphenyl, it was necessary to increase the temperature to allow the rotation passing from 60°C to 120°C and consequently H<sub>2</sub> activation.

Other than small molecules, NHC-based FLP systems were able to activate N-H bond generating the corresponding aminoborane,<sup>178</sup> the C-H bond in the case of alkyne, obtaining the corresponding alkyne-borane,<sup>181</sup> and more other.<sup>182</sup>

<sup>181</sup> M. A. Dureen, C. C. Brown, D. W. Stephan, *Organometallics* **2010**, *29*, 6594–6607.

<sup>182</sup> E. L. Kolychev, E. Theuergarten, M. Tamm, in *Frustrated Lewis Pairs II*, Springer, Berlin, Heidelberg, **2012**, pp. 121–155.

In 2015, Tamm and co-workers, succeed in the preparation of the first NHC-silylium FLP system. Starting from the tetramethyl-imidazolyliene, they were able to recover the adduct by reaction with  $\text{Me}_3\text{SiX}$  similarly to the seminal work of Kuhn presented in Chapter 2. This adduct was then employed in different type of reaction that usually works in presence of an FLP system as shown in the following scheme.



**Scheme III-21** FLP behaviour of the NHC-Silylium adduct

To our knowledge, this is the only example of an NHC-Si adduct acting like FLP. however this system was not able to split hydrogen.

## III.2 Results and Discussion

### III.2.1 Assessing the Lewis acidity of the Martin's spirosilane

Before starting the investigation of the potential application of Martin's spirosilane as a Lewis acid partner in FLP chemistry, we intent to measure its Lewis acidity. To do so, the Gutmann-Beckett<sup>183</sup> and the Hilt methods<sup>184</sup> were performed. The first one is based on the evaluation of <sup>31</sup>P NMR chemical shift of a phosphine oxide, between the free form and the coordinated one. The higher is the Lewis acidity, the stronger is the interaction with the phosphine oxide and therefore the more deshielded is the phosphorus as observed by <sup>31</sup>P NMR. The latter method is based on the same principle, quantifying the chemical shift variation, but in this case by means of <sup>2</sup>H NMR chemical shift of the deuterated pyridine. The more the chemical shift of the deuterium goes to low fields (a positive difference), the higher is the acidity. In addition, the Gutmann-Beckett method, give an access to the acceptor number, a parameter for the quantification of the Lewis acidity, calculated with the following formula<sup>185</sup>: AN= [ $\delta(\text{sample})/\text{ppm} - 41.0$ ]\*2.22. The results were reported in the following table III.1.

<i>Lewis Acid</i>	$\delta(^{31}\text{P})/\text{ppm}$	<i>AN</i>
B(C <sub>6</sub> F <sub>5</sub> ) <sub>3</sub>	77.71	81.4
Martin's spirosilane 7	79.05	84.4

**Table III.1** G.-B. Experimental values

Surprisingly, according to the Gutmann-Beckett method, the Lewis acidity of the Martin's spirosilane resulted to be a slightly more acidic than the commonly used B(C<sub>6</sub>F<sub>5</sub>)<sub>3</sub>. The results obtained with the Hilt method seems to be less relevant since the ortho, meta and para chemical shifts differences of the deuterated pyridine are not fully consistent (Table III.2).

<sup>183</sup> a) M. A. Beckett, G. C. Strickland, J. R. Holland, K. Sukumar Varma, *Polymer* **1996**, 37, 4629–4631. b) V. Gutmann, *Donor-Acceptor Approach to Molecular Interactions*, Plenum Press, **1978**. c) V. Gutmann, *Coord. Chem. Rev.* **1975**, 15, 207–237.

<sup>184</sup> G. Hilt, A. Nödling, *Eur. J. Org. Chem.* **2011**, 2011, 7071–7075.

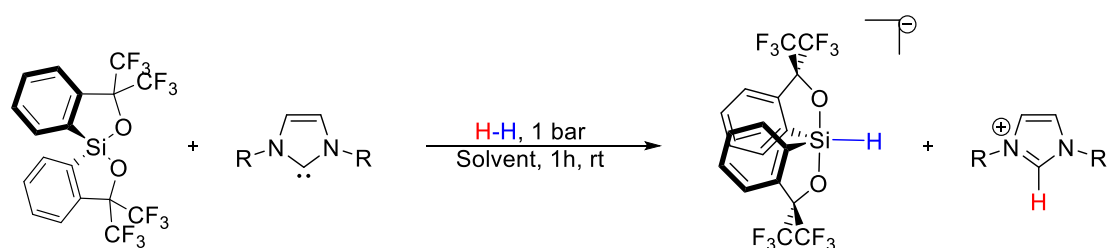
<sup>185</sup> M. A. Beckett, G. C. Strickland, J. R. Holland, K. Sukumar Varma, *Polymer* **1996**, 37, 4629–4631.

	$\delta(^2\text{H})/\text{ppm Ortho}$	$\delta(^2\text{H})/\text{ppm Meta}$	$\delta(^2\text{H})/\text{ppm Para}$
Only Pyridine-d <sub>5</sub>	8.60	7.30	7.69
B(C <sub>6</sub> F <sub>5</sub> ) <sub>3</sub>	8.67	8.26	7.76
Martin's spirosilane <b>7</b>	8.86	7.60	8.10

**Table III.2** Hilt experimental values; deuterium naturally present in CH<sub>2</sub>Cl<sub>2</sub> used as ref.: 5.30 ppm

### III.2.2 Attempts to split hydrogen

As aforementioned in Chapter II, the steric demand of the Martin's spirosilane is high since it does not interact in a classical way with IPr and ItBu NHCs. Furthermore, its Lewis acidity seems to be comparable to that of B(C<sub>6</sub>F<sub>5</sub>)<sub>3</sub>. These two features prompt us to study the reactivity of this electron-deficient silicon derivatives in some diagnostic reactions. We first focused to the challenging activation of hydrogen, using the different NHC carbenes, in deuterated toluene or dichloromethane. Splitting of hydrogen should give rise to the formation of the hydrosilicate and the imidazolium as depicted in scheme III-22.



**Scheme III-22** General H<sub>2</sub> activation scheme in mild condition

In chapter I it was mentioned that the hydride derivatives of **1**,<sup>38</sup> is characterised by <sup>1</sup>H NMR by a broad singlet around 5.3 ppm. Unfortunately, in all the preliminary attempts carried out, although the protonation of the different carbenes occurred and the hydrogen signal is present, no singlet around 5.3 ppm was evidenced by <sup>1</sup>H NMR. Each times the major product probably corresponded to the hydroxysilicate derivatives with the corresponding imidazolium as counter-cation. The same compounds were observed after just ten minutes of reaction. In order to corroborate the hydroxy formation theory, a drop of water was added to an NMR tube containing a mixture of NHC and **1**.

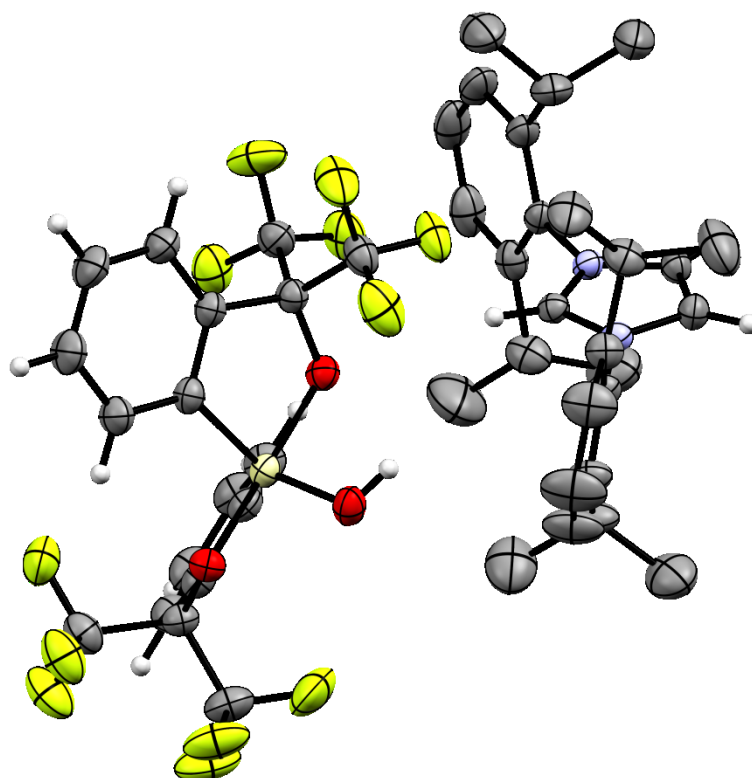


**Figure III.4** ORTEP representation of **48**, ellipsoid 50% of probability

Crystals were obtained by slow evaporation of the organic phase, allowing us to obtain the structure of the proposed compound **48**. It was also possible to obtain the same compound by bubbling air in the starting mixture. At this point, it was obvious that our system is highly sensitive to water and the purity of the gas and solvent is a critical issue. A Karl-Fischer test was performed on the different reaction components, with the purpose of locating the source of water and to quantify it. It turned out that, while the solvents and the solid reactant possess a negligible content of water, <2 ppm, addition of H<sub>2</sub>, increase the quantity of water from less than 2 ppm to more than 70 ppm. It was therefore, necessary to dry the gas.

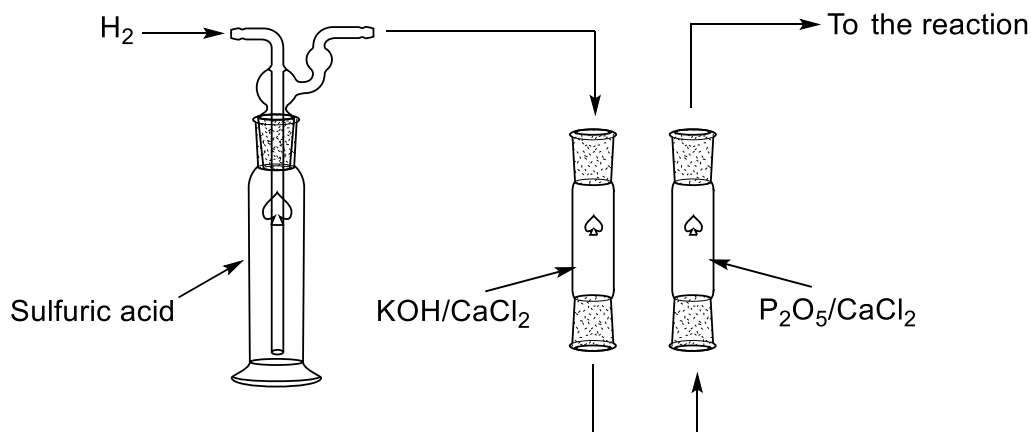


**Figure III.5** Gas drying system

The drying system was divided into three steps: first is the passage through sulfuric acid, then through a pad of KOH, to eliminate the possible acidic impurities, and a pad of activated calcium chloride and finally to a pad of phosphorus pentoxide and again on activated calcium chloride. Finally having presumably drier H<sub>2</sub> at our disposal, new experiments were carried out.

This time it was decided to change in a more radical manner the conditions, tests were performed at high pressure up to 50 bar and also by increasing the temperature up to 110°C. In order to do this reaction different techniques were employed, from the use of J-Young NMR tube and also sealed tubes. In the case where an NHC was used as basic partner, the hydroxy form was recovered together with the corresponding normal or abnormal adducts. However, it was noticed that the formation of the unwanted compound was slower than before. In accordance with this result it was decided to check other Lewis bases as the: P(iPr)<sub>3</sub>, P(tBu)<sub>3</sub> and also superbase as the BEMP and the Verkade-iPr. All these bases did not interact with the Martin's spirosilane as monitored by <sup>1</sup>H NMR (see experimental part)

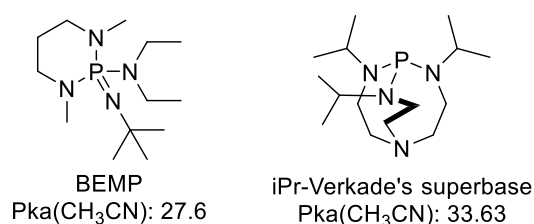
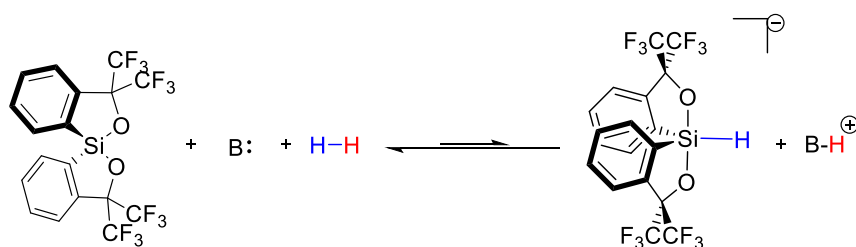


**Figure III.6** Superbase used in this study

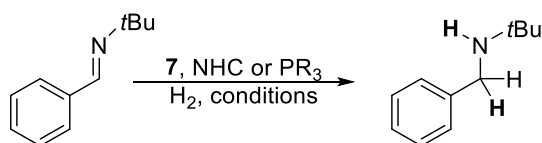
Regardless the variation of the substrates and conditions it was not possible to obtain the compounds formed by hydrogen splitting.

It could be possible that our system are able to perform the heterolytic splitting of the hydrogen, but the resulting compounds are not stable or perhaps an equilibrium would operate not in favour of the ionic pair (Scheme III-23).



**Scheme III-23** H<sub>2</sub> splitting equilibrium

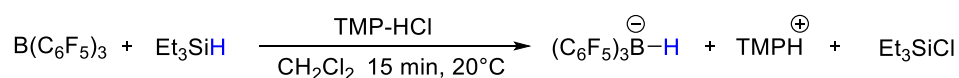
With the purpose to corroborate this theory, hydrogenation reactions were performed, engaging N-benzylidene-*tert*-butylamine as substrate.<sup>186</sup>



**Scheme III-24** hydrogenation reaction

All the Lewis bases show to this point were engaged in this investigation with catalytic or stoichiometric amounts of both Lewis partners. The reaction was carried out in toluene, dichloromethane or bromobenzene with various temperature and pressure in a range from room temperature to 110°C and from 1bar to 50 bar. However, in all the case, no hydrogenated compounds were obtained.

Due to the disappointing results obtained with the molecular hydrogen, it has been decided to get the desired ionic pair via an “indirect” route.<sup>187</sup> Indeed, it is known that in the presence of triethylsilane and a protonated form of a Lewis base (phosphine or amine),  $B(C_6F_5)_3$  react to afford an ionic pair composed of the protonated base and the borohydride (Scheme III-25).



**Scheme III-25** Reaction with  $Et_3SiH$  as hydride donor

Unfortunately, although we could reproduce this reaction with  $B(C_6F_5)_3$ , the desired product using the Martin’s spiro silane could not be obtained. From all this set of results, it seems that this silane is not prone to abstract an hydride from weak hydride-donors.

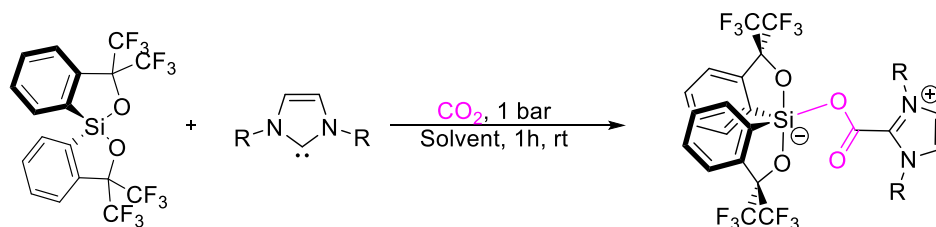
<sup>186</sup> P. A. Chase, T. Jurca, D. W. Stephan, *Chem. Commun.* **2008**, 0, 1701–1703.

<sup>187</sup> V. Morozova, P. Mayer, G. Berionni, *Angew. Chem. Int. Ed.* **2015**, 54, 14508–14512.

### III.2.3 Attempts to activate carbon dioxide

Due to the frustrating results obtained with H<sub>2</sub>, we turned our attention to the activation of carbon dioxide.

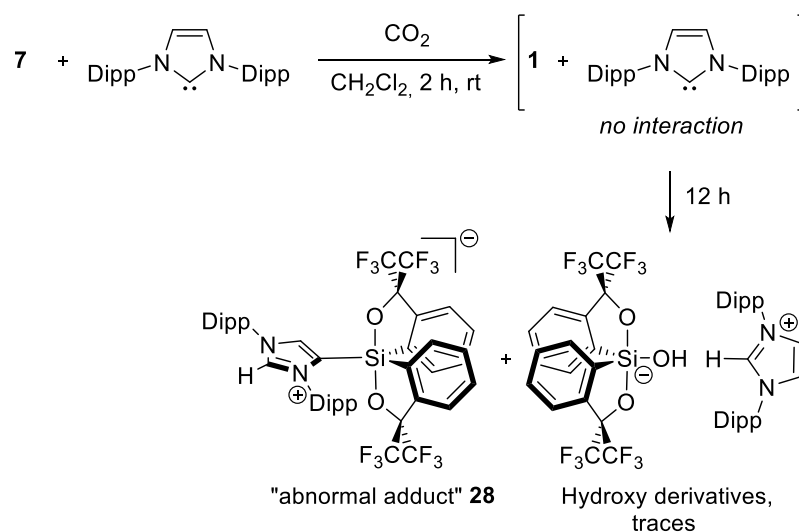
Similarly to the previous study it was followed a logical order of investigation, starting from the simple test in an NMR tube.



**Scheme III-26** General CO<sub>2</sub> activation scheme in mild condition

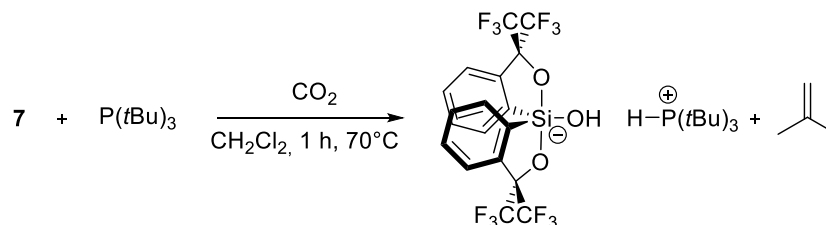
Once again after just only ten minutes at room temperature, the hydroxy form was observed. It was then realized a drying gas apparatus similar to that of the hydrogen but without KOH to avoid the possible carbonation process. The reactions were repeated expanding also the Lewis base used and the condition, and in this case, some interesting result were obtained.

Indeed in the majority of the cases, it was obtained the hydroxy form of our reactants. When IPr was employed, in a dichloromethane solution, no interactions were noticed at all, even after some hours of reaction and at the end, the abnormal adduct was obtained with trace of the hydroxysilicate (Scheme III-27).



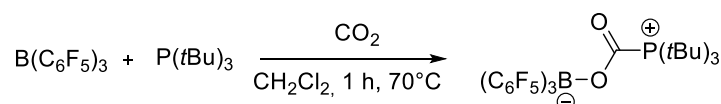
**Scheme III-27** Activation of CO<sub>2</sub> with IPr and 7

The same behaviour was observed, always in dichloromethane, with P(tBu)<sub>3</sub>, noticing the formation of the hydroxy siliconate only after 7 h at 70°C, along with the generation of isobutene due to the reaction between of phosphine with the resulting phosphonium (Scheme III-28).



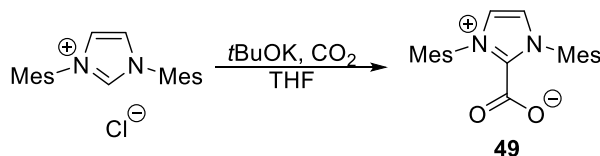
**Scheme III-28** Attempt the activation of carbon dioxide with phosphine

The experiments with the borane was reproduced, and this time the reaction with CO<sub>2</sub> in presence of P(tBu)<sub>3</sub> gave the expected product CO<sub>2</sub> adduct (Scheme III-29).



**Scheme III-29** Activation of carbon dioxide with borane and phosphine

Likewise the hydrogenation, an indirect route was attempted. Following the example of Doung *et al.*,<sup>188</sup> the carboxylate derivatives of IMes, **49**, was synthesised (Scheme III-30).



**Scheme III-30** Synthesis of **49**

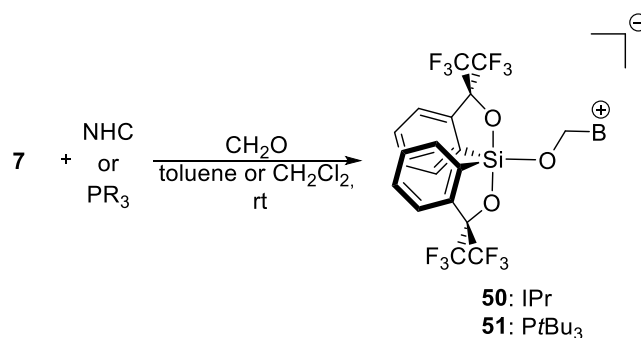
With the addition of **49** in the reactional environment, what was expected was the product derived from the nucleophilic attack of the oxygen on the silicon centre. However, no interaction was observed even after several hours at higher temperature, despite Martin's spirosilane is known to readily interacts with carboxylate.<sup>189</sup>

<sup>188</sup> H. A. Duong, T. N. Tekavec, A. M. Arif, J. Louie, *Chem. Commun.* **2004**, 112–113.

<sup>189</sup> These Hugo Lenormand, *Synthese et Utilisation de Compose Spiranique Silyle comme Sonde a Fluorures*, Universié Pierre et Marie Curie, **2012**

### III.2.4 Reaction with formaldehyde

Inspired by the work of Gabbai and co-workers,<sup>190</sup> in which they were able to activate paraformaldehyde with an antimony complex bearing a phosphine in a vicinal position, it was decided to perform the same type of reaction with our system, albeit in intermolecular fashion. This time, the expected products were obtained and it was possible to isolate them when IPr or P(*t*Bu)<sub>3</sub> were used as the base Lewis partners.



**Scheme III-31** General scheme for the formaldehyde activation

The reactions were performed by mixing the Lewis acid and the Lewis base in 1:1 ratio and paraformaldehyde in excess. Purification by subsequent precipitation afforded the two products in good yield, **50**: 59% and **51**: 61%. The proton NMR displays the presence of two signals typical of diastereotopic hydrogens, two doublets with a “roof effect”, ascribable to the two protons of the methylene (Figure III.7). This is a result of stereogenicity of the pentavalent silicate at the NMR time scale, as it will be discussed in chapter 5.

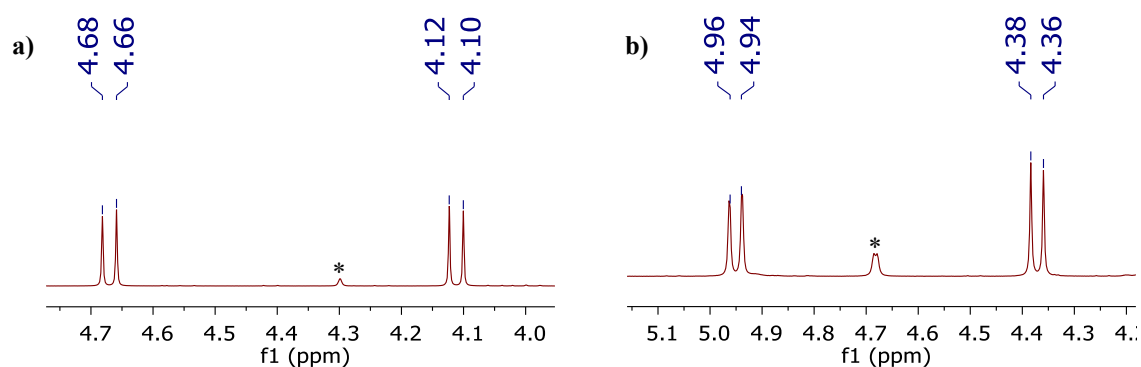


**Figure III.7** Particular of the <sup>1</sup>H NMR spectra of **50** (a) and **51** (b); \*: paraformaldehyde.

It is interesting to notice, once again, the loss of symmetry of the methyl of IPr, in this case with four different signals. Silicon NMR signals felt, as expected, in the typical area of

<sup>190</sup> D. Tofan, F. P. Gabbai, *Chem. Sci.* **2016**, 7, 6768–6778.

pentacoordinate species, -76.8 ppm for **50** and -76.7 for **51**. Moreover, as expected the phosphorus signal of the phosphonium was deshielded, compared to that of the free phosphine. Gratifyingly, we could obtain suitable crystals for the X-Ray diffraction of the compound **51**, here presented (Figure III.8).

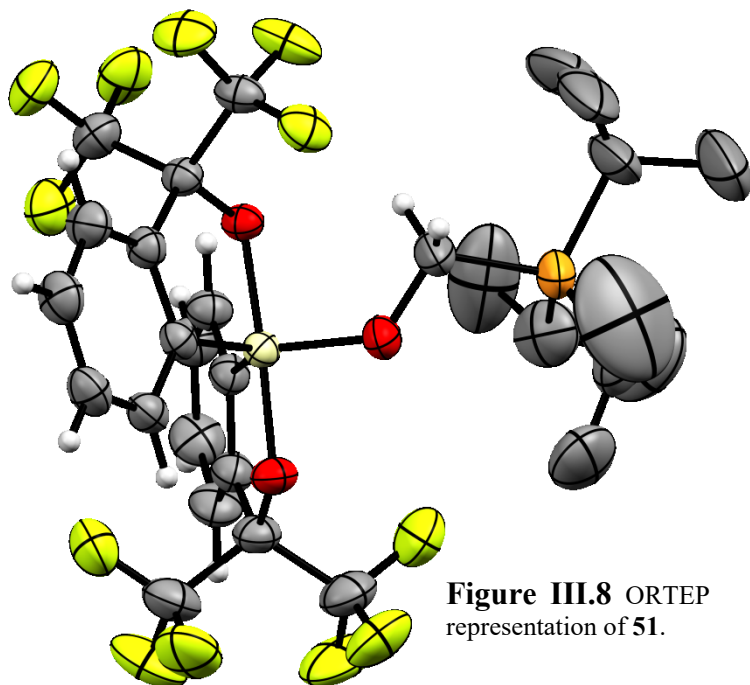


**Figure III.8** ORTEP representation of **51**.

The system belongs to the orthorhombic space group  $Pna2_1$ , the asymmetric unit contains three molecules of compound **51**, two are omitted for clarity. Again the silicon atom possesses a trigonal bipyramid geometry. The Si-O(apical) bond length, 1.80 Å, is comparable of that found in the NHC-Si adduct of the previous chapter, while the angle formed between the two

apical oxygen,  $176.71^\circ$ , is comparable with that of IMes-Martin adduct **27**. Regarding the equatorial oxygen it was observed a Si-O distance about 1.68 Å, that is longer compared with the average bond length, 1.63 Å, on the other side the O-C and C-P distances felt in the standard lengths. The reaction with ItBu and paraformaldehyde give the desired product mixed with other different impurities, in a non-negligible quantity, that we could not separate. Despite this, in one attempt of purification one single crystal of one of these different compounds was obtained. Surprisingly, the crystal was the desired compound, **52** (Figure III.9).

It belongs to the monoclinic  $Cc$  space group, with a trigonal bipyramid geometry, as the previous examples, we found a distance silicon apical oxygen of 1.80 Å, while the angle is about  $173.61^\circ$ , due to the major steric encumbrance of the carbene compared to that of the phosphine. The distance between the silicon atom and the equatorial oxygen is of 1.676 Å, similar to that of **51**, also with the O-C bond, 1.419 Å, the C-C bond result to be around 1.49 Å, slightly less than the average carbon-carbon single bond, evidence of a strong interaction.

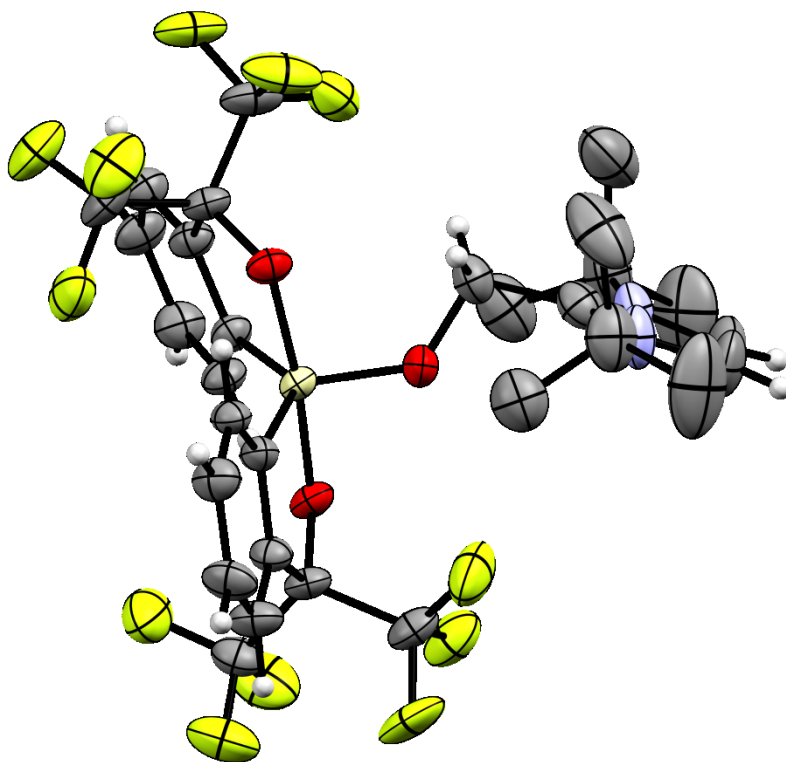
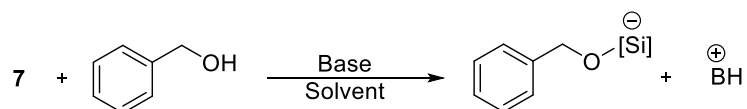


**Figure III.9** ORTEP representation of **52**

Recently, Ghattas *et al.*,<sup>191</sup> reported the activation of formaldehyde by the well-known Frustrated Lewis Pair,  $PtBu_3/B(C_6F_5)_3$ , able to activate hydrogen.<sup>192</sup>

### III.2.5 Reaction with benzyl alcohol

It was also investigated the ability of Martin's spiro-silane to coordinate benzyl alcohol in presence of weak bases as the 2,2,6,6-tetramethylpiperidine (TMP),  $pK_a = 11.07$ , or with  $PtBu_3$ ,  $pK_a = 11.40$ , in order to obtain the benzyloxysiliconate (Scheme III-32).



**Scheme III-32** General synthesis for the benzyloxysiliconate

<sup>191</sup> G. Ghattas, C. Bizzarri, M. Hölscher, J. Langanke, C. Gürtler, W. Leitner, M. A. Subhani, *Chem. Commun.* **2017**, 53, 3205–3208.

<sup>192</sup> G. C. Welch, D. W. Stephan, *J. Am. Chem. Soc.* **2007**, 129, 1880–1881.

The first test was performed with TMP and due to the precedent experiments, deuterated toluene was chosen as solvent. The NMR studies performed confirmed the presence of only the product **53**.

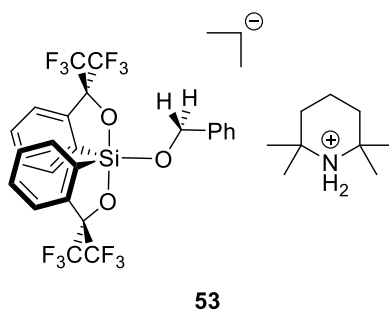


**Figure III.10** Representation of **53**

The  $^1\text{H}$  NMR showed the presence of two diastereotopic protons, ascribable to the benzylic position, confirming the formation of the alcoholate Martin adduct.

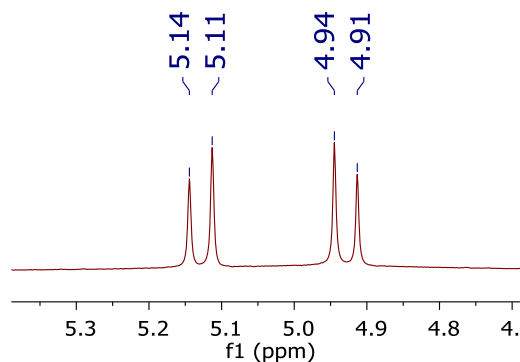


**Figure III.11**  $^1\text{H}$ NMR of **53**; clearly visible the roof effect

The same reaction was performed with tris(tert-butyl)phosphine as base, and in this case, a precipitate was formed after one hour. After isolation and dissolution in deuterated dichloromethane, a characterisation by NMR spectroscopy was possible. Likewise the last example, the typical diastereoisomeric doublet was present, and, the appearance of a doublet, with a constant of 437 Hz, ascribable to the P-H proton, confirmed the structure of **54** (Figure III.12).

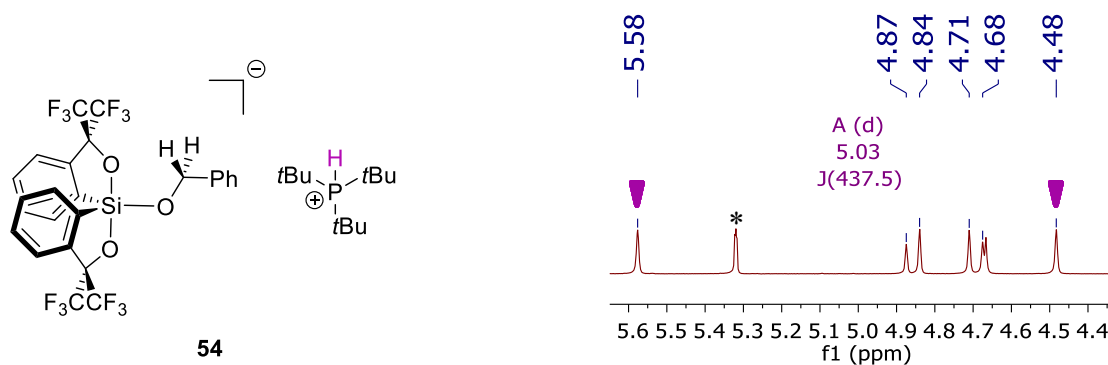
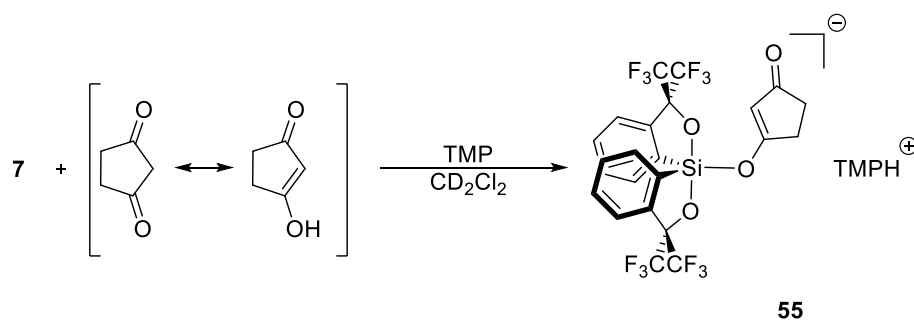


**Figure III.12** Representation of **54**;  $^1\text{H}$  NMR spectra highlighting the two benzylic protons, and the doublet corresponding to the P-H (purple triangles); \*  $\text{CD}_2\text{Cl}_2$

### III.2.6 Reaction with 1,3-cyclopentadione

After it was ascertained the ability of **7** to coordinate alcohol and aldehyde, it has been decided to test it with diones.



**Scheme III-33** Synthesis of **55**

1,3-cyclopentadione was used as sample molecule. From the NMR it was confirmed the presence of two product. The minor product can be assigned to the hydroxy form of Martin's spirosilane, while the compound in majority from preliminary analysis seems the product expected. By slow evaporation of the mixture, suitable crystals for X-Ray diffraction were obtained (Figure III.13).

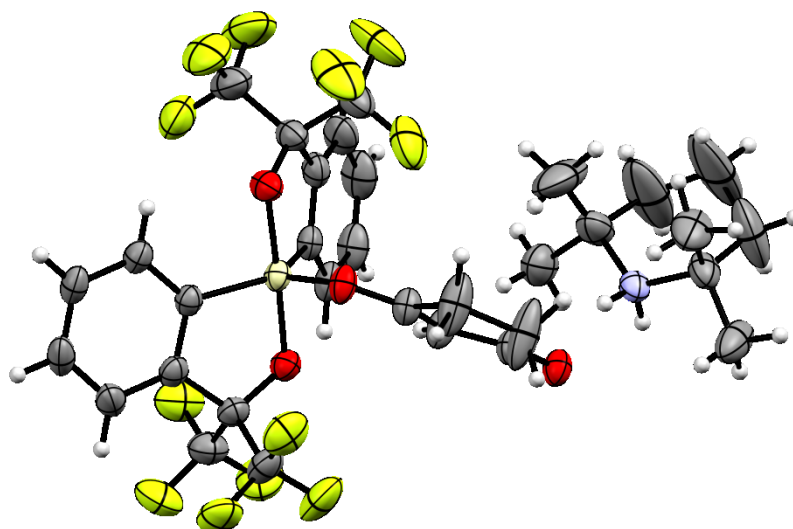


**Figure III.13** ORTEP representation of **55**, ellipsoid 50% of probability.

The system belongs to the monoclinic  $P2_1/n$  space group, and once again silicon is in a TBP configuration. Similar to the previous structure, the Si-O (apical) bond length is 1.778 Å while the angle O-Si-O is about 177.4°. the Si-O (equatorial) distance is about 1.73 Å much longer compared to the adducts **51** and **52**. As expected the coordination of **7** affected the C-O bond length with a value of 1.30 Å, the other carbonyl has a C-O distance of 1.25 Å nearer the average distance of 1.20 Å. The double bond character between the carbon and the central carbon was confirmed by a distance of 1.35 Å. A more in depth analysis of the system suggests the presence of a possible resonance as shown in the following schema.

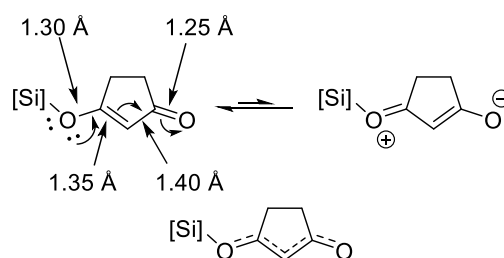


**Figure III.14** Proposed resonance equilibrium

The steric hindrance generates a dihedral angle, between the equatorial plane and the plane containing the cyclopentanedione, about  $-35.89^\circ$ .

In conclusion, Martin's spiroasilane in presence of hindered Lewis bases proved to be able to activate molecules such as aldehydes, enol and alcohol. Moreover, the presence of diastereotopic protons in these adducts confirms the prochirality of the siliconate moiety and could open the way to new applications. Although this result suggests a potential as Frustrated

Lewis partner, the activation of more challenging hydrogen and carbon monoxide gave for the moment negative results. The use of Martin's spiro silane analogues with a higher Lewis acidity could be a way to achieve such reactions.

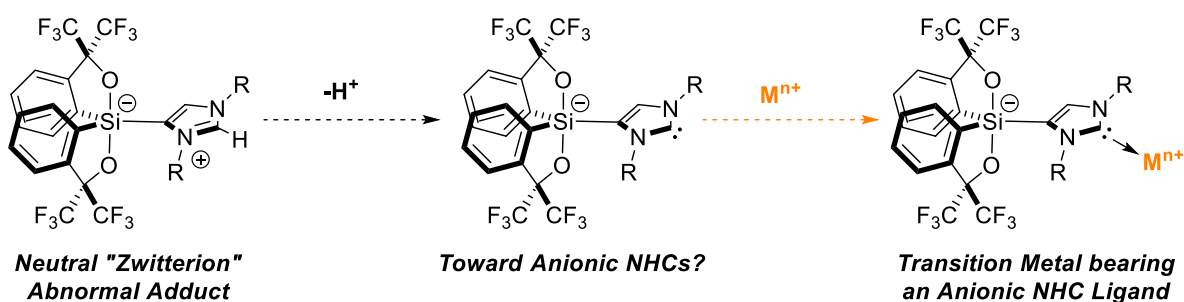


**Chapter IV**  
**Anionic NHC Carbenes Bearing a**  
**Siliconate Moiety**



## IV. Anionic NHC Carbenes Bearing a Siliconate Moiety

As it was presented in the chapter II, the interactions between NHCs and Martin's spirosilane could lead to abnormal adducts when the steric demand of the Lewis base is high. These abnormal adducts are neutral species that could be regarded as imidazolium rings functionalized by a weakly coordinating anionic NHC carbene. It prompted us to have a closer look the possibility to use them as precursors of anionic NHCs.



**Scheme IV-1** From abnormal adduct to anionic NHC ligand

## IV.1 Anionic NHC Carbene : from Synthesis to Metals Coordination and Catalysis

From their name, it is evident that anionic carbenes are carbenes possessing an overall negative charge. The first report of such species dated back to 1990 by Fehlhhammer and co-workers (Figure IV.1),<sup>193</sup> but it is only during the last decade that these compounds have drawn a deeper attention in chemistry.

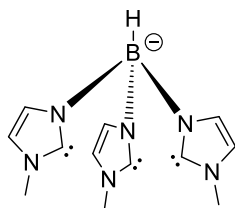
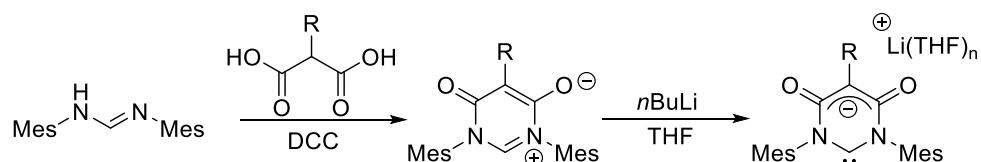


**Figure IV.1** Fehlhhammer's anionic NHC

Indeed, by now it exists a large library of anionic NHCs possessing different negatively charged atoms or groups such as oxygen derivatives,<sup>194</sup> aluminium-based moieties,<sup>195</sup> imidazolium phosphanide,<sup>196</sup> borane derivatives<sup>197</sup> or gallium.<sup>198</sup>

In 2008 the group of Lavigne described the synthesis of a *malocarbene* starting from a derivatives of the malonic acid (Scheme IV-2).<sup>199</sup>



**Scheme IV-2** Synthesis of the *malo*NHC

<sup>193</sup> U. Kernbach, M. Ramm, P. Luger, W. P. Fehlhhammer, *Angew. Chem. Int. Ed. Engl.* **1996**, *35*, 310–312.

<sup>194</sup> L. Benhamou, V. César, H. Gornitzka, N. Lugan, G. Lavigne, *Chem. Commun.* **2009**, *0*, 4720–4722.

<sup>195</sup> Y. Wang, Y. Xie, M. Y. Abraham, P. Wei, H. F. Schaefer, P. v. R. Schleyer, G. H. Robinson, *J. Am. Chem. Soc.* **2010**, *132*, 14370–14372.

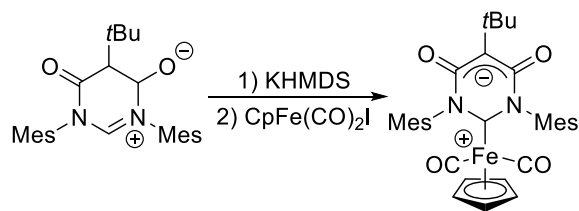
<sup>196</sup> P. K. Majhi, G. Schnakenburg, Z. Kelemen, L. Nyulaszi, D. P. Gates, R. Streubel, *Angew. Chem. Int. Ed.* **2013**, *52*, 10080–10083.

<sup>197</sup> S. Kronig, E. Theuergarten, C. G. Daniliuc, P. G. Jones, M. Tamm, *Angew. Chem.* **2012**, *124*, 3294–3298.

<sup>198</sup> a) G. Schnee, O. Nieto Faza, D. Specklin, B. Jacques, L. Karmazin, R. Welter, C. Silva López, S. Dagorne, *Chem. – Eur. J.* **2015**, *21*, 17959–17972. b) M. Uzelac, D. R. Armstrong, A. R. Kennedy, E. Hevia, *Chem. – Eur. J.* **2016**, *22*, 15826–15833.

<sup>199</sup> V. César, N. Lugan, G. Lavigne, *J. Am. Chem. Soc.* **2008**, *130*, 11286–11287.

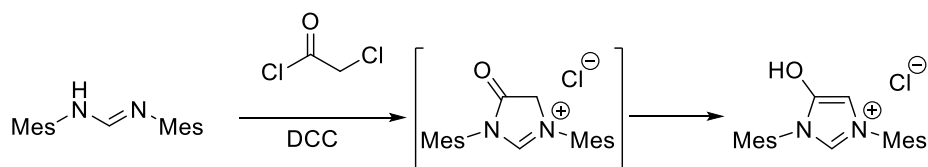
In order to study the electronic properties of the anionic carbene, a metal carbonyl complex was synthesised starting from  $\text{CpFe}(\text{CO})_2\text{I}$  (Scheme IV-4).



**Scheme IV-3** Synthesis of the iron(I) derivatives

Investigations of the TEP value showed that the *malon*NHC is more donor than the IMes or the SIMes carbene.

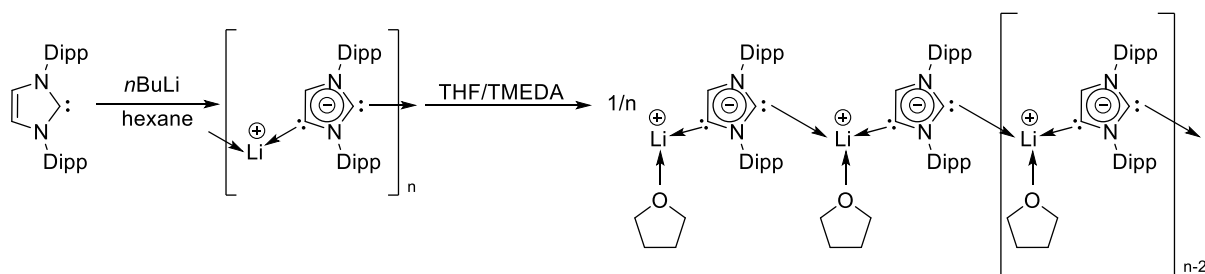
Lavigne's group also reported the synthesis of a five-member enolate NHC derivative (Scheme IV-4).<sup>200</sup>



**Scheme IV-4** Synthesis of the enol-NHC

The enol-imidazolium derivatives can be easily deprotonated by two equivalents of LiHMDS, one equivalent for the deprotonation of the alcohol and one for the deprotonation of the carbenic carbon. The obtained lithium salt can give access to different species, e.g. reaction with sulfur or  $[\text{Rh}(\text{COD})\text{Cl}]_2$ . They also demonstrated how the oxygen moiety can be post-functionalised to obtain silylether derivatives and more.

In 2010, by treatment of IPr with *n*BuLi, Robinson could obtain bis-carbene lithium derivative as a polymer (Scheme IV-5).<sup>201</sup>



**Scheme IV-5** Synthesis of the anionic NHC dicarbene

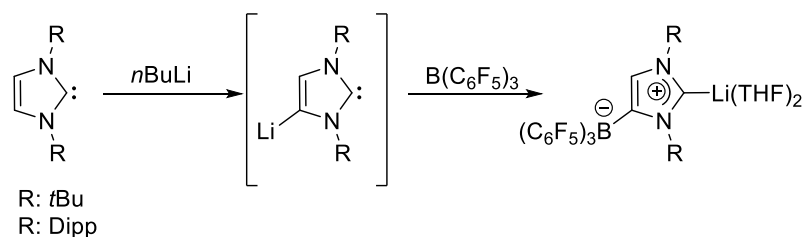
<sup>200</sup> L. Benhamou, V. César, H. Gornitzka, N. Lukan, G. Lavigne, *Chem. Commun.* **2009**, 0, 4720–4722.

<sup>201</sup> Y. Wang, Y. Xie, M. Y. Abraham, P. Wei, H. F. Schaefer, P. v. R. Schleyer, G. H. Robinson, *J. Am. Chem. Soc.* **2010**, *132*, 14370–14372.

More in-depth analysis and calculations highlighted that the positive charge is concentrated on the lithium atom and the HOMO and HOMO+1 orbitals corresponding to the Li-C bonds, suggesting the anionic character of the carbenic moiety.

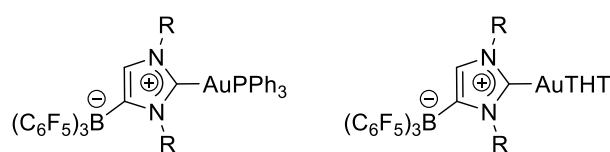
This latter enunciation was proved by reaction between the polymeric dicarbene and different Lewis acids like  $\text{BEt}_3$ ,  $\text{AlMe}_3$  and  $\text{Me}_3\text{SiCl}$  obtaining the abnormal adduct, neutral in the case of the silicon derivatives.

Inspired by the work of Robinson, Tamm and co-workers treated ItBu and IPr with  $n\text{BuLi}$ , followed by addition of  $\text{B}(\text{C}_6\text{F}_5)_3$ , generating the anionic carbene products as their lithium salts (Scheme IV-6).<sup>197</sup>



**Scheme IV-6** Synthesis proposed by Tamm

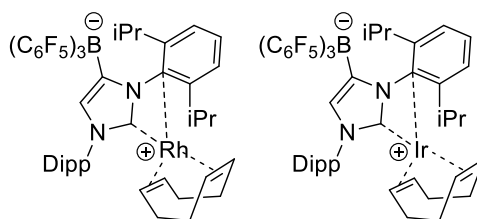
In  $^{13}\text{C}$  NMR, the carbenic carbon possesses a chemical shift between 210 and 220 ppm, a little bit more shielded than the starting carbenes. These two lithiated compounds were used in subsequent transmetalations with transition metals. Indeed the two anionic carbenes in presence of gold(I) chloride precursors such as  $\text{PPh}_3\text{AuCl}$  or  $\text{THTAuCl}$  gave the corresponding derivatives. The NHC-Au(I)THT complex resulted also to be an excellent catalyst for the skeletal rearrangement of enynes.



**Scheme IV-7** Anionic carbene Gold(I) derivatives

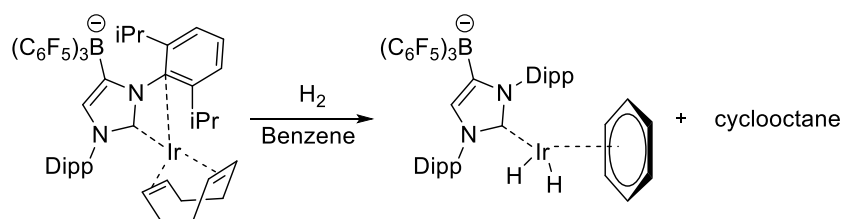
A year later, Tamm and co-workers also reported on the synthesis of Rh(I) and Ir(I) complexes using the same lithium derivatives (R=Dipp). The synthetic pathway is the same showed in the previous work, but this time,  $[\text{Rh}(\text{COD})\text{Cl}]_2$  and  $[\text{Ir}(\text{COD})\text{Cl}]_2$  were used as metal precursors. In both cases, an important shielding of the carbenic carbon signal, compared to the corresponding normal complexes, was observed suggesting a strong

$\sigma$ -donation by the anionic moiety. It was noticed a loss of equivalence for the *ipso*-carbon of the Dipp substituents that generate two distinct signals, one of them is a broad singlet representing a likely metal-arene interaction.



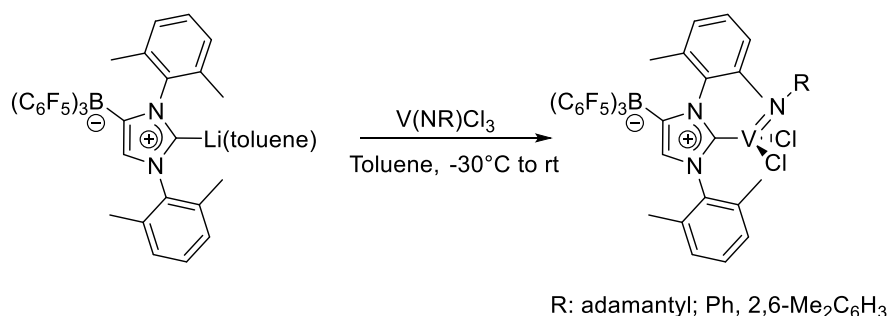
**Scheme IV-8** Rh(I), Ir(I) complexes synthesised by Tamm and co-workers

The catalyst activity of iridium(I) complex in hydrogenation reaction was regarded by analogy with the Crabtree hydrogenation catalyst  $[\text{Ir}(\text{COD})(\text{py})(\text{PCy}_3)\text{PF}_6]$ .<sup>202</sup> In the presence of dihydrogen, cyclooctane is released with the consequent formation of the dihydro complex (Scheme IV-9). This complex proved to be able to hydrogenate also internal alkenes whereas the Crabtree catalyst cannot.



**Scheme IV-9** Formation of the dihydro complex

Another example was the one reported by Igarashi and Tamm, in which a vanadium(V) complex bearing a NHC carbene with a  $\text{B}(\text{C}_6\text{F}_5)_3$  on the backbone (Scheme IV-10).<sup>203</sup>



**Scheme IV-10** Synthesis of the Igarashi's vanadium(V) complex

<sup>202</sup> R. H. Crabtree, H. Felkin, G. E. Morris, *J. Organomet. Chem.* **1977**, *141*, 205–215.

<sup>203</sup> A. Igarashi, E. L. Kolychev, M. Tamm, K. Nomura, *Organometallics* **2016**, *35*, 1778–1784.

From X-Ray investigations, the authors could evince that the V-C<sub>carbene</sub> distance is shorter than other NHC-Vanadium complexes, indicating of a strong  $\sigma$ -donation from the anionic NHC. Moreover, the V-Cl distance is also shorter than the average, indicating a high  $\pi$ -donation from the chloride to the vanadium centre. These two observations attested the high electrophilicity of the metallic centre. The complex just presented was chosen as catalyst in olefin polymerisations, because the reactive species in this kind of reactions are stabilised by  $\sigma$  and  $\pi$ -donor ligands. They successfully performed the ethylene polymerisation in the presence of the vanadium catalyst with aluminium derivatives as cocatalyst. It is noteworthy that the aluminium derivatives in presence of the more common polymerisation catalysts like metallocenes are inefficient. In contrast they had a remarkable catalytic activity coupled with the anionic NHC catalyst of Igarashi. This behaviour was rationalised as a result of the high stabilisation of the formally cationic alkyl species by the weakly coordinating anion NHC.

In summary, since the first report of Fehlhammer different WCA-NHCs were isolated and characterised. These compounds showed to be stronger  $\sigma$ -donors compared to their neutral analogues. They are able to form complexes with metals that can be used in catalysis and also compounds with main group elements. Inspired by the work of Lavigne<sup>200</sup> new synthetic strategies have been discovered for the direct synthesis of the desired modified heterorings.

However, to the best of our knowledge no such species with a silicon-based anion have been reported so far.<sup>204</sup>

---

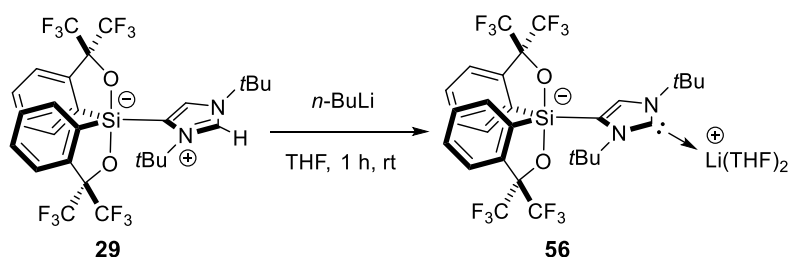
<sup>204</sup> For a recent review see: A. Nasr, A. Winkler, M. Tamm, *Coord. Chem. Rev.* **2016**, *316*, 68–124.

## IV.2 Results and Discussion

In chapter II the synthesis of two imidazolium rings bearing the Martin's spiro silane as weakly coordinated anionic moiety was devised. Inspired by the literature, it was decided to investigate the possibility to use these abnormal adducts as precursor of anionic carbene for their further application the synthesis of metal complexes stabilized by anionic NHCs.

### IV.2.1 Deprotonation of the abnormal adduct **29**

Although the anionic borane carbenes studied by Tamm<sup>197</sup> were obtained in an indirect manner, in our case it was possible to perform the deprotonation directly from the abnormal compound. Firstly, classical deprotonation conditions were investigated without any success. However, when **29** was treated with a slight excess of *n*BuLi, the lithium derivative **56** was obtained quantitatively (Scheme IV-12). These conditions were previously used by the group of Dagorne to deprotonate similar anionic ItBu carbenes functionalized at the C4 by trimethylaluminium, -indium or -gallium anions.



**Scheme IV-11** Synthesis of lithium derivatives **56**

The <sup>1</sup>H NMR analysis confirmed in an undeniable manner the success of the deprotonation. As depicted in the following figure, in the starting material two protons are present on the heteroaromatic ring characterised by two doublets in the aromatic area (green rectangles, (Figure IV.2).

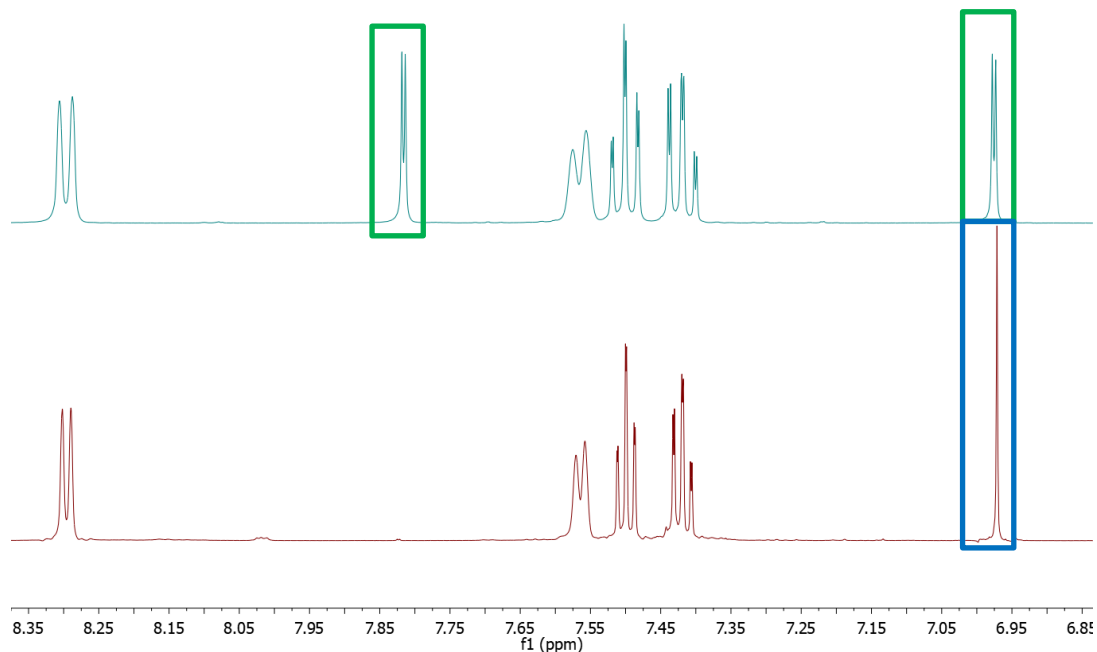


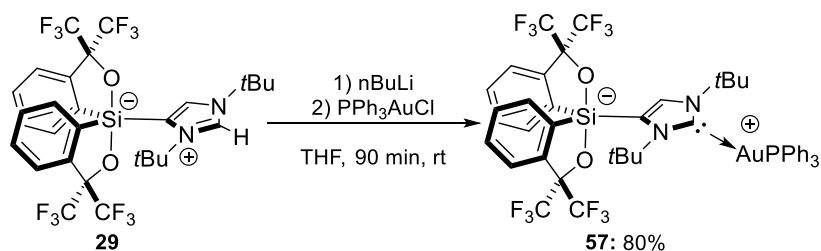
**Figure IV.2** Comparison of the aromatic area in  $^1\text{H}$  NMR spectra before and after deprotonation

Once the deprotonation was accomplished, only a singlet was observed (blue rectangle figure IV-2) and ascribed to the only proton left on the ring. By  $^{13}\text{C}$  NMR, it was not possible to detect the carbenic carbon and only a negligible shift was evidenced in the  $^{29}\text{Si}$  NMR spectrum of **56**.

#### IV.2.2 Metal complex with **29**

After having achieved the formation of the anionic carbene, the ability of its coordination to metals was then tested, starting from the triphenylphosphinegold(I) chloride complex. .

Different attempts were performed, and the best conditions resulted to be that reported in the following scheme (IV-12).



**Scheme IV-12** Synthesis of **57**

An *in situ* deprotonation was performed, followed by the addition of the gold(I) complex. The anionic nature of the ligand and the presence of the lithium cation that favoured the chloride abstraction into a silver-free process afforded the neutral gold(I) expected complex. The latter was characterised by an upfield shift of the silicon signal and a downfield shift of the phosphorus. However, chemical shifts are similar with the data of the borane complex of Tamm.<sup>205</sup>

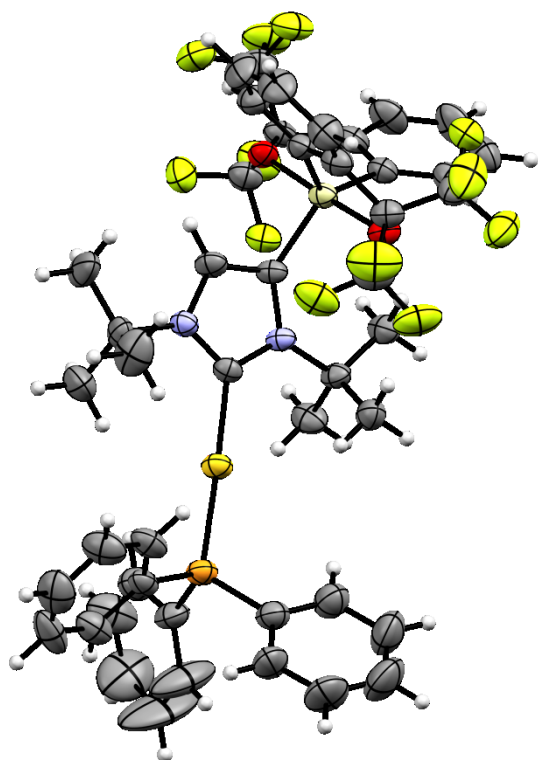


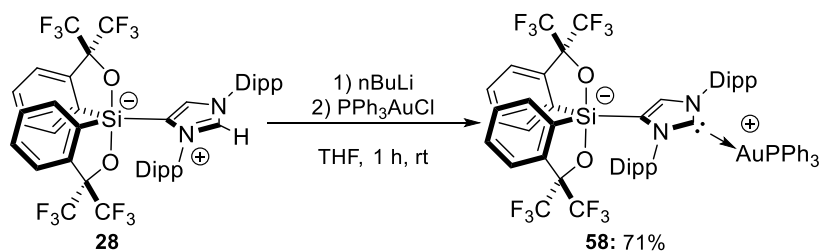
**Figure IV.3** ORTEP representation of **57**, ellipsoid 50% probability.

Slow evaporation of a dichloromethane solution of **57** afforded suitable crystals for X-Ray diffraction. The compound belongs to the orthorhombic *Pccn* space group and the Si-C distance is 0.01 Å shorter than that in the abnormal adduct, **29**. C-Au distance is about 2.044(4) Å shorter than the analogous complex of Tamm, suggesting a stronger interaction. Interesting is the deformation of the A-Au-P angle about 177.7° ascribable to the steric hindrance, and as in all the previous structure, a torsion of the heteroaromatic ring of 62.5° was found.

### IV.2.3 Metal complexes with the **28**

In a similar approach, it was possible to synthesise the analogous gold(I) derivative with abnormal IPr as ligand (Scheme IV-14). In this case, we did not isolate the organolithium intermediate, however the isolation of the metal complex suggested its formation.

<sup>205</sup> M. V. Baker, P. J. Barnard, S. J. Berners-Price, S. K. Brayshaw, J. L. Hickey, B. W. Skelton, A. H. White, *J. Organomet. Chem.* **2005**, *690*, 5625–5635.



**Scheme IV-13** Synthesis of **58**

To our delight, it was possible to find by  $^{13}\text{C}$  NMR the signal of the carbon bearing the gold(I) atom as a doublet due to the coupling with phosphorus ( $^2J = 126$  Hz) at 190.4 ppm, in line with the results obtained by Tamm. The  $^{31}\text{P}$  NMR chemical shift is only slightly deshielded as compared to the analogous normal gold(I).<sup>206</sup>

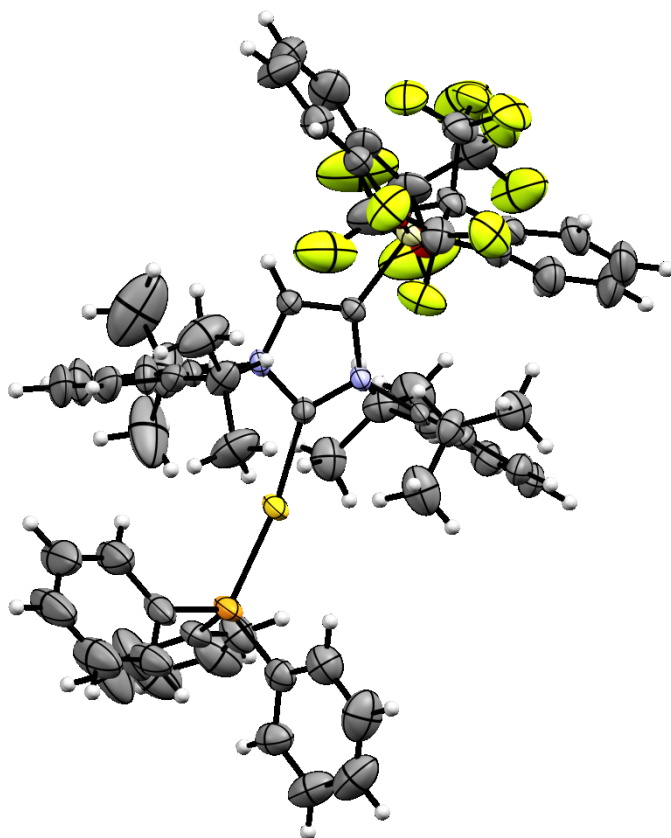


**Figure IV.4** ORTEP representation of **58**, ellipsoid 50% probability.

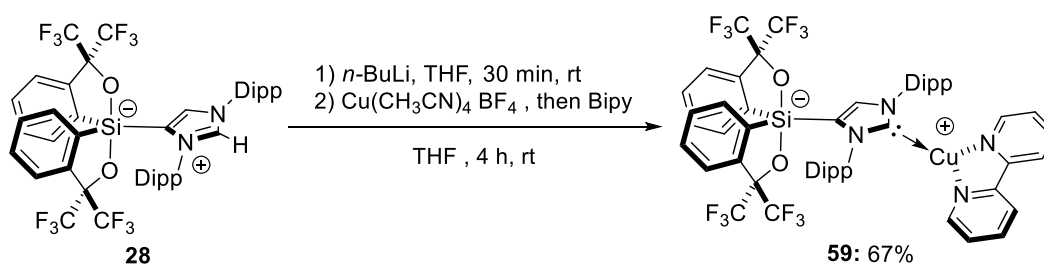
It has been possible to obtain suitable crystals for X-Ray diffraction. The compound belongs to the *P-1* triclinic space group. The Si-C distance is slightly increased, with a value of 1.911(4) Å, as compared to the abnormal adduct **28**. The C-Au distance, 2.051(3) Å, is found to be shorter than the analogous borane that possesses a bond length of 2.071 Å, probably derived from a strong interaction between the two elements. The steric hindrance can explain the greater distortion of the O-Si-O angle that from 170° in Tamm's borane complex it passed to 168.6°, as also the C-Au-P angle that has a value of 171.3°, is smaller

than the Tamm's borane complex, with a value of 177.8°. It was also noticed the increasing of the torsion angle from -27.05° to -30.6°.

<sup>206</sup> J. Fernández-Gallardo, B. T. Elie, M. Sanaú, M. Contel, *Chem. Commun.* **2016**, 52, 3155–3158.

From the abnormal aIPr-Si X, the reactivity towards Cu(I) was also investigated starting from the Cu(I)(CH<sub>3</sub>CN)<sub>4</sub>BF<sub>4</sub> complex.

Different attempts were performed but without success due to the instability of the Cu(I) centre. Indeed, even if the reaction was performed in different coordinating solvents like acetonitrile or pyridine, only products of degradation were recovered. At this point, it was decided to employ an additive, such as 2,2'-bipyridine, with the aim to enhance the stability of the metallic centre. Addition of 7 equivalent of bipy allowed the isolation of the copper(I) complex in 67% yield. Indeed, the additive was able to enhance the durability of the compound so that a solution of **59** in dichloromethane under argon was stable for at least three weeks.



**Scheme IV-14** Synthesis of the copper derivatives **59**

NMR investigations showed the accomplishment of the reaction with the presence of a single molecule of bipyridine for one anionic ligand. A solution of **59** stored at -30°C for 8 hours under argon, afforded suitable crystals for X-Ray diffraction.

The crystals belongs to the monoclinic *P2<sub>1</sub>/c* space group. The silicon-carbon bond result to be shorter than that in the other abIPr complexes, 1.898(1) Å, also if the angle O-Si-O is similar to that found in **58**, suggesting a major interaction between the two atoms. The carbon-copper bond, 1.894(1) Å, is shorter compared to the IPrCuCl,<sup>207</sup> probably due to a major interaction between the two atoms. Also the Cu-N bonds appears to be shorter compared to literature.<sup>208</sup> Moreover, the torsion between the equatorial plane and the plane containing the heteroaromatic ring is comparable to that of the compound **58** (Figure IV.5).

<sup>207</sup> H. Kaur, F. K. Zinn, E. D. Stevens, S. P. Nolan, *Organometallics* **2004**, *23*, 1157–1160.

<sup>208</sup> C. R. Woods, M. Benaglia, S. Toyota, K. Hardcastle, J. S. Siegel, *Angew. Chem. Int. Ed.* **2001**, *40*, 749–751.

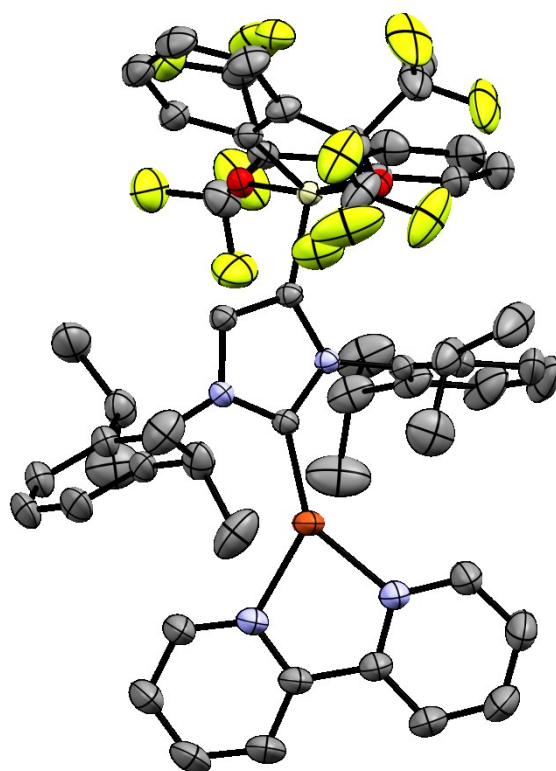


**Figure IV.5** ORTEP representation of **59**, ellipsoid 50% probability.

Up to now, our system has demonstrated to be an excellent platform for the synthesis of new metal complexes bearing an anionic NHC. We could expand the investigation to the stabilisation of main elements, in particular with boron. Indeed, NHC-borane distinguished themselves as reagents in different fields such as FLP,<sup>209</sup> reaction with electrophiles,<sup>210</sup> in radical chemistry,<sup>211</sup> as catalyst<sup>212</sup> and more other.<sup>213</sup>

<sup>209</sup> a) J. Lam, B. A. R. Günther, J. M. Farrell, P. Eisenberger, B. P. Bestvater, P. D. Newman, R. L. Melen, C. M. Crudden, D. W. Stephan, *Dalton Trans.* **2016**, 45, 15303–15316.

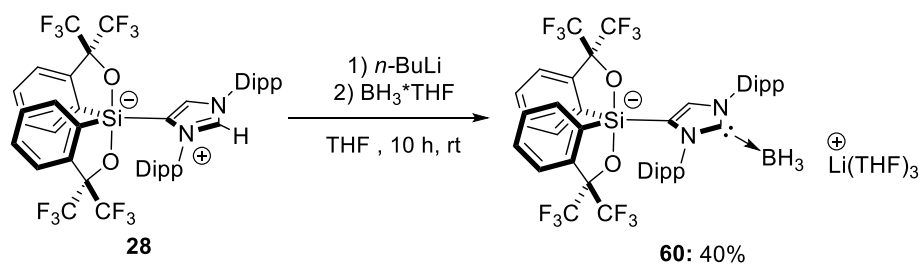
<sup>210</sup> A. Solovyev, Q. Chu, S. J. Geib, L. Fensterbank, M. Malacria, E. Lacôte, D. P. Curran, *J. Am. Chem. Soc.* **2010**, 132, 15072–15080.

<sup>211</sup> S.-H. Ueng, A. Solovyev, X. Yuan, S. J. Geib, L. Fensterbank, E. Lacôte, M. Malacria, M. Newcomb, J. C. Walton, D. P. Curran, *J. Am. Chem. Soc.* **2009**, 131, 11256–11262.

<sup>212</sup> K. Lee, A. R. Zhugralin, A. H. Hoveyda, *J. Am. Chem. Soc.* **2009**, 131, 7253–7255.

<sup>213</sup> D. P. Curran, A. Solovyev, M. Makhoulouf Brahmī, L. Fensterbank, M. Malacria, E. Lacôte, *Angew. Chem. Int. Ed.* **2011**, 50, 10294–10317.

The same protocol was used as for the previous metal complexes, with an *in situ* deprotonation followed by the addition of the precursors, in this case  $\text{BH}_3 \cdot \text{THF}$  (Scheme IV-16).



**Scheme IV-15** Synthesis of complex **60**

The compound was obtained in moderate yield. The  $^{11}\text{B}$  NMR confirmed the tetracoordinate nature of the boron atom with the presence of a broad quadruplet at  $-34.6$  ppm. Once again it was possible to obtain a X-Ray Structure.

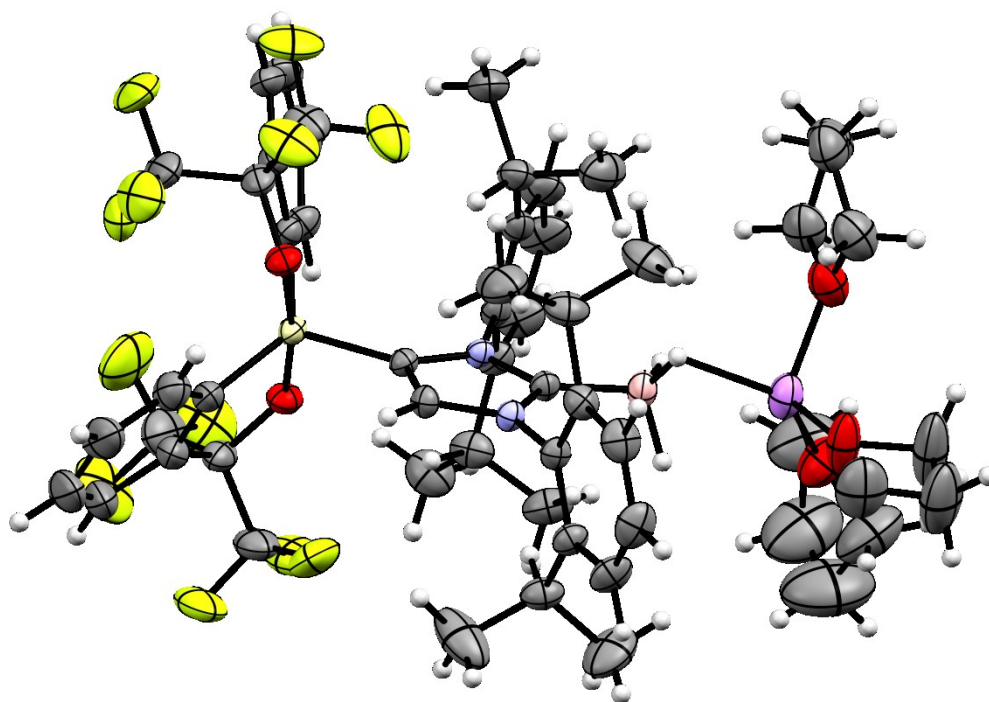


**Figure IV.6** ORTEP representation of **60**, ellipsoid 50% probability.

The crystal belongs to the monoclinic  $P2_1/c$  space group, it possessed a Si-C bond length of  $1.904(1)$  Å, similar of that found in the other compounds. The O-Si-O angle is less constrained than in the two previous cases with an angle of  $171.26^\circ$  while the dihedral angle is always around the  $-30^\circ$ . The carbon-boron distance appears to be smaller,  $1.597(2)$  Å, than

the 1.62 Å of the IPrBH<sub>3</sub>.<sup>214</sup> Intriguing characteristic in this structure is the interaction between boron and lithium mediated by a proton (Figure IV-6).

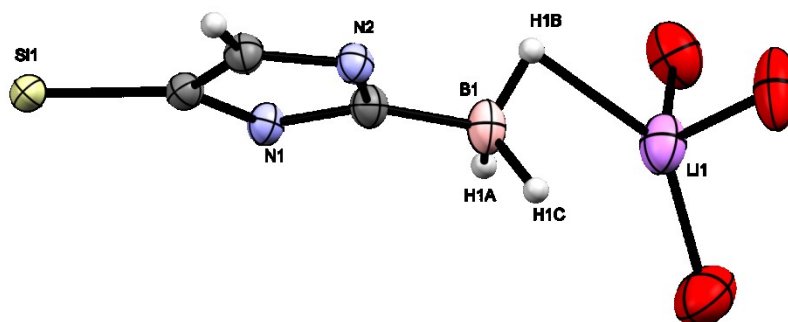


**Figure IV.7** Cross section of the structure of **60**. ORTEP representation, ellipsoid 50% probability.

The structural image showed the presence of an H-Li interaction. A bibliographic survey, allowed us to rationalise these results. Müller and co-workers in 2001, described a mono(borane)phosphides complex having lithium as counter-cation,<sup>215</sup> in which they evidenced the Li-H-B and Li---B interactions which favoured the formation of dimers. In compound **60** the Li-H1b distance is about 2.11(2) Å and the B-H1b-Li angle measured 87°. These numbers are comparable to those found by Müller with a Li-B distance of 2.315(4) Å. From the data comparison and due to the specific location of the lithium atom near the borate, we can affirm the presence of interactions between the two moieties.

<sup>214</sup> Y. Wang, B. Quillian, P. Wei, C. S. Wannere, Y. Xie, R. B. King, H. F. Schaefer, P. v. R. Schleyer, G. H. Robinson, *J. Am. Chem. Soc.* **2007**, *129*, 12412–12413.

<sup>215</sup> G. Müller, J. Brand, *Organometallics* **2003**, *22*, 1463–1467.

#### IV.2.4 Computational investigations

The deprotonated form of the aIPr, **28**, has been subjected to computational studies by Dr. Etienne Derat (IPCM). The figure below displayed the HOMO calculated at the B3LYP-D3/def2-SVPD level of theory, and it shows that the siliconate moiety, while influencing the carbene, does not modify the ability of this type of divalent carbon to be  $\sigma$ -donor. It has also been decided to calculate and compare the frontier orbital energy levels and the corresponding singlet-triplet gap for our system, IPr and CAAC-Dipp. Compared to IPr, our system in the deprotonated form displays a much higher lying HOMO, -3.34 eV vs. -5.89 eV, which indicates a stronger  $\sigma$ -donor character.

The LUMO level that attests for the  $\pi$ -accepting capabilities is also higher in energy. This last finding was evidenced experimentally by measuring the  $^{77}\text{Se}$  NMR chemical shift of the selenium adducts<sup>216</sup> of ItBu and the lithium complex **56**, where an upfield shift of about 11.5 ppm was observed.

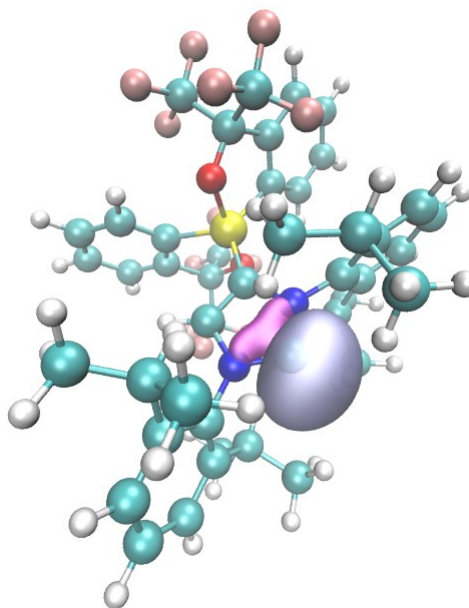


**Figure IV.8** Visualisation of the HOMO of calculated at the B3LYP-D3/def2-SVPD level of theory and plotted at an isosurface value of 0.05

<sup>216</sup> a) S. V. C. Vummaleti, D. J. Nelson, A. Poater, A. Gómez-Suárez, D. B. Cordes, A. M. Z. Slawin, S. P. Nolan, L. Cavallo, *Chem. Sci.* **2015**, *6*, 1895–1904. b) A. Liske, K. Verlinden, H. Buhl, K. Schaper, C. Ganter, *Organometallics* **2013**, *32*, 5269–5272.

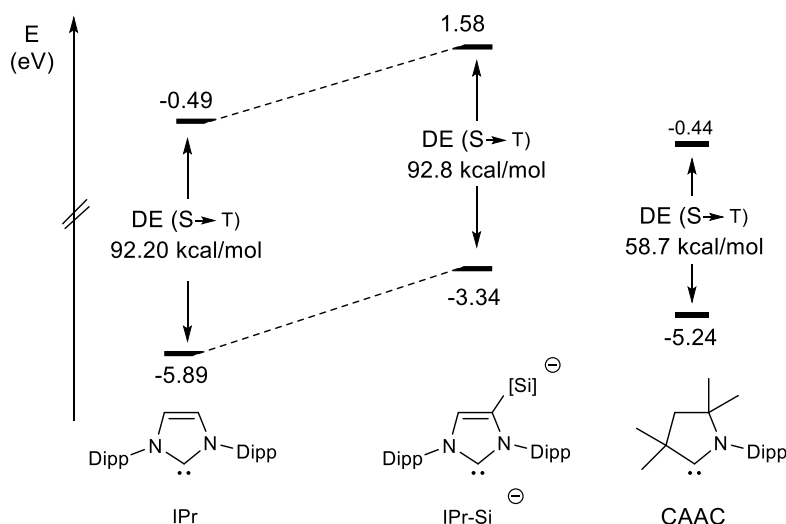


**Figure IV.9** Frontier molecular orbital comparison between **25**, **28** and CAAC carbenes

According to the DFT studies, the HOMO of AbIPr<sup>-</sup> carbene is even higher than the one calculated for the CAAC-Dipp, -5.24 eV, known to be a very strong  $\sigma$ -donor. However, the singlet-triplet gap of our compound resembles more to the one of IPr than CAAC.

In conclusion the abnormal adducts appear to be ideal platforms for the generation of anionic carbene derivatives. It has been demonstrated that the anionic carbene obtained are able to react with different metals like Cu(I) and Au(I), affording the corresponding neutral complexes. For each one, the X-Ray structure was obtained. Experimental data and theoretical calculations are consistent with a strong  $\sigma$ -donor nature of these ligands.

## **Chapter V**

# **Configurational Stability at the Pentacoordinate Silicon Adducts**



# V. Configurational Stability at the Pentacoordinate Silicon Adducts

## V.1 Introduction on Silicon Chirality

Chiral organosilicon compounds featuring a stereogenic silicon centre have attracted a lot of attention from a synthetic point of view as well as for potential applications.<sup>217</sup> The stereogenic silicon centres in tetraalkylsilanes and functionalized tetracoordinate organosilanes display a very high configurational stability under neutral conditions. In a sharp contrast, like most pentacoordinate compounds, this stability is far much weaker in pentacoordinate silicon(IV) which present most of the time non-rigid structures.<sup>218</sup> As mentioned in Chapter 1, these pentacoordinate species usually adopt a trigonal-bipyramidal geometry with two apical and three equatorial sites which are inclined to configurational isomerism with a fast substituent sites interchange. Such a process is known as the Berry pseudorotation mechanism. Nevertheless, the configuration of the stereogenic silicon atom can be controlled by formation of pseudorotamers when a rigid stereogenic element is close.<sup>219</sup>

---

<sup>217</sup> a) J. O. Bauer, C. Strohmman, *Angew. Chem. Int. Ed.* **2014**, *53*, 720–724. b) R. Shintani, E. E. Maciver, F. Tamakuni, T. Hayashi, *J. Am. Chem. Soc.* **2012**, *134*, 16955–16958. c) K. Igawa, D. Yoshihiro, N. Ichikawa, N. Kokan, K. Tomooka, *Angew. Chem. Int. Ed.* **2012**, *51*, 12745–12748. d) L.-W. Xu, L. Li, G.-Q. Lai, J.-X. Jiang, *Chem. Soc. Rev.* **2011**, *40*, 1777–1790. e) Y. Yasutomi, H. Suematsu, T. Katsuki, *J. Am. Chem. Soc.* **2010**, *132*, 4510–4511. f) S. Rendler, M. Oestreich, C. P. Butts, G. C. Lloyd-Jones, *J. Am. Chem. Soc.* **2007**, *129*, 502–503. g) S. Rendler, G. Auer, M. Keller, M. Oestreich, *Adv. Synth. Catal.* **2006**, *348*, 1171–1182. h) S. Rendler, G. Auer, M. Oestreich, *Angew. Chem. Int. Ed.* **2005**, *44*, 7620–7624. i) D. R. Schmidt, S. J. O'Malle, J. L. Leighton, *J. Am. Chem. Soc.* **2003**, *125*, 1190–1191. l) K. Tomooka, A. Nakazaki, T. Nakai, *J. Am. Chem. Soc.* **2000**, *122*, 408–409. m) K. Kobayashi, T. Kato, M. Unno, S. Masuda, *Bull. Chem. Soc. Jpn.* **1997**, *70*, 1393–1401.

<sup>218</sup> E. P. A. Couzijn, M. Schakel, F. J. J. de Kanter, A. W. Ehlers, M. Lutz, A. L. Spek, K. Lammertsma, *Angew. Chem. Int. Ed.* **2004**, *43*, 3440–3442.

<sup>219</sup> a) J. O. Bauer, C. Strohmman, *J. Am. Chem. Soc.* **2015**, *137*, 4304–4307. b) S. Schlecht, M. Finze, R. Bertermann, W. Frank, A. Domann, M. Braun, *Eur. J. Inorg. Chem.* **2013**, *2013*, 1488–1492.

## V.2 Configurational Stereomutation at Pentacoordinate Species

Stereomutation in pentacoordinate species can follow different pathway, Berry pseudorotation is the most known and common mechanism.<sup>220</sup>

Muetterties proposed five possible mechanisms for the rearrangement of compounds having a trigonal bipyramid geometry (Figure V.1).<sup>221</sup> The first mechanism proposed is the Berry pseudorotation. The second mechanism involves a 120° interchange between an axial ligand and two equatorial substituents; in the third one we have a simple 180° interchange between an axial and an equatorial ligand; the fourth mechanism is characterised by the position change of all the substituents; the last mechanism occurs thanks to a 180° interchange of two equatorial groups. Despite the mechanisms four and five are theoretically possible, they do not seem convincing due to the passage through a high energetic planar state.

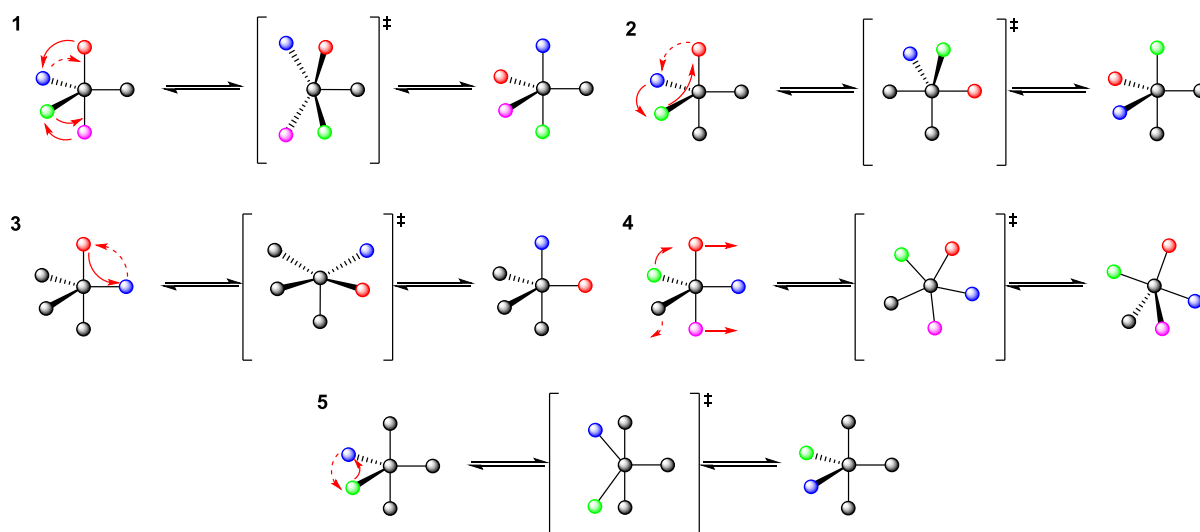


**Figure V.1** Pseudorotation mechanisms proposed by Muettterties.

<sup>220</sup> a) R. S. Berry, *J. Chem. Phys.* **1960**, *32*, 933–938. b) R. S. Berry, *Rev. Mod. Phys.* **1960**, *32*, 447–454.

<sup>221</sup> E. L. Muettterties, *J. Am. Chem. Soc.* **1969**, *91*, 4115–4122.

Another interesting mechanism is the one proposed by Ugi,<sup>222</sup> mechanism **b** in the previous scheme, the ligands were divided in two groups, a trio, and a duo. This latter can be affected by a 60° rotation, that leads to the formation of the other TBP configuration.<sup>223</sup>

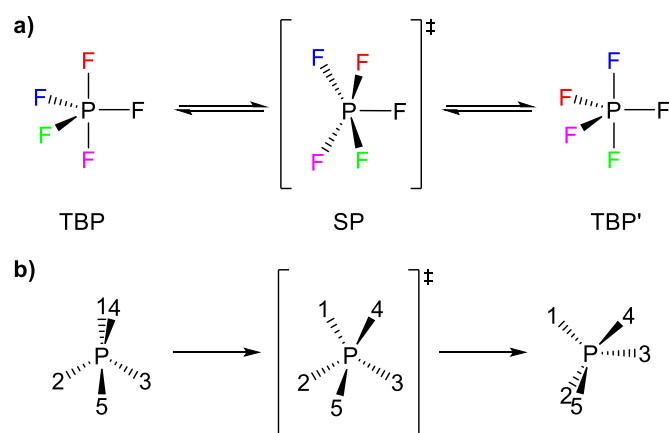
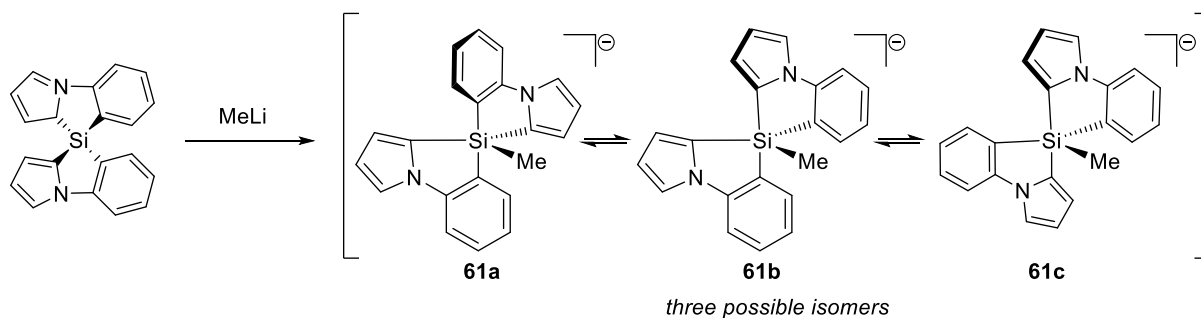


**Figure V.2** a) Berry's pseudorotation mechanism; b) Turnstile rotation Mechanism, Ugi's Pseudorotation.

Concerning silicon, an elegant investigation on the isomerisation barrier of pentaorganosilicate was realised by Lammertsma and co-workers.<sup>224</sup> From variable-temperature NMR studies, a dynamic equilibrium between the different isomers (Scheme V-1) was pointed out. Extrapolation of the experimental data stated that **61a** is more stable than **61b** of +1.8 kcal.mol<sup>-1</sup> and **61c** of +2.6 kcal.mol<sup>-1</sup>. The overall pseudorotation mechanism (**61a**→**61c**→**61b**) has an energy barrier of 15 kcal.mol<sup>-1</sup>.



**Scheme V-1** Synthetic pathway and the three isomers described by Lammertsma and co-workers

In 2009, the same group re-investigated the stereomutation in pentacoordinate silicon-based compounds (Figure V.3) and the structural parameters influencing on the

<sup>222</sup> a) P. Gillespie, P. Hoffman, H. Klusacek, D. Marquarding, S. Pfohl, F. Ramirez, E. A. Tsois, I. Ugi, *Angew. Chem. Int. Ed. Engl.* **1971**, *10*, 687–715. b) I. Ugi, D. Marquarding, H. Klusacek, G. Gokel, P. Gillespie, *Angew. Chem. Int. Ed. Engl.* **1970**, *9*, 703–730.

<sup>223</sup> P. Meakin, E. L. Muetterties, J. P. Jesson, *J. Am. Chem. Soc.* **1972**, *94*, 5271–5285.

<sup>224</sup> E. P. A. Couzijn, M. Schakel, F. J. J. de Kanter, A. W. Ehlers, M. Lutz, A. L. Spek, K. Lammertsma, *Angew. Chem. Int. Ed.* **2004**, *43*, 3440–3442.

pseudorotation barriers.<sup>225</sup> They were able to describe two different competitive pathways for the isomerisation of pentaorgano-spirocyclic silicate.

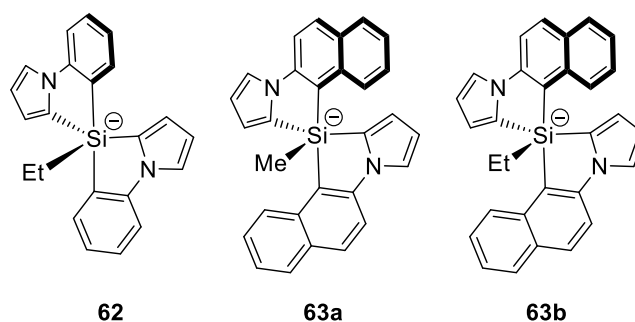


**Figure V.3** Compounds investigated

A thorough DFT study on the stereomutation mechanism allowed determining the beneficial influence of the substituent in *ortho*-position to silicon on the energy barrier. Experimentally, when the phenylpyrrole ligand in **62** was replaced by a naphthylpyrrole ligand (**63a, b**), a  $\pi$ -electron richer and hindered substituent, the energy barrier corresponding to the stereomutation was greatly enhanced from about 15 kcal.mol<sup>-1</sup> to 21 kcal.mol<sup>-1</sup> as evidenced by NMR experiments, avoiding the fast stereomutation.

### V.3 Configurational Stereomutation in Martin's Spirosilane Adduct

In 1985 an extensive work was made<sup>226</sup> for rationalising the stereomutation in pentacoordinate Martin's derivatives. In this study, they firstly synthesised various pentacoordinate silicate derivatives and investigated their interconversion by dynamic NMR experiments. As expected, in all the cases, a TBP structure was obtained, in which the two most electronegative atoms, the oxygens, occupied the apical positions while the carbon atoms and the additional nucleophilic ligand occupied the equatorial positions (Figure V.4).

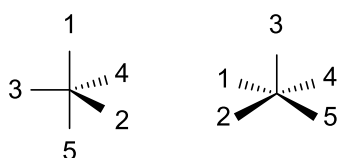


**Figure V.4** TBP and SPP configuration

<sup>225</sup> E. P. A. Couzijn, D. W. F. van den Engel, J. C. Slootweg, F. J. J. de Kanter, A. W. Ehlers, M. Schakel, K. Lammertsma, *J. Am. Chem. Soc.* **2009**, *131*, 3741–3751.

<sup>226</sup> a) W. H. Stevenson, J. C. Martin, *J. Am. Chem. Soc.* **1985**, *107*, 6352–6358. b) W. H. Stevenson, S. Wilson, J. C. Martin, W. B. Farnham, *J. Am. Chem. Soc.* **1985**, *107*, 6340–6352.

Depending on the substituents, the TBP geometry results to be, more or less, distorted towards a SPP geometry, most favoured in presence of five substituents with a comparable electronegativity. They measured the SPP character thanks to the  $\delta_{24}$  parameters,<sup>227</sup> the dihedral angle between the planes passing through 1-2-4 and 5-2-4 (Figure V.3), that for SPP is 0° and for TBP is 53,1°.

They carried out also the measurement of the energy barriers for the inversion of configuration at the silicon centre for various silicates thanks to dynamic NMR experiments.

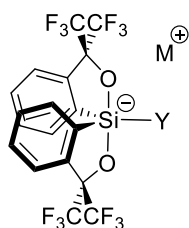


**Table V.1** Energy barriers to inversion with different substituent Y

Y	M	$\Delta G^*_{424K}$ kcal/mol	$\sigma^*Y$
<i>n</i> -Bu	Et <sub>4</sub> N	28.6 ± 0.3	-0.13
C <sub>6</sub> H <sub>5</sub> CH(CH <sub>3</sub> )	Me <sub>4</sub> N	29.0 ± 0.2	0.11
4-MeOC <sub>6</sub> H <sub>4</sub>	Et <sub>4</sub> N	26.6 ± 0.1	0.42
Ph	Et <sub>4</sub> N	26.0 ± 0.1	0.60
3-CF <sub>3</sub> C <sub>6</sub> H <sub>4</sub>	Et <sub>4</sub> N	25.6 ± 0.1	0.89
3,5-(CF <sub>3</sub> ) <sub>2</sub> C <sub>6</sub> H <sub>3</sub>	Bu <sub>4</sub> N	25.5 ± 0.1	1.18
C <sub>6</sub> F <sub>5</sub>	Bu <sub>4</sub> N	21.9 ± 0.1	2.0
C <sub>6</sub> H <sub>5</sub> O	Li	20.4 ± 0.3	2.24
F	(Me <sub>2</sub> N) <sub>3</sub> S	17.5	3.08
CN	(Me <sub>2</sub> N) <sub>3</sub> S	16.8 ± 0.2	3.64

It can be learnt from the data ( $\Delta G$  calculated by magnetization transfer experiments) that for ligands with an increasing electronegativity, the energy barrier decreases and vice versa. The Taft's factor was chosen for the calculation of the  $\Delta G$  because it describes how a substituent can influence the reaction through inductive field and resonance effects. Moreover, the Taft's equation<sup>228</sup> takes into accounts the steric factor in contrast to the Hammett equation.<sup>229</sup> To determine it, Taft studied the hydrolysis of a methyl ester (RCOOMe), an idea already suggested by Ingold in 1930<sup>230</sup>, in basic and acid conditions. Once the energy barriers were calculated, the pseudorotation mechanism was studied, and two different mechanisms were proposed.

<sup>227</sup> a) R. R. Holmes, *Acc. Chem. Res.* **1979**, *12*, 257–265. b) R. R. Holmes, J. A. Deiters, *J. Am. Chem. Soc.* **1977**, *99*, 3318–3326. c) R. R. Holmes, "Pentacoordinated Phosphorus", *American Chemical Society*, Washington D.C., **1980**, Vols. I and II.

<sup>228</sup> a) R. W. Taft, *J. Am. Chem. Soc.* **1953**, *75*, 4538–4539. b) R. W. Taft, *J. Am. Chem. Soc.* **1952**, *74*, 3120–3128. c) R. W. Taft, *J. Am. Chem. Soc.* **1952**, *74*, 2729–2732.

<sup>229</sup> L. P. Hammett, *J. Am. Chem. Soc.* **1937**, *59*, 96–103.

<sup>230</sup> C. K. Ingold, *J. Chem. Soc. Resumed* **1930**, *0*, 1032–1039.

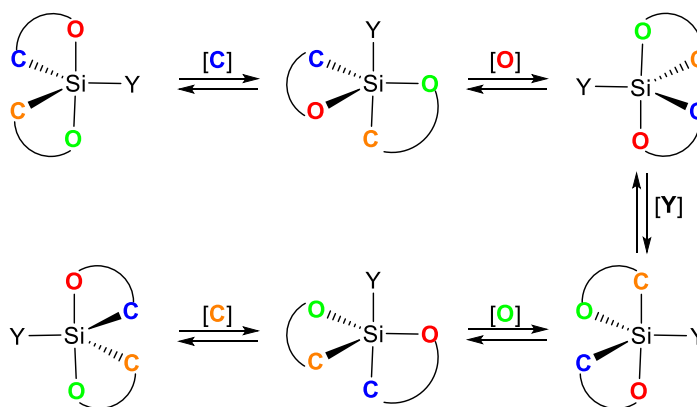


**Figure V.5** First proposed mechanism; in bracket the *pivot* ligand.

Due to the negligible entropy of activation and also a low solvent effect, the first mechanism proposed belongs to the intramolecular type (Figure V.5). Starting from a TBP structure, five consequent pseudorotations take place, each one characterised by a *pivot* ligand. This mechanism provides as intermediate a high energy TBP, in which, the aromatic carbon and the Y ligand are in apical position (Figure V.6).

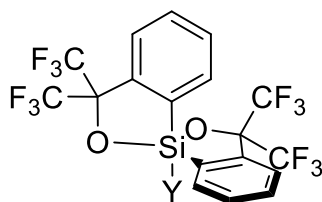


**Figure V.6** Highest transition state

This conformation allowed them to rationalise the trend shown before. In fact, the presence of a more electronegative Y ligand in apical position stabilises the high electronic density here located. The apicophilicity, in this case, is the driving force for the pseudorotation pathways.

The second proposed mechanism considered the heterolytic rupture of one Si-O bond, followed by its rotation and reformation (Figure V.7).

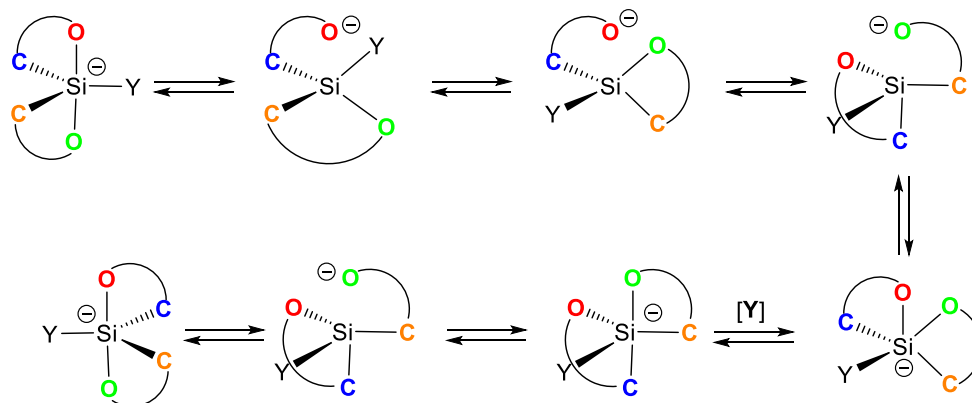


**Figure V.7** Second proposed mechanism; in bracket the *pivot* ligand.

If the latter represents the actual mechanism for the inversion of configuration, an increase of the electron-withdrawing ability of the nucleophile has to appear in an augmentation of the rotation barrier, this because the cleavage of the Si-O bond will reduce the negative charge on the silicon atom. As a consequence, the presence of an electron-withdrawing group will have to slow this mechanism. However, the experimental data indicate that this pathway is highly unlikely.

#### V.4 Configurational Stability of NHC-Si and *a*NHC-Si Adducts

To the best of our knowledge, synthesis of configurationally rigid pentacoordinate silicon(IV) derivatives at room temperature are extremely rare and limited to anionic silicates. Furthermore, the separation of their enantiomers has never been carried out. In our study, we have been able to synthesize several pentacoordinate NHC-Si normal and abnormal adducts with the Martin's spiroasilane. Our interested was to study the stereomutation associated energies and trying to physically separate the enantiomers which would be a "premiere". According to the data of Martin mentioned previously, the energy barriers corresponding to the ligand interchange should fall in a range where the racemisation might be slow enough to perform the separation of enantiomers at room temperature. Moreover, unlike the configurationally rigid pentacoordinate silicate known in the literature, our adducts are neutral and for some of them can be purified by standard chromatography on silica gel. To study their configurational stability and to resolve the racemic mixtures we envisioned to use chiral

HPLC. This work has been done in collaboration with Nicolas Vanthuyne of ISM2, Marseille. Firstly, we focused our attention to the analysis of abnormal adduct **29**, featuring two tert-butyl groups on the imidazolium ring, by HPLC with various chiral columns and conditions. The sample was dissolved in ethanol, injected on the column, and detected with an UV detector at 220 nm and a circular dichroism detector at 254 nm. To our delight, the two enantiomers of the compound **29** could be nicely separated in very standard conditions using a Chiralcel OD-3 chiral column with a heptane/isopropanol (90/10) mixture as eluent and a flow-rate of 7 mL/min. The circular dichroism unambiguously confirmed that the two peaks correspond to both enantiomers (Figure V.5). This very good result indicates first that the product are not sensitive to solvolysis and also that the racemisation is not fast at the HPLC timescale otherwise only one peak would have been obtained. Secondly, because of the neutral nature of the compound, the HPLC method is adequate for the resolution of such uncommon compounds based on pentacoordinate silicon(IV).

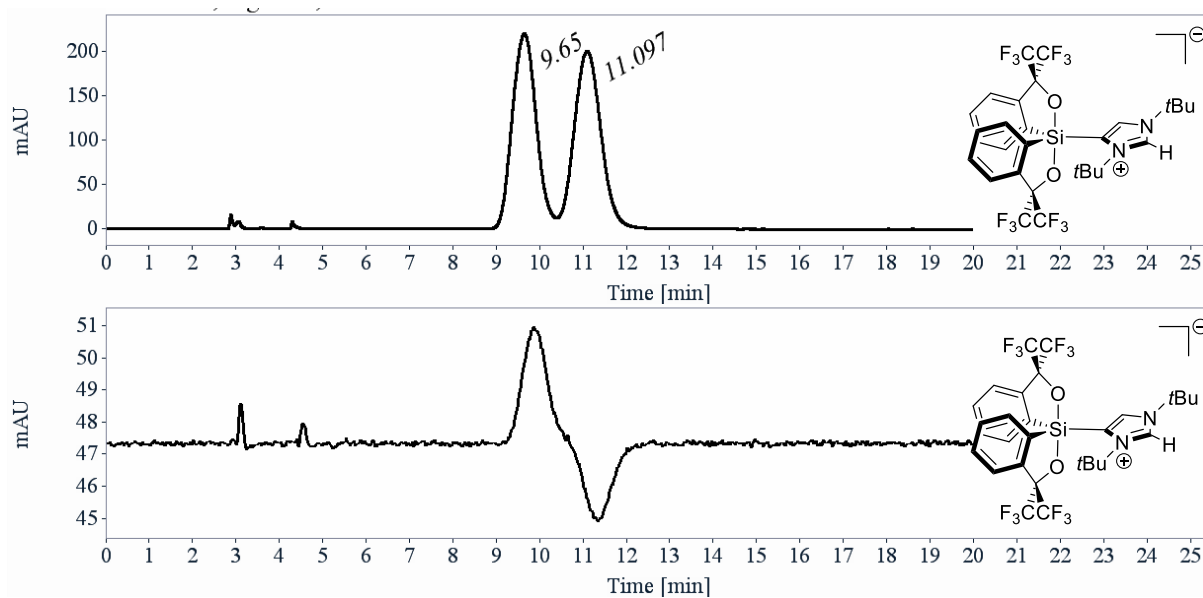


**Figure V.8** Chromatogram of **29** (up); coupled to positive and negative Circular Dichroism (down).

It was then possible to study the kinetics of the racemisation process of **29**, and then calculate the half-life time of a single enantiomer. A solution of the first eluted enantiomer in dichloromethane is thermostated at 25 °C. A part of this sample is then injected on the chiral column at different times. The percentage decrease of the first eluted enantiomer is monitored (Figure V.8).

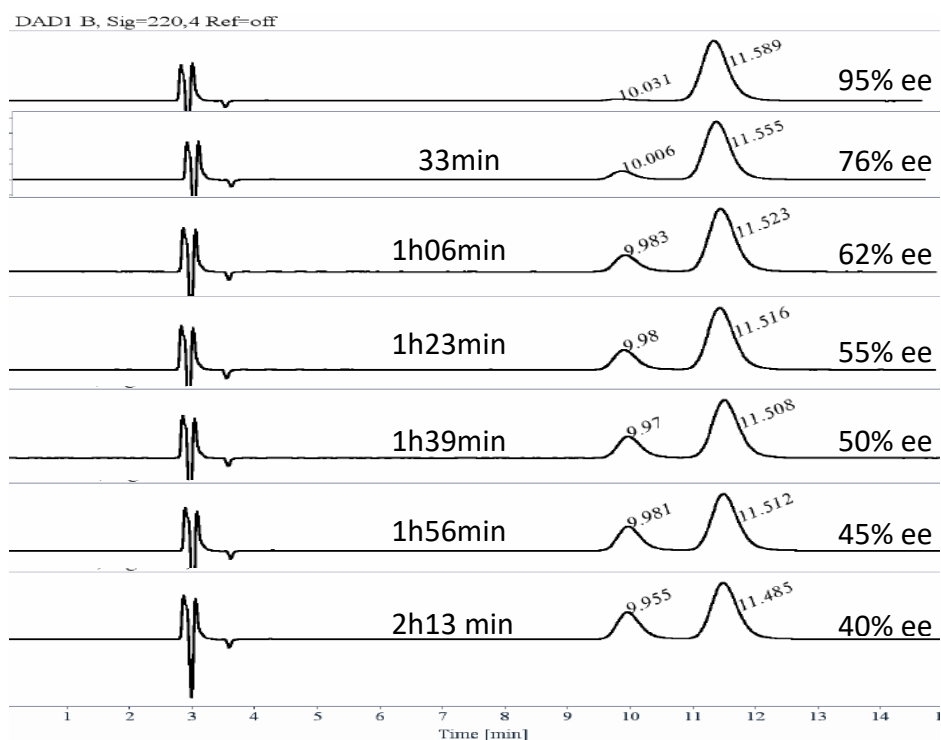


**Figure V.9** Data collected by monitoring the racemisation

From these collected data, the racemisation barrier was calculated to be 97.4 kJ/mol (23.3 kcal/mol: see experimental section) and therefore the enantiomers have a half-life of 1.81 h at 25°C, with a  $k_{\text{enantiomerisation}} = 5.3294\text{E-}0.5 \text{ s}^{-1}$ .

Conditions for the enantiomers separation of compound **26**, the less hindered normal adduct, could also be carried out using a Chiralpak IB column at 40°C with a heptane/isopropanol (99.5/0.5) eluent. Two different peaks were identified as the two enantiomers with a “plateau” in between, This "plateau" reveals the enantiomerization during the analysis (Figure V.9). By dynamic chiral HPLC, using the equation developed by O. Trapp and V. Schurig,<sup>231</sup> the barrier to racemization can be evaluated at 99 kJ/mol (23.7 kcal/mol).

<sup>231</sup> O. Trapp, V. Schurig, *Chirality* **2002**, *14*, 465-470.

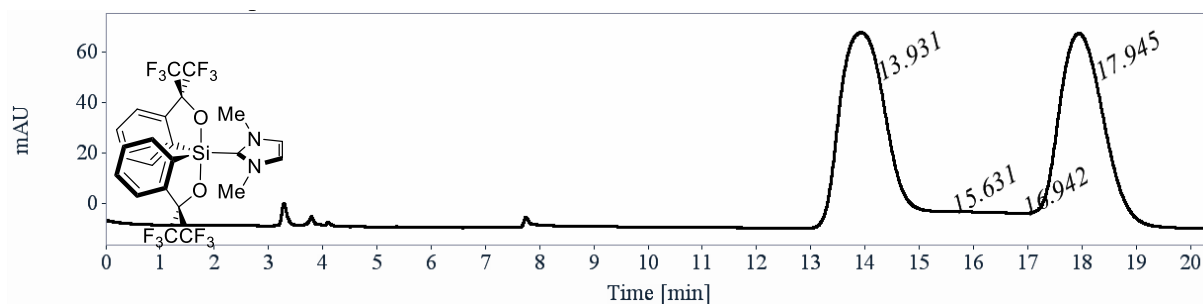


**Figure V.10** Chromatogram of **26**

The fact that we do not observe the on-column racemisation for the previous analysed compound **26**, is attributable to the lower resolution of the two enantiomers in these conditions (see experimental section). Unfortunately, for the bulkier adducts **27** and **28**, it was not possible to find suitable conditions to perform the separation of their enantiomers and therefore to quantify their racemisation barriers.

An investigation was also undertaken on the neutral gold complexes described previously in chapter IV. The first compound to be analysed was **57** and as before the sample was dissolved in ethanol, injected on the chiral column and detected with an UV detector at 220 nm, a circular dichroism detector at 254 nm and a polarimetric detector with an eluent composed of hexane/2-PrOH (95/5). Surprisingly, the complex **57** proved to be stable in the analysis conditions and the separation of enantiomers was effective using a Chiralpak IE column (Figure V.11). Once again the polarimeter detector unambiguously confirmed the two peaks correspond to both enantiomers.

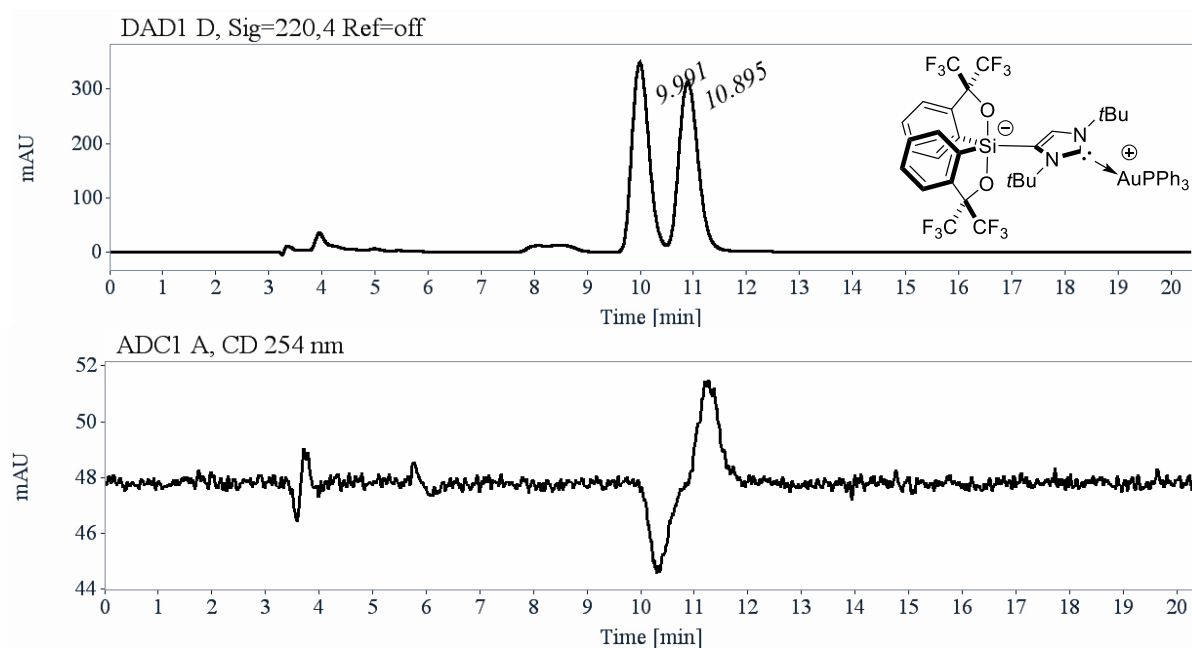


**Figure V.11** Chromatogram of **57** (up); coupled to positive and negative Circular Dichroism (down).

A kinetic study of the racemisation was also carried out on this gold complex **X**, and a value of 102 kJ/mol (24.4 kcal/mol: see experimental section) could be worked out for the inversion barrier energy. Interestingly, this value corresponds to a half-life of 10.86 h for the enantiomers, at 25°C, with a  $k_{\text{enantiomerisation}} = 8.8667\text{E-}06 \text{ s}^{-1}$ . These very good results highlighted the influence of the complexed triphenylphospinegold(I) moiety on the configurational stability of the pentacoordinate silicon with fivefold multiplied half-life time. CD spectra of the two separated enantiomers could be recorded and are presented in figure V.12.

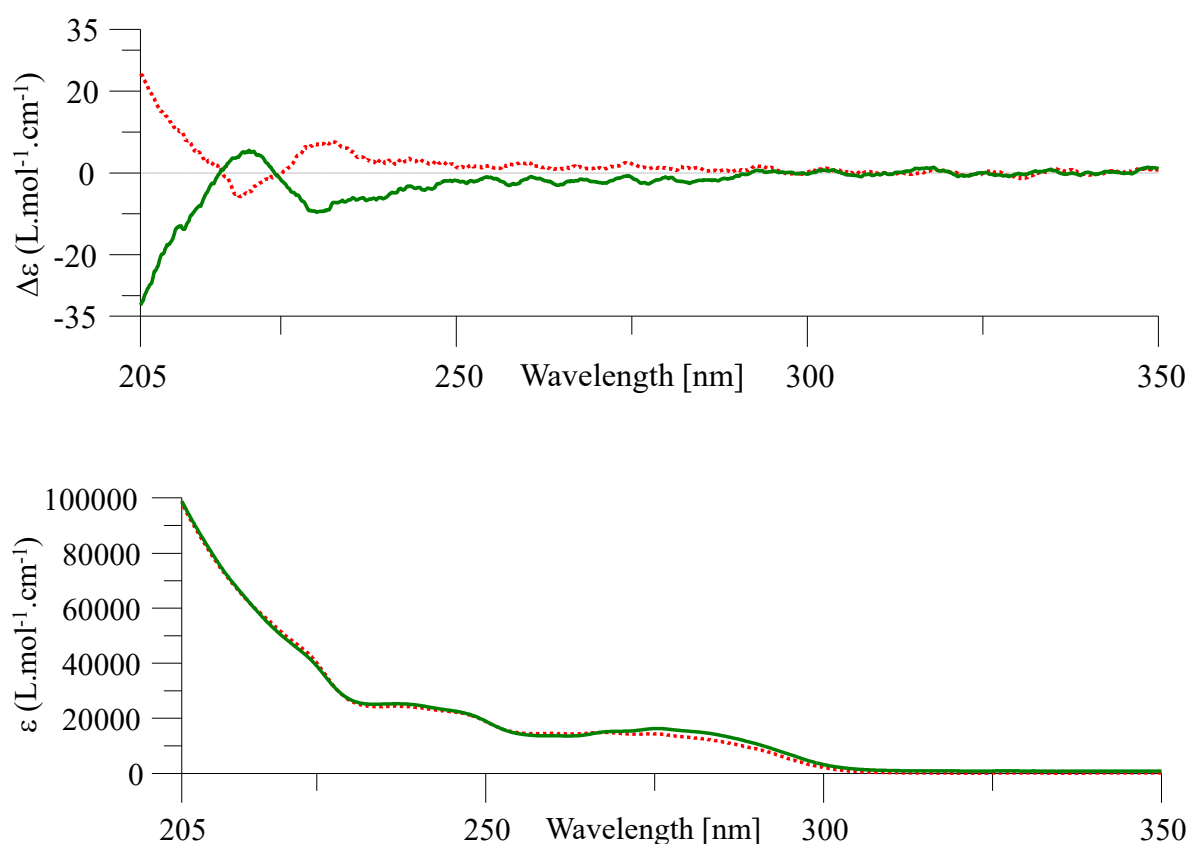


**Figure V.12** CD spectra of the two separated enantiomers

The same behaviour in identical analytical conditions was also observed for the complex **58**. Unlike the abnormal adduct **28**, this time it was possible to separate the two enantiomers of the gold complexes **58** with Dipp substituents and the racemisation barrier was evaluated at 101 kJ/mol (24.13 kcal/mol: see experimental section) with a half-life time for the racemisation of 9.07 h, at 25°C (Figure V.13)

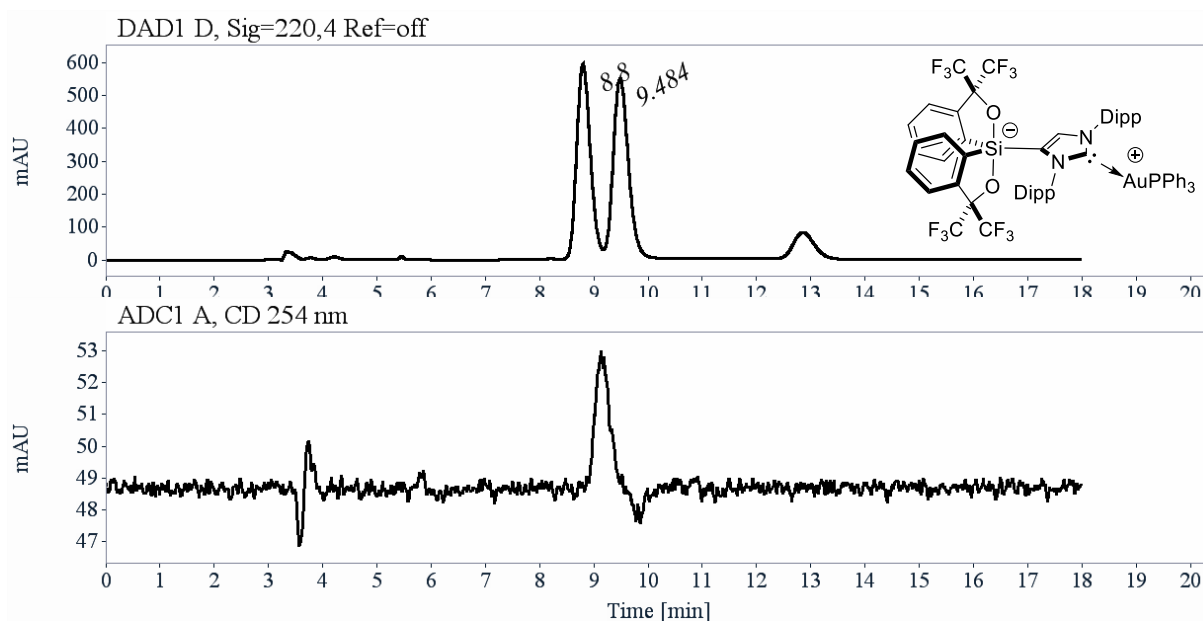


**Figure V.13** Chromatogram of **58** (up); coupled to positive and negative Circular Dichroism (down).

In conclusion, the configurational stability of novel neutral pentacoordinate adducts coming from the interaction of the Martin's spiro-silane end some NHCs was assessed and gave rise to really promising preliminary results. As previously noticed by Stevenson *et al.*, according to the nature of the additional ligand, the Martin's spiro-silane derivatives can display a strong configurational rigidity even at room temperature. Gratifyingly, chiral HPLC allowed us to separate the enantiomers of the neutral normal adduct **26** and the zwitterionic abnormal adduct **29** with an estimated racemisation barrier of about 97-99 kcal/mol. In addition, the gold(I) complex derivatives of abnormal adducts **57** and **58** could be separated as well and an effect of the metal on the isomerisation rate was found out. Indeed, we were pleased to observe an enhancement of the half-life time, multiplied fivefold in the case of complex **57** and complex **58** with a not negligible half-life time of about 10 hours. To the best of our knowledge, these are the first examples of physical separation of pentacoordinate silicon(IV) enantiomers. These outcomes open the way to applications that required a chiral environment such as enantioselective catalysis.

## **General Conclusion**



Silicon derivatives have become key reagents in chemistry, due to the possibility to tune its Lewis acidity and the ability to access the hypercoordinate state. In this thesis work, it was explored the reactivity of the Martin's spiroasilane, that proved to possess a high acidity and a relatively high steric hindrance. The first part was focused on the synthesis of the spiroasilane, thus achieving a grams-scale synthetic pathway.

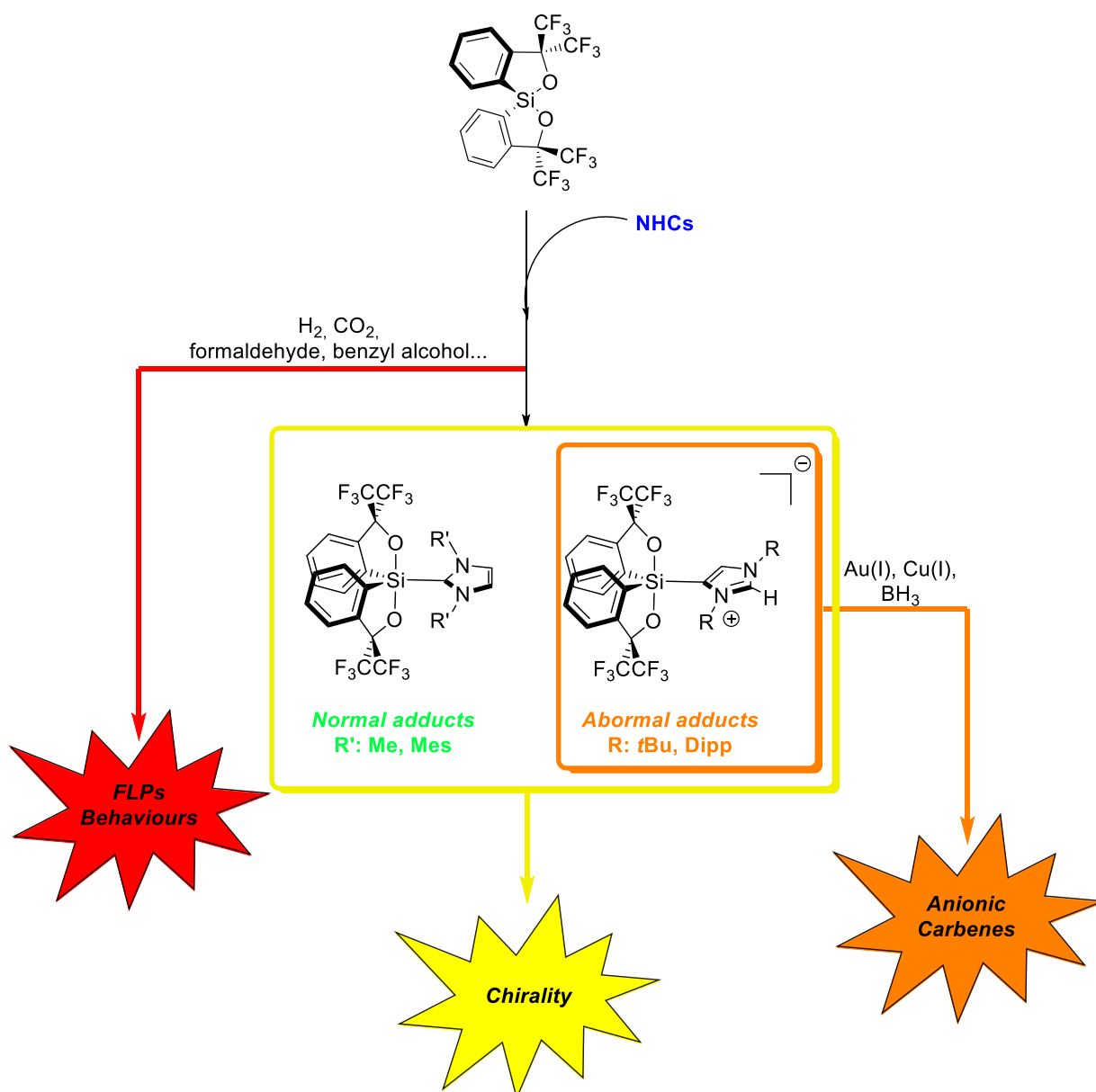
The second part of this work has been focused on the development of the interaction between the Martin's spiroasilane and NHCs. Several adducts have been synthesised, and for the first time abnormal adducts with a pentacoordinated silicon(IV) moiety have been obtained. All the compounds were characterized by X-ray crystallography which gave even greater emphasis to the results obtained.

Given the nature of the components at the base of this research work, given the first results obtained in, it was decided to investigate its potential use in FLP chemistry. Therefore, the capacity of activation of hydrogen and carbon dioxide was assessed. Unfortunately, the different attempts have not yielded the expected result as our different systems proved to not prone to these small molecules. So, attention was paid to the ability to synthesize pentacoordinated complexes with different target molecules such as formaldehyde, benzyl alcohol and diones. This time the results were positive and it was possible to isolate and characterize, even by X-ray crystallography, the different products obtained, collecting some intriguing results.

In Chapter II abnormal adducts were introduced and analysed. As well as being an exciting result, they can also serve as an entry to for the world of anionic carbenes. This is an already known class of compounds that has proved to be of great potential, in our case we are also in the presence of new potential precursors. To our immense pleasure the predictions proved to be accurate, several metal complexes were obtained and characterised as well as a complex with a main group element. The results presented in this chapter are the base of a further studies focused on their use in catalysis.

In the last part of this work we assessed the configurational stability of the adducts and complexes we made. It turned out that our compounds present relatively high racemisation barriers as we were able to separate enantiomers using chiral HPLC. In fact, the protagonist of this work has proven to be a prochiral molecule.

In Conclusion, Martin's spirosilane proved to be a pluripotent Lewis acid that allowed to pave the way for new unexplored territories.



## **Experimental Section**



Unless otherwise noted, reactions were carried out under an argon atmosphere in oven-dried glassware using Schlenk line techniques. All the solvents were distilled prior to be used. Dichloromethane and pentane were distilled over CaH<sub>2</sub>, THF was distilled over sodium/benzophenone, toluene was distilled over sodium, tetramethylethylenediamine (TMEDA) over potassium hydroxide. Sodium hydride 60% dispersion, was washed three times with distilled pentane, dried and stored in the glove box. Reagents and chemicals were purchased from commercial sources and used as received. Melting points were determined on a melting point apparatus SMP3 (Stuart scientific) and are uncorrected. HRMS were registered on a microTOF Bruker with ESI source. <sup>1</sup>H, <sup>19</sup>F, <sup>31</sup>P NMR spectra were recorded at room temperature at 300, 282, 121 MHz on a Bruker AVANCE 300 nanobay spectrometer. <sup>1</sup>H, <sup>19</sup>F, <sup>13</sup>C, <sup>31</sup>P and <sup>29</sup>Si NMR spectra were recorded at room temperature at 400, 376, 100, 161 and 79.49 MHz respectively, on a Bruker AVANCE 400 spectrometer. <sup>1</sup>H, <sup>19</sup>F, <sup>13</sup>C, <sup>29</sup>Si, <sup>31</sup>P <sup>77</sup>Se, <sup>7</sup> Li NMR were recorded, unless otherwise noted, at room temperature at 600, 564, 150, 119, 242, 114.45 and 233.23 MHz respectively, on a Bruker AVANCE III 600 spectrometer. Chemical shifts ( $\delta$ ) are reported in ppm and coupling constants ( $J$ ) are given in Hertz (Hz). Abbreviations used for peak multiplicity are: s (singlet); bs (broad singlet); d (doublet); t (triplet); q (quartet), td (triplet of doublet), dt (doublet of triplet); m (multiplet). Calibration tol-d<sub>8</sub>: 2.08; CD<sub>2</sub>Cl<sub>2</sub>: 5.32; CDCl<sub>3</sub>: 7.26; THF-d<sub>8</sub>: 3.58, 1.72. Intensity data was collected with Bruker Kappa-APEX2 systems using micro-source Cu-K $\alpha$  or fine-focus sealed tube Mo-K $\alpha$  radiation. Unit-cell parameters determination, data collection strategy, integration and absorption correction were carried out with the Bruker APEX2 suite of programs. The structures were solved with SHELXT-2014 and refined by full-matrix least-squares methods with SHELXL-2014 using the WinGX suite. Intensity data were collected with a BRUKER Kappa-APEXII diffractometer with graphite-monochromated Mo-K $\alpha$  radiation ( $\lambda = 0.71073 \text{ \AA}$ ). Data collection were performed with APEX2 suite (BRUKER). Unit-cell parameters refinement, integration and data reduction were carried out with SAINT program (BRUKER). SADABS (BRUKER) was used for scaling and multi-scan absorption corrections. In the WinGX suite of programs,<sup>232</sup> the structure were solved with SHELXT-14 program<sup>233</sup> and refined by full-matrix least-squares methods using SHELXL-14.<sup>233</sup>

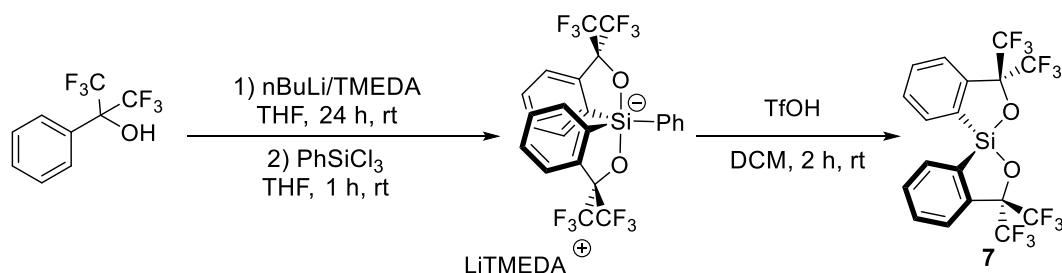
---

<sup>232</sup> L. J. Farrugia, *J. Appl. Crystallogr.* **1999**, *32*, 837–838.

<sup>233</sup> G. M. Sheldrick, *Acta Crystallogr. Sect. C Struct. Chem.* **2015**, *71*, 3–8.

## Chapter I

### Synthesis of 7



To a stirred solution of  $n\text{BuLi}$  (2.5 M in hexane, 110.0 mmol, 44 mL, 2.25 eq.), distilled TMEDA (5.0 mmol, 749  $\mu\text{L}$ , 0.1 eq.) was added at RT. After 30 min the mixture was cooled down to  $0^\circ\text{C}$  and then a solution of 1,1,1,3,3,3-hexafluoro-2-phenyl-2-propanol (50.0 mmol, 12 g, 1.0 eq.) in THF (15 mL) was added dropwise over 20 min. The reaction mixture was stirred for 24 h at room temperature and then was cooled again to  $0^\circ\text{C}$  and  $\text{PhSiCl}_3$  (26 mmol, 4.16 mL, 0.52 eq.) was added dropwise over 15 min. The reaction mixture was stirred for 4 h and quenched with 10 mL of HCl (0.5 M) and diluted with 150 mL of diethyl ether and washed with water. The organic layer was dried over  $\text{MgSO}_4$  and evaporated under reduced pressure. The silicate **1-Ph [LiTMEDA]** was obtained by precipitation after solubilisation of the crude product in the minimal amount of dichloromethane and addition of pentane, filtration and drying under vacuum for 6h afford silicate **1-Ph [LiTMEDA]** as a light- yellow solid (10.2 g, 81%).

$^1\text{H NMR}$  (400 MHz, acetone- $d_6$ ):  $\delta$  8.43 (d,  $J = 7.29$  Hz, 2H), 7.76 (dd, 2H), 7.44 (d,  $J = 7.70$  Hz, 1H), 7.34 (m, 2H), 7.26 (m, 2H), 6.97 (m, 4H), 3.13 (m, 4H), 2.71 (m, 12H).  $^{19}\text{F NMR}$  (376 MHz, acetone- $d_6$ ):  $\delta$  -74.44 (q, 6F), -75.74 (q, 6F).

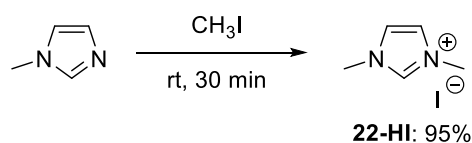
Triflic acid (1.7 mL, 19.6 mmol, 7.0 eq.) was added dropwise to a solution of **1-Ph [LiTMEDA]** (2.0 g, 2.8 mmol, 1.0 eq.) in dichloromethane (70 mL). The reaction mixture was stirred for 13 h at room temperature and then was cooled down to  $0^\circ\text{C}$ , quenched with distilled water and diluted with diethyl ether. After washing with distilled water, the organic layer was dried over  $\text{MgSO}_4$  and evaporated under reduced pressure. The crude product recrystallized in pentane to afford spirosilane **7** as off-white crystals. (1.0 g, 70%).  $^1\text{H NMR}$  (400 MHz,  $\text{tol-}d_8$ ):  $\delta$  7.55 (d,  $J = 8.0$  Hz, 2H), 7.34 (d,  $J = 6.4$  Hz, 2H), 7.05 (dd,  $J = 7.5, 1.3$  Hz, 2H), 6.93 (dd,  $J = 7.4, 1.1$  Hz, 2H);  $^{19}\text{F NMR}$  (376 MHz,  $\text{tol-}d_8$ ):  $\delta$  -75.9 (q,  $J = 8.6$  Hz, 6F), -76.24 (q,  $J = 8.7$  Hz, 6F).  $^{13}\text{C NMR}$  (100 MHz,  $\text{tol-}d_8$ ): 142.0, 133.4, 133.4, 131.5, 122.6

(q,  $^1J_{C-F} = 285$  Hz,  $CF_3$ ), 83.14 (sept,  $^2J_{C-F} = 31.8$  Hz,  $C(CF_3)_2$ )  $^{29}Si$  NMR (119 MHz,  $CDCl_3$ ):  $\delta$  7.5. NMR data are consistent with those found in literature.<sup>34</sup>

## Chapter II

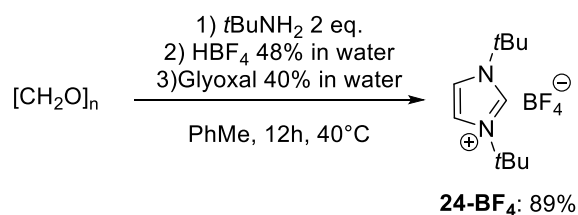
### Synthesis of Carbenes

#### Synthesis of 22-HI



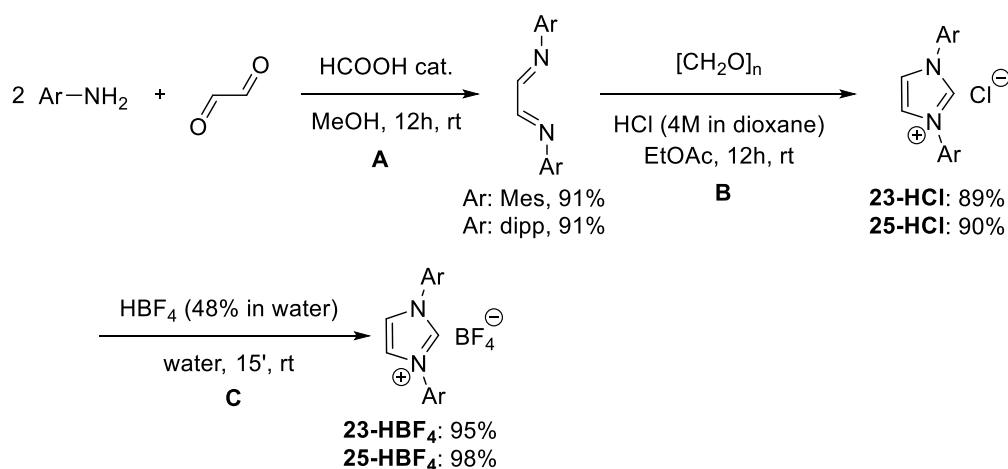
The compound was synthesised following the literature procedure.<sup>107</sup> To a solution of N-methylimidazole (1.0 g, 12.2 mmol, 1.0 eq.) in  $CH_2Cl_2$  (12 mL), methyl iodide (0.91 mL, 14.6 mmol, 1.2 eq.) was added dropwise in 15 minutes. The reaction was allowed to stir for 30 minutes. The solution was dried under vacuum to afford a pale yellow solid, 2.6 g 95%. NMR data are consistent with those found in literature.

#### Synthesis of 24-HBF<sub>4</sub>



The compound was synthesised following the literature procedure.<sup>111</sup> Paraformaldehyde (3.0 g, 100 mmol, 1.0 eq.) was dissolved in toluene (100 mL), then *tert*-butylamine (10.6 mL, 100 mmol, 1.0 eq.) was added dropwise. The mixture was stirred until a clear solution was obtained. The solution was then cooled at 0°C and another equivalent of *tert*-butylamine (10.6 mL, 100 mmol, 1.0 eq.) was added. Always at 0°C  $HBF_4$  48% in water (13.0 mL, 100 mmol, 1.0 eq.) was added dropwise to the mixture. The cooling was removed and once the reaction had reached room temperature, glyoxal 40% in water (11.5 mL, 100.0 mmol, 1.0 eq.) was added. The mixture was heated at 40°C and stirred overnight, a colorless solid precipitate. the mixture was filtrate and the solid obtained was washed with 50 mL of water and with 50 mL of  $Et_2O$ , then dried under vacuum. Obtained a white solid, 22.5 g 84%. NMR data are consistent with those found in literature.

## General procedure for the synthesis of 23-HBF<sub>4</sub> and 25-HBF<sub>4</sub><sup>109</sup>



### Step A

In a round bottom flask containing methanol (2 M) the corresponding aniline (2.0 mmol, 1.0 eq.) was added, the solution was then stirred for five minutes. Glyoxal (1.0 mmol, 0.5 eq.), 40% solution in water, was added followed by few drop of formic acid as catalyst, a yellow precipitate appeared. The reaction was allowed to stir overnight. The mixture was then filtered and the yellow solid was washed with methanol, 5x20 mL, and then dried under vacuum for 4 h. The NMR analysis of the diazabutadiene are consistent with that found in literature.<sup>109</sup>

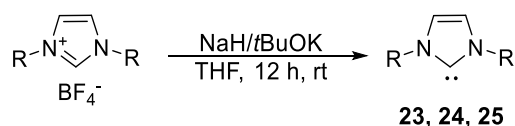
### Step B

In a round bottom flask paraformaldehyde (2.1 mmol, 1.05 eq.) was added to a solution of HCl 4 M in dioxane (3.0 mmol, 1.5 eq.), the mixture was allowed to stir until total dissolution. The first solution was added dropwise to a round bottom flask containing a solution of diazabutadiene (2.0 mmol, 1.0 eq.) in ethyl acetate (0.5 M), a white precipitate appeared. The reaction was allowed to stir overnight. The mixture was then filtered and the solid was washed with ethyl acetate, 5x 20 mL. the off-white solid obtained was dried under argon for 4 h. The NMR analysis of the imidazolium chloride obtained are consistent with that found in literature.<sup>109</sup>

### Step C

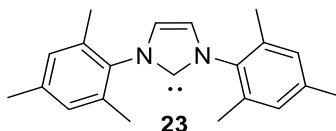
To a round bottom flask containing imidazolium chloride (1.0 mmol, 1.0 eq.) distilled water was added until dissolution of the solid occur. Then  $\text{HBF}_4$  (1.1 mmol, 1.1 eq.), 48% in water, was added dropwise to the solution and a white precipitate instantly appeared. The mixture was allowed to stir for fifteen minutes. The water solution was extracted with dichloromethane, 3x150 mL. the organic phase was dried over  $\text{MgSO}_4$ , filtrated and the solvent was evaporated affording a white solid that was dried under vacuum for 4 h. The NMR analysis of the imidazolium tetrafluoroborate obtained are consistent with that found in literature.<sup>109</sup>

### General Procedure for the synthesis of carbenes, 23, 24, 25



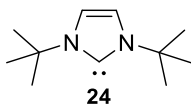
In a flame-dried Schlenk tube, imidazolium tetrafluoroborate (8.3 mmol, 1.0 eq.), NaH (398 mg, 16.6 mmol, 2.0 eq.) and *t*BuOK (93.13 mg, 0.83 mmol, 0.1 eq.), were added followed by the addition of THF (0.2 M). The reaction was stirred for 12 h, after that time the agitation was stopped and the solution was decanted. The liquid phase was transferred in another flame dried Schlenk tube using a filtrating canula. The remaining solid was washed with THF and the liquid phase was transferred. After concentration of the liquid phase, pentane (20 mL) was added and a precipitate appeared. The solid was filtered off using a filtrating cannula, washed with pentane (20 mL) and filtered again. The free carbene was dried under vacuum for 4 h, then stored in the glove box.

### 1,3-Bis(2,4,6-trimethylphenyl)imidazol-2-ylidene (23)



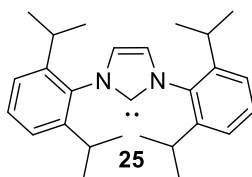
Carbene **23** (IMes) was synthesized following the general procedure. Yield: 84%.  $^1\text{H NMR}$  (400 MHz,  $\text{tol-d}_8$ ): 6.77 (s, 4H), 6.5 (s, 2H), 2.16 (s, 6H), 2.11 (s, 12H);  $^{13}\text{C NMR}$  (100 MHz,  $\text{tol-d}_8$ ): 219.7, 139.2, 137.0, 135.3, 129.0, 120.4, 21.0, 18.0. NMR data are consistent with those found in literature.<sup>109</sup>

### 1,3-bis(2,6-di-tert-butyl)imidazol-2-ylidene (**24**)



Carbene **24** (*ItBu*) was synthesized following the general procedure. Yield: 61%.  $^1\text{H NMR}$  (400 MHz,  $\text{tol-d}_8$ ): 6.75 (s, 2H), 1.47 (s, 18H);  $^{13}\text{C NMR}$  (100 MHz,  $\text{tol-d}_8$ ): 213.1, 114.8, 55.7, 31.4. NMR data are consistent with those found in literature.<sup>109</sup>

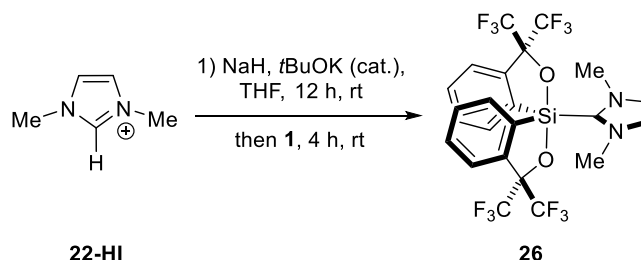
### 1,3-bis(2,6-diisopropylphenyl)imidazol-2-ylidene (**25**)



Carbene **25** (*IPr*) following the general procedure. Yield: 78%.  $^1\text{H NMR}$  (400 MHz,  $\text{tol-d}_8$ ): 7.25 (q, 2H), 7.14 (d,  $J = 7.7\text{Hz}$ , 4H), 6.64 (s, 2H), 2.91 (m, 4H), 1.24 (d,  $J = 6.9\text{Hz}$ , 12H), 1.17 (d,  $J = 7.0\text{ Hz}$ , 12H);  $^{13}\text{C NMR}$  (100 MHz,  $\text{tol-d}_8$ ): 220.7, 146.2, 138.9, 123.5, 121.5, 28.7, 24.7, 23.6. NMR data are consistent with those found in literature.<sup>109</sup>

## Synthesis of NHC-Martin's Adducts

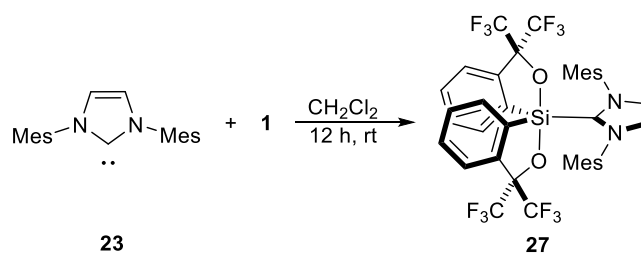
### Synthesis of adduct **26**



In a flame-dried Schlenk tube under argon, imidazolium salt **22-HI** (218 mg, 0.97 mmol, 1.0 eq.), NaH (46 mg, 1.95 mmol, 2.0 eq.) and *t*BuOK (10.88 mg, 0.097 mmol, 0.1 eq.), were added followed by the addition of THF (1.9 mL). The reaction was stirred for 12 h then **7** (500 mg, 0.97 mmol, 1.0 eq.) was added and the reaction mixture was stirred for 4 h. After this time the solvent was evaporated and the white solid was dissolved in the minimal amount of dichloromethane and was passed over a short pad of silica ( $R_f$ : 0.96), washed three times with 15 mL of dichloromethane. The solvent was evaporated and a white solid was obtained. 496 mg, 84%. Melting Point: 255-263°C. **HRMS-ESI** Mass calculated for  $\text{C}_{23}\text{H}_{16}\text{F}_{12}\text{N}_2\text{NaO}_2\text{Si}$ : 631.0682; found: 631.0691.  $^1\text{H NMR}$  (600 MHz,  $\text{CD}_2\text{Cl}_2$ ): 8.26 (d,  $J = 7.4\text{ Hz}$ , 2H), 7.63 (d,  $J = 7.6\text{ Hz}$ , 2H), 7.55 (td,  $J = 7.2, 1.0\text{ Hz}$ , 2H), 7.50 (td,  $J = 7.5, 1.4\text{ Hz}$ ,

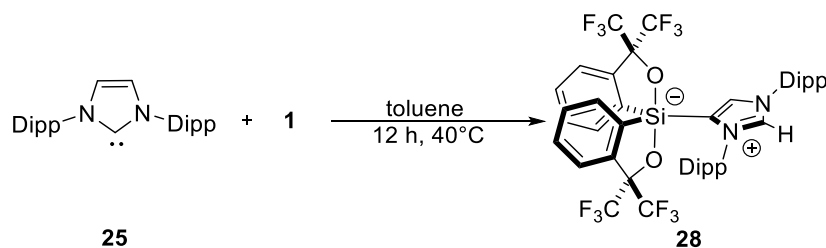
2H), 6.80 (s, 2H), 3.74 (s, 6H);  $^{19}\text{F}$  NMR (564 MHz,  $\text{CD}_2\text{Cl}_2$ ): -75.93 (q,  $J = 9.2$  Hz, 6F), -77.10 (q,  $J = 9.2$  Hz, 6F);  $^{13}\text{C}$  NMR (150 MHz,  $\text{CD}_2\text{Cl}_2$ ): 160.1, 142.1, 138.2, 138.1, 131.0, 130.2, 124.7, 124.4 (q,  $^1J_{\text{C-F}} = 287$  Hz,  $\text{CF}_3$ ), 124.2 (q,  $^1J_{\text{C-F}} = 287$  Hz,  $\text{CF}_3$ ), 122.3, 82.1 (sept,  $^2J_{\text{C-F}} = 29.6$  Hz,  $\text{C}(\text{CF}_3)_2$ ), 37.6;  $^{29}\text{Si}$  NMR (119 MHz,  $\text{CD}_2\text{Cl}_2$ ): -83.54.

### Synthesis of adduct **27**



In a flame-dried Schlenk tube, **23** (304 mg, 1.0 mmol, 1.0 eq.) and **7** (461 mg, 0.9 mmol, 0.9 eq.) and  $\text{CH}_2\text{Cl}_2$  (19.6 mL) were added. The reaction was stirred for 12 h, after the mixture was filtered through a pad of silica ( $R_f$ : 0.96), washed with dichloromethane (3x20 mL). The filtrate was evaporated and a pale yellow solid was obtained. 568 mg, 77%. Melting Point: 205-215°C. **HRMS-ESI** Mass calculated for  $\text{C}_{39}\text{H}_{33}\text{F}_{12}\text{N}_2\text{O}_2\text{Si}$ : 817.2114; found: 817.2138.  $^1\text{H}$ NMR (400MHz,  $\text{tol-d}_8$ ): 7.57 (d,  $J = 7.7$  Hz, 2H), 7.24 (d,  $J = 7.6$  Hz, 2H), 7.06 (td,  $J = 7.5, 1.4$  Hz, 2H), 6.92 (td,  $J = 7.3, 1.1$  Hz, 2H), 6.86 (bs, 2H), 6.21 (bs, 2H), 5.72 (bs, 2H), 2.14 (s, 6H), 2.11 (s, 6H), 1.14 (s, 6H);  $^{19}\text{F}$ NMR (376MHz,  $\text{tol-d}_8$ ): -71.82 (q,  $J = 10.7$  Hz, 6F), -73.56 (q,  $J = 10.6$  Hz, 6F);  $^{13}\text{C}$ NMR(100MHz,  $\text{tol-d}_8$ ): 160.1, 141.6, 140.1, 140.0, 138.8, 136.7, 136.2, 133.7, 129.6, 129.4, 129.0, 128.7, 125.1 (q,  $^1J_{\text{C-F}} = 287$  Hz,  $\text{CF}_3$ ), 124.2 (q,  $^1J_{\text{C-F}} = 290$  Hz,  $\text{CF}_3$ ), 123.5, 123.2, 82.6 (sept,  $^2J_{\text{C-F}} = 28.9$  Hz,  $\text{C}(\text{CF}_3)_2$ ), 18.5 (q,  $J = 3.3$  Hz), 16.5 (q,  $^9J_{\text{C-F}} = 3.3$  Hz);  $^{29}\text{Si}$ NMR (119MHz,  $\text{CD}_2\text{Cl}_2$ ): -81.82

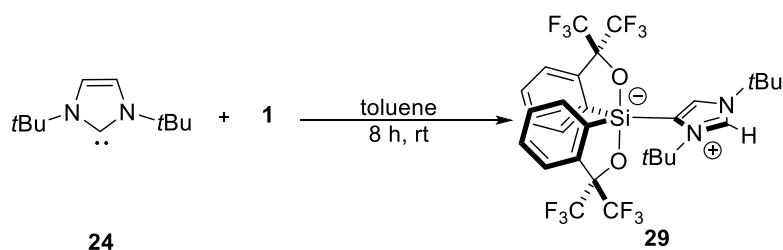
### Synthesis of adduct **28**



In a flame-dried Schlenk tube under argon, **25** (389mg, 1.0 mmol, 1.0 eq.), **7** (461mg, 0.9 mmol, 0.9 eq) and distilled toluene (0.05 M) were added, and the solution was stirred for 12 h at 40°C. After this time the solvent was evaporated and the white solid was dissolved in the minimal amount of dichloromethane and was passed over a silica pad ( $R_f$ : 0.93), that was

washed five times with 20mL of dichloromethane. The solvent was evaporated and the abnormal adduct **28** was obtained as a white solid, 631 mg, yield: 70%. 226.5-230°C HRMS-ESI Mass calculated for C<sub>45</sub>H<sub>43</sub>F<sub>12</sub>N<sub>2</sub>O<sub>2</sub>Si: 899.2891; found: 899.2909. <sup>1</sup>H NMR (600 MHz, CD<sub>2</sub>Cl<sub>2</sub>) δ 7.98 (d, *J* = 7.26 Hz, 2H), 7.91 (d, *J* = 1.74Hz, 1H), 7.54 (t, *J* = 7.82 Hz, 1H), 7.50 (d, *J* = 7.7 Hz 2H), 7.46 (t, *J* = 7.74Hz, 1H), 7.41 (m, 2H), 7.34 (dd, *J* = 7.91, 1.34, 2H), 7.29 (m, 5H), 7.18 (d, *J* = 6.9 Hz, 1H), 7.03 (dd, *J* = 7.69, 1.58, 1H), (d, 7.8 Hz, 1H), 2.94 (m, *J* = 6.62Hz, 1H), 2.40 (m, *J* = 6.87 Hz, 1H), 2.33 (m, *J* = 6.71 Hz 1H), 2.25 (m, *J* = 6.97 Hz, 1H), 1.35 (d, *J* = 6.5 Hz, 3H), 1.24 (d, *J* = 6.78 Hz, 3H), 1.15 (t, *J* = 6.62 Hz, 6H), 1.02 (d, *J* = 6.86 Hz, 3H), 0.97 (d, *J* = 6.76 Hz, 3H), 0.77 (d, *J* = 6.82 Hz, 3H), 0.59 (d, *J* = 6.53 Hz, 3H). <sup>19</sup>F NMR (564 MHz, CD<sub>2</sub>Cl<sub>2</sub>) δ -74.47 (q, *J* = 9.8, 9.74 Hz 6F), -75.45 (q, *J* = 9.82, 9.7 Hz, 6F). <sup>13</sup>C NMR (150 MHz, CD<sub>2</sub>Cl<sub>2</sub>): 148.0, 146.0, 146.0, 145.9, 145.8, 145.3, 142.4, 141.1, 137.6, 136.8, 133.4, 132.4, 132.1, 131.4, 130.3, 129.4, 129.3, 129.2, 128.6, 125.7, 125.5, 125.1, 125.0, 124.6, 124.6 (q, <sup>1</sup>*J*<sub>C-F</sub> = 287 Hz, CF<sub>3</sub>), 124.3, 124.3 (q, <sup>1</sup>*J*<sub>C-F</sub> = 289 Hz, CF<sub>3</sub>), 124.1, 82.0 (sept, <sup>2</sup>*J*<sub>C-F</sub> = 28.8 Hz, C(CF<sub>3</sub>)<sub>2</sub>), 29.6, 29.1, 29.0, 28.6, 28.5, 27.3, 26.8, 24.7, 24.5, 24.4, 24.1, 24.0, 23.8, 22.6, 21.6, 21.1; <sup>29</sup>Si NMR (119 MHz, CD<sub>2</sub>Cl<sub>2</sub>) δ -81.96.

### Synthesis of adduct **29**



In a flame-dried Schlenk tube under argon, **24** ( 774 mg, 4.3 mmol, 1.1eq.), **7** ( 2.0 g, 3.9 mmol, 1.0 eq) and distilled toluene (0.05 M) were added, and the solution was stirred for 8 h. After this time the solvent was evaporated and the white solid was dissolved in the minimal amount of dichloromethane and was passed over a short pad of silica (R<sub>f</sub>: 0.86), that was washed five times with 20 mL of dichloromethane. The solvent was evaporated and the abnormal adduct **29** was obtained as a white solid, 2.1 g, yield: 77%. <sup>1</sup>H NMR (400 MHz, CD<sub>2</sub>Cl<sub>2</sub>): 8.30 (d, *J* = 7.2 Hz, 2H), 7.82 (d, *J* = 2.0 Hz, 1H), 7.57 (d, *J* = 7.8 Hz, 2H), 7.50 (td, *J* = 7.3, 1.2 Hz, 2H), 7.42 (td, *J* = 7.5, 7.4, 1.4 Hz, 2H), 6.98 (d, *J* = 2.0 Hz, 1H), 1.51 (s, 9H), 1.45 (s, 9H); <sup>19</sup>F NMR (376 MHz, CD<sub>2</sub>Cl<sub>2</sub>): -75.27 (q, *J* = 9.6 Hz, 6F), -75.62 (q, *J* = 9.6 Hz, 6F); <sup>13</sup>C NMR (100 MHz, CD<sub>2</sub>Cl<sub>2</sub>): 147.3, 142.2, 141.3, 137.9, 129.9, 129.7, 128.4, 126.5, 124.7 (q, <sup>1</sup>*J*<sub>C-F</sub> = 287 Hz, CF<sub>3</sub>), 124.5 (q, <sup>1</sup>*J*<sub>C-F</sub> = 290 Hz, CF<sub>3</sub>), 124.4, 82.1 (sept, <sup>2</sup>*J*<sub>C-F</sub> = 28.9 Hz, C(CF<sub>3</sub>)<sub>2</sub>), 61.9, 58.7, 31.0, 29.9; <sup>29</sup>Si NMR (119 MHz, CD<sub>2</sub>Cl<sub>2</sub>): -79.0

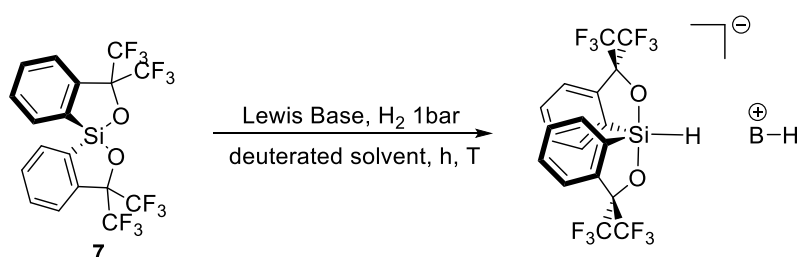
## Chapter III

### Hydrogen Activation Reactions

#### Summary of the Conditions

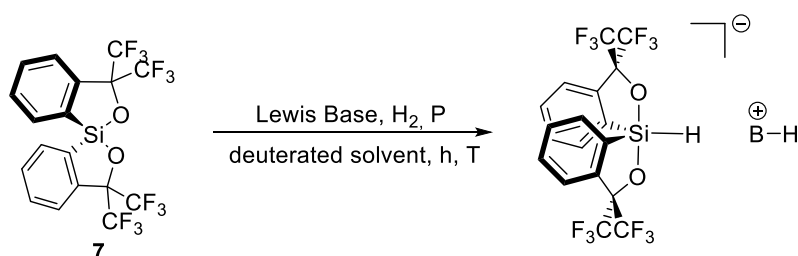
<i>Temperature (°C)</i>	<i>Pressure (bar)</i>	<i>Solvent</i>
25, 40, 50, 70, 80, 100, 110, 120	1, 5, 10, 15, 20, 25, 50	Dichloromethane, Toluene, Bromobenzene and deuterated analogue

#### General procedure for NMR-scale reactions



In an oven-dried screw-cap NMR tube in the glow box, **7** (20 mg, 0.04 mmol, 1.0 eq.), Lewis base (0.04 mmol, 1.0 eq.) and the deuterated solvent (0.065 M) were added. After it was sorted from the glow box, H<sub>2</sub> was bubbled in the solution for ten minutes. NMR analysis were performed just after the addition of hydrogen or after an established amount of time. The reaction was also heated at different temperature by immersion in an oil bath.

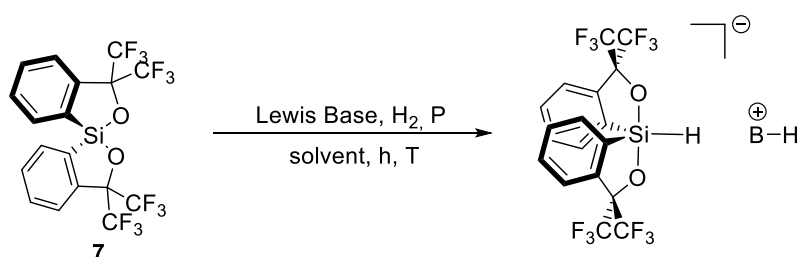
#### General procedure for High-Pressure NMR-scale reactions



In an oven-dried J-Young NMR tube in the glow box, **7** (20 mg, 0.04 mmol, 1.0 eq.), Lewis base (0.04 mmol, 1.0 eq.) and the deuterated solvent, volume in dependence of the

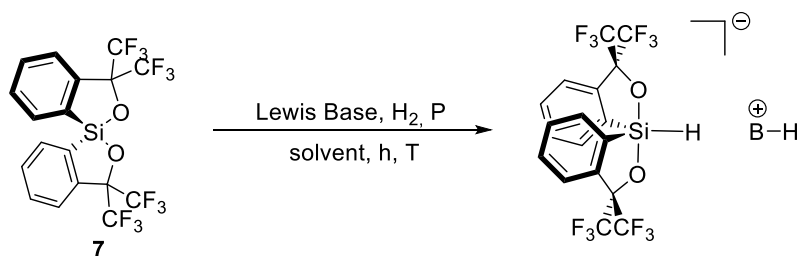
pressure, were added. For the addition of H<sub>2</sub> at the required pressure, it was used the  $PV=nRT$ . Hydrogen was added with the freeze-pump-thaw technique.

### General procedure for Microwave vial scale reactions



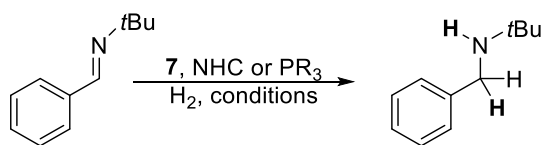
In flame-dried Microwave vial in the glow box, **7** (100 mg, 0.2 mmol, 1.0 eq.), Lewis base (0.2 mmol, 1.0 eq.) and distilled solvent, volume in dependence of the pressure, were added. The gas was added or bubbling it in the solution or with freeze-pump-thaw technique. Once the reaction is finished the solvent was removed under vacuum, and then the vial was put inside the glow box, where the NMR tube was prepared.

### General procedure for High Pressure reactions



In flame-dried Microwave vial in the glow box, **7** (100 mg, 0.2 mmol, 1.0 eq.), Lewis base (0.2 mmol, 1.0 eq.) and distilled solvent (0.065 M) were added. The open vial was put inside a steel autoclave under argon and filled with 3 Å molecular sieves, pre-activated at 300°C for 20 h under vacuum. Purged two times with 10 bar of hydrogen and the filled with the desired pressure. If it was necessary to heat it, a heater was put around the reactor. Once the reaction was finished the solvent was evaporated and the crude product was analysed by NMR.

## General procedure for the hydrogenation of imine



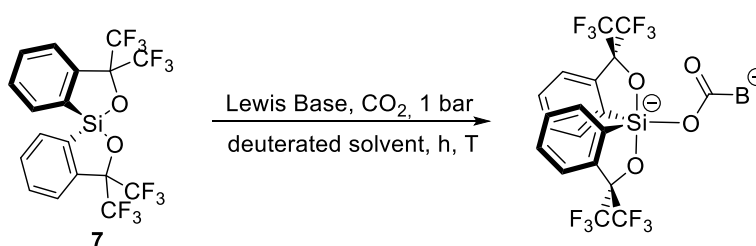
In flame-dried Microwave vial in the glow box, **7** (50 mg, 0.1 mmol, 1.0 eq.), Lewis base (0.1 mmol, 1.0 eq.), imine (17.79  $\mu$ L, 0.1 mmol, 1.0 eq.) and distilled solvent (0.065 M) were added. The vial was then sealed and put under hydrogen atmosphere with the Freeze-pump-thaw technique. Reaction was performed in different conditions of temperature pressure and solvent. Once the reaction was ended, the solvent was evaporated and an NMR tube of the crude was prepared in the glove box.

## Activation of the Carbon Dioxide

### Summary of the Conditions

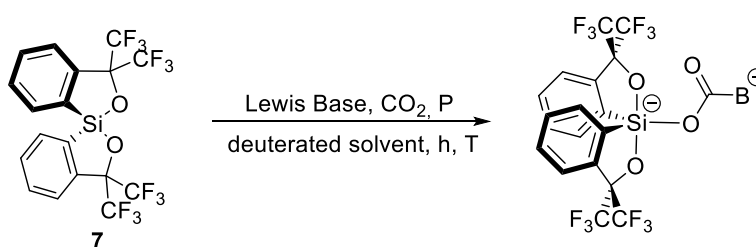
<i>Temperature (°C)</i>	<i>Pressure (bar)</i>	<i>Solvent</i>
25, 40, 50, 70, 80, 100, 110, 120	1, 5, 10, 15	Dichloromethane, Toluene, Bromobenzene and deuterated analogue

### General procedure for NMR-scale reactions



In an oven-dried screw-cap NMR tube in the glow box, **7** (20 mg, 0.04 mmol, 1.0 eq.), Lewis base (0.04 mmol, 1.0 eq.) and the deuterated solvent (0.065 M) were added. After it was sorted from the glow box, CO<sub>2</sub> was bubbled in the solution for ten minutes. NMR analysis were performed just after the addition of hydrogen or after an established amount of time. The reaction was also heated at different temperature by immersion in an oil bath.

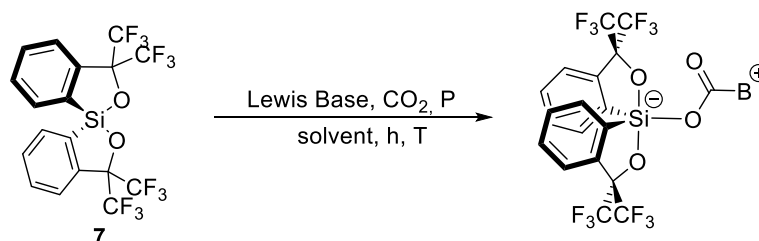
### General procedure for High-Pressure NMR-scale reactions



In an oven-dried J-Young NMR tube in the glow box, **7** (20 mg, 0.04 mmol, 1.0 eq.), Lewis base (0.04 mmol, 1.0 eq.) and the deuterated solvent, volume in dependence of the pressure, were added. For the addition of CO<sub>2</sub> at the required pressure, it was used the  $PV=nRT$ . The NMR tube was degassed by freeze-pump-thaw and leave under vacuum at -196°C then the carbon dioxide, passed over the dried system, was took from a flask,

connected at the end of the dry system, filled with molecular sieves (activated at 300°C for 20 h under vacuum) by syringe and added by injection in the NMR tube. The latter was allowed to heat at room temperature and NMR analysis was performed.

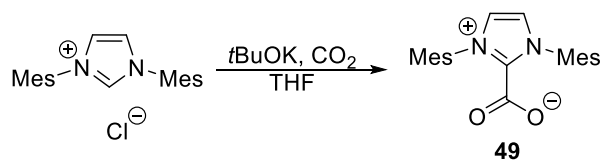
### General procedure for Microwave vial scale reactions



In flame-dried Microwave vial in the glow box, **7** (100 mg, 0.2 mmol, 1.0 eq.), Lewis base (0.2 mmol, 1.0 eq.) and distilled solvent, volume in dependence of the pressure, were added. The gas was added by bubbling it in the solution or with freeze-pump-thaw technique. Once the reaction is finished the solvent was removed under vacuum, and then the vial was put inside the glow box, where the NMR tube was prepared.

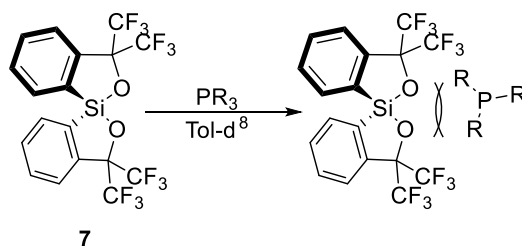
### Indirect activation

#### Synthesis of **49**



Product **49** was synthesised following the literature procedure.<sup>188</sup> In an flame-dried Schlenk tube under argon, **23-HCl** (200.0 mg, 0.58 mmol, 1.0 eq.) and *t*BuOK (78.1 mg, 0.69 mmol, 1.2 eq.) were added. The argon was substituted by CO<sub>2</sub> and then distilled THF (3 mL) was added. The reaction was allowed to stir for 6 h. then the solvent was removed and the crude product was dissolved with CH<sub>2</sub>Cl<sub>2</sub> and passed through a Celite pad. The filtrate was evaporated and washed with Et<sub>2</sub>O and the remaining solid was dried under vacuum. **49** was obtained as a white solid, 139.4 mg 69%. NMR data are consistent with those found in literature.

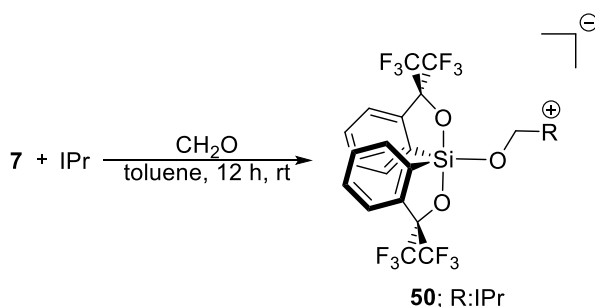
## Interactions between **7** and phosphine



In a screw cap NMR tube under argon, spirosilane **7** (20.0 mg, 0.04 mmol, 1.0 eq.), the corresponding phosphine (0.04 mmol, 1.0 eq.) and Tol- $d_8$  (0.75 mL) were added. The NMR tube was shaken until all the reagents were solubilised. Then NMR was performed. No formation of adduct was noticed.

## Synthesis of the Formaldehyde adducts

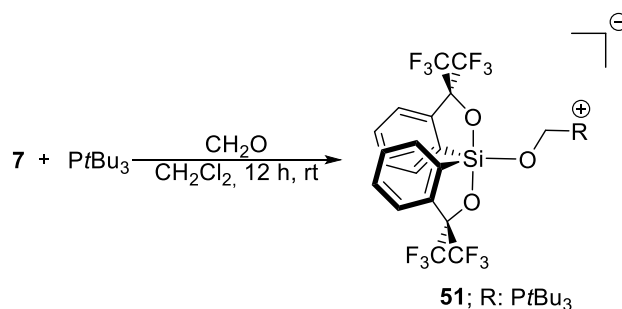
### Synthesis of formaldehyde adduct **50**



In an flame-dried Schlenk tube under argon, IPr (77.7 mg, 0.2 mmol, 1.0 eq. ), **7** (102.5 mg, 0.2 mmol, 1.0 eq. ), paraformaldehyde (12.0 mg, 0.4 mmol, 2 eq.) and toluene (1.4 mL, 0.14 M) were added, the resulting mixture was allowed to stir for 12 h. Then the solvent was concentrated, and pentane was added. The liquid phase was removed and toluene (0.5 M) was added, the mixture was stirred for 5 min. Pentane was added in order to form a precipitate which was filtered off. The purification was repeated two other times. The solid was dried under vacuum for 8h. **50** was obtained as an off-white solid 109 mg, 59%. **HRMS-ESI** Mass calculated for  $C_{46}H_{46}F_{12}N_2NaO_3Si$ : 953.2984; found: 953.2957.  **$^1H$  NMR** (600 MHz,  $CD_2Cl_2$ ): 7.78 (d,  $J = 6.7$  MHz, 2H), 7.53 (t,  $J = 7.8$  Hz, 2H), 7.39 (dd,  $J = 7.8, 1.4$  Hz, 4H), 7.28 (s, 2H), 7.21 (ddd,  $J = 7.1, 5.0, 1.6$  Hz, 4H), 7.16 (dd,  $J = 7.8, 1.3$  Hz, 2H), 4.67 (d,  $J = 13.6$  Hz, 1H), 4.11 (d,  $J = 13.6$ , 1H), 2.49 (s,  $J = 6.8$  Hz, 2H), 2.15 (s,  $J = 6.8$  Hz, 2H), 1.39 (d,  $J = 6.8$  Hz, 6H), 1.13 (d,  $J = 6.9$  Hz, 6H), 1.05 (d,  $J = 6.8$  Hz, 6H), 0.70 (d,  $J = 6.8$  Hz,

6H);  $^{19}\text{F}$  NMR (564 MHz,  $\text{CD}_2\text{Cl}_2$ ): -74.1 (q,  $J = 9.6$  Hz, 6F), -75.77 (q,  $J = 9.6$  Hz, 6F);  $^{13}\text{C}$  NMR (150 MHz,  $\text{CD}_2\text{Cl}_2$ ): 150.7, 146.1, 145.3, 142.9, 141.0, 137.2, 132.4, 130.2, 128.8, 128.7, 125.3, 125.1, 124.8, 124.8 (q,  $^1J_{\text{C-F}} = 288$  Hz,  $\text{CF}_3$ ), 124.5 (q,  $^1J_{\text{C-F}} = 288$  Hz,  $\text{CF}_3$ ), 123.7, 80.6 (sept,  $^2J_{\text{C-F}} = 27.9$  Hz,  $\text{C}(\text{CF}_3)_2$ ), 29.4, 29.2, 25.7, 25.5, 22.7, 21.9;  $^{29}\text{Si}$  NMR (119MHz,  $\text{CD}_2\text{Cl}_2$ ): -76.82.

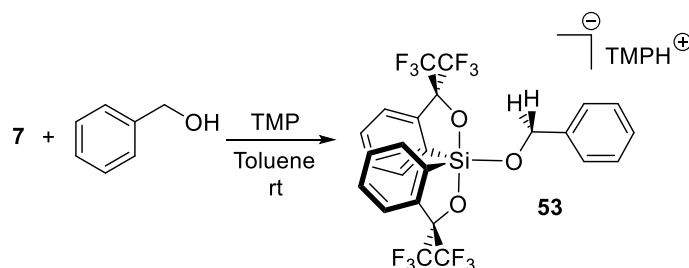
### Synthesis of formaldehyde adduct **51**



In a flame-dried Schlenk tube under argon,  $\text{PtBu}_3$  (40.5 mg, 0.2 mmol, 1.0 eq. ), **7** (102.5 mg, 0.2 mmol, 1.0 eq. ), paraformaldehyde (24.0 mg, 0.8 mmol, 4 eq.) and  $\text{CH}_2\text{Cl}_2$  (1.4 mL) were added, the resulting mixture was allowed to stir for 4 h at RT. The reaction was then filtered through a pad of celite to get rid of the excess of paraformaldehyde. Pentane was added to the filtrate and the precipitate was collected by filtration and washed with pentane (2x 7mL). The white solid was dried for 4 h under vacuum. **51** was obtained as a white solid, 85.7 mg, 61%. Melting Point: 223-227°C. HRMS-ESI Mass calculated for  $\text{C}_{28}\text{H}_{31}\text{F}_{12}\text{NaO}_3\text{PSi}$ : 725.1486; found: 725.1483.  $^1\text{H}$  NMR (600 MHz  $\text{CDCl}_3$ ): 8.16 (d,  $J = 7.2$  Hz, 2H), 7.56 (d,  $J = 7.6$  Hz, 2H), 7.37 (m, 4H), 4.95 (d,  $J = 14.6$  Hz, 1H), 4.37 (d,  $J = 14.6$  Hz, 1H), 2.46 (m, 3H), 1.29 (q,  $J = 7.3$  Hz, 9H), 1.20 (q,  $J = 7.3$  Hz, 9H);  $^{19}\text{F}$  NMR (564 MHz,  $\text{CDCl}_3$ ): -74.07 (q,  $J = 9.3$  Hz, 6F), -75.09 (q,  $J = 9.2$  Hz, 6F);  $^{13}\text{C}$  NMR (150 MHz,  $\text{CDCl}_3$ ): 141.3, 141.0, 137.5, 129.3, 128.7, 124.8 (q,  $^1J_{\text{C-F}} = 288$  Hz,  $\text{CF}_3$ ), 124.3 (q,  $^1J_{\text{C-F}} = 288$  Hz,  $\text{CF}_3$ ), 123.6, 80.8 (sept,  $^2J_{\text{C-F}} = 28.4$  Hz,  $\text{C}(\text{CF}_3)_2$ ), 52.0 (d,  $^2J_{\text{C-P}} = 62.0$  Hz,  $\text{CH}_2\text{O}$ ), 19.3 (d,  $J = 40.4$  Hz,  $\text{CHP}$ ), 16.8 (d,  $J = 3.5$  Hz,  $\text{CH}_3\text{CP}$ ), 16.8 (d,  $J = 3.6$  Hz,  $\text{CH}_3\text{CP}$ );  $^{31}\text{P}$  NMR (243 MHz,  $\text{CDCl}_3$ ): 38.78;  $^{29}\text{Si}$  NMR(119 MHz,  $\text{CDCl}_3$ ): -76.7 (d,  $J = 13.4$  Hz).

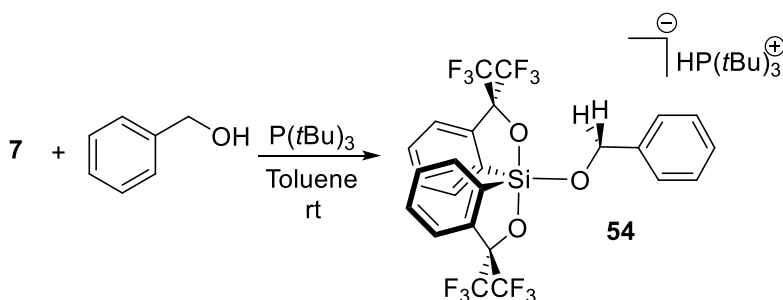
## Synthesis of the benzyl alcohol adducts

### Synthesis of benziloxysiliconate **53**



In an oven-dried screw cap NMR tube, under argon, spirosilane **7** (20 mg, 0.039 mmol, 1.0 eq. ) benzyl alcohol (3.63  $\mu\text{L}$ , 0.039 mmol, 1.0 eq. ), TMP (6.58  $\mu\text{L}$ , 0.039 mmol, 1.0 eq. ) and tol- $d_8$  (0.75 mL, 0.052M) were added. The tube was shaken for 10 min, and leave at RT for 7 h. NMR showed the desired product, with a slight excess of **7**.  **$^1\text{H}$  NMR** (400 MHz, tol- $d_8$ ): 8.57 (dd,  $J = 7.5, 1.3$  Hz, 2H), 7.82 (d,  $J = 7.9$  Hz, 2H), 7.32 (td,  $J = 7.3, 1.1$  Hz, 2H), 7.20 (td,  $J = 7.5, 1.4$  Hz, 2H), 7.03 (m, 3H), 6.88 (dd,  $J = 5.0, 2.0$  Hz, 2H), 5.13 (d,  $J = 12.6$  Hz, 1H), 4.93 (d,  $J = 12.6$  Hz, 1H), 0.77 (bs, 18H);  **$^{19}\text{F}$  NMR** (376 MHz, tol- $d_8$ ): -73.22 (q,  $J = 9.6$  Hz, 6F), -74.81 (q,  $J = 9.6$  Hz, 6F).  **$^{13}\text{C}$  NMR**,  **$^{29}\text{Si}$  NMR** cannot be obtained due to the degradation of the sample during the analysis.

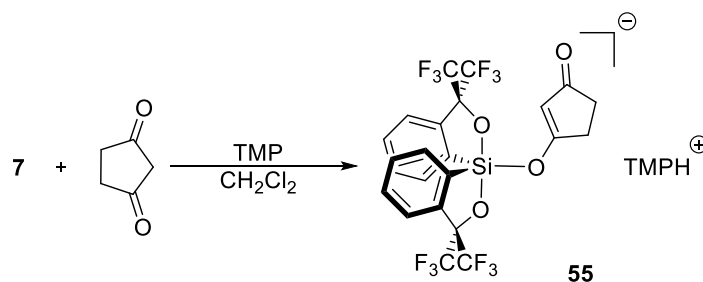
### Synthesis of benziloxysiliconate **54**



In an oven-dried screw cap NMR tube, under argon, spirosilane **7** (20 mg, 0.039 mmol, 1.0 eq. ) benzyl alcohol (3.63  $\mu\text{L}$ , 0.039 mmol, 1.0 eq. ), tri-tert-butyl phosphine (7.9 mg, 0.039 mmol, 1.0 eq. ) and tol- $d_8$  (0.75 mL, 0.052M) were added. The tube was shaken for 10 minutes then after 7 h, a white precipitate appeared. The mixture was filtrate and the solid was dried under vacuum. The solid was dissolved in  $\text{CD}_2\text{Cl}_2$  and NMR was performed. **54** was obtained as a white solid (28.7 mg, 85%).  **$^1\text{H}$  NMR** (400 MHz,  $\text{CD}_2\text{Cl}_2$ ): 8.20 (d,  $J = 6.80$  Hz, 2H), 7.55 (d,  $J = 6.5$  Hz, 2H), 7.36 (m, 5H), 7.22 (d,  $J = 7.1$  Hz, 2H), 7.13 (t,  $J = 7.5$  Hz, 2H), 5.03 (d,  $J = 437$  Hz, 1H P-H), 4.86 (d,  $J = 13.9$  Hz, 1H, CH benzyl), 4.69 (d,  $J = 14.0$

Hz, 1H, CH benzyl), 1.44 (d,  $J = 15.7$  Hz, 27H);  $^{19}\text{F}$  NMR (376 MHz,  $\text{CD}_2\text{Cl}_2$ ): -74.48 (q,  $J = 9.5$  Hz, 6F), -75.37 (q,  $J = 9.3$  Hz, 6F);  $^{13}\text{C}$  NMR (100 MHz,  $\text{CD}_2\text{Cl}_2$ ): 144.9, 144.0, 137.8, 137.1, 128.8, 128.8, 128.7, 127.9, 127.3, 127.0, 125.9, 123.8, 81.0 (sept,  $^2J_{\text{C-F}} = 28.9$  Hz,  $\text{C}(\text{CF}_3)_2$ ), 65.4, 37.7 ( $J = 27.5$  Hz, CP), 30.2;  $^{31}\text{P}$  NMR (161 MHz,  $\text{CD}_2\text{Cl}_2$ ): 57.54.  $^{29}\text{Si}$  NMR cannot be obtained due to the degradation of the sample during the analysis.

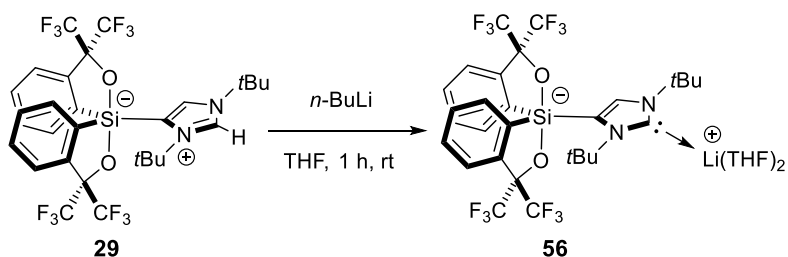
### Synthesis of the 1,3-cyclopentanedione adduct



In a flame-dried Schlenk tube under argon, 1,3-cyclopentanedione (23.0 mg, 0.23 mmol, 1.0 eq.), TMP (39.5  $\mu\text{L}$ , 0.23 mmol, 1.0 eq.) and distilled  $\text{CH}_2\text{Cl}_2$  (0.065 M) were added, the solution was allowed to stir for five minute. After that time, **7** (120 mg, 0.23 mmol, 1.0 eq.) was added at once. The reaction was allowed to stir for 2 h, a precipitate appeared. After the reaction time the solution was allowed to decant and the liquid phase was removed. Suitable crystals were obtained by slow evaporation from a dichloromethane solution of the crude product.

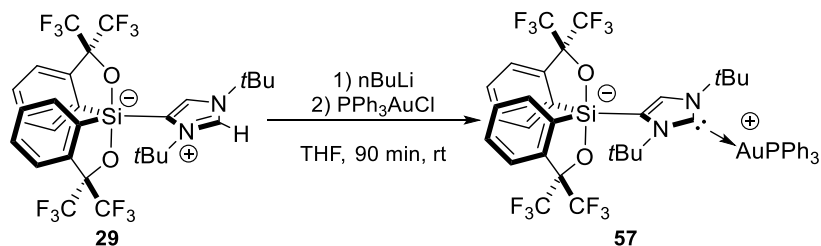
## Chapter IV

### Synthesis of the lithium derivatives **56**



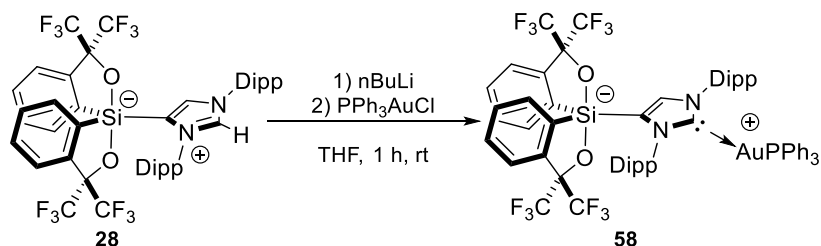
In a flame-dried Schlenk under argon abnormal adduct **29** (692 mg, 1.0 mmol, 1.0 eq) and distilled THF (10 mL, 0.1 M) were added. After total solubilisation, *n*BuLi (2.5 M, 396  $\mu$ L, 1.1 eq) was added dropwise at room temperature and the reaction was allowed to stir for 7 h. The solvent was evaporated, and the lithium complex **56** was obtained as a red solid. Quantitatively. <sup>1</sup>H NMR (400 MHz, CD<sub>2</sub>Cl<sub>2</sub>): 8.29 (d, *J* = 8.1 Hz, 2H), 7.56 (d, *J* = 7.8 Hz, 2H), 7.50 (td, *J* = 7.3, 1.2 Hz, 2H), 7.42 (td, *J* = 7.5, 7.4, 1.4 Hz, 2H), 6.97 (s, 1H), 3.68 (m, 8H), 1.8 (m, 8H) 1.51 (s, 9H), 1.45 (s, 9H); <sup>19</sup>F NMR 376 MHz, CD<sub>2</sub>Cl<sub>2</sub>): -75.28 (q, *J* = 9.5 Hz, 6F), -75.64 (q, *J* = 9.5 Hz, 6F); <sup>13</sup>C NMR (150 MHz, CD<sub>2</sub>Cl<sub>2</sub>): 147.2, 142.2, 141.3, 137.8, 129.9, 129.7, 128.4, 126.5, 124.7 (q, <sup>1</sup>*J*<sub>C-F</sub> = 288 Hz, CF<sub>3</sub>), 124.5 (q, <sup>1</sup>*J*<sub>C-F</sub> = 288 Hz, CF<sub>3</sub>), 124.4, 82.1 (sept, <sup>2</sup>*J*<sub>C-F</sub> = 28.9 Hz, C(CF<sub>3</sub>)<sub>2</sub>), 68.2, 61.9, 58.7, 31.0, 29.9, 26.0; <sup>29</sup>Si NMR (79 MHz, CD<sub>2</sub>Cl<sub>2</sub>): -79.33; <sup>7</sup>Li NMR (155 MHz, CD<sub>2</sub>Cl<sub>2</sub>): 1.34.

## Synthesis of gold(I) complex **57**



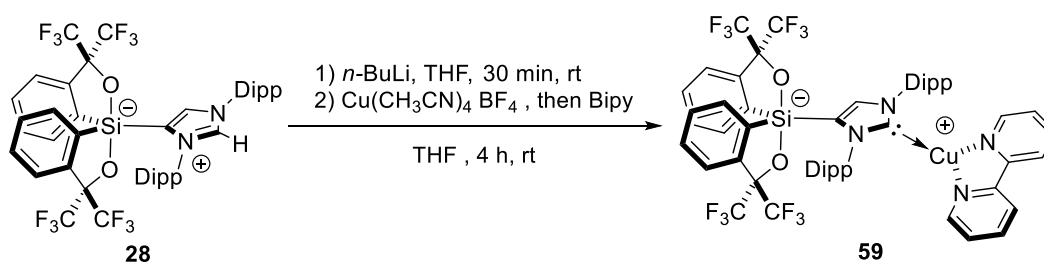
In a flame-dried Schlenk tube under argon, abnormal adduct **29** (100 mg, 0.14 mmol, 1.0 eq) was dissolved in distilled THF (2 mL, 0.07 M). *n*BuLi (2 M, 79.2  $\mu$ L, 1.1 eq) was added dropwise at room temperature and the solution was allowed to stir for 30 min before adding PPh<sub>3</sub>AuCl (71.2 mg, 0.14 mmol, 1.0 eq) at once. The reaction was stirred for another hour and then the solvent was concentrated, and distilled pentane was added to trigger the precipitation of the product. After filtration, the solid was washed with pentane then was dried under vacuum. Gold complex **57** was obtained as 129 mg, 80%. <sup>1</sup>H NMR (400 MHz, CD<sub>2</sub>Cl<sub>2</sub>): 8.21 (bd, *J* = 27.4 Hz, 2H), 7.52 (m, 17H), 7.42 (m, 2H), 7.35 (td, *J* = 7.4, 1.4 Hz, 2H), 6.85 (s, 1H), 1.81 (s, 9H), 1.61 (s, 9H); <sup>13</sup>C NMR (150 MHz, CD<sub>2</sub>Cl<sub>2</sub>): 143.0, 134.3 (d, *J*<sub>CP</sub> = 13.4 Hz), 132.5 (d, *J*<sub>CP</sub> = 2.6 Hz), 129.9 (d, *J*<sub>CP</sub> = 11.5 Hz), 129.5, 129.2, 126.2, 124.1 (bs, CH<sub>imid</sub>), 60.3, 57.7, 34.4, 32.5; <sup>19</sup>F NMR (376 MHz, CD<sub>2</sub>Cl<sub>2</sub>): -75.23 (bm, 9F), -75.89 (bs, 3F); <sup>31</sup>P NMR (161 MHz, CD<sub>2</sub>Cl<sub>2</sub>): 39.86; <sup>29</sup>Si NMR (79 MHz, CD<sub>2</sub>Cl<sub>2</sub>): -76.54.

## Synthesis of the gold(I) complex **58**



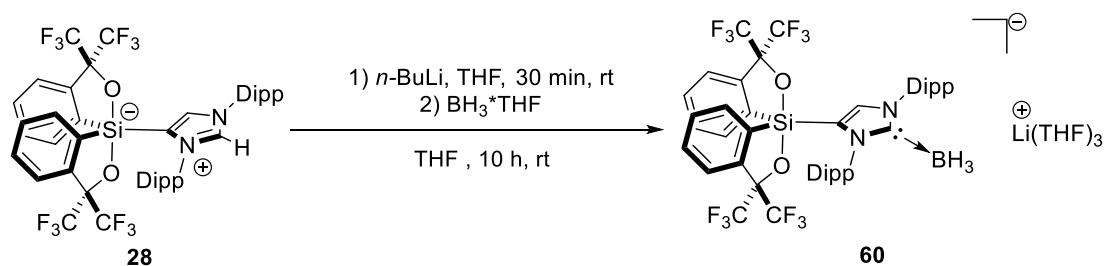
In a flame-dried Schlenk tube under argon, abnormal adduct **28** (100 mg, 0.11 mmol, 1.0 eq) was dissolved in distilled THF (1.6 mL, 0.07 M). *n*BuLi (2.5 M, 48.4  $\mu$ L, 1.1eq) was added dropwise at room temperature and the solution was allowed to stir for 30 minute before adding PPh<sub>3</sub>AuCl (54.4 mg, 0.11 mmol, 1.0 eq) at once. The reaction was stirred for another hour. The solvent was concentrated, and distilled pentane was added to trigger the precipitation of the product. After filtration, the solid was washed with pentane then was dried under vacuum. Gold complex **58** was obtained as a white solid, 106 mg, 71%. **<sup>1</sup>H NMR** (600 MHz, CD<sub>2</sub>Cl<sub>2</sub>): 8.11 (d, *J* = 7.1 Hz, 2H), 7.47-7.41 (m, 6H), 7.37 (t, *J* = 7.8 Hz, 1H), 7.31 (td, *J* = 7.9, 2.5 Hz, 6H), 7.27-7.22 (m, 6H), 7.17 (d, *J* = 7.8 Hz, 1H), 7.12 (d, *J* = 7.8 Hz, 1H), 6.94 (dd, *J* = 13, 8.1 Hz, 6H), 2.71 (m, *J* = 6.8 Hz, 1H), 2.58 (m, *J* = 6.8 Hz, 2H), 2.4 (m, *J* = 6.8 Hz, 1H), 1.10-1.04 (m, 15H), 0.99 (dd, *J* = 6.9, 4.6 Hz, 6H), 0.72 (d, *J* = 6.7 Hz, 3H); **<sup>13</sup>C NMR** (150 MHz, CD<sub>2</sub>Cl<sub>2</sub>): 190.4 (d, <sup>2</sup>*J*<sub>CP</sub> = 126 Hz, NCN), 147, 146.9, 146.8, 146.6, 145, 144, 140.9, 137.9, 137.5, 134.6, 134.2 (d, <sup>2</sup>*J*<sub>CP</sub> = 13.7 Hz, *o*-C<sub>6</sub>H<sub>3</sub>), 132.5 (d, <sup>4</sup>*J*<sub>CP</sub> = 2.6 Hz, *p*-C<sub>6</sub>H<sub>3</sub>), 130.5, 129.6 (d, <sup>3</sup>*J*<sub>CP</sub> = 11.2 Hz, *m*-C<sub>6</sub>H<sub>3</sub>), 128.8 (d, <sup>1</sup>*J*<sub>CP</sub> = 57.8 Hz, *i*-C<sub>6</sub>H<sub>3</sub>), 128.6, 128.5, 126.2 (q, <sup>1</sup>*J*<sub>C-F</sub> = 287 Hz, CF<sub>3</sub>), 124.5 (q, <sup>1</sup>*J*<sub>C-F</sub> = 290 Hz, CF<sub>3</sub>), 124.3, 124.2, 124.2, 123.9, 123.5 (bs, CH<sub>imid</sub>), 28.8, 28.7, 28.7, 28.6, 27.1, 26.4, 24.7, 24.3, 24.2, 24.2, 23.1, 22.6; **<sup>19</sup>F NMR** (376 MHz, CD<sub>2</sub>Cl<sub>2</sub>): -73.31 (q, *J* = 10 Hz, 9F), -74.92 (q, *J* = 10 Hz, 6F); **<sup>31</sup>P NMR** (161 MHz, CD<sub>2</sub>Cl<sub>2</sub>): 39.98; **<sup>29</sup>Si NMR**: the signal was not detected.

## Synthesis of the copper(I) complex **59**



In a flame dried Schlenk tube under argon, abnormal adduct **28** (75 mg, 0.083 mmol, 1.0 eq) was dissolved in distilled THF (1.2 mL, 0.07 M). *n*BuLi (2.5 M, 36.5  $\mu$ L, 1.1 eq) was added dropwise at room temperature and the solution was allowed to stir for 30 minute. Then  $\text{Cu}(\text{CH}_3\text{CN})_4\text{BF}_4$  (24.2 mg, 0.083 mmol, 1.0 eq) was added, the mixture was allowed to stir for five minutes before addition of 2,2'-bipyridine (13 mg, 0.083 mmol, 1.0 eq), the reaction was allowed to stir for 3 h. The solvent was evaporated under vacuum, the solid then, was solubilised in the minimum amount of distilled  $\text{CH}_2\text{Cl}_2$  and stored  $-30^\circ\text{C}$  for 8h. Copper complex **59** was obtained as orange cubic crystal. 62.6 mg, yield: 67%.  $^1\text{H NMR}$  (600 MHz,  $\text{CD}_2\text{Cl}_2$ ): 7.96 (dd,  $J = 6.8, 1.9$  Hz, 2H), 7.87 (d,  $J = 7.9$  Hz, 2H), 7.81 (td,  $J = 7.9, 7.76, 1.69$  Hz, 2H), 7.58 (t, 7.8 Hz, 1H), 7.48 (t,  $J = 7.7$  Hz, 1H), 7.44 (m, 3H), 7.37 (dd,  $J = 7.8, 1.4$  Hz, 1H), 7.32 (dd,  $J = 7.8, 1.4$  Hz, 1H), 7.21 (m, 5H), 7.12 (ddd,  $J = 7.5, 5.1, 1.16$  Hz, 2H), 7.01 (dd,  $J = 7.6, 1.63$  Hz, 1H), 6.30 (ddd,  $J = 5.0, 1.6, 0.9$  Hz, 2H), 3.10 (m, 1H), 2.68 (m, 1H), 2.62 (m, 1H), 2.48 (m, 1H), 1.26 (d,  $J = 6.6$  Hz, 3H), 1.20 (d,  $J = 6.8$  Hz, 3H), 1.03 (d,  $J = 6.8$  Hz, 3H), 0.97 (d,  $J = 6.8$  Hz, 3H), 0.94 (t,  $J = 8.2, 6.9$  Hz, 6H), 0.87 (d,  $J = 6.76$  Hz, 3H), 0.54 (d,  $J = 6.5$  Hz, 3H);  $^{13}\text{C NMR}$  (150 MHz,  $\text{CD}_2\text{Cl}_2$ ): 182.8 (NCN), 152.1, 150.8, 147.6, 147.5, 147.2, 147.2, 145.2, 143.6, 140.8, 140.4, 139.3, 137.6, 137.6, 131.6, 129.8, 129.0, 128.6, 128.2, 126.0, 124.8 (q,  $^1J_{\text{C-F}} = 288$  Hz,  $\text{CF}_3$ ), 124.6, 124.6 (q,  $^1J_{\text{C-F}} = 290$  Hz,  $\text{CF}_3$ ), 124.6, 124.3, 124.1, 123.7, 120.9, 81.7 (sept,  $^2J_{\text{C-F}} = 28.9$  Hz,  $\text{C}(\text{CF}_3)_2$ ), 28.6, 28.5, 28.5, 28.2, 27.7, 27.4, 24.5, 24.5, 24.1, 24.0, 23.2, 22.1;  $^{19}\text{F NMR}$  (564 MHz,  $\text{CD}_2\text{Cl}_2$ ): -73.88 (q,  $J = 9.8, 9.7$  Hz, 6F), -75.42 (q,  $J = 10.0, 9.7$  Hz, 6F);  $^{29}\text{Si NMR}$  (119 MHz,  $\text{CD}_2\text{Cl}_2$ ): -80.6.

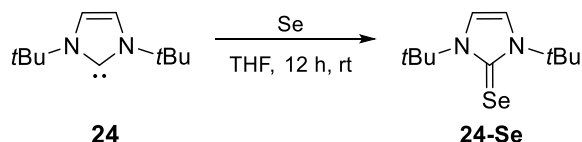
## Synthesis of the borate complex **60**



In a flame dried schlenk under argon, **28** (75 mg, 0.083 mmol, 1eq) was dissolved in distilled THF (0.07 M). *n*BuLi (2.5M, 36.5  $\mu$ L, 1.1eq) was added dropwise and the solution was allowed to stir for 30'. After  $\text{BH}_3 \cdot \text{THF}$  (1M, 83  $\mu$ L, 1eq) was added and the reaction was allowed to stir for 3h. The solvent was evaporated under vacuum, after the solid was solubilize in the minimum amount of distilled  $\text{CH}_2\text{Cl}_2$  and put at  $-30^\circ\text{C}$  for 13h. The white needle formed, were recuperated one by one. Obtained 37.77 mg, yield: 40%.  $^1\text{HNMR}$  (400 MHz,  $\text{CD}_2\text{Cl}_2$ ): 8.07 (dd,  $J = 6.63, 2.21$  Hz, 2H), 7.35 (m, 4H), 7.22 (m, 7H), 7.10 (dd,  $J = 7.80, 1.50$  Hz, 1H), 7.04 (dd,  $J = 7.68, 1.49$  Hz, 1H), 3.42 (m, 12H, THF), 2.67 (m, 1H), 2.55 (m, 1H), 2.43 (m, 1H), 2.31 (m, 1H), 1.7 (m, 12H, THF), 1.14 (d,  $J = 6.87$  Hz, 3H), 1.09 (d,  $J = 6.87$  Hz, 3H), 1.01 (m, 9H), 0.94 (d,  $J = 6.81$  Hz, 3H), 0.91 (d,  $J = 6.82$  Hz, 3H), 0.65 (d,  $J = 6.72$  Hz, 3H), -0.01 (bq, 3H);  $^{13}\text{CNMR}$  (150 MHz, THF- $d_8$ ): 146.7, 146.6, 146.5, 146.4, 141.1, 140.4, 139.1, 137.8, 136.4, 133.3, 129.3, 128.3, 128.3, 127.8, 125.1(q,  $^1J_{\text{C-F}} = 290$  Hz,  $\text{CF}_3$ ), 124.9 (q,  $^1J_{\text{C-F}} = 291$  Hz,  $\text{CF}_3$ ), 124.2, 123.8, 123.7, 123.5, 123.4, 123.2, 82.2(sept,  $^2J_{\text{C-F}} = 28.7$  Hz,  $\text{C}(\text{CF}_3)_2$ ), 68 (THF, O- $\text{CH}_2$ ), 28.8, 28.8, 28.7, 28.7, 26.2(THF,  $\text{CH}_2\text{-CH}_2$ ), 25.6, 25.4, 24.7, 24.5, 23.9, 23.3, 23, 22.9;  $^{19}\text{FNMR}$  (564 MHz, THF- $d_8$ ): -73.42 (q,  $J = 9.91, 9.86$  Hz, 6F), -75.12 (q,  $J = 10.07, 9.98$  Hz, 6F);  $^{11}\text{BNMR}$  (192 MHz, THF- $d_8$ ): -34.6 (bq,  $J = 94.53$  Hz,  $\text{BH}_3$ );  $^{29}\text{SiNMR}$  (119 MHz, THF- $d_8$ ): -80.6;  $^7\text{LiNMR}$  (233 MHz, THF- $d_8$ ): -0.6.

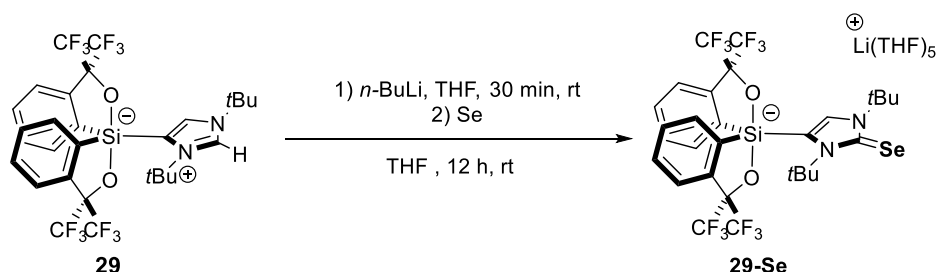
## Selenium Derivatives

### Synthesis of selenium adduct 24-Se



The selenium derivatives was synthesised following the slightly modified literature procedure.<sup>234</sup> In a flame-dried Schlenk tube under argon, **24** (50 mg, 0.27 mmol, 1.0 eq.), Se(0) (87 mg, 1.1 mmol, 4.0 eq.) were dissolved in distilled THF (5 mL, 0.054M), and stirred overnight. After that time the solvent was evaporated, and the crude product was dissolved in dichloromethane and was passed over a short pad of Celite<sup>®</sup>, that was washed five times with 5 mL of dichloromethane. The filtrate was evaporated and the selenium complex **24-Se** was obtained as a white solid, 48 mg, 67%. <sup>1</sup>H NMR (600 MHz, THF-d<sub>8</sub>): 7.13 (s, 2H), 1.87 (s, 18H); <sup>77</sup>Se NMR (114.4 MHz, THF-d<sub>8</sub>): 204.98.

### Synthesis of selenium adduct 29-Se



In a flame-dried Schlenk tube under argon, abnormal adduct **29** ( 50 mg, 0.072 mmol, 1.0 eq.), was dissolved in distilled THF (5 mL, 0.14 M). *n*BuLi (2.5 M, 31.7  $\mu$ L, 1.1 eq) was added dropwise at room temperature and the solution was allowed to stir for 30 minute. Then metallic selenium (22.74 mg, 0.28 mmol, 4.0 eq.) was added in one portion and the reaction was allowed to stir for 12 h at room temperature. The mixture was passed over a short pad of Celite<sup>®</sup>, washed five times with 5 mL of dichloromethane. The orange solution was evaporated, then leaved under vacuum for 7 h. The selenium derivatives **29-Se** was obtained as an orange sticky solid. The <sup>1</sup>H NMR spectra shows unseparable mixture of two

<sup>234</sup> S. V. C. Vummaleti, D. J. Nelson, A. Poater, A. Gómez-Suárez, D. B. Cordes, A. M. Z. Slawin, S. P. Nolan, L. Cavallo, *Chem. Sci.* **2015**, *6*, 1895–1904.

compounds, the desired product and the starting material in a 15:1 ratio. Five molecules of THF are probably coordinated to the lithium cation. Over time degradation was observed. **<sup>1</sup>H NMR** (600 MHz, THF-*d*<sub>8</sub>): 8.26 (d, *J* = 7.4 Hz, 1H), 8.15 (d, *J* = 7.5 Hz, 1H), 7.47 (d, *J* = 7.7 Hz, 1H), 7.40 (d, *J* = 7.5 Hz, 1H), 7.28 (dt, *J* = 16.4, 7.3 Hz, 2H), 7.21 (q, *J* = 8.5 Hz, 2H), 6.85 (s, 1H), 3.62 (m, 20H), 1.83 (s, 9H), 1.77 (m, 20H), 1.64 (s, 9H); **<sup>19</sup>F NMR** (564 MHz, THF-*d*<sub>8</sub>): -75.29 (t, *J* = 8.6 Hz, 5F), -75.36 (d, *J* = 8.9 Hz, 10F), -75.55 (bs, 3F), -75.84 (q, *J* = 9.8 Hz, 6F); **<sup>77</sup>Se NMR** (114.4 MHz, THF-*d*<sub>8</sub>): 193.52.

## Chapter V

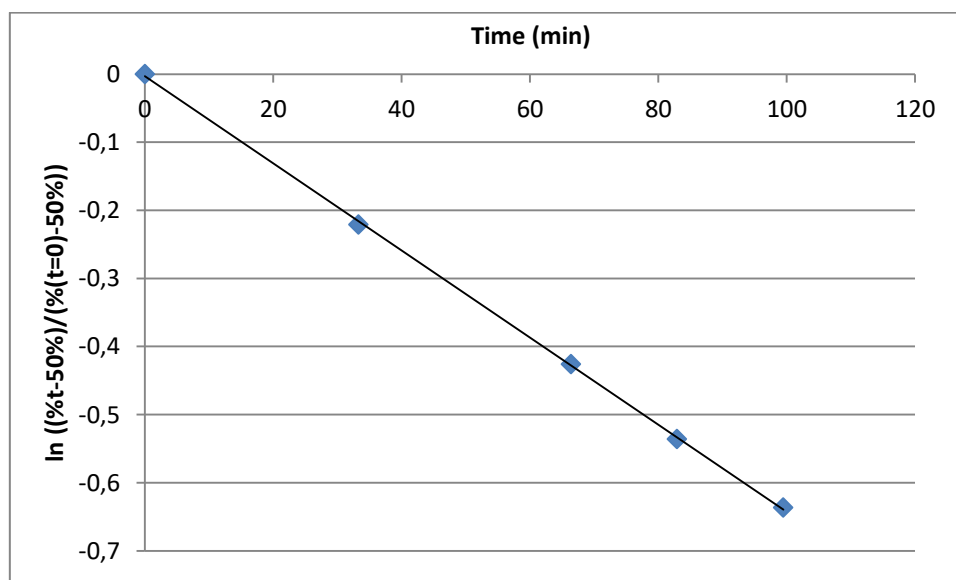
### Separation of 29

Conditions :

Column	Mobile Phase	t1	k1	t2	k2	$\alpha$	Rs
Chiralcel OD-3	Heptane / 2-PrOH (90/10)	9.65 (+)	2.27	11.10(-)	2.76	1.22	1.35

Kinetic of Enantiomerisation :

Time (min)	% first eluted enantiomer	$\ln ((\%t-\%e)/(\%0-\%e))$
0.00	97.33	0.0000
33.27	87.95	-0.2209
66.38	80.91	-0.4261
82.92	77.69	-0.5361
99.48	75.04	-0.6367



- Equation:  $y = -0.0064x - 0.0032$ ;  $R^2 = 0.9998$
- $k_{\text{enantiomerisation}} = 5.3294 \times 10^{-5} \text{ s}^{-1}$
- $\Delta G^\ddagger = 97.4 \text{ kJ/mol}$
- $t_{1/2} = 1.81 \text{ h}$

## Separation of 26

*Conditions :*

Chiralpak IB, 40°C, heptane/isopropanol (99.5/0.5), 7 mL/min

*Kinetic of racemization:*

By dynamic chiral HPLC, using the equation developed by O. Trapp and V. Schurig,<sup>235</sup> the barrier to enantiomerization can be evaluated at 99 kJ/mol.

## Separation of 57

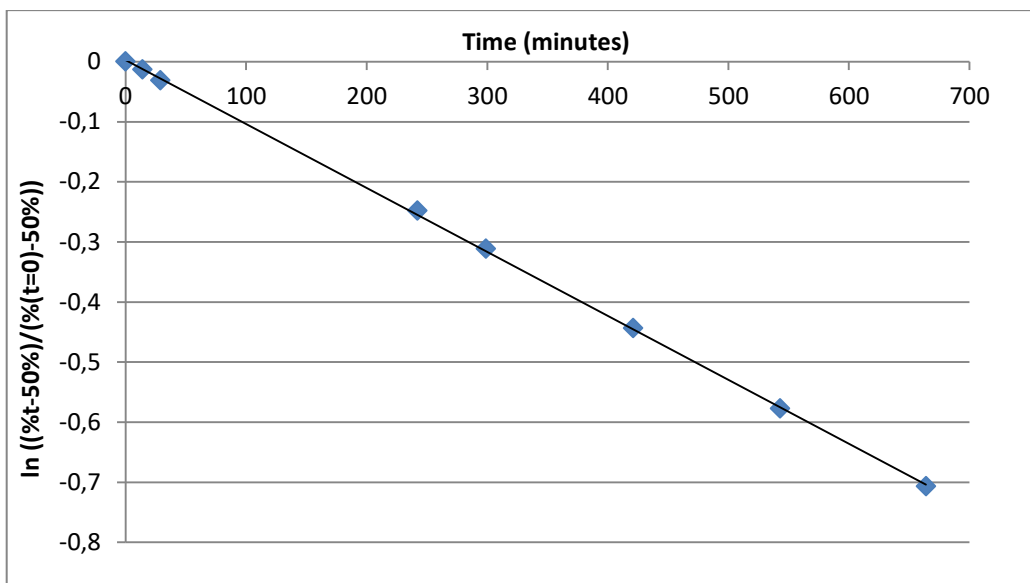
*Conditions :*

Column	Mobile Phase	t1	k1	t2	k2	$\alpha$	Rs
Chiralpak IE	Heptane / 2-PrOH (95/5)	9.99 (-)	2.39	10.90 (+)	2.69	1.13	1.46

*Kinetic of Enantiomerisation :*

Time (min)	% first eluted enantiomer	$\ln ((\%t-\%e)/(\%0-\%e))$
0	88.82	0.0000
14	88.31	-0.0132
29	87.63	-0.0311
242	80.29	-0.2481
299	78.43	-0.3115
421	74.91	-0.4437
543	71.79	-0.5775
664	69.15	-0.7066

<sup>235</sup> O. Trapp, V. Schurig, *Chirality* **2002**, *14*, 465-470.



- Equations:  $y = -0,0011x + 0,0027$ ;  $R^2 = 0,9998$
- $k_{\text{enantiomerisation}} = 8.8667\text{E-}06 \text{ s}^{-1}$  (25°C, dichloromethane)
- $\Delta G^\ddagger = 101.9 \text{ kJ/mol}$  (25°C, dichloromethane)
- $t_{1/2} = 10.86 \text{ h}$  (25°C, dichloromethane)

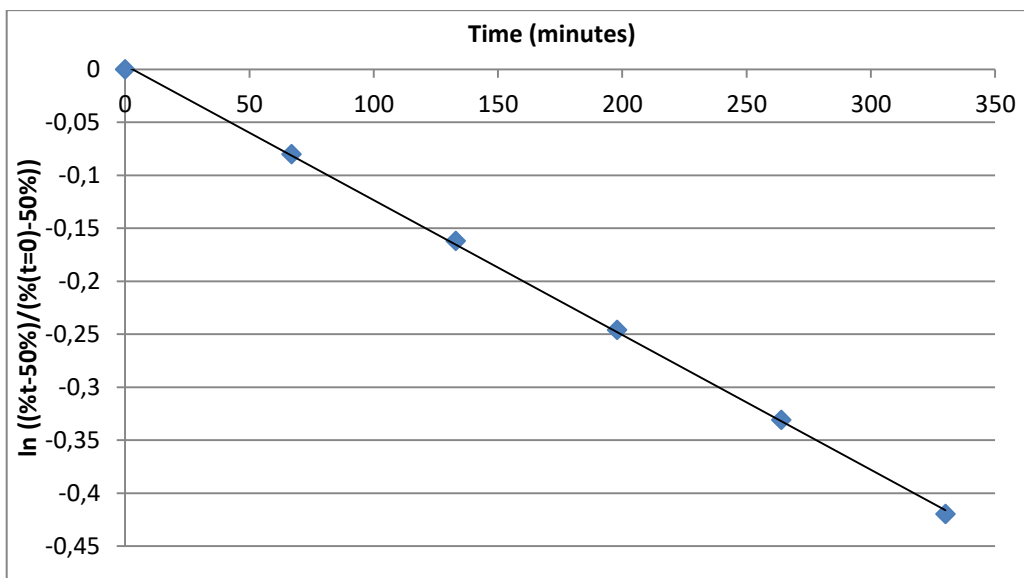
### Separation of 58

*Conditions :*

Column	Mobile Phase	t1	k1	t2	k2	$\alpha$	Rs
Chiralpak IE	Heptane / 2-PrOH (95/5)	8.80 (+)	1.98	9.48 (-)	2.22	1.12	1.41

*Kinetic of enantiomerisation :*

Time (min)	% first eluted enantiomer	ln ((%t-%e)/(%0-%e))
0	81.12	0.0000
67	78.72	-0.0803
133	76.46	-0.1622
198	74.33	-0.2461
264	72.35	-0.3310
330	70.45	-0.4199



- Equations:  $y = -0,0013x + 0,0039$ ;  $R^2 = 0,9996$
- $k_{\text{enantiomerisation}} = 1.0617\text{E-}05 \text{ s}^{-1}$  (25°C, dichloromethane)
- $\Delta G^\ddagger = 101.4 \text{ kJ/mol}$  (25°C, dichloromethane)
- $t_{1/2} = 9.07 \text{ h}$  (25°C, dichloromethane)

## Crystallographic Data

Compound	26	27	28	29
CCDC Number	1523668	1523669	1523670	To register
Empirical formula	C <sub>23</sub> H <sub>16</sub> F <sub>12</sub> N <sub>2</sub> O <sub>2</sub> Si	C <sub>42.5</sub> H <sub>11</sub> F <sub>12</sub> N <sub>2</sub> O <sub>2</sub> Si	C <sub>48.5</sub> H <sub>48</sub> F <sub>12</sub> N <sub>2</sub> O <sub>2</sub> Si	C <sub>29</sub> H <sub>28</sub> F <sub>12</sub> N <sub>2</sub> O <sub>2</sub> Si
Formula weight	608.47	862.82	946.98	692.62
Crystal system	Orthorhombic	Monoclinic	Triclinic	Monoclinic
Space group	P b c a	P 2 <sub>1</sub> /n	P -1	P 2 <sub>1</sub> /n
Unit cell dimensions	a = 12.7028(10) Å	a = 10.9559(4) Å	a = 10.8510(3) Å	a = 10.3357(5) Å
	b = 11.9895(10) Å	b = 40.9680(16) Å	b = 11.2578(3) Å	b = 18.8236(10) Å
	c = 31.828(3) Å	c = 18.0864(7) Å	c = 19.0950(5) Å	c = 15.9436(8) Å
	α = 90°	α = 90°	α = 85.788(2)°	α = 90°
	β = 90°	β = 100.232(2)°	β = 89.285(2)°	β = 96.026(2)°
	γ = 90°	γ = 90°	γ = 87.827(2)°	γ = 90°
Volume	4847.5(7) Å <sup>3</sup>	7988.8(5) Å <sup>3</sup>	2324.53(11) Å <sup>3</sup>	3084.8(3) Å <sup>3</sup>
Z	8	8	2	4
Crystal description	colourless fragment	colourless fragment	colourless prism	colourless fragment
Crystal size	0.4 x 0.3 x 0.2 mm <sup>3</sup>	0.3 x 0.2 x 0.2 mm <sup>3</sup>	0.2 x 0.15 x 0.1 mm <sup>3</sup>	0.35 x 0.25 x 0.05 mm <sup>3</sup>
Density (calculated)	1.667 g.cm <sup>-3</sup>	1.435 g.cm <sup>-3</sup>	1.353 g.cm <sup>-3</sup>	1.491 g.cm <sup>-3</sup>
Absorption coefficient	0.216 mm <sup>-1</sup>	1.376 mm <sup>-1</sup>	0.139 mm <sup>-1</sup>	0.179 mm <sup>-1</sup>
Min. and max. transmission	0.93 and 0.98	0.75 and 0.83	0.73 and 0.75	0.95 and 1.00
Temperature	200(1) K	200(1) K	200(1) K	200(1) K
Wavelength	0.71073 Å	1.54178 Å	0.71073 Å	0.71073 Å
θ range for data collection	3.02° to 30.07°	2.71° to 66.64°	1.07° to 30.66°	1.68° to 30.54°
Index ranges	-14 ≤ h ≤ 17	-13 ≤ h ≤ 12	-15 ≤ h ≤ 15	-14 ≤ h ≤ 14
	-12 ≤ k ≤ 16	-48 ≤ k ≤ 44	-15 ≤ k ≤ 16	-26 ≤ k ≤ 26
	-44 ≤ l ≤ 35	-21 ≤ l ≤ 21	-27 ≤ l ≤ 27	-16 ≤ l ≤ 22
Reflections (all / independent)	45794 / 7098	53393 / 14060	56212 / 14342	30249 / 9432
R(int)	2.21 %	2.33 %	1.96 %	2.72 %
Completeness	99.8 %	99.6 %	99.7 %	99.8 %
Data / parameters / restraints	7098 / 363 / 0	14060 / 1085 / 0	14342 / 622 / 72	9432 / 415 / 6
Goodness-of-fit on F <sup>2</sup>	1.038	1.023	1.037	1.041
Final R indices [I > 2σ(I)]	R1 = 4.00 % wR2 = 10.89 %	R1 = 3.93 % wR2 = 10.36 %	R1 = 4.80 % wR2 = 13.19 %	R1 = 4.58 % wR2 = 11.34 %
Final R indices (all data)	R1 = 4.83 % wR2 = 11.61 %	R1 = 4.29 % wR2 = 10.66 %	R1 = 6.33 % wR2 = 14.59 %	R1 = 7.34 % wR2 = 12.66 %
Largest difference peak and hole	0.39 and -0.36 e.Å <sup>-3</sup>	0.50 and -0.30 e.Å <sup>-3</sup>	0.88 and 0.49 e.Å <sup>-3</sup>	0.619 and -0.359 e.Å <sup>-3</sup>

Compound	51	52	55	57
CCDC number	<i>To register</i>	<i>To register</i>	<i>To register</i>	<i>To register</i>
Empirical formula	C <sub>28</sub> H <sub>31</sub> F <sub>12</sub> O <sub>3</sub> Si	C <sub>30</sub> H <sub>30</sub> F <sub>12</sub> N <sub>2</sub> O <sub>3</sub> Si	C <sub>32</sub> H <sub>33.5</sub> F <sub>12</sub> NO <sub>4.25</sub> Si	C <sub>52</sub> H <sub>54</sub> AuF <sub>12</sub> N <sub>2</sub> O <sub>2</sub> PSi
Formula weight	702.59	722.65	756.19	1223.00
Crystal system	Orthorhombic	Monoclinic	Monoclinic	Orthorhombic
Space group	P n a 21	C c	P 21/n	P c c n
Unit cell dimensions	a = 11.8599(4) Å	a = 10.2900(5) Å	a = 12.6543(2) Å	a = 25.4459(13) Å
	b = 41.2824(14) Å	b = 20.3888(7) Å	b = 16.0038(3) Å	b = 20.4754(9) Å
	c = 19.2532(6) Å	c = 16.2827(7) Å	c = 16.7692(4) Å	c = 22.0282(9) Å
	α = 90°	α = 90°	α = 90°	α = 90°
	β = 90°	β = 107.231(5)°	β = 94.323(2)°	β = 90°
	γ = 90°	γ = 90°	γ = 90°	γ = 90°
Volume	9426.5(5) Å <sup>3</sup>	3262.8(2) Å <sup>3</sup>	3386.38(12) Å <sup>3</sup>	11477.0(9) Å <sup>3</sup>
Z	12	4	4	8
Crystal description	colourless prism	colourless prism	colourless block	colourless prism
Crystal size	0.7 x 0.3 x 0.1 mm <sup>3</sup>	0.34 x 0.08 x 0.06 mm <sup>3</sup>	0.3 x 0.25 x 0.15 mm <sup>3</sup>	0.55 x 0.05 x 0.02 mm <sup>3</sup>
Density (calculated)	1.485 g.cm <sup>-3</sup>	1.471 g.cm <sup>-3</sup>	1.483 g.cm <sup>-3</sup>	1.416 g.cm <sup>-3</sup>
Absorption coefficient	2.072 mm <sup>-1</sup>	1.584 mm <sup>-1</sup>	0.174 mm <sup>-1</sup>	2.689 mm <sup>-1</sup>
Min. and max. transmission	0.45 and 0.87	0.62 and 1.00	0.92 and 0.94	0.50 and 0.98
Temperature	200(1) K	181(2) K	200(1) K	200(1) K
Wavelength	1.54178 Å	1.54184 Å	0.71073 Å	0.71073 Å
θ range for data collection	3.95° to 66.79°	4.34° to 68.55°	1.95° to 30.58°	1.85° to 28.36°
Index ranges	-11 ≤ h ≤ 14	-12 ≤ h ≤ 12	-18 ≤ h ≤ 18	-33 ≤ h ≤ 33
	-49 ≤ k ≤ 48	-24 ≤ k ≤ 24	-22 ≤ k ≤ 18	-27 ≤ k ≤ 24
	-22 ≤ l ≤ 22	-18 ≤ l ≤ 19	-16 ≤ l ≤ 23	-29 ≤ l ≤ 25
Reflections (all / independent)	88418 / 16619	9920 / 4521	35146 / 10373	74398 / 14298
R(int)	5.30 %	2.56 %	2.07 %	8.68 %
Completeness	99.7 %	99.0 %	99.8 %	99.6 %
Data / parameters / restraints	16619 / 1225 / 17	4521 / 434 / 2	10373 / 464 / 36	14298 / 685 / 56
Goodness-of-fit on F <sup>2</sup>	1.022	1.088	1.036	0.994
Final R indices [I > 2σ(I)]	R1 = 3.85 % wR2 = 10.23 %	R1 = 6.05 % wR2 = 18.72 %	R1 = 5.94 % wR2 = 16.39 %	R1 = 4.33 % wR2 = 8.42 %
Final R indices (all data)	R1 = 4.10 % wR2 = 10.43 %	R1 = 6.15 % wR2 = 18.79 %	R1 = 5.53 % wR2 = 18.45 %	R1 = 11.09 % wR2 = 10.52 %
Largest difference peak and hole	0.38 and -0.35 e.Å <sup>-3</sup>	0.78 and -0.34 e.Å <sup>-3</sup>	0.75 and 0.55 e.Å <sup>-3</sup>	1.523 and -0.629 e.Å <sup>-3</sup>

Compound	58	59	60
CCDC Number	1575949	1575951	1575950
Empirical formula	C <sub>63</sub> H <sub>58</sub> AuF <sub>12</sub> N <sub>2</sub> O <sub>2</sub> PSi	C <sub>58</sub> H <sub>57</sub> C <sub>16</sub> CuF <sub>12</sub> N <sub>4</sub> O <sub>2</sub> Si	C <sub>57</sub> H <sub>70</sub> BF <sub>12</sub> LiN <sub>2</sub> O <sub>5</sub> Si
Formula weight	1359.14	1374.40	1136.99
Crystal system	Triclinic	Monoclinic	Monoclinic
Space group	P -1	P 21/c	P 21/c
Unit cell dimensions	a = 12.8739(9) Å	a = 15.2050(7) Å	a = 11.4845(4) Å
	b = 13.2923(9) Å	b = 23.6591(10) Å	b = 23.8536(8) Å
	c = 18.6706(14) Å	c = 17.7121(8) Å	c = 21.7031(7) Å
	α = 84.008(3)°.	α = 90°.	α = 90°.
	β = 72.333(3)°.	β = 104.7380(10)°.	β = 99.918(2)°.
	γ = 76.619(3)°.	γ = 90°.	γ = 90°.
Volume	2959.6(4) Å <sup>3</sup>	6162.1(5) Å <sup>3</sup>	5856.6(3) Å <sup>3</sup>
Z	2	4	4
Crystal description	colourless fragment	yellow stick	colourless block
Crystal size	0.15 x 0.10 x 0.03 mm <sup>3</sup>	0.24 x 0.13 x 0.12 mm <sup>3</sup>	0.35 x 0.27 x 0.22 mm <sup>3</sup>
Density (calculated)	1.525 Mg/m <sup>3</sup>	1.481 Mg/m <sup>3</sup>	1.289 Mg/m <sup>3</sup>
Absorption coefficient	2.615 mm <sup>-1</sup>	0.715 mm <sup>-1</sup>	0.126 mm <sup>-1</sup>
Min. and max. transmission	0.961 and 0.724	0.746 and 0.683	0.746 and 0.717
Temperature	200(1) K	200(2) K	200(2) K
Wavelength	0.71073 Å	0.71073 Å	0.71073 Å
θ range for data collection	1.914 to 26.441°.	1.721 to 30.103°.	1.955 to 30.137°.
Index ranges	-16<=h<=15	-21<=h<=21	-15<=h<=16
	-16<=k<=13	-33<=k<=33	-33<=k<=33
	-23<=l<=23	-24<=l<=24	-30<=l<=30
Reflections (all / independent)	60945 / 12156	171774 / 18112	143489 / 17266
R(int)	0.0444	0.0286	0.0327
Completeness	99.9 %	100.0 %	99.9 %
Data / parameters / restraints	12156 / 0 / 739	18112 / 0 / 765	17266 / 75 / 769
Goodness-of-fit on F <sup>2</sup>	1.039	0.999	1.081
Final R indices [I > 2σ(I)]	R1 = 0.0407 wR2 = 0.0901	R1 = 0.0392 wR2 = 0.1082	R1 = 0.0621, wR2 = 0.1739
Final R indices (all data)	R1 = 0.0626 wR2 = 0.0982	R1 = 0.0574 wR2 = 0.1198	R1 = 0.0803 wR2 = 0.1879
Largest difference peak and hole	2.488 and -0.944 e.Å <sup>-3</sup>	0.328 and -0.247 e.Å <sup>-3</sup>	0.724 and -0.372 e.Å <sup>-3</sup>



# Index



## Figure's Index

<b>Figure I.1</b> a) Fragment of flint; b) Base unit cell of silica; c) Disordered 3D network typical of glass; d) Ordered 3D network typical of the crystalline form of silica quartz.....	13
<b>Figure I.2</b> Schematic representation of the <i>d</i> atomic orbitals.....	15
<b>Figure I.3</b> Example of $\sigma$ , $\pi$ and $\delta$ bonding.....	15
<b>Figure I.4</b> Equilibrium arrangements for electron pairs on the surface of a sphere repelling each other according to a force law of the form $1/r^n$ . (a) and (b) are the most stable arrangements for $n = \infty$ . (c) is the form of the square-pyramidal configuration for $n < \infty$ ; preferential conformation of AX <sub>5</sub> molecules (I) and AX <sub>5</sub> E (I). ....	16
<b>Figure I.5</b> Hybridisation and electron density in hypervalent silicon.....	16
<b>Figure I.6</b> Orbital picture and hybridisation of silicon complex.....	17
<b>Figure I.7</b> Molecular orbital diagram of three-centre four-electron molecule.....	18
<b>Figure I.8</b> Original letter of Pr. Schleyer.....	19
<b>Figure I.9</b> Denmark's intermediate for silanol-based cross-coupling.....	22
<b>Figure I.10</b> Fluorescence spectra ( $\lambda_{\text{ex}} = 266 \text{ nm}$ ) of <b>7</b> and <b>8a</b> in DCM.....	27
<b>Figure I.11</b> X-ray structure of <b>14</b> *TBA (CCDC: 692252), the counteranion is omitted for clarity.....	29
<b>Figure I.12</b> X-Ray structure of <b>20</b> .....	32
<b>Figure I.13</b> <sup>19</sup> FNMR of <b>20</b> at different T ( <i>dioxane-d</i> <sub>8</sub> ).....	33
<b>Figure I.14</b> <sup>1</sup> HNMR spectra ((CD <sub>3</sub> ) <sub>2</sub> CO) of <b>21</b> . * THF. ....	35
<b>Figure I.15</b> <sup>1</sup> HNMR (toluene- <i>d</i> <sub>8</sub> ) of Martin's spiroasilane.....	36
<b>Figure I.16</b> <sup>19</sup> FNMR (toluene- <i>d</i> <sub>8</sub> ) of Martin's spiroasilane.....	37
<b>Figure II.1</b> Linear and bent structure of carbene.....	41
<b>Figure II.2</b> Some class of NHC carbene.....	42
<b>Figure II.3</b> X-Ray structure of 1, 3-di(1-adamantyl)imidazole-2-ylidene (CCDC number: 1283930).....	43
<b>Figure II.4</b> Frontier orbitals and electron configurations for carbene carbon atoms.....	44
<b>Figure II.5</b> Representation of the limit forms of the carbene in NHCs.....	44
<b>Figure II.6</b> Consequence of steric effect on multiplicity state.....	45
<b>Figure II.7</b> NHC classes used in pK <sub>a</sub> (H <sub>2</sub> O) evaluation put in a decreasing acidity scale.....	46
<b>Figure II.8</b> Nucleophilicity parameters measured by Lupton.....	47
<b>Figure II.9</b> NHCs used for this study in steric hindrance scale.....	55

<b>Figure II.10</b> comparison of the $^1\text{H}$ NMR of <b>7</b> (red) and <b>26</b> (blue). $\text{CD}_2\text{Cl}_2$ .....	58
<b>Figure II.11</b> ORTEP representation of <b>26</b> , ellipsoid 50% probability. ....	59
<b>Figure II.12</b> ORTEP representation of the NHC-Si derivatives of Roschenthaler.....	59
<b>Figure II.13</b> <b>26</b> X-Ray structure divided in quadrant.....	60
<b>Figure II.14</b> Decomposition product of <b>27</b> after water treatment. ....	61
<b>Figure II.15</b> ORTEP representation of <b>27</b> , 50% probability ellipsoid. For the sake of clarity the second molecule of adduct present in the asymmetric unit is omitted.....	61
<b>Figure II.16</b> $^{13}\text{C}$ NMR spectrum detail of <b>27</b> .....	62
<b>Figure II.17</b> C-F (orange), H-F (blue) distance.....	62
<b>Figure II.18</b> Comparison between the $^1\text{H}$ NMR in the aliphatic area of <b>IPr</b> and <b>28</b> in $\text{CD}_2\text{Cl}_2$ .....	64
<b>Figure II.19</b> ORTEP representation of <b>28</b> ellipsoid 50% probability. ....	65
<b>Figure II.20</b> ORTEP Cross section of <b>28</b> . Highlighted the imidazole ring.....	65
<b>Figure II.21</b> ORTEP representation of <b>29</b> , ellipsoid 50% probability. ....	67
<b>Figure II.22</b> Comparison of the NMR spectra of <b>27</b> at room temperature (red) and at $80\text{ }^\circ\text{C}$ (green) .....	68
<b>Figure III.1</b> chiral borane derived from the (+)- $\alpha$ -pinene .....	79
<b>Figure III.2</b> Activated form of catalyst .....	80
<b>Figure III.3</b> Top: classical adduct transformed in FLP; bottom: Hoshimoto's system .....	91
<b>Figure III.4</b> ORTEP representation of <b>48</b> , ellipsoid 50% of probability .....	96
<b>Figure III.5</b> Gas drying system .....	96
<b>Figure III.6</b> Superbase used in this study.....	97
<b>Figure III.7</b> Particular of the $^1\text{H}$ NMR spectra of <b>50</b> (a) and <b>51</b> (b); *: paraformaldehyde. 101	
<b>Figure III.8</b> ORTEP representation of <b>51</b> . ....	102
<b>Figure III.9</b> ORTEP representation of <b>52</b> .....	103
<b>Figure III.10</b> Representation of <b>53</b> .....	104
<b>Figure III.11</b> $^1\text{H}$ NMR of <b>53</b> ; clearly visible the roof effect.....	104
<b>Figure III.12</b> Representation of <b>54</b> ; $^1\text{H}$ NMR spectra highlighting the two benzylic protons, and the doublet corresponding to the P-H (purple triangles); * $\text{CD}_2\text{Cl}_2$ .....	105
<b>Figure III.13</b> ORTEP representation of <b>55</b> , ellipsoid 50% of probability. ....	106
<b>Figure III.14</b> Proposed resonance equilibrium .....	106
<b>Figure IV.1</b> Fehllhammer's anionic NHC.....	112
<b>Figure IV.2</b> Comparison of the aromatic area in $^1\text{H}$ NMR spectra before and after deprotonation.....	118

<b>Figure IV.3</b> ORTEP representation of <b>57</b> , ellipsoid 50% probability.....	119
<b>Figure IV.4</b> ORTEP representation of <b>58</b> , ellipsoid 50% probability.....	120
<b>Figure IV.5</b> ORTEP representation of <b>59</b> , ellipsoid 50% probability.....	122
<b>Figure IV.6</b> ORTEP representation of <b>60</b> , ellipsoid 50% probability.....	123
<b>Figure IV.7</b> Cross section of the structure of <b>60</b> . ORTEP representation, ellipsoid 50% probability. ....	124
<b>Figure IV.8</b> Visualisation of the HOMO of calculated at the B3LYP-D3/def2-SVPD level of theory and plotted at an isosurface value of 0.05 .....	125
<b>Figure IV.9</b> Frontier molecular orbital comparison between <b>25</b> , <b>28</b> and CAAC carbenes...	126
<b>Figure V.1</b> Pseudorotation mechanisms proposed by Muetterties.....	130
<b>Figure V.2</b> a) Berry's pseudorotation mechanism; b) Turnstile rotation Mechanism, Ugi's Pseudorotation.....	131
<b>Figure V.3</b> Compounds investigated .....	132
<b>Figure V.4</b> TBP and SPP configuration .....	132
<b>Figure V.5</b> First proposed mechanism; in bracket the <i>pivot</i> ligand.....	134
<b>Figure V.6</b> Highest transition state.....	134
<b>Figure V.7</b> Second proposed mechanism; in bracket the <i>pivot</i> ligand.....	135
<b>Figure V.8</b> Chromatogram of <b>29</b> (up); coupled to positive and negative Circular Dichroism (down). ....	136
<b>Figure V.9</b> Data collected by monitoring the racemisation.....	137
<b>Figure V.10</b> Chromatogram of <b>26</b> .....	138
<b>Figure V.11</b> Chromatogram of <b>57</b> (up); coupled to positive and negative Circular Dichroism (down). ....	138
<b>Figure V.12</b> CD spectra of the two separated enantiomers.....	139
<b>Figure V.13</b> Chromatogram of <b>58</b> (up); coupled to positive and negative Circular Dichroism (down). ....	140

## Scheme's Index

<b>Scheme I-1</b> First C-C bond formation with organosilane by Kumada <i>et al.</i> ....	20
<b>Scheme I-2</b> General example of the first reported Hiyama cross-coupling .....	21
<b>Scheme I-3</b> Proposed catalytic cycle for of Pd-catalysed cross-coupling of organosilicon reagent .....	21
<b>Scheme I-4</b> In bracket the active hypercoordinate compound in the Hosomi's example.....	22
<b>Scheme I-5</b> General intermediate proposed by Leighton .....	23
<b>Scheme I-6</b> Cyclosilane as transfer reagent.....	23
<b>Scheme I-7</b> Pentacoordinate silicate as radical precursor .....	23
<b>Scheme I-8</b> Reactions scheme for the synthesis of the hypercoordinate compounds from hexafluorocumyl alcohol.....	24
<b>Scheme I-9</b> Reaction with different nucleophiles.....	25
<b>Scheme I-10</b> Synthesis of hydrosilicate <b>7-H</b> and its application in the enone's reduction	26
<b>Scheme I-11</b> polymerisation of oxetanes.....	26
<b>Scheme I-12</b> Reactivity of <b>7</b> toward different fluoride source .....	27
<b>Scheme I-13</b> Synthesis of the modified spirosilane <b>13a-i</b> .....	28
<b>Scheme I-14</b> Synthesis and reactivity of disilicate <b>14</b> .....	29
<b>Scheme I-15</b> Interconversion among the Disilicates, silylsilicates and Disilane .....	30
<b>Scheme I-16</b> Oxidative bond cleavage of <b>14-M</b> .....	31
<b>Scheme I-17</b> Proposed mechanism for Si-Si cleavage .....	31
<b>Scheme I-18</b> Synthesis of the phenanthroline's adduct <b>20</b> .....	32
<b>Scheme I-19</b> General reaction between <b>7</b> with a large excess of nucleophile.....	34
<b>Scheme I-20</b> First synthetic attempt .....	34
<b>Scheme I-21</b> Synthesis of Ph-Martin Spirosilane.....	35
<b>Scheme I-22</b> Final step of Martin's spirosilane synthesis .....	36
<b>Scheme II-1</b> Synthesis of the phosphinocarbene used by Bertrand and co-workers in their studies.....	42
<b>Scheme II-2</b> Synthesis of 1, 3-di(1-adamantyl)imidazole-2-ylidene .....	43
<b>Scheme II-3 a)</b> Electrophiles used by Lupton in his studies; <b>b)</b> Reaction used to calculate the nucleophilicity.....	47
<b>Scheme II-4</b> Synthetic pathway used by Dorta (a) and Plenio (b) .....	48
<b>Scheme II-5</b> First examples of NHC-Silanes realised by Kuhn .....	49

<b>Scheme II-6</b> Polysiloxane for the protection of carbene .....	50
<b>Scheme II-7</b> Polymerisation of polysiloxane .....	50
<b>Scheme II-8</b> Synthetic strategy adopted by Robinson to stabilize low-valent oxidation states of silicon.....	51
<b>Scheme II-9</b> Dichlorosilene stabilised by IPr and its reactivity .....	52
<b>Scheme II-10</b> Synthesis of the Filippou's complex.....	52
<b>Scheme II-11</b> Example of ring opening reaction described by Radius .....	53
<b>Scheme II-12</b> Disilyne stabilised by NHC .....	53
<b>Scheme II-13</b> Silicon-based acylium ion.....	54
<b>Scheme II-14</b> synthesis of the precursor IDM.....	55
<b>Scheme II-15</b> Synthesis of carbenes <b>23</b> and <b>25</b> .....	56
<b>Scheme II-16</b> Synthetic strategy for <b>24</b> .....	57
<b>Scheme II-17</b> Interaction between Martin's spirosilane <b>7</b> and IDM.....	57
<b>Scheme II-18</b> Formation of the normal adduct <b>27</b> by interaction between Martin's spirosilane <b>7</b> and IMes <b>23</b> .....	60
<b>Scheme II-19</b> Synthesis of abnormal adduct <b>28</b> .....	63
<b>Scheme II-20</b> Synthesis of abnormal adduct <b>29</b> .....	66
<b>Scheme II-21</b> NMR comparison between the <i>n</i> NHC adduct with IMes (red) and the mixture <i>n</i> NHC/ <i>a</i> NHC (green). Tol-d <sub>8</sub> .....	68
<b>Scheme II-22</b> Mechanism formation of abnormal adduct proposed by Hevia.....	69
<b>Scheme II-23</b> DFT-computed (M06/def2-SVP) mechanism for the normal-to-abnormal NHC rearrangement in the presence of THF proposed by Dagorne and coworker. Gibbs free energies in THF solution.....	70
<b>Scheme III-1</b> Examples of Brønsted adduct formation (up) and Lewis adduct formation (bottom).....	75
<b>Scheme III-2</b> Brown's experiments. ....	76
<b>Scheme III-3</b> Tochtermann trapping product.....	76
<b>Scheme III-4</b> Reactivity of tris(pentafluorophenyl) borane and a phosphorus ylide .....	77
<b>Scheme III-5</b> First example of FLP.....	78
<b>Scheme III-6</b> Catalytic cycle proposed for the imine reduction .....	79
<b>Scheme III-7</b> Synthesis of chiral borane <b>37</b> and <b>38</b> .....	80
<b>Scheme III-8</b> General condition for hydrogenation reaction .....	81
<b>Scheme III-9</b> Reversible CO <sub>2</sub> binding.....	82
<b>Scheme III-10</b> Proposed mechanism for the CO <sub>2</sub> reduction .....	83

<b>Scheme III-11</b> General reaction conditions for the synthesis of benzimidazoles .....	84
<b>Scheme III-12</b> Proposed mechanism for benzimidazoles formation .....	84
<b>Scheme III-13</b> Silyl ion split hydrogen .....	86
<b>Scheme III-14</b> Hydrogen activation and rearrangement of silylenium cation .....	86
<b>Scheme III-15</b> a) CO <sub>2</sub> activation by the Cantat's FLP system; b) Example hydroboration of carbon dioxide .....	87
<b>Scheme III-16</b> First proposed catalytic cycle .....	88
<b>Scheme III-17</b> Mitzel's adduct .....	88
<b>Scheme III-18</b> Hydrogen activation and dehydrogenation of water .....	89
<b>Scheme III-19</b> First time NHC were employed in FLP chemistry .....	90
<b>Scheme III-20</b> Synthesis and conversion of <b>46</b> and <b>47</b> .....	92
<b>Scheme III-21</b> FLP behaviour of the NHC-Silylium adduct .....	93
<b>Scheme III-22</b> General H <sub>2</sub> activation scheme in mild condition .....	95
<b>Scheme III-23</b> H <sub>2</sub> splitting equilibrium .....	97
<b>Scheme III-24</b> hydrogenation reaction .....	98
<b>Scheme III-25</b> Reaction with Et <sub>3</sub> SiH as hydride donor .....	98
<b>Scheme III-26</b> General CO <sub>2</sub> activation scheme in mild condition .....	99
<b>Scheme III-27</b> Activation of CO <sub>2</sub> with IPr and <b>7</b> .....	99
<b>Scheme III-28</b> Attempt the activation of carbon dioxide with phosphine .....	100
<b>Scheme III-29</b> Activation of carbon dioxide with borane and phosphine .....	100
<b>Scheme III-30</b> Synthesis of <b>49</b> .....	100
<b>Scheme III-31</b> General scheme for the formaldehyde activation .....	101
<b>Scheme III-32</b> General synthesis for the benzyloxysiliconate .....	103
<b>Scheme III-33</b> Synthesis of <b>55</b> .....	105
<b>Scheme IV-1</b> From abnormal adduct to anionic NHC ligand .....	111
<b>Scheme IV-2</b> Synthesis of the <i>malo</i> NHC .....	112
<b>Scheme IV-3</b> Synthesis of the iron(I) derivatives .....	113
<b>Scheme IV-4</b> Synthesis of the enol-NHC .....	113
<b>Scheme IV-5</b> Synthesis of the anionic NHC dicarbene .....	113
<b>Scheme IV-6</b> Synthesis proposed by Tamm .....	114
<b>Scheme IV-7</b> Anionic carbene Gold(I) derivatives .....	114
<b>Scheme IV-8</b> Rh(I), Ir(I) complexes synthesised by Tamm and co-workers .....	115
<b>Scheme IV-9</b> Formation of the dihydro complex .....	115
<b>Scheme IV-10</b> Synthesis of the Igarashi's vanadium(V) complex .....	115

<b>Scheme IV-11</b> Synthesis of lithium derivatives <b>56</b> .....	117
<b>Scheme IV-12</b> Synthesis of <b>57</b> .....	118
<b>Scheme IV-13</b> Synthesis of <b>58</b> .....	120
<b>Scheme IV-14</b> Synthesis of the copper derivatives <b>59</b> .....	121
<b>Scheme IV-15</b> Synthesis of complex <b>60</b> .....	123
<b>Scheme V-1</b> Synthetic pathway and the three isomers described by Lammertsma and co-workers .....	131

## Table's Index

<b>Table II.1</b> Thermodynamic parameters obtained by DFT calculations for the formation of normal adduct. Distance are given in Å and energies in Kcal.mol <sup>-1</sup> .....	70
<b>Table II.2</b> Thermodynamic parameters obtained by DFT calculations for normal-to-abnormal adducts interconversion. Distance are given in Å and energies in Kcal.mol <sup>-1</sup> .....	71
<b>Table III.1</b> G.-B. Experimental values .....	94
<b>Table III.2</b> Hilt experimental values; deuterium naturally present in CH <sub>2</sub> Cl <sub>2</sub> used as ref.: 5.30 ppm.....	95
<b>Table V.1</b> Energy barriers to inversion with different substituent Y .....	133



## Résumé

Ce travail de thèse est consacré à l'étude de la réactivité du spirosilane de Martin, une molécule présentant des propriétés intéressantes notamment en présence de bases de Lewis, qui a trouvé des applications diverses comme la détection d'ions fluorures. En ce qui nous concerne, nous avons choisi d'étudier l'interaction de ce dérivé du silicium avec des bases de Lewis neutres fortes tels que les Carbènes N-Hétérocycliques (NHC) qui ont été beaucoup utilisés pour stabiliser les espèces de basse valence des éléments du bloc p. Alors que les NHC sont connus pour former avec les chlorosilanes des adduits pentacoordinés stables, aucun exemple avec des silanes non halogénés n'avaient été décrits avant notre étude. Nous avons montré qu'en fonction de l'encombrement stérique des NHC étudiés, ils forment avec le spirosilane de Martin des adduits de Lewis normaux et anormaux stables. Les propriétés « Paires de Lewis Frustrées » (FLP) du spirosilane avec des NHC encombrés ont été examinées ainsi que l'accès à des nouveaux ligands NHC anioniques portant un motif silicate.

## Mots Clés

Silicium, Paire de Lewis Frustrée, Ligand Anionique, Spirosilane, Carbène N-Hétérocyclique, Chiralité,

## Abstract

This thesis work is focused on the reactivity of Martin's Spirosilane, a molecule that displays some interesting properties in particular with different Lewis base, founding some interesting application such as fluoride sensing. In our study, we chose N-Heterocyclic Carbenes (NHC) because they are well-known for stabilising low-valence states of p-block elements. Besides, NHC are known to form relatively stable adducts with tetravalent halosilanes and also to stabilise silicon(0), but, to the best of our knowledge, no pentacoordinated NHC-adducts with a non-halogenated silane partner has been synthesised to date.

We investigate the interaction between different NHC carbene and Martin's spirosilane that afforded some normal and abnormal adducts that were fully characterised. The different systems were then studied as potential Frustrated Lewis Pair and as precursors of anionic-type ligands for the metal coordination.

## Keywords

Silicon, Frustrated Lewis Pair, Anionic Ligand, Spirosilane, N-Heterocyclic Carbene, Chirality.